



**HAL**  
open science

# Contributions in shape optimization and inverse problems for some partial differential equations

Fabien Caubet

► **To cite this version:**

Fabien Caubet. Contributions in shape optimization and inverse problems for some partial differential equations. Mathematics [math]. Université Toulouse 3 Paul Sabatier (UT3 Paul Sabatier), 2018. tel-01973336

**HAL Id: tel-01973336**

**<https://hal.science/tel-01973336>**

Submitted on 8 Jan 2019

**HAL** is a multi-disciplinary open access archive for the deposit and dissemination of scientific research documents, whether they are published or not. The documents may come from teaching and research institutions in France or abroad, or from public or private research centers.

L'archive ouverte pluridisciplinaire **HAL**, est destinée au dépôt et à la diffusion de documents scientifiques de niveau recherche, publiés ou non, émanant des établissements d'enseignement et de recherche français ou étrangers, des laboratoires publics ou privés.

---

## Mémoire

présenté en vue de l'obtention du diplôme d'

### HABILITATION À DIRIGER DES RECHERCHES

en Mathématiques

par

**Fabien Caubet**

---

---

## Contributions en optimisation de forme et problèmes inverses pour quelques équations aux dérivées partielles

---

Soutenance publique le 11 décembre 2018

**Parrain :** Franck BOYER Professeur, Université Paul Sabatier – Toulouse III

**Rapporteurs :** Grégoire ALLAIRE Professeur, École Polytechnique  
Fioralba CAKONI Professeur, Université Rutgers  
Antoine HENROT Professeur, École des Mines de Nancy

### Composition du jury

Grégoire ALLAIRE	Professeur, École Polytechnique
Amel BEN ABDA	Professeur, École Nationale d'Ingénieurs de Tunis
Marc BONNET	Directeur de Recherche CNRS, ENSTA ParisTech
Franck BOYER	Professeur, Université Paul Sabatier – Toulouse III
Dorin BUCUR	Professeur, Université de Savoie
Marc DAMBRINE	Professeur, Université de Pau et des pays de l'Adour
Antoine HENROT	Professeur, École des Mines de Nancy



À Léon et Martin



---

# Remerciements

Avant toute chose, je tiens ici à remercier chaleureusement les personnes qui m'ont accompagné au cours de ces dernières années, tant sur le plan professionnel que personnel.

Je remercie tout d'abord très chaleureusement Grégoire Allaire, Fioralba Cakoni et Antoine Henrot d'avoir accepté de lire mon manuscrit et de m'avoir fait bénéficier de leur expertise sur les sujets évoqués. Je remercie à nouveau Grégoire Allaire et Antoine Henrot, ainsi que Amel Ben Abda, Marc Bonnet et Dorin Bucur d'avoir assisté à ma soutenance ; nos échanges ont été et sont toujours très enrichissants et j'espère que nous aurons très vite l'occasion d'aborder de nouveaux sujets ensemble. Je remercie naturellement mon "parrain" Franck Boyer d'avoir en particulier géré et maîtrisé les difficultés administratives liées à ma soutenance. Merci enfin au dernier membre de mon jury, Marc Dambrine, pour... beaucoup de choses ! Merci de m'avoir formé à la recherche, merci pour tes conseils et tes avis toujours pertinents et merci pour nos discussions continuellement positives et bénéfiques. La transition est toute trouvée pour remercier Mehdi Badra. Merci là encore pour ton accompagnement depuis toutes ces années, merci pour nos repas toulousains et merci pour nos nombreux échanges scientifiques et non scientifiques.

J'ai eu la chance de réaliser les recherches présentées dans ce manuscrit au sein de l'IMT, dans un environnement extrêmement favorable à mon développement professionnel. Je remercie ainsi sincèrement les membres de l'équipe MIP pour leur accueil lors de mon arrivée à Toulouse et pour l'ambiance de travail conviviale et stimulante à l'institut. Merci en particulier au petit groupe de travail que nous avons formé avec notamment Jérémie Dardé, Frédéric de Gournay, Sylvain Ervedoza, Jérôme Fehrenbach et Jean-Pierre Raymond. Merci pour nos échanges et nombreuses pistes de recherche ouvertes. Merci également aux membres du département GMP de l'IUT A pour leur hospitalité et les nombreux repas et pots rythmant l'année universitaire. Je remercie particulièrement Bernard Ferret en tant que chef de département à mon arrivée ainsi que Stefan Le Coz et Michel Fournié pour nos échanges et pour vos conseils sur l'intégration d'un mathématicien en GMP. Je remercie enfin ici les membres du LMAP, en particulier Chérif Amrouche, Daniel Delabre, Jean-Matthieu Etancelin, Isabelle Greff, Charles Pierre, Bénédicte Puig et Guy Vallet, pour nos discussions et nos projets en commun.

J'ai eu l'opportunité grâce à Carlos Conca de co-encadrer la thèse de Matías Godoy. Merci à tous les deux pour cette merveilleuse aventure et merci pour votre chaleureux accueil lors de ma venue en famille à Santiago. J'espère avoir l'occasion de revenir vous rendre visite prochainement. Je remercie en particulier Matías pour sa motivation et son implication lors de sa thèse. Ce fut un réel plaisir pour moi de t'encadrer et de t'accompagner dans tes premiers pas de chercheur. Je te souhaite beaucoup de réussite pour la suite et serai ravi de poursuivre notre collaboration.

Je remercie particulièrement Loïc Bourdin : merci pour nos très bons moments depuis notre première année et pour nos diverses discussions, aussi riches que variées. J'en profite pour glisser un mot

## Remerciements

---

à Paul Sauvy pour nos années passées tous les trois à découvrir les mathématiques et la vie d'étudiant. J'ai eu la chance et le plaisir de travailler avec divers collaboratrices et collaborateurs que je remercie pour leurs contributions dans ce manuscrit : merci à Samir Adly, Pierre Bonnelie, Thibaut Deheuvels, Housseem Haddar, Djalil Kateb, Frédérique Le Louër, Jing-Rebecca Li, Yannick Privat, Olivier Ruatta et Dang Van Nguyen.

Je remercie enfin mes proches non mathématiciens, mes amis et ma famille. Merci en particulier à Sophia pour sa relecture et ses corrections (dès la première phrase!), merci à Thomas d'avoir assisté à la soutenance, merci également à Christine, Maurice et Grégory. Un grand merci naturellement à ma mère, mon frère, Marlène, Raphaël et Julia ainsi que mon père et Françoise. Merci également à Alban, Pascal et Thibaut pour leur amitié et ce qu'elle implique. Et bien entendu un immense merci à Sarah pour son soutien, sa patience et ses conseils toujours bienveillants. Je termine naturellement ces remerciements en pensant à Léon et Martin : merci de m'apprendre autant chaque jour et merci pour tout le bonheur que vous m'apportez à chaque instant.

Merci encore à toutes et tous et bonne lecture pour celles et ceux qui ont le courage de continuer!

**Fabien**



## Remerciements

---

---

# Table des matières

<b>Préambule</b>	<b>1</b>
<b>Introduction générale</b>	<b>3</b>
<b>Notations</b>	<b>7</b>
<b>I Études de stabilité en mécanique des fluides</b>	<b>9</b>
I.1 Stabilité de formes optimales . . . . .	10
I.1.1 Un résultat de stabilité pour la minimisation de la trainée . . . . .	10
I.1.1.1 Le problème étudié . . . . .	11
I.1.1.2 Coercivité de la Hessienne . . . . .	12
I.1.1.3 Stabilité du problème de minimisation de la trainée et estimation de stabilité . . . . .	14
I.1.2 Perspectives . . . . .	15
I.2 Instabilité d'un problème inverse . . . . .	16
I.2.1 Estimations de stabilité pour le problème de reconstruction de données . . . . .	16
I.2.1.1 Inégalités de Carleman . . . . .	17
I.2.1.2 Inégalités de stabilité . . . . .	18
I.2.2 Deux applications . . . . .	20
I.2.2.1 Identification de paramètres . . . . .	20
I.2.2.2 Taux de convergence de méthodes numériques de reconstruction . . . . .	22
I.2.3 Perspectives . . . . .	24
<b>II De nouvelles approches pour la détection d'objets immergés en 2D</b>	<b>27</b>
II.1 Une méthode mixte . . . . .	28
II.1.1 Objectifs et principales difficultés de la dimension deux . . . . .	28
II.1.2 Position du problème . . . . .	30
II.1.3 Les résultats principaux . . . . .	31

## Table des matières

---

II.1.3.1	Développement asymptotique de la solution du problème de Stokes . . . . .	32
II.1.3.2	Gradient topologique de la fonctionnelle de Kohn-Vogelius . . . . .	34
II.1.4	Simulations numériques . . . . .	35
II.2	Une paramétrisation par des courbes de Bézier . . . . .	35
II.2.1	Une façon de modifier la topologie du domaine . . . . .	36
II.2.1.1	Rappels généraux sur les courbes de Bézier par morceaux . . . . .	36
II.2.1.2	Détection d'intersections des polygones de contrôle et procédure de flip . . . . .	38
II.2.2	Application à la détection d'obstacle . . . . .	38
II.3	Perspectives . . . . .	41
<b>III</b>	<b>Le problème inverse d'obstacle sur de nouveaux modèles pour l'équation de Laplace</b>	<b>45</b>
III.1	Prise en compte de données de Cauchy partielles : un problème de complétion de données	46
III.1.1	Analyse du problème de complétion de données et reconstruction numérique d'une inclusion . . . . .	48
III.1.1.1	Le problème de complétion de données . . . . .	48
III.1.1.2	Le problème inverse d'obstacle avec des données de Cauchy partielles . . . . .	52
III.1.2	Mise en place de la méthode de l'essai . . . . .	54
III.1.2.1	Le problème de complétion de données : une méthode de Newton . . . . .	55
III.1.2.2	Le problème inverse d'obstacle : la méthode de l'essai . . . . .	59
III.1.3	Perspectives . . . . .	60
III.2	Avec des conditions d'impédance généralisées de type Wentzell . . . . .	61
III.2.1	Le problème inverse d'obstacle avec des conditions de Wentzell . . . . .	61
III.2.2	Les résultats principaux et les reconstructions numériques . . . . .	62
III.2.2.1	Un résultat d'identifiabilité dans un anneau . . . . .	62
III.2.2.2	Calcul de forme . . . . .	63
III.2.3	Conclusion . . . . .	65
<b>IV</b>	<b>Modélisation mathématique : prise en compte de couches minces</b>	<b>67</b>
IV.1	Conditions d'impédance généralisée pour l'Imagerie par Résonance Magnétique (IRM) de diffusion . . . . .	68
IV.1.1	Modélisation du signal de l'IRM de diffusion par l'équation de Bloch-Torrey . . . . .	69
IV.1.1.1	Compartiments géométriques . . . . .	70
IV.1.1.2	Modèle asymptotique classique pour une diffusion isotropique dans la couche . . . . .	71
IV.1.2	Obtention formelle des conditions de transmission . . . . .	71
IV.1.2.1	Expression des opérateurs différentiels en coordonnées curvilignes . . . . .	71
IV.1.2.2	Mise à l'échelle et développement asymptotique formel . . . . .	72
IV.1.2.3	Une première famille de conditions . . . . .	73
IV.1.2.4	Une seconde famille de conditions . . . . .	74
IV.1.3	Validation numérique . . . . .	76

IV.2	Conditions d'impédance généralisée et forme optimale pour l'élasticité linéaire . . . . .	77
IV.2.1	Le problème étudié . . . . .	77
IV.2.1.1	Introduction et notations . . . . .	77
IV.2.1.2	Introduction du problème de transmission et du problème avec GIBC . . . . .	79
IV.2.2	Résultats principaux . . . . .	80
IV.2.2.1	Brève description de l'analyse asymptotique . . . . .	80
IV.2.2.2	Analyse de sensibilité par rapport à la forme et minimisation de la compliance . . . . .	82
IV.2.3	Simulations numériques pour un cantilever en 2D . . . . .	83
IV.3	Perspectives . . . . .	84
<b>V</b>	<b>Analyse de sensibilité pour des problèmes de contact</b>	<b>87</b>
V.1	Notations et rappels d'analyse convexe . . . . .	88
V.2	L'opérateur $f$ -proximal . . . . .	90
V.2.1	Introduction de l'opérateur $f$ -proximal et résultat principal . . . . .	90
V.2.2	Relation avec l'opérateur de Douglas-Rachford . . . . .	92
V.3	Conclusion . . . . .	93
V.3.1	Application à l'analyse de sensibilité . . . . .	93
V.3.2	Perspectives . . . . .	94
<b>VI</b>	<b>Répartition optimale de ressources en dynamique des populations</b>	<b>97</b>
VI.1	Le modèle biologique et l'état de l'art . . . . .	97
VI.1.1	Le modèle biologique . . . . .	97
VI.1.2	Un problème de valeur propre principale avec un poids indéfini . . . . .	99
VI.1.3	État de l'art . . . . .	100
VI.2	Modélisation du problème de design optimal et résultats principaux . . . . .	101
VI.2.1	Modélisation . . . . .	101
VI.2.2	Résolution du problème de design optimal . . . . .	102
VI.2.3	Propriétés qualitatives et commentaires . . . . .	104
VI.3	Perspectives . . . . .	105
	<b>Références bibliographiques</b>	<b>107</b>

## Table des matières

---

---

# Préambule

Ce manuscrit contient le résumé d'une partie de mes activités de recherche depuis mon arrivée à l'Institut de Mathématiques de Toulouse (IMT) de l'université Toulouse III - Paul Sabatier, en 2013. En particulier les articles issus de ma thèse de doctorat ((*xii*) à (*xvi*) ci-dessous) ne sont pas présentés dans ce mémoire; je ferai néanmoins référence à certains résultats qu'ils contiennent dans le corps du texte. La suite du présent document sera rédigée en langue anglaise.

Ce manuscrit vise à présenter succinctement les résultats et les idées principales contenus dans les articles (*i*) à (*xi*) ci-dessous. Plus précisément, le chapitre I concerne les études de stabilité en mécanique des fluides (*viii*) et (*xi*); le chapitre II expose les nouvelles approches pour la détection d'inclusions en 2D développées dans (*vii*) et (*ix*); le chapitre III étudie le problème inverse d'obstacle couplé avec une reconstruction de données, analysé dans (*i*) et (*iv*), ou lorsque l'obstacle possède une couche mince, détaillé dans (*x*); le chapitre IV se concentre sur les travaux (*ii*) et (*vi*) concernant la construction et l'analyse de conditions d'impédance généralisée pour des problèmes issus de la médecine et de la mécanique du solide; le chapitre V présente les premiers résultats démontrés dans (*iii*) d'un projet en cours concernant l'étude de sensibilité pour des problèmes de contact; le chapitre VI synthétise l'article (*v*) sur la répartition optimale de ressources dans un contexte de dynamique des populations.

Les articles (*iv*) et (*ix*) ont été réalisés dans le cadre de la thèse de Matías Godoy que j'ai co-encadrée avec Carlos Conca de l'université du Chili entre 2013 et 2016.

## Prépublications

- (*i*) F. Caubet, M. Dambrine et H. Harbrecht. A new method for the data completion problem and application to obstacle detection. *Soumis*.

## Publications dans des revues internationales à comité de lecture

- (*ii*) F. Caubet, D. Kateb et F. Le Louër. Shape sensitivity analysis for elastic structures with generalized impedance boundary conditions of the Wentzell type – Application to minimization of the compliance. *J. of Elasticity*, à paraître, 2018.
- (*iii*) S. Adly, L. Bourdin et F. Caubet. On a decomposition formula for the proximal operator of the sum of two convex functions. *J. of Convex Anal.*, à paraître, 2018.

- (iv) F. Caubet, J. Dardé et M. Godoy. On the data completion problem and the inverse obstacle problem with partial Cauchy data for Laplace's equation. *ESAIM Control Optim. Calc. Var.*, à paraître, 2017.
- (v) F. Caubet, T. Deheuvels et Y. Privat. Optimal location of resources for biased movement of species: the 1D case. *SIAM J. Appl. Math.*, 77(6):1876–1903, 2017.
- (vi) F. Caubet, H. Haddar, J.-R. Li et D. V. Nguyen. New transmission condition accounting for diffusion anisotropy in thin layers applied to diffusion MRI. *ESAIM Math. Model. Numer. Anal.*, 51(4):1279–1301, 2017.
- (vii) P. Bonnelie, L. Bourdin, F. Caubet et O. Ruatta. Flip procedure in geometric approximation of multiple-component shapes – application to multiple-inclusion detection. *SMAI J. Comput. Math.*, 2:255–276, 2016.
- (viii) M. Badra, F. Caubet et J. Dardé. Stability estimates for Navier-Stokes equations and application to inverse problems. *Discrete Contin. Dyn. Syst. Ser. B*, 21(8):2379–2407, 2016.
- (ix) F. Caubet, C. Conca et M. Godoy. On the detection of several obstacles in 2D Stokes flow: topological sensitivity and combination with shape derivatives. *Inverse Probl. Imaging*, 10(2):327–367, 2016.
- (x) F. Caubet, M. Dambrine et D. Kateb. Shape optimization methods for the inverse obstacle problem with generalized impedance boundary conditions. *Inverse Problems*, 29(11):115011, 26, 2013.
- (xi) F. Caubet et M. Dambrine. Stability of critical shapes for the drag minimization problem in Stokes flow. *J. Math. Pures Appl. (9)*, 100(3):327–346, 2013.
- (xii) F. Caubet. Instability of an Inverse Problem for the Stationary Navier-Stokes Equations. *SIAM J. Control Optim.*, 51(4):2949–2975, 2013.
- (xiii) F. Caubet, M. Dambrine, D. Kateb et C. Z. Timimoun. A Kohn-Vogelius formulation to detect an obstacle immersed in a fluid. *Inverse Probl. Imaging*, 7(1):123–157, 2013.
- (xiv) F. Caubet et M. Dambrine. Localization of small obstacles in Stokes flow. *Inverse Problems*, 28(10):105007, 31, 2012.
- (xv) M. Badra, F. Caubet et M. Dambrine. Detecting an obstacle immersed in a fluid by shape optimization methods. *Math. Models Methods Appl. Sci.*, 21(10):2069–2101, 2011.

## Actes de conférences

- (xvi) F. Caubet. Detecting an obstacle immersed in a fluid (the Stokes case). *Eleventh Intern. Conf. Zaragoza-Pau on Applied Math. and Stat.*, vol. 37 of Monogr. Mat. García Galdeano, p. 91–101, 2012.

---

# General introduction

This manuscript deals with two main mathematical areas: **shape optimization** and **inverse problems**. It presents a summary of my contributions about these themes on some **partial differential equations** (PDE) and underlines the fields of possible applications of the results.

This work was motivated by the following main questions:

- *how to **justify theoretically the efficiency of a numerical method** or the need of regularization to solve a problem?*
- *how to **solve numerically the inverse obstacle problem** according to the physical context?*
- *how to **model mathematically a shape optimization problem** in several fields of applications?*

This introduction aims at exploring the main ideas and at giving an overview of the main topics which will be treated in this manuscript. Each part and each notion is detailed hereafter in the corresponding chapter.

## (In)stability for problems arising in fluid mechanics

In order to **study the efficiency of a numerical method**, for a (shape) optimization problem or for an inverse problem such as the well-known Cauchy problem, it is mandatory to understand the (in)stability of the considered problem.

Indeed this preliminary theoretical study enables to build a suitable algorithm in order to numerically solve a problem. For instance, in finite dimension, it is well-known that one can easily find the minimum of a smooth functional such that the Hessian is positive-definite. Conversely some *regularization methods* are needed in order to solve a linear problem of the form  $Au = b$ , where  $A$  is a matrix of size  $d \times d$  and  $b$  a vector of  $\mathbb{R}^d$ , if the matrix  $A$  is ill-conditioned. In an infinite dimension context, technical tools are used in order to study the (in)stability of a problem even if one can expect the same kind of results.

Keeping this in mind, we use a second order shape sensitivity analysis in order to prove the **stability of the drag minimization problem** for the *Stokes equations*. Here stability means that a critical shape is, under some conditions, a local strict minimum. The main difficulty is to overcome the so-called *two norms discrepancy problem*: the coercivity norm is weaker than the differentiability norm. To do this we study precisely the second order shape derivative of the energy functional: we first compute the shape Hessian using the so-called Hadamard's formula, then we prove its coerciveness and finally we obtain the stability of the minimization problem by constructing appropriate modulus of continuity and perturbation fields, see Theorem I.1.6.

In an inverse problem context, we prove the **instability of the Cauchy problem** for the *Stokes and Navier-Stokes equations*. Using new *Carleman inequalities*, we obtain a log type estimate which quantifies the well-known associated unique continuation result. Especially, for boundary observations, we obtain new stability estimates which only depend on the data, that is on the Cauchy pair (Dirichlet and Neumann boundary conditions), see Theorem I.2.4. Then we apply it to obtain a stability inequality for the identification of Robin parameter and to obtain the rate of convergence of some numerical methods of reconstruction of the solution of the Stokes equations from partial boundary measurements.

These two theoretical analyses of stability are detailed in Chapter I which summarizes my articles [33, 86].

## The inverse obstacle problem: new approaches and new models

Inverse problems arise in many application fields such as medical issues as well as other imaging problems, location of immersed objects, finding cracks within materials, identification in growth processes, etc. A well-known inverse problem is the so-called **inverse obstacle problem** which consists in recovering an unknown inclusion in a known domain from boundary measurements. As most of the inverse problems, this problem is known to be unstable and some regularization methods are needed to numerically solve it.

Several methods exist in order to reconstruct the inclusions. Among these methods, the shape optimization approach is an efficient way to consider such a problem. A difficulty is to reconstruct at the same time the number of obstacles, their locations and their shapes. Indeed, for instance, a classical geometrical shape optimization approach enables to detect the shape if the number of inclusions is known while a topological shape optimization approach is efficient to find the number of obstacles but is often not accurate to reconstruct the shapes.

The existing literature contains several methods in order to overcome this difficulty, with its advantages and its drawbacks for each of them, depending on the context. We have explored two methods in order to deal with this problem of **finding both the number of obstacles and their shapes**, in the two-dimensional case. The first one is a *blending method* which couples the topological gradient and the shape gradient. Even if the main objective is to obtain an efficient numerical reconstruction of the unknown obstacle(s), this approach needs a technical theoretical part. Indeed one difficulty is to rigorously obtain the expression of the topological gradient of the considered functional (see Theorem II.1.3), considering the two dimensional *Stokes equations* and taking into account the *Stokes paradox*. The second one uses a *Bézier parametrization* of the inclusion and a procedure in order to modify the topology of the domain in a geometrical shape optimization algorithm. The key point is the representation of the boundary using the control polygons which seems to be well-suited in order to numerically deal with this problem. We performed this method in the classical *Laplace's equation* (see Figure II.2.10). These two methods are described in Chapter II which corresponds to my papers [56, 84].

Beyond the methods of resolution of the inverse obstacle problem, an important issue concerns the model inspired by the physical context. If the computation of the solution obviously depends on the considered PDE, the techniques strongly depend on the data, especially on the domain of measurements, or on the characteristics of the inclusions as, e.g., if the obstacle has a membrane or some defects.

Considering the context of *electrical impedance tomography*, we aim at studying these two problems. Firstly, assuming that the measurements are done only on a part of the exterior boundary, that is in the case of **partial Cauchy data** (which is physically relevant), we study the so-called **data completion problem** in order to solve the initial inverse obstacle problem. Indeed, to implement a shape optimization algorithm, we complete first the data in order to obtain a well-posed (shape)

functional. Thus, after obtaining several theoretical results concerning the data completion problem, we implement two numerical methods in order to numerically solve the inverse obstacle problem coupled with the problem of recovering the data on an inaccessible part of the boundary: the first one is a classical gradient method recovering both the data and the inclusion (see Figure III.1.4), the second one uses an efficient Newton approach combined with a trial method (see Figure III.1.6). Secondly, if the inclusion has a thin layer, such as a rough boundary, one can model it using some **nonclassical boundary conditions**. Precisely, in the context of *Laplace's equation*, we consider the so-called **Wentzell boundary conditions on the obstacle**. Since these second order conditions are imposed on the unknown boundary, we differentiate them with respect to the shape in order to implement a shape optimization algorithm. The proof of the existence and the computation of the shape derivative contain theoretical difficulties in this context, see Propositions III.2.2 and III.2.3. Then we solve the inverse obstacle problem using a classical gradient method for instance. These two studies are explained in Chapter III which exposes my works [87, 88, 90].

## Mathematical modeling: asymptotic expansions, contact problems and population dynamics

Shape optimization can be used in several topics, for several contexts of applications such as in medicine, in fluid mechanics, in solid mechanics, in biology, etc. One challenge, before solving a concrete problem, is to find a *good model*, in the sense that **the considered model has to be realistic but also mathematically tractable**. The following problems are linked with shape optimization tools, even if it is not always in the classical sense.

As mentioned above, an interesting case is to deal with domains with a thin layer, such as a membrane of a cell or a corroded object. It is interesting to obtain a model without this thin layer but which takes it into account, especially for a numerical point of view, in order not to have to finely mesh the thin layer. If the Wentzell boundary conditions are well-known concerning Laplace's equation, the derivation of some *Generalized Impedance Boundary Conditions* (GIBC) for others PDE is still a mathematical challenge.

We focus on the derivations of GIBC in two contexts. Firstly, in a medicine context, we consider the so-called *Bloch-Torrey equation*, used to deal with the diffusion Magnetic Resonance Imaging (dMRI). Hence, in order to take into account the anisotropic behavior of the exchanges in the membrane of a human cell, we use an **asymptotic expansion with two scales of diffusion in the membrane**. However the formal derivation of boundary conditions leads to some unstable results: then we correct the conditions in order to obtain a coherent model, see Equations (IV.1.16). Secondly, we focus on the *linear elasticity model* and on the optimal design problem of **finding the structure that minimizes the compliance**, taking into account that (a part of) this structure is corroded. Then, using an asymptotic expansion, we obtain GIBC that we then differentiate with respect to the shape in order to implement a shape optimization algorithm that minimizes the cost functional, see Theorem IV.2.4. These two asymptotic analyses and the computation of the shape gradient of the compliance in the context of GIBC of order two are treated in Chapter IV which presents my articles [92, 93].

Concerning the solid mechanics applications, an important emerging field, especially in a shape optimization point of view, is the contact problems. Several models can be considered in order to characterize the contact between two solids that touch each other. Particularly one can take into account some friction effects that can be modeled by the so-called *Tresca's conditions*.

With the perspective to study the (shape) sensitivity of the Tresca problem, we use the variational inequalities theory. Indeed this sensitivity analysis goes through the study of *parametrized variational inequalities of the second kind*. Especially we can express the corresponding solution as the proximal operator of the sum of two proper, lower semicontinuous and convex functions. Hence, in order to differentiate this solution with respect to the parameter, we introduce and study a new operator, which

is an extension of the classical proximal operator. It enables particularly to obtain a **decomposition formula of the proximal operator of the sum of two functions**, see Theorem V.2.6. This first step in the shape sensitivity analysis is exposed in Chapter V which synthesizes my paper [6].

Finally we focus on a biological problem, arising in population dynamics. The question is to study the equilibrium state of a *diffusive-logistic equation* with Robin boundary conditions. The main concern is to find an optimal location of resources in order to maximize the survival ability of a species.

Chapter VI gives an abstract of my work [91]: it deals with the modeling and the resolution of this problem, in the one dimensional case. This optimal design problem is modeled with the help of an extremal indefinite weight linear eigenvalue problem and the aim is to **minimize the positive principal eigenvalue with respect to the weight**, under constraints motivated by some biological issues. Due to the Robin boundary conditions and to the drift term, we use appropriate unimodal rearrangements in order to solve this problem by computing the optimality conditions. We then obtain the optimal configurations which depend on the value of the Robin coefficient, see Theorem VI.2.6.

---

# Notations

## General notations

$d$	:	natural number, dimension of the space of work ( $d = 2, 3$ )
$\mathbf{I}$	:	identity matrix of size $d \times d$
$\mathbf{1}$	:=	${}^t(1, \dots, 1)$ , unit vector of size $d$
supp	:	support of a function
$\Omega$	:	non-empty bounded connected smooth open set of $\mathbb{R}^d$
$\omega$	:	non-empty bounded smooth open set strictly included in $\Omega$
$\partial\Omega, \partial\omega$	:	boundary of $\Omega$ , boundary of $\omega$
$ \Omega ,  \omega $	:=	$\mathcal{L}^d(\Omega), \mathcal{L}^d(\omega)$ , the Lebesgue measure of $\Omega$ and of $\omega$ ( <i>volume of <math>\Omega</math> and <math>\omega</math></i> )
$\mathbf{n}$	:	exterior unit normal of the considered domain
$\partial_n u$	:	normal derivative of a function $u$

## Functional spaces

$\mathcal{C}^k$	:	space of functions with $k$ continuous derivatives
$L^p$	:	classical Lebesgue space
$W^{m,p}$	:	classical Sobolev space
$H^m$	:=	$W^{m,2}$
$\mathcal{C}^k, \mathbf{L}^p$ , etc.	:	vectorial functions spaces
$L_0^2(\Omega)$	:=	$\{p \in L^2(\Omega); \int_{\Omega} p = 0\}$
$ \cdot _{H^m(\Omega)}$	:	semi-norm $H^m(\Omega)$

## Fluid mechanics: Stokes and Navier-Stokes equations

$\nu$	:	non-negative constant which represents the kinematic viscosity of the fluid
$(\mathbf{u}, p)$	:	couple velocity/pressure, solution of the considered PDE (Stokes, Navier-Stokes)
$\mathcal{D}(\mathbf{u})$	:=	$\frac{1}{2}(\nabla \mathbf{u} + {}^t \nabla \mathbf{u})$ , symmetrized gradient of $\mathbf{u}$
$\sigma(\mathbf{u}, p)$	:=	$\nu(\nabla \mathbf{u} + {}^t \nabla \mathbf{u}) - p\mathbf{I}$ , stress tensor
$(E, \mathbf{P})$	:	fundamental solution of the Stokes system in $\mathbb{R}^2$

## Notations

---

### Solid mechanics: linear elasticity equations

$\mathbf{u}$	:	solution of the linear elasticity equations
$\mathcal{D}(\mathbf{u})$	:=	$\frac{1}{2}(\nabla\mathbf{u} + {}^t\nabla\mathbf{u})$ , symmetrized gradient of $\mathbf{u}$
$\mu_e, \lambda_e$	:	non-negative constants, the Lamé coefficients of the given material
$A_e$	:	elasticity tensor defined for any symmetric matrix $\xi$ by $A_e \xi := 2\mu_e \xi + \lambda_e \text{Tr}(\xi) \mathbf{I}$
$\mathbf{T}_e(\mathbf{u})$	:=	$A_e \mathcal{D}(\mathbf{u}) \mathbf{n}$ , stress tensor

### Shape optimization, functionals, differential operators

$d_0$	:	non-negative real number
$\Omega_{d_0}$	:	smooth open set such that $\{x \in \Omega; d(x, \partial\Omega) > \frac{d_0}{2}\} \subset \Omega_{d_0} \subset \{x \in \Omega; d(x, \partial\Omega) > \frac{d_0}{3}\}$
$\mathcal{O}$	:	set of admissible shapes
$\mathcal{U}$	:	set of admissible perturbations (supported in $\Omega_{d_0}$ )
$J$	:	energy functional (drag, compliance)
$\mathcal{J}$	:	least squares functional
$\mathcal{K}$	:	Kohn-Vogelius functional
$H$	:	mean curvature of a domain
$b$	:	signed distance to a boundary of a domain
$\nabla_\tau, \text{div}_\tau, \Delta_\tau$	:	classical tangential differential operators

### Inverse problems, asymptotic analysis, convex analysis

$\Gamma_{\text{obs}}$	:	non-empty open subset of $\partial\Omega$ ( <i>domain of observations or of measurements</i> )
$\Gamma_{\text{ina}}$	:	open subset of $\partial\Omega$ such that $\partial\Omega = \overline{\Gamma_{\text{obs}}} \cup \overline{\Gamma_{\text{ina}}}$ ( <i>inaccessible domain</i> )
$(g_N, g_D)$	:	Cauchy data on $\Gamma_{\text{obs}}$
$\varepsilon$	:	positif real number, regularization parameter
$\eta$	:	positif real number, thickness of the considered thin layer
$[\cdot]$	:	jump relative to the direction $\mathbf{n}$ through an interface
$\langle \cdot \rangle$	:	average through an interface
$H$	:	a general Hilbert space
$\Gamma_0(H)$	:=	$\{f : H \rightarrow \mathbb{R} \cup \{+\infty\}, \text{ proper, lower semi-continuous and convex}\}$
$\text{prox}_f$	:=	$(\mathbf{I} + \partial f)^{-1}$ , proximal operator of $f \in \Gamma_0(H)$
$\text{Fix}(A)$	:=	$\{x \in H; x \in A(x)\}$ , set of fixed points of a set-valued map $A : H \rightrightarrows H$

---

---

# Chapter I

---

## Studies of stability in fluid mechanics

This chapter focuses on the notion of *stability* of a problem and summarizes the two following articles:

- [86] F. Caubet and M. Dambrine. Stability of critical shapes for the drag minimization problem in Stokes flow. *J. Math. Pures Appl. (9)*, 100(3):327–346, 2013;
- [33] M. Badra, F. Caubet and J. Dardé. Stability estimates for Navier-Stokes equations and application to inverse problems. *Discrete Contin. Dyn. Syst. Ser. B*, 21(8):2379–2407, 2016.

The notion of stability is very important since it enables especially to characterize the efficiency of a numerical method in order to solve a problem. It is well-known that one can expect to obtain an efficient reconstruction of the solution of a *stable problem* whereas a regularization method should be used in order to numerically solve an *unstable problem*.

In an optimization problem, the study of the stability consists in knowing if a critical point of a functional is a local strict minimizer. This is particularly crucial in order to make numerical simulations: as already mentioned, if the problem is *unstable*, regularization is required in the numerical minimization of the functional (see, e.g., the book of Engl *et al.* [125] or the articles [8, 89, 100]). Usually, the question of stability is dealt with the second order derivative of the functional at a critical point. In finite dimension, the knowledge of the sign of the Hessian enables to fully answer the question of stability using Taylor-Young expansion. However, in shape optimization or in infinite dimension, the *two norms discrepancy problem* can occur: the coercivity norm is often weaker than the differentiability norm. Let us refer to the paper [117] by Descloux for a concrete example of such a situation known as the magnetic shaping problem: on this example, the coercivity at a critical point holds in the  $H^{1/2}$  norm while the differentiability holds in  $C^2$  topology. Since the quantity  $o(\|\cdot\|_{C^2}^2)$  is not smaller than  $C \|\cdot\|_{H^{1/2}}^2$ , the classical argument using the Taylor-Young formula does not insure that this critical point is a local strict minimum. A method to overcome this problem is given by Dambrine *et al.* in [107, 111] in the case of Poisson's equation and of a strictly and uniformly elliptic operator for a shape optimization problem. The key is a precise estimate of the variations of the second order shape derivative of the functional with respect to the coercivity and differentiability norms around a critical shape.

In an other context, the inverse problems are well-known to be usually *ill-posed* in the sense that the solution does not depend continuously on the data, that is especially on the *measurements*. However, using Carleman estimates, one can obtain *stability estimates* which are usually of log type (or log-log type in the case of the inverse obstacle problem, see for instance the work of Ballerini [35]). These estimates firstly characterize the ill-posedness (showing that the inverse problem is typically exponentially ill-posed) and secondly enable to obtain several properties such as the uniqueness of the solution, some stability inequalities for the problem of recovering some boundary coefficients or the rate of convergence of some reconstructions methods. One challenge in the obtention of such estimates is to fit with a unique continuation result which implies, roughly speaking, that if some specified

measurements are null (such as some Cauchy data), then the solution is equal to zero. For instance, in a fluid mechanics context, Fabre and Lebeau prove in [127] that under some *observations* (that we specified below) the uniqueness of the solution of the Navier-Stokes system occurs. Nevertheless a previous recent stability result (see [60, Theorem 1.4] by Boulakia *et al.*) does not depend exclusively on the needed observations and then does not fit the Fabre and Lebeau's Theorem, as underlined by the authors themselves.

*The aim of this chapter is to prove the stability of a shape optimization problem (see Section I.1) and the instability of an inverse problem (see Section I.2), for vectorial problems in the context of fluid mechanics.* Section I.1 aims at presenting the extension of the results of Dambrine *et al.* [107, 111] for the Stokes system: we obtain the stability of the drag minimization problem dealing with the two norms discrepancy problem explained above. Section I.2 presents an improvement of the results of Boulakia *et al.* [60]: establishing new Carleman estimates, we obtain new stability inequalities characterizing Fabre and Lebeau's unique continuation result and we present some applications of such a result.

## I.1 Stability of optimal shapes

This section is devoted to the study of the stability of critical shapes for the *drag minimization problem* in Stokes flow. This work was done in collaboration with Marc Dambrine (university of Pau) and is published in *Journal de Mathématiques Pures et Appliquées* (see [86], 20 pages).

### I.1.1 A stability result for drag minimization

In fluid mechanics, the study of the minimization of the drag of a body in a fluid (i.e. the computation of optimal profiles) is a very popular problem. A typical application is the study of the geometry of blunt bodies in flow at low Reynolds numbers (see, e.g., [198]). In this study, the parameter is the shape of the body immersed in the fluid and we are interested in studying the stability of this shape optimization problem. The used strategy is the following.

A first step is to prove the existence of second order shape derivatives. It is classically obtained through an implicit function theorem: this is due to Simon [206] for Stokes equations and to Bello *et al.* [42, 43] for the Navier-Stokes equations.

In a second step we obtain the Euler-Lagrange equation, then we compute the shape Hessian. These shape derivatives of the drag (at least at the first order) was computed by some authors (see for instance [206] for the Stokes equations and [41, 43] for the Navier-Stokes equations). However, in this work, we need a different expression of the shape Hessian. Then we use the Euler-Lagrange equations and some computations to derive a sufficient condition of positivity of the shape Hessian computed at a critical shape.

In a third step, we prove the stability of the minimization. As mentioned above, the two norms discrepancy problem occurs: the coercivity norm  $\mathbf{H}^{1/2}$  is weaker than the differentiability norm  $\mathcal{C}^{2,1}$ . Following the previous works of Dambrine *et al.* in [107, 111], we obtain the main result of this work which is a stability result for the drag minimization problem: it claims that a critical shape can be a local strict minimum if a given criterion is satisfied.

Finally, in a fourth and last step, we derive a precise version of the minimality inequality: we provide a lower bound of the variations of the drag in term of a geometrical quantity following some ideas introduced by Fusco *et al.* [3, 137].

I.1.1.1 The considered problem

**The drag functional.** Let  $\Omega$  be a bounded and connected open subset of  $\mathbb{R}^d$  (with  $d = 2$  or  $d = 3$ ) containing a Newtonian and incompressible fluid with a constant coefficient of kinematic viscosity  $\nu > 0$ . We assume that  $\Omega$  is smooth (at least with a  $\mathcal{C}^{2,1}$  boundary). Let  $d_0 > 0$  fixed (large). We define the set of admissible shapes by

$$\mathcal{O} := \left\{ \omega \subset \Omega \text{ open set with a } \mathcal{C}^{2,1} \text{ boundary such that } d(x, \partial\Omega) > d_0, \forall \mathbf{x} \in \omega \right. \\ \left. \text{and such that } \Omega \setminus \bar{\omega} \text{ is connected} \right\}$$

and we consider  $\omega \in \mathcal{O}$ .

Let us consider  $\mathbf{g} \in \mathcal{C}^{2,\alpha}(\partial\Omega)$ , with  $\alpha \in (0, 1)$ , satisfying the compatibility condition  $\int_{\partial\Omega} \mathbf{g} \cdot \mathbf{n} = 0$  and the unique solution  $(\mathbf{u}, p) \in \mathcal{C}^{2,\alpha}(\overline{\Omega \setminus \bar{\omega}}) \times \left[ \mathcal{C}^{1,\alpha}(\overline{\Omega \setminus \bar{\omega}}) \cap L_0^2(\Omega \setminus \bar{\omega}) \right]$  of

$$\begin{cases} -\nu \Delta \mathbf{u} + \nabla p = \mathbf{0} & \text{in } \Omega \setminus \bar{\omega}, \\ \operatorname{div} \mathbf{u} = 0 & \text{in } \Omega \setminus \bar{\omega}, \\ \mathbf{u} = \mathbf{g} & \text{on } \partial\Omega, \\ \mathbf{u} = \mathbf{0} & \text{on } \partial\omega. \end{cases} \quad (\text{I.1.1})$$

The existence and uniqueness of the solution of such a problem is classical (see, e.g., the book of Galdi [138, Theorems IV.7.1 and IV.7.2]). The energy dissipated by the fluid is given by

$$J(\omega) := \frac{1}{2} \int_{\Omega \setminus \bar{\omega}} \nu |\mathcal{D}(\mathbf{u})|^2,$$

where  $\mathcal{D}(\mathbf{u}) := \frac{1}{2} (\nabla \mathbf{u} + {}^t \nabla \mathbf{u})$ . The drag minimization problem is to minimize  $J$  over all subdomains  $\omega$  of  $\Omega$  with a given measure  $M > 0$ :

$$\omega^* := \operatorname{argmin} \{ J(\omega); \omega \in \mathcal{O} \text{ such that } |\omega| = M \}.$$

We also define the *stress tensor* as  $\sigma(\mathbf{u}, p) := \nu (\nabla \mathbf{u} + {}^t \nabla \mathbf{u}) - p \mathbf{I}$ .

**Admissible deformations.** Let us define some admissible deformations of the domain  $\omega \in \mathcal{O}$  we use in this work. Since we want to perturb only  $\omega$  (and not  $\Omega$  which is fixed), we define  $\Omega_{d_0}$  an open set with a  $\mathcal{C}^\infty$  boundary and such that

$$\{ \mathbf{x} \in \Omega; d(\mathbf{x}, \partial\Omega) > d_0/2 \} \subset \Omega_{d_0} \subset \{ \mathbf{x} \in \Omega; d(\mathbf{x}, \partial\Omega) > d_0/3 \}.$$

We then consider a diffeomorphism

$$\Theta \in \mathfrak{U} := \{ \boldsymbol{\theta} \in \mathcal{C}^{2,1}(\mathbb{R}^d); \boldsymbol{\theta} \equiv \mathbf{I} \text{ in } \mathbb{R}^d \setminus \Omega_{d_0} \}.$$

The principle of Hadamard's approach is to consider here the flow  $\Phi_{\Theta,t}$  of an adequate autonomous vector field

$$\mathbf{V}_\Theta \in \mathfrak{U} := \{ \mathbf{V} \in \mathcal{C}^{2,1}(\mathbb{R}^d); \operatorname{supp}(\mathbf{V}) \subset \overline{\Omega_{d_0}} \},$$

i.e. the solution of

$$\begin{cases} \partial_t \Phi = \mathbf{V}_\Theta(\Phi), \\ \Phi(0, \mathbf{x}) = \mathbf{x}, \end{cases}$$

such that  $\mathbf{V}_\Theta$  is a (normal) vector field defining a path  $t \in [0, 1] \mapsto \omega_t := \Phi_{\Theta,t}(\omega)$  in  $\Omega_{d_0}$  within domains connecting  $\omega_0 = \omega$  and  $\omega_1 = \Theta(\omega)$ . This enables especially to classically characterize the shape derivative of  $(\mathbf{u}, p)$  and to compute the shape derivatives of  $J$  in a perturbation direction  $\mathbf{V}_\Theta$  using the Hadamard's formula (see, e.g., [152, Theorem 5.2.2]). In the following we will use the notation  $\mathbf{V}$  instead of  $\mathbf{V}_\Theta$ .

### I.1.1.2 Coercivity of the shape Hessian

We assume the existence of a critical shape  $\omega^* \in \mathcal{O}$  with a  $\mathcal{C}^{4,\alpha}$  boundary. Let  $\mathbf{V} \in \mathcal{U}$  be a normal perturbation which is divergence free (in order to preserve the volume of  $\omega^*$ ). We recall that the existence of the second order shape derivatives is proved in some previous works (see for instance [32, 89, 206] for the Stokes case and [42, 83] for the Navier-Stokes case).

**Remark I.1.1.** *The fact that we have to impose a  $\mathcal{C}^{4,\alpha}$  regularity of the boundary of the initial shape (whereas we can work with shapes with a  $\mathcal{C}^{2,1}$  boundary in order to have the twice differentiability with respect to the domain) comes to the fact that we consider normal perturbations (so we loose one rank of regularity) which are divergence free (which imposes the lost of an additional derivative by construction): see [107, Section 2.1].*

Firstly, Simon proves in [206, Theorem 3] that

$$DJ(\omega^*) \cdot \mathbf{V} = -\frac{1}{2} \int_{\partial\omega^*} \nu |\partial_n \mathbf{u}|^2 (\mathbf{V} \cdot \mathbf{n}).$$

Since we work under the constraint of constant volume and since  $\omega^*$  is a critical point, there exists  $\Lambda_0 \in \mathbb{R}$  such that  $DJ(\omega^*) \cdot \mathbf{V} + \Lambda_0 D\mathcal{V}(\omega^*) \cdot \mathbf{V} = 0$  for any perturbation  $\mathbf{V}$  (where  $\mathcal{V}(\omega^*)$  is the volume of  $\omega^*$ ). Hence, for all  $\mathbf{V} \in \mathcal{U}$ ,

$$-\frac{1}{2} \int_{\partial\omega^*} \nu |\partial_n \mathbf{u}|^2 (\mathbf{V} \cdot \mathbf{n}) + \Lambda_0 \int_{\partial\omega^*} \mathbf{V} \cdot \mathbf{n} = 0,$$

and then we obtain the Euler-Lagrange equation satisfied at the critical shape: there exists  $\Lambda \in \mathbb{R}$  such that

$$|\partial_n \mathbf{u}|^2 = \frac{2}{\nu} \Lambda_0 =: \Lambda. \quad (\text{I.1.2})$$

Notice that this result is also proved in [206, Theorem 7] in a different way.

Secondly, using the classical shape calculus, we prove that

$$D^2J(\omega^*) \cdot \mathbf{V} \cdot \mathbf{V} = 2 \int_{\partial\omega^*} \mathbf{u}' \cdot (\sigma(\mathbf{u}', p') \mathbf{n}) - \frac{1}{2} \int_{\partial\omega^*} \nu \nabla(|\mathcal{D}(\mathbf{u})|^2) \cdot \mathbf{V} (\mathbf{V} \cdot \mathbf{n}), \quad (\text{I.1.3})$$

where the couple  $(\mathbf{u}, p) \in \mathcal{C}^{2,\alpha}(\overline{\Omega \setminus \omega^*}) \times [\mathcal{C}^{1,\alpha}(\overline{\Omega \setminus \omega^*}) \cap L_0^2(\Omega \setminus \omega^*)]$  solves (I.1.1) (with  $\omega = \omega^*$ ) and the couple  $(\mathbf{u}', p') \in \mathcal{C}^{2,\alpha}(\overline{\Omega \setminus \omega^*}) \times [\mathcal{C}^{1,\alpha}(\overline{\Omega \setminus \omega^*}) \cap L_0^2(\Omega \setminus \omega^*)]$  solves

$$\begin{cases} -\nu \Delta \mathbf{u}' + \nabla p' &= \mathbf{0} & \text{in } \Omega \setminus \overline{\omega^*}, \\ \operatorname{div} \mathbf{u}' &= 0 & \text{in } \Omega \setminus \overline{\omega^*}, \\ \mathbf{u}' &= \mathbf{0} & \text{on } \partial\Omega, \\ \mathbf{u}' &= -\partial_n \mathbf{u} (\mathbf{V} \cdot \mathbf{n}) & \text{on } \partial\omega^*. \end{cases} \quad (\text{I.1.4})$$

In order to prove the coerciveness of the shape Hessian, we claim the two following results.

**Lemma I.1.2.** *We consider  $\Omega$  and  $\omega$  two Lipschitz open sets of  $\mathbb{R}^d$  such that  $\omega \subset\subset \Omega$  and  $\Omega \setminus \overline{\omega}$  is connected. For  $\mathbf{h} \in \mathbf{H}^{1/2}(\partial\omega)$ , let us define the following Steklov-Poincaré operator:*

$$D_N : \begin{array}{l} \mathbf{H}^{1/2}(\partial\omega) \\ \mathbf{h} \end{array} \longrightarrow \begin{array}{l} \mathbf{H}^{-1/2}(\partial\omega) \\ \sigma(\mathbf{U}, P) \mathbf{n}, \end{array}$$

where  $(\mathbf{U}, P) \in \mathbf{H}^1(\Omega \setminus \overline{\omega}) \times L^2(\Omega \setminus \overline{\omega})$  solves

$$\begin{cases} -\operatorname{div}(\sigma(\mathbf{U}, P)) &= \mathbf{0} & \text{in } \Omega \setminus \overline{\omega}, \\ \operatorname{div} \mathbf{U} &= 0 & \text{in } \Omega \setminus \overline{\omega}, \\ \mathbf{U} &= \mathbf{0} & \text{on } \partial\Omega, \\ \mathbf{U} &= \mathbf{h} & \text{on } \partial\omega. \end{cases}$$

Then there exists a constant  $C$  depending on  $\Omega$  and  $\omega$  such that

$$\langle D_N(\mathbf{h}), \mathbf{h} \rangle_{\mathbf{H}^{-1/2}(\partial\omega), \mathbf{H}^{1/2}(\partial\omega)} \geq C \|\mathbf{h}\|_{\mathbf{H}^{1/2}(\partial\omega)}^2. \quad (\text{I.1.5})$$

**Lemma I.1.3.** *It holds*

$$\nu \nabla \left( |\mathcal{D}(\mathbf{u})|^2 \right) \cdot \mathbf{n} = 4 \left( \nu(d-1)\text{H}\Lambda + \nu^t \mathbf{b} \mathfrak{F} \mathbf{b} + \nabla_{\tau} p \cdot \mathbf{b} \right) \quad \text{on } \partial\omega^*, \quad (\text{I.1.6})$$

where  $\mathbf{b}$  is the projection of  $\partial_n \mathbf{u}$  on the tangential space of  $\partial\omega^*$  and  $\mathfrak{F}$  is the second fundamental form of the surface  $\partial\omega^*$ .

Then, considering Problem (I.1.4) solved by the shape derivative  $(\mathbf{u}', p')$  and noticing that, since  $\text{div } \mathbf{u}' = 0$ ,

$$-\nu \Delta \mathbf{u}' + \nabla p' = -\text{div}(\nu \mathcal{D}(\mathbf{u}')) + \nabla p' = -\text{div}(\sigma(\mathbf{u}', p')),$$

and that  $\mathbf{u}' = -\partial_n \mathbf{u}(\mathbf{V} \cdot \mathbf{n})$  on  $\partial\omega^*$ , we get

$$\int_{\partial\omega^*} \mathbf{u}' \cdot (\sigma(\mathbf{u}', p') \mathbf{n}) = \int_{\partial\omega^*} \partial_n \mathbf{u}(\mathbf{V} \cdot \mathbf{n}) D_N(\partial_n \mathbf{u}(\mathbf{V} \cdot \mathbf{n})).$$

Hence there exists a constant  $C > 0$  such that

$$2 \int_{\partial\omega^*} \mathbf{u}' \cdot (\sigma(\mathbf{u}', p') \mathbf{n}) \geq C \|\partial_n \mathbf{u}(\mathbf{V} \cdot \mathbf{n})\|_{\mathbf{H}^{1/2}(\partial\omega^*)}^2 = C \Lambda \|\mathbf{V} \cdot \mathbf{n}\|_{\mathbf{H}^{1/2}(\partial\omega^*)}^2. \quad (\text{I.1.7})$$

We used the coercivity of the operator  $D_N$  (given by (I.1.5) in Lemma I.1.2) and the Euler-Lagrange equation  $|\partial_n \mathbf{u}|^2 = \Lambda$  according to (I.1.2).

Finally, gathering (I.1.3), (I.1.7) and (I.1.6), we obtain

$$D^2 J(\omega^*) \cdot \mathbf{V} \cdot \mathbf{V} \geq C \Lambda \|\mathbf{V} \cdot \mathbf{n}\|_{\mathbf{H}^{1/2}(\partial\omega^*)}^2 - 2 \int_{\partial\omega^*} \left( \nu(d-1)\text{H}\Lambda + \nu^t \mathbf{b} \mathfrak{F} \mathbf{b} + \nabla_{\tau} p \cdot \mathbf{b} \right) (\mathbf{V} \cdot \mathbf{n})^2.$$

Hence, using the regularity of  $\partial\omega^*$  and of the solution  $\mathbf{u}$ , the quantity

$$\nu(d-1)\text{H}\Lambda + \nu^t \mathbf{b} \mathfrak{F} \mathbf{b} + \nabla_{\tau} p \cdot \mathbf{b}$$

belongs to  $L^\infty(\partial\omega^*)$  and the second term behaves like  $\|\mathbf{V} \cdot \mathbf{n}\|_{L^2(\partial\omega^*)}^2$ . Thus a natural assumption is that the shape Hessian is coercive in the  $\mathbf{H}^{1/2}(\partial\omega^*)$  sense. This is the case if

$$\nu(d-1)\text{H}\Lambda + \nu^t \mathbf{b} \mathfrak{F} \mathbf{b} + \nabla_{\tau} p \cdot \mathbf{b} < 0 \quad \text{on } \partial\omega^*. \quad (\text{I.1.8})$$

Note that this condition couples geometrical effect with the solution itself. In practice, the condition (I.1.8) cannot easily be tested theoretically since it couples the curvature of the object with derivatives of the flow. It might be tested numerically, however it will require a curved mesh for the surface and the fluid domain and high order elements to catch the desired effects of curvature and the derivatives of the couple  $(\mathbf{u}, p)$ . Such a precise computation requires specific numerical attention.

**Theorem I.1.4.** *Let us assume that Estimate (I.1.8) is satisfied. Then there exists a constant  $C > 0$  such that, for all  $\mathbf{V} \in \mathcal{U}$  with  $\text{div } \mathbf{V} = 0$ ,*

$$D^2 J(\omega^*) \cdot \mathbf{V} \cdot \mathbf{V} \geq C \|\mathbf{V} \cdot \mathbf{n}\|_{\mathbf{H}^{1/2}(\partial\omega^*)}^2.$$

### I.1.1.3 Stability of the drag minimization problem and accurate stability estimate

In this section, the shape Hessian is assumed to be coercive at  $\omega^*$  in the following sense: for any  $\mathbf{V}$  in the tangent space defined by the constraints that is with

$$\int_{\partial\omega^*} \mathbf{V} \cdot \mathbf{n} = 0,$$

it holds

$$D^2J(\omega^*) \cdot \mathbf{V} \cdot \mathbf{V} \geq C \|\mathbf{V} \cdot \mathbf{n}\|_{H^{1/2}(\partial\omega^*)}^2. \quad (\text{I.1.9})$$

The following main result of this section states the stability of the drag minimization problem.

**Theorem I.1.5.** *If  $\omega^*$  is a critical shape for  $J$  where (I.1.9) holds, there exists  $\eta > 0$  such that, for all  $\Theta \in \mathfrak{U}$  with  $\|\Theta - \mathbf{I}\|_{\mathcal{C}^{2,1}(\mathbb{R}^d)} < \eta$ ,  $|\Theta(\omega^*)| = |\omega^*|$  and  $\Theta \neq \mathbf{I}$ ,*

$$J(\Theta(\omega^*)) > J(\omega^*).$$

Let us define, for  $t \in [0, 1]$ ,

$$j(t) := J(\omega_t) := \frac{1}{2} \int_{\Omega \setminus \overline{\omega_t}} \nu |\mathcal{D}(\mathbf{u}_t)|^2,$$

where  $(\mathbf{u}_t, p_t) \in \mathcal{C}^{2,\alpha}(\overline{\Omega \setminus \overline{\omega_t}}) \times [\mathcal{C}^{1,\alpha}(\overline{\Omega \setminus \overline{\omega_t}}) \cap L_0^2(\Omega \setminus \overline{\omega_t})]$  is the solution of the following perturbed problem:

$$\begin{cases} -\nu \Delta \mathbf{u}_t + \nabla p_t = \mathbf{0} & \text{in } \Omega \setminus \overline{\omega_t}, \\ \operatorname{div} \mathbf{u}_t = 0 & \text{in } \Omega \setminus \overline{\omega_t}, \\ \mathbf{u}_t = \mathbf{g} & \text{on } \partial\Omega, \\ \mathbf{u}_t = \mathbf{0} & \text{on } \partial\omega_t. \end{cases}$$

with  $\omega_t := \Phi_{\Theta,t}(\omega)$ . Then, by the order two Taylor expansion

$$J(\omega) = j(1) = j(0) + \int_0^1 (1-s)j''(s)ds = J(\omega^*) + \int_0^1 (1-s)j''(s)ds,$$

Theorem I.1.5 is a direct consequence of the following theorem (and of the assumption of the  $H^{1/2}$  coercivity (I.1.9) of the shape Hessian). Notice that we have  $j''(0) = D^2J(\omega^*) \cdot \mathbf{V} \cdot \mathbf{V}$ .

**Theorem I.1.6.** *There exist  $\eta_0 > 0$  and a function  $w : (0, \eta_0) \rightarrow \mathbb{R}$  with  $\lim_{r \searrow 0} w(r) = 0$  (which depends only on  $\Omega$ ,  $\omega^*$  and the data) such that, for all  $\eta \in (0, \eta_0)$  and for all  $\Theta \in \mathfrak{U}$  with  $\|\Theta - \mathbf{I}\|_{\mathcal{C}^{2,1}(\mathbb{R}^d)} < \eta$  and  $|\Theta(\omega^*)| = |\omega^*|$ , there exists a divergence free vector field  $\mathbf{V} \in \mathfrak{U}$  whose the flow  $\Phi_t$  defines a path  $(\omega_t := \Phi_t(\omega^*))_{t \in [0,1]}$  between  $\omega^*$  and  $\Theta(\omega^*)$ , such that, for all  $t \in [0, 1]$ , the following estimate holds:*

$$|j''(t) - j''(0)| \leq w(\eta) \|\mathbf{V} \cdot \mathbf{n}\|_{H^{1/2}(\partial\omega^*)}^2.$$

Indeed we obtain Theorem I.1.5 by noticing that there is a non-negative  $\eta$  such that  $w(\eta) \leq C/2$ , so that

$$J(\omega) \geq J(\omega^*) + \frac{C}{4} \|\mathbf{V} \cdot \mathbf{n}\|_{H^{1/2}(\partial\omega^*)}^2 > J(\omega^*). \quad (\text{I.1.10})$$

Finally, in order to obtain a stability estimate, we use the following purely geometrical result which gives the existence of a constant  $C > 0$  (depending only on the domains) such that

$$|\Omega \Delta \Theta(\omega^*)| \leq C \|\mathbf{V} \cdot \mathbf{n}\|_{L^1(\partial\omega^*)},$$

for all  $\Theta \in \mathfrak{U}$  with  $\|\Theta - \mathbf{I}\|_{\mathcal{C}^{2,1}(\mathbb{R}^d)} < \eta$  and  $|\Theta(\omega^*)| = |\omega^*|$  and with  $\operatorname{div} \mathbf{V} = 0$ . Moreover, Cauchy-Schwarz inequality provides

$$\|\mathbf{V} \cdot \mathbf{n}\|_{L^1(\partial\omega^*)} \leq |\partial\omega^*|^{1/2} \|\mathbf{V} \cdot \mathbf{n}\|_{L^2(\partial\omega^*)} \leq |\partial\omega^*|^{1/2} \|\mathbf{V} \cdot \mathbf{n}\|_{H^{1/2}(\partial\omega^*)},$$

so that our previous stability estimates (I.1.10) provides the existence of a non-negative real  $\eta$  and of a constant  $C$  such that, for any diffeomorphism  $\Theta \in \mathfrak{U}$  with  $\|\Theta - \mathbf{I}\|_{\mathcal{C}^{2,1}(\mathbb{R}^d)} < \eta$  and  $|\Theta(\omega^*)| = |\omega^*|$ , it holds

$$J(\omega) \geq J(\omega^*) + \frac{C}{4} \|\mathbf{V} \cdot \mathbf{n}\|_{H^{1/2}(\partial\omega^*)}^2 \geq J(\omega^*) + C |\omega^* \Delta \Theta(\omega^*)|^2.$$

Hence we have shown the following accurate estimate.

**Theorem I.1.7.** *If  $\omega^*$  is a critical shape for  $J$  where (I.1.9) holds, there exist  $\eta > 0$  and  $C > 0$  depending only on  $\Omega$  and  $\omega^*$  such that, for all  $\Theta \in \mathfrak{U}$  with  $\|\Theta - \mathbf{I}\|_{\mathcal{C}^{2,1}(\mathbb{R}^d)} < \eta$ ,  $|\Theta(\omega^*)| = |\omega^*|$  and  $\Theta \neq \mathbf{I}$ ,*

$$J(\Theta(\omega^*)) > J(\omega^*) + C |\omega^* \Delta \Theta(\omega^*)|^2.$$

Let us make a final comment: this result can be understood as a quantitative estimate of the deviation from minimality for sets close to  $\omega^*$  in a strong sense (here the  $\mathcal{C}^{2,\alpha}$  norm). Then the present work corresponds to the first step in extending to the drag functional ideas and results on isoperimetric problems, see [3]. In a second step, using additional regularity properties provided by the perimeter, Acerbi *et al.* manage to extend this result on smooth domains to less regular sets.

## I.1.2 Perspectives

We first notice that this work can be adapted to other classical boundary conditions. This could be interested in order to deal with more specific physical applications.

Moreover this may be extended to the case where the fluid motion is assumed to be governed by the (stationary) Navier-Stokes equations (using the same assumptions and notations than above)

$$\begin{cases} -\nu \Delta \mathbf{u} + \nabla \mathbf{u} \mathbf{u} + \nabla p = \mathbf{0} & \text{in } \Omega \setminus \bar{\omega}, \\ \operatorname{div} \mathbf{u} = 0 & \text{in } \Omega \setminus \bar{\omega}, \\ \mathbf{u} = \mathbf{g} & \text{on } \partial\Omega, \\ \mathbf{u} = \mathbf{0} & \text{on } \partial\omega. \end{cases}$$

The adaptation is far to be trivial and the most difficult part in order to obtain analogous results seems to be the coercivity of the shape Hessian. Indeed Bello *et al.* prove in [41, Theorem 5] that

$$DJ(\omega^*) \cdot \mathbf{V} = \int_{\partial\omega^*} \nu (\partial_n \mathbf{w} - \partial_n \mathbf{u}) \cdot \partial_n \mathbf{u} (\mathbf{V} \cdot \mathbf{n}),$$

where  $(\mathbf{w}, \pi)$  solves the following adjoint problem

$$\begin{cases} -\nu \Delta \mathbf{w} + {}^t \nabla \mathbf{u} \mathbf{w} - \nabla \mathbf{w} \mathbf{u} + \nabla \pi = -2\nu \Delta \mathbf{u} & \text{in } \Omega \setminus \bar{\omega}^*, \\ \operatorname{div} \mathbf{w} = 0 & \text{in } \Omega \setminus \bar{\omega}^*, \\ \mathbf{w} = \mathbf{0} & \text{on } \partial\Omega, \\ \mathbf{w} = \mathbf{0} & \text{on } \partial\omega^*. \end{cases}$$

As previously, since we work under the constraint of constant volume and since  $\omega^*$  is a critical point, there exists  $\Lambda_0 \in \mathbb{R}$  such that  $DJ(\omega^*) \cdot \mathbf{V} + \Lambda_0 D\mathcal{V}(\omega^*) \cdot \mathbf{V} = 0$  for all  $\mathbf{V} \in \mathfrak{U}$ , i.e.,

$$\int_{\partial\omega^*} \nu (\partial_n \mathbf{w} - \partial_n \mathbf{u}) \cdot \partial_n \mathbf{u} (\mathbf{V} \cdot \mathbf{n}) + \Lambda_0 \int_{\partial\omega^*} \mathbf{V} \cdot \mathbf{n} = 0,$$

and we obtain the Euler-Lagrange equation satisfied at the critical shape: there exists  $\Lambda \in \mathbb{R}$  such that

$$|\partial_n \mathbf{u}|^2 - \partial_n \mathbf{w} \cdot \partial_n \mathbf{u} = \frac{\Lambda_0}{\nu} =: \Lambda.$$

Then we obtain, after lengthly computations, the following expression for the shape Hessian of the drag

$$\begin{aligned} D^2 J(\omega^*) \cdot \mathbf{V} \cdot \mathbf{V} &= 2 \int_{\partial\omega^*} \mathbf{u}' \cdot (\sigma(\mathbf{u}', p') \mathbf{n}) - \frac{1}{2} \int_{\partial\omega^*} \nu \nabla (|\mathcal{D}(\mathbf{u})|^2) \cdot \mathbf{V} (\mathbf{V} \cdot \mathbf{n}) \\ &+ \frac{1}{2} \int_{\partial\omega^*} \nu (\mathcal{D}(\mathbf{u}') : \mathcal{D}(\mathbf{w})) (\mathbf{V} \cdot \mathbf{n}) + \frac{1}{2} \int_{\partial\omega^*} \nu (\mathcal{D}(\mathbf{u}) : \mathcal{D}(\mathbf{w}')) (\mathbf{V} \cdot \mathbf{n}) \\ &+ \frac{1}{2} \int_{\partial\omega^*} \nu \nabla (\mathcal{D}(\mathbf{u}) : \mathcal{D}(\mathbf{w})) \cdot \mathbf{V} (\mathbf{V} \cdot \mathbf{n}), \end{aligned}$$

where  $(\mathbf{u}', p')$  and  $(\mathbf{w}', \pi')$  denote respectively the shape derivatives of  $(\mathbf{u}, p)$  and  $(\mathbf{w}, \pi)$ . Even if some terms could be treated as the Stokes case (see the expression of the shape Hessian (I.1.3)), the stability result seems to be hardly tractable following the same strategy than above. We expect to conclude using some recent results of Dambrine *et al.* in [109] where the authors identify structural hypotheses on the Hessian of a shape functional in order that critical stable domains (i.e. such that the first order derivative vanishes and the second order one is positive) are local minima for smooth perturbations.

Finally one can mention that it should be possible to adapt these results to unbounded domain. However, due to the approach using derivatives, removing the regularity assumptions on the boundary and the deformations seems out of reach without new ideas.

## I.2 Instability of an inverse problem

This part focuses on the instability of an inverse problem, that is *the data completion problem* for the Stokes and Navier-Stokes equations, and more precisely on the derivation of some stability estimates for this problem. This work was done in collaboration with Mehdi Badra and Jérémi Dardé (University Paul Sabatier – Toulouse III) and is published in *Discrete and Continuous Dynamical Systems - Series B* (see [33], 29 pages).

### I.2.1 Stability estimates for data completion problem

The data completion problem, or more generally recovering the solution of a partial differential equation from (boundary or distributed) measurements, finds several applications in various areas. For instance, this enables to reconstruct boundary coefficients containing the properties of a material immersed in a fluid. Even if these inverse problems are well-known to be unstable, one can expect to obtain some stability estimates which firstly characterize the (exponential) ill-posedness and secondly enable to obtain several properties such as the uniqueness of the solution of the inverse problem.

We focus on the fluid mechanics context. Hence, considering the classical Navier-Stokes equations in a bounded domain, Fabre and Lebeau prove in [127] that if one has some additional observation, such as the value of the velocity in a non-empty (and arbitrary small) open subset of the considered domain or the value of the Cauchy data (i.e. the Dirichlet and the Neumann boundary conditions) on a non-empty open subset of the boundary of the domain, then the corresponding pair velocity-pressure is unique. One of the difficulty is to obtain a stability inequality expressing the (conditional) continuous dependence of the solution with respect to the data and to some norms of the above mentioned observations.

To do this, we present new global Carleman inequalities for Stokes and Oseen equations with non-homogeneous boundary conditions. These estimates lead to log type stability inequalities for the

problem of recovering the solution of the Stokes and Navier-Stokes equations from both boundary and distributed observations. These inequalities fit the well-known unique continuation result of Fabre and Lebeau [127]: the distributed observation only depends on interior measurement of the velocity, and the boundary observation only depends on the trace of the velocity and of the Cauchy stress tensor measurements.

Notice that quantitative results for unique continuation are classically obtained thanks to Carleman inequalities and three-spheres inequalities. We refer to the topical review of Alessandrini *et al.* [12] and to the references therein for elliptic cases; see also the works of Le Rousseau *et al.* in [171]. However there is not so much results available on quantitative uniqueness for systems. About Stokes system we mention the works of Boulakia *et al.* in [59, 60] for stability estimates and of Ballerini in [35, 36] and Lin *et al.* in [173] for some other connected results.

### I.2.1.1 Carleman inequalities

Let  $\Omega$  be a non-empty bounded open subset of  $\mathbb{R}^d$  (with  $d = 2$  or  $d = 3$ ) of class  $\mathcal{C}^2$ ,  $\omega$  be a non-empty bounded open subset such that  $\omega \subset \subset \Omega$  and  $\psi : \Omega \rightarrow \mathbb{R}$  be a function satisfying

$$\psi \in \mathcal{C}^2(\Omega; \mathbb{R}); \quad \psi > c_0 \quad \text{and} \quad |\nabla \psi| > 0 \quad \text{in} \quad \Omega \setminus \bar{\omega}; \quad \psi = c_0 \quad \text{on} \quad \partial\Omega,$$

for some positive constant  $c_0 > 0$ . For the existence of such a function see for instance [136] or [214, Appendix III].

The main useful result is a Carleman inequality for the non homogeneous Oseen equations

$$\begin{cases} -\nu \Delta \mathbf{v} + (\mathbf{z}_1 \cdot \nabla) \mathbf{v} + (\mathbf{v} \cdot \nabla) \mathbf{z}_2 + \nabla p = \mathbf{f} & \text{in } \Omega, \\ \operatorname{div} \mathbf{v} = d & \text{in } \Omega. \end{cases} \quad (\text{I.2.1})$$

To obtain it, we first prove a Carleman inequality for a pair velocity-pressure in  $\mathbf{H}_0^2(\Omega) \times \mathbf{H}_0^1(\Omega)$  for the Stokes equations and then we use a domain extension argument to recover the non-homogeneous case. Above and in the following,  $\nu > 0$  is a constant which represents the kinematic viscosity of the fluid,  $\mathbf{f} \in \mathbf{L}^2(\Omega)$  and  $d \in \mathbf{H}^1(\Omega)$ . Moreover we assume that

$$\mathbf{z}_1 \in \mathbf{L}^\infty(\Omega) \quad \text{and} \quad \mathbf{z}_2 \in \mathbf{W}^{1,r}(\Omega) \quad \text{with} \quad \begin{cases} r > 2 & \text{if } d = 2, \\ r = 3 & \text{if } d = 3, \end{cases} \quad (\text{I.2.2})$$

and we use the following notation for the particular constant:

$$\tilde{\mathbf{m}}(\mathbf{z}_1, \mathbf{z}_2) := \max \left\{ 1, \|\mathbf{z}_1\|_{\mathbf{L}^\infty(\Omega)}, \|\nabla \mathbf{z}_2\|_{\mathbf{L}^r(\Omega)} \right\}.$$

**Theorem I.2.1.** *There exist  $C > 0$ ,  $\hat{c} > 0$  and  $\hat{s} > 1$  such that for all  $\mathbf{z}_1 \in \mathbf{L}^\infty(\Omega)$ ,  $\mathbf{z}_2 \in \mathbf{W}^{1,r}(\Omega)$ , for all  $\lambda \geq \hat{\lambda} := \tilde{\mathbf{m}}(\mathbf{z}_1, \mathbf{z}_2)\hat{c}$  and for all  $s \geq \hat{s}$ , every solution  $(\mathbf{v}, p) \in \mathbf{H}^2(\Omega) \times \mathbf{H}^1(\Omega)$  of System (I.2.1) satisfies*

$$\begin{aligned} \int_{\Omega} (|\nabla \mathbf{v}|^2 + se^{\lambda\psi} |\operatorname{curl} \mathbf{v}|^2 + s^2 \lambda^2 e^{2\lambda\psi} |\mathbf{v}|^2) e^{2se^{\lambda\psi}} &\leq C \left( \int_{\Omega} (s^{-1} \lambda^{-2} e^{-\lambda\psi} |\nabla d|^2 + \lambda^{-2} |\mathbf{f}|^2) e^{2se^{\lambda\psi}} \right. \\ &\quad \left. + \int_{\omega} s^3 \lambda^2 e^{3\lambda\psi} |\mathbf{v}|^2 e^{2se^{\lambda\psi}} + e^{2se^{\lambda c_0}} \left( \|\mathbf{v}\|_{\mathbf{H}^2(\Omega)}^2 + \|p\|_{\mathbf{H}^1(\Omega)}^2 \right) \right) \end{aligned}$$

and

$$\begin{aligned} \int_{\Omega} se^{\lambda\psi} |p - d|^2 e^{2se^{\lambda\psi}} &\leq C \left( \int_{\omega} (s^3 \lambda^2 e^{3\lambda\psi} |\mathbf{v}|^2 + se^{\lambda\psi} |p - d|^2) e^{2se^{\lambda\psi}} \right. \\ &\quad \left. + \int_{\Omega} (s^{-1} \lambda^{-2} e^{-\lambda\psi} |\nabla d|^2 + \lambda^{-2} |\mathbf{f}|^2) e^{2se^{\lambda\psi}} + e^{2se^{\lambda c_0}} \left( \|\mathbf{v}\|_{\mathbf{H}^2(\Omega)}^2 + \|p\|_{\mathbf{H}^1(\Omega)}^2 \right) \right). \end{aligned}$$

### I.2.1.2 Stability inequalities

We use the Carleman inequalities given in the previous Theorem I.2.1 to obtain several stability estimates for both distributed and boundary observation. We first prove a Hölder type interior estimates and a global log type estimates for a distributed observation. Then we use an extension of the domain procedure to obtain a global log type estimates for a boundary observation.

Using the same assumptions and notations than in Section I.2.1.1, we consider a pair velocity-pressure  $(\mathbf{v}, p) \in \mathbf{H}^2(\Omega) \times H^1(\Omega)$  solution of the linearized Navier-Stokes equations (I.2.1). We recall that if  $\mathbf{z}_1$  and  $\mathbf{z}_2$  are two solutions of the Navier-Stokes equations, then their difference  $\mathbf{v} = \mathbf{z}_1 - \mathbf{z}_2$  verifies (I.2.1). Moreover,  $\mathbf{n}$  is the outward unit normal to  $\partial\Omega$  which is assumed to be of class  $\mathcal{C}^2$  and the *stress tensor* is defined by  $\sigma(\mathbf{u}, p) := 2\nu\mathcal{D}(\mathbf{u}) - p\mathbf{I}$ , where  $\mathcal{D}(\mathbf{u}) := \frac{1}{2}(\nabla\mathbf{u} + {}^t\nabla\mathbf{u})$  is the *symmetrized gradient*.

The pair  $(\mathbf{v}, p)$  is not completely determined by System (I.2.1). However, if we have some additional *observation*, such as the value of the velocity  $\mathbf{v}$  in a non-empty (and arbitrary small) open subset  $\omega \subset \Omega$ , namely

$$\mathbf{v} = \mathbf{v}_{\text{obs}} \quad \text{in } \omega, \quad (\text{I.2.3})$$

or the value of the Cauchy data  $(\mathbf{v}, \sigma(\mathbf{v}, p)\mathbf{n})$  on a non-empty open subset  $\Gamma_{\text{obs}}$  of  $\partial\Omega$ , namely

$$\begin{cases} \mathbf{v} = \mathbf{g}_D & \text{on } \Gamma_{\text{obs}}, \\ \sigma(\mathbf{v}, p)\mathbf{n} = \mathbf{g}_N & \text{on } \Gamma_{\text{obs}}, \end{cases} \quad (\text{I.2.4})$$

then Fabre and Lebeau's Theorem guarantees the uniqueness of the corresponding pair  $(\mathbf{v}, p)$  (see [127]). Nevertheless, as previously mentioned, the related stability inequality expressing the (conditional) continuous dependence of  $(\mathbf{v}, p)$  with respect to  $\|\mathbf{f}\|_{\mathbf{L}^2(\Omega)}$ ,  $\|d\|_{H^1(\Omega)}$  and to some norm  $\|(\mathbf{v}, p)\|_{\text{obs}}$  (corresponding to one of the above mentioned observation) was not yet proved for system (I.2.1). Indeed, up to my knowledge, the most recent result quantifying the Fabre and Lebeau's unique continuation theorem in the Stokes case was the following one given in [60, Theorem 1.4] by Boulakia *et al.*

**Theorem I.2.2** (Boulakia *et al.* in [60]). *Assume that  $\Omega$  is of class  $\mathcal{C}^\infty$ . There exists  $\eta_0 > 0$  such that for all  $\eta > \eta_0$ , there exists  $C > 0$  such that, for all solution  $(\mathbf{v}, p) \in \mathbf{H}^2(\Omega) \times H^2(\Omega)$  of the Stokes equations*

$$\begin{cases} -\nu\Delta\mathbf{v} + \nabla p = \mathbf{0} & \text{in } \Omega, \\ \operatorname{div}\mathbf{v} = 0 & \text{in } \Omega, \end{cases}$$

we have

$$\|\mathbf{v}\|_{\mathbf{H}^1(\Omega)} + \|p\|_{H^1(\Omega)} \leq C \frac{\|\mathbf{v}\|_{\mathbf{H}^2(\Omega)} + \|p\|_{H^2(\Omega)}}{\left(\ln\left(\eta \frac{\|\mathbf{v}\|_{\mathbf{H}^2(\Omega)} + \|p\|_{H^2(\Omega)}}{\|\mathbf{v}\|_{\mathbf{H}^1(\omega)} + \|p\|_{H^1(\omega)}}\right)\right)^{1/2}}$$

and

$$\|\mathbf{v}\|_{\mathbf{H}^1(\Omega)} + \|p\|_{H^1(\Omega)} \leq C \frac{\|\mathbf{v}\|_{\mathbf{H}^2(\Omega)} + \|p\|_{H^2(\Omega)}}{\left(\ln\left(\eta \frac{\|\mathbf{v}\|_{\mathbf{H}^2(\Omega)} + \|p\|_{H^2(\Omega)}}{\|\mathbf{v}\|_{\mathbf{L}^2(\Gamma_{\text{obs}})} + \|\frac{\partial\mathbf{v}}{\partial\mathbf{n}}\|_{\mathbf{L}^2(\Gamma_{\text{obs}})} + \|p\|_{\mathbf{L}^2(\Gamma_{\text{obs}})} + \|\frac{\partial p}{\partial\mathbf{n}}\|_{\mathbf{L}^2(\Gamma_{\text{obs}})}}\right)\right)^{1/2}}.$$

As underlined by the authors themselves, this result does not depend exclusively on the needed observations (I.2.3) or (I.2.4) and then does not fit the Fabre and Lebeau's Theorem. The first main results claimed below are stability inequalities for the Oseen equations (I.2.1) which are quantified versions of Fabre and Lebeau's uniqueness Theorem (see Theorem I.2.3 below) and, in this sense, improve the previous work of Boulakia *et al.*

We introduce a constant  $K \geq e^e$  which satisfies:

$$\max\left\{1, \|\mathbf{z}_1\|_{\mathbf{L}^\infty(\Omega)}, \|\nabla\mathbf{z}_2\|_{\mathbf{L}^r(\Omega)}\right\} \leq \ln(\ln K). \quad (\text{I.2.5})$$

**Theorem I.2.3.** *Assume (I.2.2) and (I.2.5) and that  $(\mathbf{v}, p) \in \mathbf{H}^2(\Omega) \times \mathbf{H}^1(\Omega)$  is a solution of the Oseen equations (I.2.1). There exists  $C > 0$  such that, for any  $M > 0$  such that  $\|\mathbf{v}\|_{\mathbf{H}^2(\Omega)} + \|p\|_{\mathbf{H}^1(\Omega)} \leq M$ , the following estimates hold:*

$$\|\mathbf{v}\|_{\mathbf{L}^2(\Omega)} \leq CK \frac{M}{\ln \left( 1 + \frac{M}{\|\mathbf{f}\|_{\mathbf{L}^2(\Omega)} + \|d\|_{\mathbf{H}^1(\Omega)} + \|\mathbf{v}\|_{\mathbf{L}^2(\omega)}} \right)} \quad (\text{I.2.6})$$

and

$$\|\mathbf{v}\|_{\mathbf{L}^2(\Omega)} \leq CK \frac{M}{\ln \left( 1 + \frac{M}{\|\mathbf{f}\|_{\mathbf{L}^2(\Omega)} + \|d\|_{\mathbf{H}^1(\Omega)} + \|\mathbf{v}\|_{\mathbf{H}^{3/2}(\Gamma_{\text{obs}})} + \|\sigma(\mathbf{v}, p)\mathbf{n}\|_{\mathbf{H}^{1/2}(\Gamma_{\text{obs}})}} \right)}. \quad (\text{I.2.7})$$

Moreover we have

$$\begin{aligned} & \|\text{curl } \mathbf{v}\|_{(\mathbf{L}^2(\Omega))^{2d-3}} + \|p - \text{div } \mathbf{v}\|_{\mathbf{L}^2(\Omega)} \\ & \leq CK \frac{M}{\left( \ln \left( 1 + \frac{M}{\|\mathbf{f}\|_{\mathbf{L}^2(\Omega)} + \|d\|_{\mathbf{H}^1(\Omega)} + \|\mathbf{v}\|_{\mathbf{H}^{3/2}(\Gamma_{\text{obs}})} + \|\sigma(\mathbf{v}, p)\mathbf{n}\|_{\mathbf{H}^{1/2}(\Gamma_{\text{obs}})}} \right) \right)^{1/2}}. \end{aligned} \quad (\text{I.2.8})$$

The above theorem allows us to obtain stability estimates for the Navier-Stokes equations. Let us consider two couples  $(\mathbf{z}_i, \pi_i) \in \mathbf{H}^2(\Omega) \times \mathbf{H}^1(\Omega)$ ,  $i = 1, 2$ , that satisfy

$$\begin{cases} -\nu \Delta \mathbf{z}_i + (\mathbf{z}_i \cdot \nabla) \mathbf{z}_i + \nabla \pi_i = \mathbf{f} & \text{in } \Omega, \\ \text{div } \mathbf{z}_i = d & \text{in } \Omega. \end{cases} \quad (\text{I.2.9})$$

Note that the  $\mathbf{H}^2$  regularity of  $\mathbf{z}_1, \mathbf{z}_2$  implies (I.2.2). Then the following theorem is a simple consequence of Theorem I.2.3 applied to the pair  $(\mathbf{v}, p) := (\mathbf{z}_1 - \mathbf{z}_2, \pi_1 - \pi_2)$  which is solution of the linearized Navier-Stokes equations:

$$\begin{cases} -\nu \Delta \mathbf{v} + (\mathbf{z}_1 \cdot \nabla) \mathbf{v} + (\mathbf{v} \cdot \nabla) \mathbf{z}_2 + \nabla p = \mathbf{0} & \text{in } \Omega, \\ \text{div } \mathbf{v} = 0 & \text{in } \Omega, \\ \mathbf{v} = \mathbf{z}_1 - \mathbf{z}_2 & \text{on } \Gamma_{\text{obs}}, \\ \sigma(\mathbf{v}, p)\mathbf{n} = \sigma(\mathbf{z}_1, \pi_1)\mathbf{n} - \sigma(\mathbf{z}_2, \pi_2)\mathbf{n} & \text{on } \Gamma_{\text{obs}}. \end{cases}$$

Hence, using (I.2.6), (I.2.7) and (I.2.8), we obtain the following estimates.

**Theorem I.2.4.** *Assume that  $(\mathbf{z}_i, \pi_i) \in \mathbf{H}^2(\Omega) \times \mathbf{H}^1(\Omega)$ ,  $i = 1, 2$ , are two solutions of (I.2.9) which satisfy (I.2.5) for some  $K > e^e$ . Then there exists  $C > 0$  such that, for any  $M > 0$  such that  $\|\mathbf{z}_1 - \mathbf{z}_2\|_{\mathbf{H}^2(\Omega)} + \|\pi_1 - \pi_2\|_{\mathbf{H}^1(\Omega)} \leq M$ , the following estimates hold:*

$$\|\mathbf{z}_1 - \mathbf{z}_2\|_{\mathbf{L}^2(\Omega)} \leq CK \frac{M}{\ln \left( 1 + \frac{M}{\|\mathbf{z}_1 - \mathbf{z}_2\|_{\mathbf{L}^2(\omega)}} \right)}$$

and

$$\|\mathbf{z}_1 - \mathbf{z}_2\|_{\mathbf{L}^2(\Omega)} \leq CK \frac{M}{\ln \left( 1 + \frac{M}{\|\mathbf{z}_1 - \mathbf{z}_2\|_{\mathbf{H}^{3/2}(\Gamma_{\text{obs}})} + \|\sigma(\mathbf{z}_1, \pi_1)\mathbf{n} - \sigma(\mathbf{z}_2, \pi_2)\mathbf{n}\|_{\mathbf{H}^{1/2}(\Gamma_{\text{obs}})}} \right)}.$$

Moreover we have

$$\begin{aligned} & \|\operatorname{curl}(\mathbf{z}_1 - \mathbf{z}_2)\|_{(\mathbf{L}^2(\Omega))^{2d-3}} + \|\pi_1 - \pi_2\|_{\mathbf{L}^2(\Omega)} \\ & \leq CK \frac{M}{\left( \ln \left( 1 + \frac{M}{\|\mathbf{z}_1 - \mathbf{z}_2\|_{\mathbf{H}^{3/2}(\Gamma_{\text{obs}})} + \|\sigma(\mathbf{z}_1, \pi_1)\mathbf{n} - \sigma(\mathbf{z}_2, \pi_2)\mathbf{n}\|_{\mathbf{H}^{1/2}(\Gamma_{\text{obs}})}} \right) \right)^{1/2}}. \end{aligned}$$

To conclude this part, let us stress that these stability estimates respect the well-known unique continuation result of Fabre and Lebeau since the observation in  $\omega$  only concerns the velocity, and since the observation on  $\Gamma_{\text{obs}}$  only concerns  $\mathbf{v}|_{\Gamma_{\text{obs}}}$  and  $\sigma(\mathbf{v}, p)\mathbf{n}|_{\Gamma_{\text{obs}}}$ . Indeed Fabre and Lebeau's Theorem states that every velocity  $\mathbf{v}$  solution of

$$\begin{cases} -\Delta \mathbf{v} + \nabla p = \mathbf{0} & \text{in } \Omega, \\ \operatorname{div} \mathbf{v} = 0 & \text{in } \Omega, \end{cases} \quad (\text{I.2.10})$$

which is identically zero in  $\omega$  must be zero in  $\Omega$  (and then  $p$  is constant, see [127, Proposition 1.1] for precise statements). Particularly, no information is required on  $p$  to obtain this result. Moreover, as a direct consequence of the above mentioned uniqueness result, we can easily deduce that, if a smooth solution  $(\mathbf{v}, p)$  of System (I.2.10) satisfies  $\mathbf{v} = \mathbf{0}$  and  $\sigma(\mathbf{v}, p)\mathbf{n} = \mathbf{0}$  on  $\Gamma_{\text{obs}}$ , then,  $\mathbf{v} = \mathbf{0}$  and  $p = 0$  in  $\Omega$ . Therefore inequalities (I.2.6), (I.2.7) and (I.2.8) are quantifications of Fabre and Lebeau's uniqueness theorem.

## I.2.2 Two applications

Additionally to the quantification aspect of the unique continuation result, we can deduce from the above theorems some results on parameter identification problems as well as some error estimates for numerical reconstruction methods.

We use the same assumptions and notations than above.

### I.2.2.1 Parameter identification

We obtain stability inequalities for the problem of recovering Navier or Robin boundary coefficients. For this, we assume that  $\Gamma_{\text{obs}}$  and  $\Gamma_0$  are two non-empty open subsets of  $\partial\Omega$  such that  $\Gamma_{\text{obs}} \cap \Gamma_0 = \emptyset$  and we consider on  $\Gamma_0$  a non penetration condition given by  $\mathbf{z} \cdot \mathbf{n} = 0$  and a friction law given by  $2\nu [\mathcal{D}(\mathbf{z})\mathbf{n}]_{\tau} + \alpha \mathbf{z} = \mathbf{0}$  (where the subscript  $\tau$  denotes the tangential component). The aim is to reconstruct the unknown friction coefficient  $\alpha$  from given Cauchy data on  $\Gamma_{\text{obs}}$ . Thus we consider two solutions  $(\mathbf{z}_i, \pi_i) \in \mathbf{H}^2(\Omega) \times \mathbf{H}^1(\Omega)$  ( $i = 1, 2$ ) of the Navier-Stokes equations (I.2.9), associated to two friction coefficients  $\alpha_i \in \mathbf{H}^{1/2}(\Gamma_0) \cap \mathbf{L}^\infty(\Gamma_0)$  ( $i = 1, 2$ ) in the Navier type boundary conditions on  $\Gamma_0$  given by:

$$\begin{cases} \mathbf{z}_i \cdot \mathbf{n} = 0 & \text{on } \Gamma_0, \\ 2\nu [\mathcal{D}(\mathbf{z}_i)\mathbf{n}]_{\tau} + \alpha_i \mathbf{z}_i = \mathbf{0} & \text{on } \Gamma_0. \end{cases} \quad (\text{I.2.11})$$

We also consider the reconstruction of the Robin coefficient, still denoted  $\alpha$ , in the case of the classical Robin boundary conditions on  $\Gamma_0$  given by:

$$\sigma(\mathbf{z}_i, \pi_i)\mathbf{n} + \alpha_i \mathbf{z}_i = \mathbf{0} \quad \text{on } \Gamma_0. \quad (\text{I.2.12})$$

Notice that the  $\mathbf{H}^{1/2}(\Gamma_0)$ -regularity of  $\alpha_i$  is necessary to have a  $\mathbf{H}^2(\Omega) \times \mathbf{H}^1(\Omega)$ -regularity of the solutions.

**Theorem I.2.5.** *Let  $\alpha_i \in H^{1/2}(\Gamma_0) \cap L^\infty(\Gamma_0)$ ,  $i = 1, 2$  be two given coefficients. Let us consider two pairs  $(z_i, \pi_i) \in \mathbf{H}^2(\Omega) \times H^1(\Omega)$ ,  $i = 1, 2$ , solution of the Navier-Stokes equations (I.2.9) with the boundary conditions (I.2.11) or (I.2.12) which satisfy (I.2.5) for some  $K \geq e^e$ . Let*

$$\mathcal{N} := \{\mathbf{x} \in \Gamma_0, z_1(\mathbf{x}) = \mathbf{0} \text{ and } z_2(\mathbf{x}) = \mathbf{0}\},$$

*let us assume that  $\mathcal{K}$  is a compact subset of  $\Gamma_0 \setminus \mathcal{N}$  with a non-empty interior and let  $m > 0$  be a constant such that  $\max(|z_1|, |z_2|) \geq m$  on  $\mathcal{K}$ . Then there exists  $C > 0$  such that, for any  $M > 0$  such that  $\|z_1 - z_2\|_{\mathbf{H}^2(\Omega)} + \|\pi_1 - \pi_2\|_{H^1(\Omega)} \leq M$ , the following inequality holds:*

$$\begin{aligned} & \|\alpha_1 - \alpha_2\|_{L^2(\mathcal{K})} \\ & \leq \frac{CK}{m} \frac{M}{\left( \ln \left( 1 + \frac{M}{\|z_1 - z_2\|_{\mathbf{H}^{3/2}(\Gamma_{\text{obs}})} + \|\sigma(z_1, \pi_1)\mathbf{n} - \sigma(z_2, \pi_2)\mathbf{n}\|_{\mathbf{H}^{1/2}(\Gamma_{\text{obs}})}} \right) \right)^{1/4}}. \end{aligned} \quad (\text{I.2.13})$$

*Here, the constant  $C$  does not depend only on the geometry but also on  $\|\alpha_i\|_{L^\infty(\Gamma_0)}$ , for  $i = 1, 2$ .*

**Remark I.2.6.** *We stress the fact that the previous estimate (I.2.13) depends on the solutions  $z_1$  and  $z_2$  through the choice of the compact set  $\mathcal{K}$  and the constant  $m$ . To complete this result, it would be interesting to obtain a quantitative estimate of the vanishing rate of  $z$ , like what is done in [13] in the case of Laplace's equation.*

**Remark I.2.7.** *Note that the assumptions of Theorem I.2.5 guarantee that  $z_1, z_2$  are continuous. Then if  $\mathcal{K}$  exists, the constant  $m > 0$  exists and depends on  $z_1, z_2$  on  $\mathcal{K}$ . The existence of  $\mathcal{K}$  is known in the case of Robin boundary conditions (I.2.12) if  $z_1$  (or  $z_2$ ) is not identically equal to zero in  $\Omega$ . It is an easy consequence of Fabre and Lebeau's theorem. But in the case of Navier conditions (I.2.11) and if one of the  $z_i$  is not trivial, the existence of a non-empty open subset of  $\Gamma_0$  on which  $z_1$  and  $z_2$  both vanish is a difficult issue. Indeed it reduces to study the existence of a non trivial vector field  $\mathbf{v}$  solution to an homogeneous Oseen equation and such that  $\mathbf{v} = \partial_{\mathbf{n}}\mathbf{v} = \mathbf{0}$  on a non-empty open subset of  $\Gamma_0$ . The difficulty relies on the fact that, unlike the Robin case, no additional information on the pressure is available.*

**Remark I.2.8.** *We can obtain a better estimate assuming more regularity on the solution  $(\mathbf{v}, p)$ . More precisely, for  $k \geq 2$  and  $n \in \mathbb{N}$ , assume that  $(\mathbf{v}, p) \in \mathbf{H}^k(\Omega) \times H^{k-1}(\Omega)$ ,  $k \geq 2$  and  $\alpha_i \in H^n(\mathcal{K})$ ,  $i = 1, 2$ . Then, using an interpolation argument, we can obtain the existence of  $C > 0$  such that, for any  $M > 0$  and  $N > 0$  such that  $\|\mathbf{v}\|_{\mathbf{H}^2(\Omega)} + \|p\|_{H^1(\Omega)} \leq M$  and  $\|\mathbf{v}\|_{\mathbf{H}^k(\Omega)} + \|p\|_{H^{k-1}(\Omega)} \leq N$  and for all  $\theta \in [0, 1]$ ,*

$$\begin{aligned} & \|\alpha_1 - \alpha_2\|_{H^{\theta n}(\mathcal{K})} \\ & \leq \frac{\left(\frac{CK}{m}N\right)^{1-\theta} \|\alpha_1 - \alpha_2\|_{H^n(\mathcal{K})}^\theta}{\left( \ln \left( 1 + \frac{M}{\|\mathbf{v}_1 - \mathbf{v}_2\|_{\mathbf{H}^{3/2}(\Gamma_{\text{obs}})} + \|\sigma(\mathbf{v}_1, p_1)\mathbf{n} - \sigma(\mathbf{v}_2, p_2)\mathbf{n}\|_{\mathbf{H}^{1/2}(\Gamma_{\text{obs}})}} \right) \right)^{\frac{(2k-3)(1-\theta)}{2k}}}. \end{aligned}$$

*For  $k = 3$  and  $\theta = n = 0$ , we then obtain a result similar to the one presented in [59, Theorem 4.3].*

To conclude this part, let us underline that Theorem I.2.5, which completes the previous results given by Boulakia *et al* in [59, 60], finds applications in the modeling of biological problems as blood flow in the cardiovascular system (see [191] and [216]) or airflow in the lungs (see [34]). For Laplace's equation, these kind of stability estimates for the Robin coefficient have been widely studied: see for instance the works of Chaabane *et al.* in [94, 95], Alessandrini *et al.* in [11], Sincich in [207], Bellassoued *et al.* in [40] and Cheng *et al.* in [96].

### I.2.2.2 Rate of convergence for numerical reconstruction methods

Finally we present another application of our stability estimates in the context of numerical reconstruction methods. More precisely we focus on the stable reconstruction of the solution of a data completion problem (also known as Cauchy problem) for the Stokes equations: for given Cauchy data  $(\mathbf{g}_N, \mathbf{g}_D) \in \mathbf{H}^{1/2}(\Gamma_{\text{obs}}) \times \mathbf{H}^{3/2}(\Gamma_{\text{obs}})$ , we search  $(\mathbf{v}, p) \in \mathbf{H}^2(\Omega) \times \mathbf{H}^1(\Omega)$  solution of the following system

$$\begin{cases} -\nu\Delta\mathbf{v} + \nabla p = \mathbf{f} & \text{in } \Omega, \\ \operatorname{div} \mathbf{v} = 0 & \text{in } \Omega, \end{cases} \quad (\text{I.2.14})$$

and such that

$$\mathbf{v} = \mathbf{g}_D \quad \text{and} \quad \sigma(\mathbf{v}, p)\mathbf{n} = \mathbf{g}_N \quad \text{on } \Gamma_{\text{obs}}.$$

Estimates (I.2.7) and (I.2.8) imply the uniqueness of the solution of the data completion problem. However there exists Cauchy data  $(\mathbf{g}_N, \mathbf{g}_D)$  for which it does not admit any solution. Hence regularization methods are needed to stably reconstruct  $(\mathbf{v}, p)$  from the couple  $(\mathbf{g}_N, \mathbf{g}_D)$ . We study two standard regularization methods: a quasi-reversibility regularization and a penalized Kohn-Vogelius regularization.

In the quasi-reversibility method, we consider, for  $\varepsilon > 0$ , the following variational problem: find a pair  $(\mathbf{v}_\varepsilon, p_\varepsilon) \in \mathbf{H}^2(\Omega) \times \mathbf{H}^1(\Omega)$  such that  $\mathbf{v}_\varepsilon = \mathbf{g}_D$  on  $\Gamma_{\text{obs}}$ ,  $\sigma(\mathbf{v}_\varepsilon, p_\varepsilon)\mathbf{n} = \mathbf{g}_N$  on  $\Gamma_{\text{obs}}$ , and for all couple  $(\mathbf{w}, q) \in \mathbf{H}^2(\Omega) \times \mathbf{H}^1(\Omega)$  such that  $\mathbf{w} = \mathbf{0}$  and  $\sigma(\mathbf{w}, q)\mathbf{n} = \mathbf{0}$  on  $\Gamma_{\text{obs}}$ , we have

$$\begin{aligned} \int_{\Omega} (-\nu\Delta\mathbf{v}_\varepsilon + \nabla p_\varepsilon) \cdot (-\nu\Delta\mathbf{w} + \nabla q) + \left( \operatorname{div}(\mathbf{v}_\varepsilon), \operatorname{div}(\mathbf{w}) \right)_{\mathbf{H}^1(\Omega)} \\ + \varepsilon(\mathbf{v}_\varepsilon, \mathbf{w})_{\mathbf{H}^2(\Omega)} + \varepsilon(p_\varepsilon, q)_{\mathbf{H}^1(\Omega)} = \int_{\Omega} \mathbf{f} \cdot (-\nu\Delta\mathbf{w} + \nabla q). \end{aligned} \quad (\text{I.2.15})$$

Let  $\Gamma_{\text{ina}} := \partial\Omega \setminus \overline{\Gamma_{\text{obs}}}$ . The penalized Kohn-Vogelius approach that we consider here consists in, for  $\varepsilon > 0$ , defining the functional  $\mathcal{K}_\varepsilon : \mathbf{H}^{1/2}(\Gamma_{\text{ina}}) \times \mathbf{H}^{3/2}(\Gamma_{\text{ina}}) \rightarrow \mathbb{R}$  given by

$$\begin{aligned} \mathcal{K}_\varepsilon(\boldsymbol{\varphi}, \boldsymbol{\psi}) := & \|\mathbf{v}_\varphi^{g_D} - \mathbf{v}_\psi^{g_N}\|_{\mathbf{H}^2(\Omega)}^2 + \|\mathbf{v}_\varphi^{g_D} - \mathbf{v}_\psi^{g_N}\|_{\mathbf{H}^1(\Omega)}^2 \\ & + \varepsilon\|(\mathbf{v}_\varphi^{g_D}, p_\varphi^{g_D})\|_{\mathbf{H}^2(\Omega) \times \mathbf{H}^1(\Omega)}^2 + \varepsilon\|(\mathbf{v}_\psi^{g_N}, p_\psi^{g_N})\|_{\mathbf{H}^2(\Omega) \times \mathbf{H}^1(\Omega)}^2, \end{aligned}$$

where  $|\cdot|_{\mathbf{H}^1(\Omega)} := \|\nabla(\cdot)\|_{\mathbf{L}^2(\Omega)}$  and  $|\cdot|_{\mathbf{H}^2(\Omega)} := \|\nabla^2(\cdot)\|_{\mathbf{L}^2(\Omega)}$  are the respective  $\mathbf{H}^1$  and  $\mathbf{H}^2$ -seminorms and where  $(\mathbf{v}_\varphi^{g_D}, p_\varphi^{g_D}) \in \mathbf{H}^2(\Omega) \times \mathbf{H}^1(\Omega)$  and  $(\mathbf{v}_\psi^{g_N}, p_\psi^{g_N}) \in \mathbf{H}^2(\Omega) \times \mathbf{H}^1(\Omega)$  are the respective solutions of the following problems

$$\left\{ \begin{array}{l} -\nu\Delta\mathbf{v}_\varphi^{g_D} + \nabla p_\varphi^{g_D} = \mathbf{f} \quad \text{in } \Omega, \\ \operatorname{div} \mathbf{v}_\varphi^{g_D} = 0 \quad \text{in } \Omega, \\ \mathbf{v}_\varphi^{g_D} = \mathbf{g}_D \quad \text{on } \Gamma_{\text{obs}}, \\ \sigma(\mathbf{v}_\varphi^{g_D}, p_\varphi^{g_D})\mathbf{n} = \boldsymbol{\varphi} \quad \text{on } \Gamma_{\text{ina}}, \end{array} \right. \quad \text{and} \quad \left\{ \begin{array}{l} -\nu\Delta\mathbf{v}_\psi^{g_N} + \nabla p_\psi^{g_N} = \mathbf{f} \quad \text{in } \Omega, \\ \operatorname{div} \mathbf{v}_\psi^{g_N} = 0 \quad \text{in } \Omega, \\ \sigma(\mathbf{v}_\psi^{g_N}, p_\psi^{g_N})\mathbf{n} = \mathbf{g}_N \quad \text{on } \Gamma_{\text{obs}}, \\ \mathbf{v}_\psi^{g_N} = \boldsymbol{\psi} \quad \text{on } \Gamma_{\text{ina}}. \end{array} \right.$$

Then we define

$$(\mathbf{v}_\varepsilon, p_\varepsilon) := (\mathbf{v}_{\varphi_\varepsilon^*}^{g_D}, p_{\psi_\varepsilon^*}^{g_N})$$

where  $(\varphi_\varepsilon^*, \psi_\varepsilon^*) \in \mathbf{H}^{1/2}(\Gamma_{\text{ina}}) \times \mathbf{H}^{3/2}(\Gamma_{\text{ina}})$  is such that

$$\mathcal{K}_\varepsilon(\varphi_\varepsilon^*, \psi_\varepsilon^*) = \inf_{(\boldsymbol{\varphi}, \boldsymbol{\psi}) \in \mathbf{H}^{1/2}(\Gamma_{\text{ina}}) \times \mathbf{H}^{3/2}(\Gamma_{\text{ina}})} \mathcal{K}_\varepsilon(\boldsymbol{\varphi}, \boldsymbol{\psi}). \quad (\text{I.2.16})$$

For this second method, we specify that we assume  $\overline{\Gamma_{\text{obs}}} \cap \overline{\Gamma_{\text{ina}}} = \emptyset$ , for instance  $\Gamma_{\text{obs}}$  could be one of the connected components of  $\partial\Omega$ .

For any Cauchy pair  $(\mathbf{g}_N, \mathbf{g}_D) \in \mathbf{H}^{1/2}(\Gamma_{\text{obs}}) \times \mathbf{H}^{3/2}(\Gamma_{\text{obs}})$ , both the quasi-reversibility problem (I.2.15) and the Kohn-Vogelius minimization problem (I.2.16) admit a unique solution  $(\mathbf{v}_\varepsilon, p_\varepsilon)$ . Moreover, if the initial data completion problem admits a solution  $(\mathbf{v}, p)$ , we prove that  $\mathbf{v}_\varepsilon$  converges to  $\mathbf{v}$  strongly in  $\mathbf{H}^2(\Omega)$  and  $p_\varepsilon$  converges to  $p$  strongly in  $\mathbf{H}^1(\Omega)$ . Furthermore the previous stability estimates provide the rate of convergence of both methods (for a survey on the connection between stability estimates and rates of convergence of regularization methods, we refer to [164]) as claimed by the following result.

**Theorem I.2.9.** *For any  $M > 0$  such that  $\|\mathbf{v}\|_{\mathbf{H}^2(\Omega)} + \|p\|_{\mathbf{H}^1(\Omega)} \leq M$ , where  $(\mathbf{v}, p)$  is the exact solution (which is assumed to exist) of the data completion problem (I.2.14), we have the following error estimates for both quasi-reversibility method and penalized Kohn-Vogelius method:*

$$\|\mathbf{v}_\varepsilon - \mathbf{v}\|_{\mathbf{L}^2(\Omega)} \leq \frac{M}{\ln(1 + \frac{M}{\sqrt{\varepsilon}})}, \quad \|\mathbf{v}_\varepsilon - \mathbf{v}\|_{\mathbf{H}^1(\Omega)} \leq \frac{M}{\left(\ln(1 + \frac{M}{\sqrt{\varepsilon}})\right)^{1/2}}$$

and

$$\|p_\varepsilon - p\|_{\mathbf{L}^2(\Omega)} \leq \frac{M}{\left(\ln(1 + \frac{M}{\sqrt{\varepsilon}})\right)^{1/2}}.$$

Let us conclude this part by giving a sketch of the proof of this result. The main idea is to obtain suitable bounds and to use the estimates (I.2.7) and (I.2.8)

The proof for the quasi-reversibility method is based on the fact that  $(\mathbf{u}, q) := (\mathbf{v}_\varepsilon - \mathbf{v}, p_\varepsilon - p)$  is such that  $\mathbf{u} = \mathbf{0}$  and  $\sigma(\mathbf{u}, q)\mathbf{n} = \mathbf{0}$  on  $\Gamma_{\text{obs}}$  and that one can prove that the following estimates hold

$$\begin{aligned} \|(\mathbf{u}, q)\|_{\mathbf{H}^2(\Omega) \times \mathbf{H}^1(\Omega)} &\leq \|(\mathbf{v}, p)\|_{\mathbf{H}^2(\Omega) \times \mathbf{H}^1(\Omega)}, \\ \|- \nu \Delta \mathbf{u} + \nabla q\|_{\mathbf{L}^2(\Omega)} &\leq \sqrt{\varepsilon} \|(\mathbf{v}, p)\|_{\mathbf{H}^2(\Omega) \times \mathbf{H}^1(\Omega)}, \\ \|\text{div}(\mathbf{u})\|_{\mathbf{L}^2(\Omega)} &\leq \sqrt{\varepsilon} \|(\mathbf{v}, p)\|_{\mathbf{H}^2(\Omega) \times \mathbf{H}^1(\Omega)}. \end{aligned}$$

Hence, applying estimates (I.2.7) and (I.2.8), we directly obtain the result.

Concerning the penalized Kohn-Vogelius method, we first note that, using the definition of  $(\varphi_\varepsilon^*, \psi_\varepsilon^*)$ ,

$$\mathcal{K}_\varepsilon(\varphi_\varepsilon^*, \psi_\varepsilon^*) \leq \mathcal{K}_\varepsilon(\sigma(\mathbf{v}, p)\mathbf{n}|_{\Gamma_{\text{ina}}}, \mathbf{v}|_{\Gamma_{\text{ina}}}) = 2\varepsilon \|(\mathbf{v}, p)\|_{\mathbf{H}^2(\Omega) \times \mathbf{H}^1(\Omega)}^2,$$

which implies

$$|\mathbf{v}_\varepsilon - \mathbf{v}_{\psi_\varepsilon^*}|_{\mathbf{H}^2(\Omega)}^2 + |\mathbf{v}_\varepsilon - \mathbf{v}_{\psi_\varepsilon^*}|_{\mathbf{H}^1(\Omega)}^2 \leq 2\varepsilon \|(\mathbf{v}, p)\|_{\mathbf{H}^2(\Omega) \times \mathbf{H}^1(\Omega)}^2$$

and

$$\|\mathbf{v}_\varepsilon - \mathbf{v}\|_{\mathbf{H}^2(\Omega)} \leq C(\mathbf{v}, p),$$

where  $C(\mathbf{v}, p)$  is a constant depending only on  $\|(\mathbf{v}, p)\|_{\mathbf{H}^2(\Omega) \times \mathbf{H}^1(\Omega)}$ . Thus, using the two previous inequalities, we obtain

$$\begin{aligned} \|\sigma(\mathbf{v}_\varepsilon, p_\varepsilon)\mathbf{n} - \mathbf{g}_N\|_{\mathbf{H}^{1/2}(\Gamma_{\text{obs}})} &= \|\sigma(\mathbf{v}_{\varphi_\varepsilon^*}, p_{\psi_\varepsilon^*})\mathbf{n} - \sigma(\mathbf{v}_{\psi_\varepsilon^*}, p_{\psi_\varepsilon^*})\mathbf{n}\|_{\mathbf{H}^{1/2}(\Gamma_{\text{obs}})} \\ &\leq |\mathbf{v}_\varepsilon - \mathbf{v}_{\psi_\varepsilon^*}|_{\mathbf{H}^2(\Omega)} + |\mathbf{v}_\varepsilon - \mathbf{v}_{\psi_\varepsilon^*}|_{\mathbf{H}^1(\Omega)} \leq \sqrt{\varepsilon} C(\mathbf{v}, p), \end{aligned}$$

where  $C(\mathbf{v}, p)$  is another constant depending only on  $\|(\mathbf{v}, p)\|_{\mathbf{H}^2(\Omega) \times \mathbf{H}^1(\Omega)}$ . Hence, applying again estimates (I.2.7) and (I.2.8), we conclude.

### I.2.3 Perspectives

All the previous results, for both the linear and nonlinear cases, concern the stationary case. A natural extension is to study the non-stationary case: for  $T > 0$ , we consider a pair velocity-pressure  $(\mathbf{v}, p) \in \mathbf{L}^2(0, T; \mathbf{H}^2(\Omega)) \times \mathbf{L}^2(0, T; \mathbf{H}^1(\Omega))$  solution of the following linearized Navier-Stokes equations:

$$\begin{cases} \partial_t \mathbf{v} - \nu \Delta \mathbf{v} + (\mathbf{z}_1 \cdot \nabla) \mathbf{v} + (\mathbf{v} \cdot \nabla) \mathbf{z}_2 + \nabla p = \mathbf{f} & \text{in } \Omega_T, \\ \operatorname{div} \mathbf{v} = d & \text{in } \Omega_T, \end{cases} \quad (\text{I.2.17})$$

where

$$\Omega_T := \Omega \times (0, T), \quad \mathbf{f} \in \mathbf{L}^2(\Omega_T) \quad \text{and} \quad d \in \mathbf{H}^{1,1/2}(\Omega_T) := \mathbf{L}^2(0, T; \mathbf{H}^1(\Omega)) \cap \mathbf{H}^{1/2}(0, T; \mathbf{L}^2(\Omega)),$$

and

$$\mathbf{z}_1 \in \mathbf{L}^\infty(\Omega_T) \quad \text{and} \quad \mathbf{z}_2 \in \mathbf{L}^\infty(0, T; \mathbf{W}^{1,r}(\Omega)) \quad \text{with} \quad \begin{cases} r > 2 & \text{if } d = 2, \\ r = 3 & \text{if } d = 3. \end{cases}$$

We expect to obtain Carleman inequalities for the non-homogeneous Oseen equations through Carleman inequalities for a pair velocity-pressure in  $\mathbf{L}^2(0, T; \mathbf{H}_0^2(\Omega)) \times \mathbf{L}^2(0, T; \mathbf{H}_0^1(\Omega))$  and the use of a domain extension argument to recover the non-homogeneous case (in the same spirit as what is done in the stationary case).

To be more precise, we could introduce some suitable functions  $\alpha(t, \mathbf{x})$  and  $\varphi(t, \mathbf{x})$  and, using the following notations

$$\hat{\alpha}(t) := \min_{\mathbf{x} \in \Omega} \alpha(t, \mathbf{x}), \quad \tilde{\mathbf{m}}(\mathbf{z}_1, \mathbf{z}_2) := \max \left\{ 1, \|\mathbf{z}_1\|_{\mathbf{L}^\infty(\Omega_T)}, \|\nabla \mathbf{z}_2\|_{\mathbf{L}^\infty(0, T; \mathbf{L}^r(\Omega))} \right\} \quad \text{and} \quad \omega_T := \sigma \times (0, T),$$

we expect to prove a Carleman inequality for the Oseen equations:

$$\begin{cases} \partial_t \mathbf{v} - \nu \Delta \mathbf{v} + (\mathbf{z}_1 \cdot \nabla) \mathbf{v} + (\mathbf{v} \cdot \nabla) \mathbf{z}_2 + \nabla p = \mathbf{f} & \text{in } \Omega_T, \\ \operatorname{div} \mathbf{v} = d & \text{in } \Omega_T, \end{cases} \quad (\text{I.2.18})$$

that is the existence of  $C > 0$ ,  $\hat{c} > 0$  and  $\hat{s} > 1$  such that for all  $\mathbf{z}_1 \in \mathbf{L}^\infty(\Omega_T)$ ,  $\mathbf{z}_2 \in \mathbf{L}^\infty(0, T; \mathbf{W}^{1,r}(\Omega))$ , for all  $\lambda \geq \hat{\lambda} := \tilde{\mathbf{m}}(\mathbf{z}_1, \mathbf{z}_2) \hat{c}$  and for all  $s \geq \hat{s} := \hat{c}(T^m + T^{m-1}/\varepsilon)$ , every solution  $(\mathbf{v}, p)$  of (I.2.18) which belongs to  $\mathbf{L}^2(0, T; \mathbf{H}^2(\Omega)) \times \mathbf{L}^2(0, T; \mathbf{H}^1(\Omega))$  satisfies

$$\begin{aligned} & \int_{\Omega_T} (|\nabla \mathbf{v}|^2 + s\varphi |\operatorname{curl} \mathbf{v}|^2 + s^2 \lambda^2 \varphi^2 |\mathbf{v}|^2) e^{2s\alpha} d\mathbf{x} dt \\ & \leq C \left( \int_{\Omega_T} (s^{-1} \lambda^{-2} \varphi^{-1} |\nabla d|^2 + \lambda^{-2} |\mathbf{f}|^2) e^{2s\alpha} d\mathbf{x} dt + \int_{\omega_T} s^3 \lambda^2 \varphi^3 |\mathbf{v}|^2 e^{2s\alpha} d\mathbf{x} dt \right. \\ & \quad \left. + \lambda^{-2} \int_0^T \left( \|\partial_t \mathbf{v}\|_{\mathbf{L}^2(\Omega)}^2 + \|\mathbf{v}\|_{\mathbf{H}^2(\Omega)}^2 + \|p\|_{\mathbf{H}^1(\Omega)}^2 \right) e^{2s\hat{\alpha}} dt \right) \end{aligned}$$

and

$$\begin{aligned} & \int_{\Omega_T} s\varphi |p - d|^2 e^{2s\alpha} d\mathbf{x} dt \\ & \leq C \left( \int_{\Omega_T} (s^3 \lambda^2 \varphi^3 |\mathbf{v}|^2 + s\varphi |p - d|^2) e^{2s\alpha} d\mathbf{x} dt + \int_{\Omega_T} (s^{-1} \lambda^{-2} \varphi^{-1} |\nabla d|^2 + \lambda^{-2} |\mathbf{f}|^2) e^{2s\alpha} d\mathbf{x} dt \right. \\ & \quad \left. + \lambda^{-2} \int_0^T \left( \|\partial_t \mathbf{v}\|_{\mathbf{L}^2(\Omega)}^2 + \|\mathbf{v}\|_{\mathbf{H}^2(\Omega)}^2 + \|p\|_{\mathbf{H}^1(\Omega)}^2 \right) e^{2s\hat{\alpha}} dt \right). \end{aligned}$$

Then we expect to prove the existence of  $C > 0$ ,  $c^* > 0$  (which depends particularly on  $\mathbf{z}_1$  and  $\mathbf{z}_2$ ) and  $\widehat{\lambda} > 1$  such that, for all  $\lambda \geq \widehat{\lambda}$ ,

$$\begin{aligned} & \|\mathbf{v}\|_{\mathbf{L}^2(\Omega \times (\varepsilon, T-\varepsilon))} \\ & \leq C \frac{e^{e^{c^* \lambda}(1+1/(T\varepsilon))} (\|\mathbf{v}\|_{\mathbf{H}^{2,1}(\Omega_T)} + \|p\|_{\mathbf{L}^2(0,T;\mathbf{H}^1(\Omega))})}{\ln \left( 1 + \frac{\|\mathbf{v}\|_{\mathbf{H}^{2,1}(\Omega_T)} + \|p\|_{\mathbf{L}^2(0,T;\mathbf{H}^1(\Omega))}}{\|\mathbf{f}\|_{\mathbf{L}^2(\Omega_T)} + \|\nabla d\|_{\mathbf{L}^2(\Omega)} + \|\mathbf{v}\|_{\mathbf{H}^{3/2,3/4}(\Gamma_{\text{obs},T})} + \|\sigma(\mathbf{v}, p) \mathbf{n}\|_{\mathbf{H}^{1/2,1/4}(\Gamma_{\text{obs},T})}} \right)} \end{aligned}$$

and

$$\begin{aligned} & \|\text{curl } \mathbf{v}\|_{\mathbf{L}^2(\Omega \times (\varepsilon, T-\varepsilon))} + \|p - \text{div } \mathbf{v}\|_{\mathbf{L}^2(\Omega \times (\varepsilon, T-\varepsilon))} \\ & \leq C \frac{e^{e^{c^* \lambda}(1+1/(T\varepsilon))} (\|\mathbf{v}\|_{\mathbf{H}^{2,1}(\Omega_T)} + \|p\|_{\mathbf{L}^2(0,T;\mathbf{H}^1(\Omega))})}{\left( \ln \left( 1 + \frac{\|\mathbf{v}\|_{\mathbf{H}^{2,1}(\Omega_T)} + \|p\|_{\mathbf{L}^2(0,T;\mathbf{H}^1(\Omega))}}{\|\mathbf{f}\|_{\mathbf{L}^2(\Omega_T)} + \|\nabla d\|_{\mathbf{L}^2(\Omega)} + \|\mathbf{v}\|_{\mathbf{H}^{3/2,3/4}(\Gamma_{\text{obs},T})} + \|\sigma(\mathbf{v}, p) \mathbf{n}\|_{\mathbf{H}^{1/2,1/4}(\Gamma_{\text{obs},T})}} \right) \right)^{1/2}}, \end{aligned}$$

where  $\Gamma_{\text{obs},T} := \Gamma_{\text{obs}} \times (0, T)$ .



---

---

## Chapter II

---

# Some new approaches for the detection of immersed objects in 2D

The works exposed in the second part of the previous chapter (see Section I.2) quantify the instability of an inverse problem, that is the reconstruction of the solution of a PDE from Cauchy data. In my PhD thesis [82] (see also my previous works [32, 81, 83, 89]), we proved that the *inverse obstacle problem*, for the Stokes and Navier-Stokes equations, is ill-posed. This is proved through a local regularity argument showing that the Riesz operator associated to the shape Hessian of the considered shape functional (a least squares functional or a Kohn-Vogelius functional) is compact. This theoretical result explains why we need to use a *regularization method* in order to numerically reconstruct the inclusion. This chapter presents two approaches in order to numerically solve the inverse obstacle problem and summarizes the two following articles:

- [84] F. Caubet, C. Conca and M. Godoy. On the detection of several obstacles in 2D Stokes flow: topological sensitivity and combination with shape derivatives. *Inverse Probl. Imaging*, 10(2):327–367, 2016;
- [56] P. Bonnelie, L. Bourdin, F. Caubet and O. Ruatta. Flip procedure in geometric approximation of multiple-component shapes – application to multiple-inclusion detection. *SMAI J. Comput. Math.*, 2:255–276, 2016.

The simplest way to regularize a shape cost functional in order to solve the inverse obstacle problem is to parametrize the shape by a truncated Fourier series and to use the classical *geometrical shape optimization approach*. This is for instance done in [8, 89]. This enables to reconstruct an approximation of the shape, using a descent method. One can reconstruct several obstacles, if the number of obstacles is given. Indeed this geometrical method does not enable to modify the topology of the domain and is commonly based on successive shape deformations, where the boundary of the approximated shape is parametrized and evolves at each step in a direction given by the deformation flow. Hence, for the geometric approximation of multiple-component shapes, especially when the number of components is *a priori* unknown, starting a parametrization method with a one-component initial shape in order to approximate a multiple-component target shape usually leads the deformation flow to make the boundary evolve until it surrounds all the components of the target shape (see Figure II.0.1 for illustrations). This classical phenomenon tends to create double points on the boundary of the approximated shape.

Several alternatives exist, with its own advantages and drawbacks, that depend on the nature of the problem studied. One can mention the recent developments on topological sensitivity based iterative schemes made by Carpio *et al.* in [78–80]. We also refer to some works using the level set method by Lesselier *et al.* in [119, 120, 174]. Combinations of several shape optimization methods was also recently tested by several authors. Allaire *et al.* propose in [17] to couple the classical geometrical shape optimization through the level set method and the topological gradient in order to minimize the

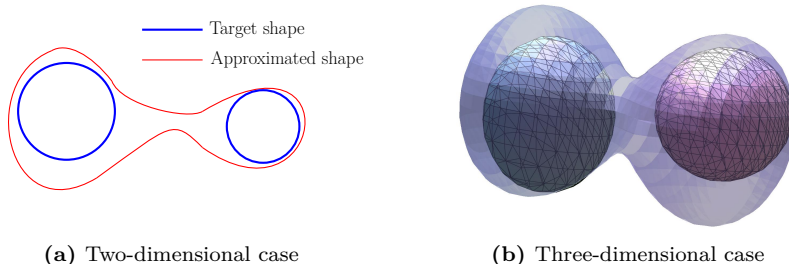


**Figure II.0.1** – Geometrical shape approximation of a two-component target shape starting from a one-component initial shape.

compliance. The same combination is made for another problem by He *et al.* in [150] or by Burger *et al.* in [71] for inverse problems. Concerning the minimization of the compliance, Pantz *et al.* propose in [184] an algorithm using boundary variations, topological derivatives and homogenization methods (without a level set approach). We can also mention the work of Christiansen *et al.* in [97] which couples topological and boundary variations approaches.

*In this chapter, two methods are explored in order to improve the approximation of multiple-component shapes, especially concerning the two dimensional case: a mixed method (see Section II.1) and a parametrization method (see Section II.2).* Firstly a blending method coupling the geometrical and the topological approaches is performed. In this part one of the difficulty is the obtention of the *topological asymptotic expansion* of the solution of the Stokes system for the two dimensional case. Then this method allows to numerically find the number of objects, their relative location and their approximative shape. Secondly a numerical method based on a Bézier parametrization is established. The main idea is that this polynomial parametrization can be approximated by its *control polygon*. This enables to prevent the potential formation of double points, i.e. to locate the parts of the boundary that are close to each other and this parametrization is suitable in order to easily change the topology of the approximated shape, precisely in order to divide a one-component shape into a two-component shape.

## II.1 A blending method

This section focuses on the inverse obstacle problem for a two-dimensional Stokes flow using a topological sensibility analysis and a combination with shape derivatives. This work was done in collaboration with Carlos Conca and Matías Godoy (university of Chile) as part of the PhD thesis of Matías Godoy, and is published in *Inverse Problems and Imaging* (see [84], 41 pages).

### II.1.1 Aims and main difficulties of the dimension two

The two main shape optimization techniques used in order to study the inverse obstacle problem in the literature are *topological* and *geometrical* shape optimization methods. The *topological* gradient approach was introduced by Schumacher in [199] and Sokolowski *et al.* in [209]. This method is based on asymptotic expansions and consequently is essentially appropriate to relatively small inclusions. Moreover, even if the topological optimization is useful in order to find the number of inclusions, it may be not well-suited in order to find a satisfactory approximation of the shape of the inclusions (see, e.g., [85] and references therein; see also [20] and references therein for a comprehensive mathematical treatment with theoretical and numerical results about reconstruction of small inclusions from boundary measurements). In the *geometrical* shape optimization category, two main techniques are

addressed in the literature. They are both based on the computation of a shape gradient used as a flow making the shape evolve. These two methods use different representations of the shape and different techniques to deform it. The first approach is the so-called level set approach (see, e.g., the survey [72] of Burger *et al.* and references therein, or [202]). It is originally based on an implicit representation of the approximated shape on a fixed mesh and, in the case of inverse problems, some regularization methods are usually needed (as curve shortening in, e.g., [197, Section 8]). In order to detect several inclusions, this method does not need any *a priori* knowledge on the number of inclusions. The second approach is based on boundary variations *via* mesh variations and, in the case of inverse problems, on an explicit representation of the approximated shape. This method is used e.g. in the work [7] of Afraites *et al.* (where a regularization by parametrization is used). Note that the standard algorithm based on shape derivatives moving the mesh does not provide the opportunity to change the topology of the shape and consequently the number of inclusions has to be known in advance.

In order to numerically solve the inverse obstacle problem, detecting both the topology (i.e. the number of obstacles) and the shape of the inclusions, recent works propose to mix several shape optimization approaches (see, e.g., the non-exhaustive list of references given in the introduction of this chapter). The aim of our approach is to couple a topological gradient method with a classical shape gradient method for the detection of immersed obstacles in a two dimensional Stokes flow. In order to reconstruct the obstacle(s), we assume that a Cauchy pair is given on a part of the surface of the fluid, that is a Dirichlet boundary condition and the measurement of the Cauchy forces. Hence the identifiability result of Alvarez *et al.* [19, Theorem 1.2] implies that this problem could be seen as the minimisation of a cost functional, which in our case will be a Kohn-Vogelius type cost functional.

Notice that this inverse obstacle problem arises, for instance, in mold filling during which small gas bubbles can be created and trapped inside the material (as it is mentioned in [44]). We can also mention the fact that the most common devices used to spot immersed bodies, such as submarines or banks of fish, are sonars, using acoustic waves: active sonars emit acoustic waves (making themselves detectable), while passive sonars only listen (and can only detect targets that are noisy enough). To overcome those limitations, one wants to design systems imitating the *lateral line systems* of fish, a sense organ they use to detect movement and vibration in the surrounding water (as emphasized in [105]).

Topological sensitivity analysis related to Stokes equations have been studied in the past by several authors, especially relevant are the works of Guillaume *et al.* [140], Maatoug [149], Amstutz [21] with steady-state Navier-Stokes equations and [22] with generalization for some non-linear systems and Sid Idris [205] which develops a detailed work in the two-dimensional case. In all of these works the focus is set to find topological asymptotic expansions for a general class of functionals where the system satisfies only Dirichlet boundary conditions. Closer works to our problem have been presented in the past by Ben Abda *et al.* [44] and in my previous work [85]. In the first reference they consider a Neumann boundary condition on the small objects obtaining general results in two and three dimensional cases, with a complete development of the theory only in the three dimensional case. In [85] we deal with the same problem as the one we consider here but only again in the three-dimensional case.

In our two-dimensional case, due to the impossibility to have an asymptotic expansion of the solution of Stokes equations by means of an exterior problem (phenomena which is related to the Stokes paradox), we have to approximate it by means of a different problem. The deduction of this approximation is influenced by the work of Bonnaillie-Noël *et al.* [53]. Indeed the same problem appears for Laplace's equation: it is based on the fact that the existence of a solution of the boundary value problem

$$\begin{cases} -\Delta V = 0 & \text{in } \mathbb{R}^2 \setminus \bar{\omega}, \\ V = u_0(\mathbf{z}) & \text{on } \partial\omega, \\ V \rightarrow 0 & \text{at infinity,} \end{cases} \quad (\text{II.1.1})$$

is not guaranteed except when  $u_0(\mathbf{z}) = 0$ . The classical analysis of elliptic equation in unbounded domain is made in the functional setting of weighted Sobolev spaces. It is known that (II.1.1) has a

unique solution in a space containing the constants, hence this solution is the constant  $u_0(\mathbf{z})$  which prohibits the condition at infinity if  $u_0(\mathbf{z}) \neq 0$ . Taking this into account, we can define the asymptotic expansion for the Stokes system which is a crucial part in order to obtain the desired expansion for the functional involved. It is important to remark that (for a given real number  $u_0(\mathbf{z})$ ) several technical results which lead to the main result are different to the ones in the three-dimensional setting which involves additional difficulties to our problem.

From the obtained theoretical results, we present some numerical simulations and propose an algorithm which joins the topological optimization procedure with the classical shape optimization method using the computation of the shape gradient for the Kohn-Vogelius functional made in my previous work [89]. This blending method allows not only to obtain the number and qualitative location of the objects, moreover it allows to approximate their shapes.

### II.1.2 Setting of the problem

Let  $\Omega$  be a bounded Lipschitz open set of  $\mathbb{R}^2$  containing a Newtonian and incompressible fluid with a constant coefficient of kinematic viscosity  $\nu > 0$ . Let  $\omega \subset \mathbb{R}^2$  a fixed bounded Lipschitz domain containing the origin. For  $\mathbf{z} \in \Omega$  and  $0 < \varepsilon \ll 1$ , we denote

$$\omega_{\mathbf{z},\varepsilon} := \mathbf{z} + \varepsilon\omega.$$

The aim of this work is to detect some unknown objects included in  $\Omega$ . We assume that a finite number  $m^*$  of obstacles  $\omega_{\mathbf{z}_i,\varepsilon}^* \subset \Omega$  have to be detected. Moreover we assume that they are well separated (that is:  $\overline{\omega_{\mathbf{z}_i,\varepsilon_i}^*} \cap \overline{\omega_{\mathbf{z}_j,\varepsilon_j}^*} = \emptyset$  for all  $1 \leq i, j \leq m^*$  with  $i \neq j$ ) and have the geometry form

$$\omega_{\mathbf{z}_k,\varepsilon_k}^* = \mathbf{z}_k^* + \varepsilon_k \omega_k^*, \quad 1 \leq k \leq m^*,$$

where  $\varepsilon_k$  is the diameter and  $\omega_k^* \subset \mathbb{R}^2$  are bounded Lipschitz domains containing the origin. The points  $\mathbf{z}_k^* \in \Omega$ ,  $1 \leq k \leq m^*$ , determine the location of the objects. Finally we assume that, for all  $1 \leq k \leq m^*$ ,  $\omega_{\mathbf{z}_k,\varepsilon_k}^*$  is far from the boundary  $\partial\Omega$ .

Let  $\mathbf{g}_D \in \mathbf{H}^{1/2}(\partial\Omega)$  such that  $\mathbf{g}_D \neq \mathbf{0}$  satisfying the compatibility condition

$$\int_{\partial\Omega} \mathbf{g}_D \cdot \mathbf{n} = 0.$$

In order to determine the location of the objects, we make a measurement  $\mathbf{g}_N \in \mathbf{H}^{-1/2}(\Gamma_{\text{obs}})$  on a part  $\Gamma_{\text{obs}}$  of the exterior boundary  $\partial\Omega$  with  $\Gamma_{\text{obs}} \subset \partial\Omega$ ,  $\Gamma_{\text{obs}} \neq \partial\Omega$ . Then we denote  $\omega_\varepsilon^* := \bigcup_{k=1}^{m^*} \omega_{\mathbf{z}_k,\varepsilon_k}^*$  and consider the following overdetermined Stokes problem

$$\left\{ \begin{array}{ll} -\nu\Delta \mathbf{u} + \nabla p = \mathbf{0} & \text{in } \Omega \setminus \overline{\omega_\varepsilon^*}, \\ \operatorname{div} \mathbf{u} = 0 & \text{in } \Omega \setminus \overline{\omega_\varepsilon^*}, \\ \mathbf{u} = \mathbf{g}_D & \text{on } \partial\Omega, \\ \mathbf{u} = \mathbf{0} & \text{on } \partial\omega_\varepsilon^*, \\ \sigma(\mathbf{u}, p)\mathbf{n} = \mathbf{g}_N & \text{on } \Gamma_{\text{obs}} \subset \partial\Omega. \end{array} \right. \quad (\text{II.1.2})$$

Here  $\sigma(\mathbf{u}, p)$  represents the *stress tensor* defined by  $\sigma(\mathbf{u}, p) := 2\nu\mathcal{D}(\mathbf{u}) - p\mathbf{I}$ , with  $\mathcal{D}(\mathbf{u}) := \frac{1}{2}(\nabla\mathbf{u} + {}^t\nabla\mathbf{u})$ . Thus we consider the following geometric inverse problem:

$$\text{Find } \omega_\varepsilon^* \subset \subset \Omega \text{ and a pair } (\mathbf{u}, p) \text{ which satisfy the overdetermined problem (II.1.2).} \quad (\text{II.1.3})$$

To study this inverse problem, we consider two forward problems:

$$\left\{ \begin{array}{l} \text{Find } (\mathbf{u}_D^\varepsilon, p_D^\varepsilon) \in \mathbf{H}^1(\Omega \setminus \overline{\omega_\varepsilon}) \times L_0^2(\Omega \setminus \overline{\omega_\varepsilon}) \text{ such that} \\ -\nu\Delta \mathbf{u}_D^\varepsilon + \nabla p_D^\varepsilon = \mathbf{0} & \text{in } \Omega \setminus \overline{\omega_\varepsilon}, \\ \operatorname{div} \mathbf{u}_D^\varepsilon = 0 & \text{in } \Omega \setminus \overline{\omega_\varepsilon}, \\ \mathbf{u}_D^\varepsilon = \mathbf{g}_D & \text{on } \partial\Omega, \\ \mathbf{u}_D^\varepsilon = \mathbf{0} & \text{on } \partial\omega_\varepsilon, \end{array} \right. \quad (\text{II.1.4})$$

and

$$\left\{ \begin{array}{l} \text{Find } (\mathbf{u}_N^\varepsilon, p_N^\varepsilon) \in \mathbf{H}^1(\Omega \setminus \overline{\omega_\varepsilon}) \times L^2(\Omega \setminus \overline{\omega_\varepsilon}) \text{ such that} \\ -\nu \Delta \mathbf{u}_N^\varepsilon + \nabla p_N^\varepsilon = \mathbf{0} \quad \text{in } \Omega \setminus \overline{\omega_\varepsilon}, \\ \operatorname{div} \mathbf{u}_N^\varepsilon = 0 \quad \text{in } \Omega \setminus \overline{\omega_\varepsilon}, \\ \sigma(\mathbf{u}_N^\varepsilon, p_N^\varepsilon) \mathbf{n} = \mathbf{g}_N \quad \text{on } \Gamma_{\text{obs}}, \\ \mathbf{u}_N^\varepsilon = \mathbf{g}_D \quad \text{on } \partial \Omega \setminus \overline{\Gamma_{\text{obs}}}, \\ \mathbf{u}_N^\varepsilon = \mathbf{0} \quad \text{on } \partial \omega_\varepsilon, \end{array} \right. \quad (\text{II.1.5})$$

where  $\omega_\varepsilon := \bigcup_{k=1}^m \omega_{z_k, \varepsilon_k}$  for a finite number  $m$  of objects located in  $\mathbf{z}_1, \dots, \mathbf{z}_m$ . These two forward problems are classically well-defined (see, e.g., [69, 138] concerning (II.1.4) and [85, Theorem A.1] concerning (II.1.5)).

One can remark that if  $\omega_\varepsilon$  coincides with the actual domain  $\omega_\varepsilon^*$ , then  $\mathbf{u}_D^\varepsilon = \mathbf{u}_N^\varepsilon$  in  $\Omega \setminus \overline{\omega_\varepsilon}$ . According to this observation, we propose a resolution of the inverse problem (II.1.3) of reconstructing  $\omega_\varepsilon^*$  based on the minimization of the following Kohn-Vogelius functional

$$\mathcal{K}(\Omega \setminus \overline{\omega_\varepsilon}) := \frac{1}{2} \int_{\Omega \setminus \overline{\omega_\varepsilon}} \nu |\mathcal{D}(\mathbf{u}_D^\varepsilon) - \mathcal{D}(\mathbf{u}_N^\varepsilon)|^2.$$

We can notice that, integrating by parts the expression of  $\mathcal{K}(\Omega \setminus \overline{\omega_\varepsilon})$ , we get that

$$\mathcal{K}(\Omega \setminus \overline{\omega_\varepsilon}) = \nu \int_{\Gamma_{\text{obs}}} (\mathbf{g}_D - \mathbf{u}_N^\varepsilon) \cdot (\sigma(\mathbf{u}_D^\varepsilon, p_D^\varepsilon) \mathbf{n} - \mathbf{g}_N).$$

This expression shows that the error can be expressed by an integral involving only the part of the boundary where we make the measurement and reveals the coupling of the solutions *via* this functional. Finally we can notice that the Dirichlet error is weighted by the Neumann error, and *vice versa*.

**Remark II.1.1.** *In order to guarantee that the inverse problem of finding  $\omega_\varepsilon^*$  and a pair  $(\mathbf{u}, p)$  satisfying (II.1.2) has a solution, we have to assume the existence of such a  $\omega_\varepsilon^*$ . This means that the measurement  $\mathbf{g}_N$  is perfect, that is to say without error. Then, according to the identifiability result [19, Theorem 1.2] proved by Alvarez et al., the domain  $\omega_\varepsilon^*$  is unique. Hence, if we find  $\omega_\varepsilon^*$  such that  $\mathcal{K}(\Omega \setminus \omega_\varepsilon^*) = 0$ , then  $\mathbf{u}_D^\varepsilon = \mathbf{u}_N^\varepsilon$  in  $\Omega \setminus \omega_\varepsilon^*$ , i.e.  $\mathbf{u}_D^\varepsilon$  satisfies (II.1.2) and thus  $\omega_\varepsilon = \omega_\varepsilon^*$  is the real domain.*

For  $\varepsilon = 0$ , we consider as a convention that  $\omega_0 = \emptyset$  (instead of  $\omega_0 = \bigcup_{k=1}^m \{z_k\}$ , which comes from the definition of  $\omega_\varepsilon$ ), and therefore:  $\Omega_0 = \Omega$ . Then we denote  $(\mathbf{u}_D^0, p_D^0) \in \mathbf{H}^1(\Omega) \times L_0^2(\Omega)$  and  $(\mathbf{u}_N^0, p_N^0) \in \mathbf{H}^1(\Omega) \times L^2(\Omega)$  the respective solutions of the following systems:

$$\left\{ \begin{array}{l} -\nu \Delta \mathbf{u}_D^0 + \nabla p_D^0 = \mathbf{0} \quad \text{in } \Omega, \\ \operatorname{div} \mathbf{u}_D^0 = 0 \quad \text{in } \Omega, \\ \mathbf{u}_D^0 = \mathbf{g}_D \quad \text{on } \partial \Omega, \end{array} \right. \quad \text{and} \quad \left\{ \begin{array}{l} -\nu \Delta \mathbf{u}_N^0 + \nabla p_N^0 = \mathbf{0} \quad \text{in } \Omega, \\ \operatorname{div} \mathbf{u}_N^0 = 0 \quad \text{in } \Omega, \\ \sigma(\mathbf{u}_N^0, p_N^0) \mathbf{n} = \mathbf{g}_N \quad \text{on } \Gamma_{\text{obs}}, \\ \mathbf{u}_N^0 = \mathbf{g}_D \quad \text{on } \partial \Omega \setminus \overline{\Gamma_{\text{obs}}}. \end{array} \right.$$

### II.1.3 Main results

From now on, we consider that we seek a single obstacle  $\omega_{z, \varepsilon} := \mathbf{z} + \varepsilon \omega$ , located at a point  $\mathbf{z} \in \Omega$ . Notice that in the case of several inclusions, we proceed by detecting the objects one by one. Thus, after detecting a first obstacle  $\omega_{z_1, \varepsilon_1}$ , we work replacing the whole domain  $\Omega$  by  $\Omega \setminus \overline{\omega_{z_1, \varepsilon_1}}$  (and then we have  $\partial \omega_{z_1, \varepsilon_1} \subset \partial(\Omega \setminus \overline{\omega_{z_1, \varepsilon_1}}) \setminus \overline{\Gamma_{\text{obs}}}$ ) and the results presented below (particularly the topological derivative) are still valid for a new inclusion  $\omega_{z, \varepsilon}$ . Note that the asymptotic expansion of the solution of elliptic boundary value problem in multiply perforated domains is studied in [55, 180].

We recall that the topological sensitivity analysis consists in studying the variations of a design functional  $\mathcal{F}$  with respect to the insertion of a small obstacle  $\omega_{z, \varepsilon}$  at the point  $\mathbf{z} \in \Omega$  (with no-slip boundary conditions). The aim is to obtain an asymptotic expansion of  $\mathcal{F}$  of the form

$$\mathcal{F}(\Omega_{z, \varepsilon}) = \mathcal{F}(\Omega) + \xi(\varepsilon) \delta \mathcal{F}(\mathbf{z}) + o(\xi(\varepsilon)), \quad \forall \mathbf{z} \in \Omega, \quad (\text{II.1.6})$$

where  $\varepsilon > 0$ ,  $\xi$  is a positive scalar function intended to tend to zero with  $\varepsilon$  and where

$$\Omega_{z,\varepsilon} := \Omega \setminus \overline{\omega_{z,\varepsilon}}, \quad \text{with } \omega_{z,\varepsilon} := z + \varepsilon\omega.$$

We summarize the notations concerning the domains in Figure II.1.2.

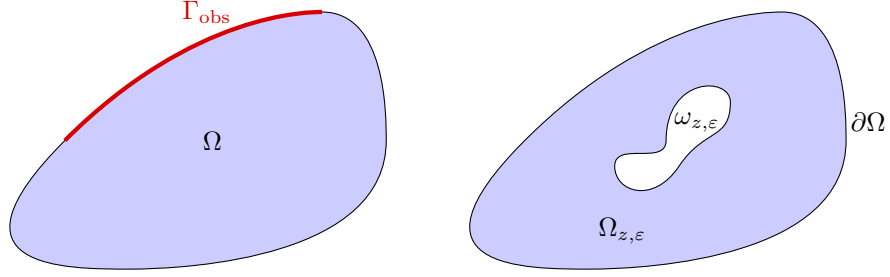


Figure II.1.2 – The initial domain and the same domain after inclusion of an object

The computation of the topological gradient  $\delta\mathcal{F}$  in this work is mainly based on my previous work [85] which deals with the presented problem in the three-dimensional setting. The work of Bonnaillie-Noël *et al.* [53], which deals with asymptotic expansions for Laplace's equation in a domain with several obstacles, was the basis for the choice of the approximating problem in the two-dimensional setting. We also have been inspired by the works of Guillaume *et al.* [139, 140], where the authors study topological asymptotic expansions for Laplace and Stokes equations in two and three dimensions. Finally, let us point out the works of Amstutz [21, 22], where the author develops a topological asymptotic expansion for a cost functional in the context of a fluid governed by the stationary Navier-Stokes equations, which contribute to understand better the possibilities for the asymptotic expansion of the solutions for our considered systems. It is important to underline that in all these situations the problem involves only Dirichlet boundary conditions.

We recall the expression of the fundamental solution  $(E, \mathbf{P})$  to the Stokes system in  $\mathbb{R}^2$  given by

$$E(\mathbf{x}) = \frac{1}{4\pi\nu} (-\log \|\mathbf{x}\| \mathbf{I} + \mathbf{s}_r {}^t \mathbf{s}_r), \quad \mathbf{P}(\mathbf{x}) = \frac{\mathbf{x}}{2\pi \|\mathbf{x}\|^2}, \quad (\text{II.1.7})$$

with  $\mathbf{s}_r := \frac{\mathbf{x}}{\|\mathbf{x}\|}$ ; that is  $-\nu\Delta E_j + \nabla P_j = \delta \mathbf{e}_j$ , where  $E_j$  denotes the  $j^{\text{th}}$  column of  $E$ ,  $(\mathbf{e}_j)_{j=1}^2$  is the canonical basis of  $\mathbb{R}^2$  and  $\delta$  is here the Dirac distribution.

### II.1.3.1 Asymptotic expansion of the solution of the Stokes problem

In order to provide an asymptotic expansion of the Kohn-Vogelius functional  $\mathcal{K}$ , we first obtain an asymptotic expansion of the solution of the Stokes problems (II.1.4) and (II.1.5). This section gives the idea of the proof of the following result.

**Proposition II.1.2.** *The respective solutions  $\mathbf{u}_D^\varepsilon \in \mathbf{H}^1(\Omega_{z,\varepsilon})$  and  $\mathbf{u}_N^\varepsilon \in \mathbf{H}^1(\Omega_{z,\varepsilon})$  of Problems (II.1.4) and (II.1.5) admit the following asymptotic expansions (with the subscript  $\natural = D$  and  $\natural = N$  respectively):*

$$\mathbf{u}_\natural^\varepsilon(\mathbf{x}) = \mathbf{u}_\natural^0(\mathbf{x}) + \frac{1}{-\log \varepsilon} (\mathbf{C}_\natural(\mathbf{x}) - \mathbf{U}_\natural(\mathbf{x})) + O_{\mathbf{H}^1(\Omega_{z,\varepsilon})} \left( \frac{1}{-\log \varepsilon} \right),$$

where  $(\mathbf{U}_\natural, P_\natural) \in \mathbf{H}^1(\Omega) \times L_0^2(\Omega)$  solves the following Stokes problem defined in the whole domain  $\Omega$

$$\begin{cases} -\nu\Delta \mathbf{U}_\natural + \nabla P_\natural = \mathbf{0} & \text{in } \Omega, \\ \operatorname{div} \mathbf{U}_\natural = 0 & \text{in } \Omega, \\ \mathbf{U}_\natural = \mathbf{C}_\natural & \text{on } \partial\Omega, \end{cases} \quad (\text{II.1.8})$$

with  $\mathbf{C}_{\mathfrak{h}}(\mathbf{x}) := -4\pi\nu E(\mathbf{x} - \mathbf{z})\mathbf{u}_{\mathfrak{h}}^0(\mathbf{z})$ , where  $E$  is the fundamental solution of the Stokes equations in  $\mathbb{R}^2$  given by (II.1.7). The notation  $O_{\mathbf{H}^1(\Omega_{z,\varepsilon})}\left(\frac{1}{-\log\varepsilon}\right)$  means that there exist a constant  $C > 0$  (independent of  $\varepsilon$ ) and  $\varepsilon_1 > 0$  such that, for all  $0 < \varepsilon < \varepsilon_1$ ,

$$\left\| \mathbf{u}_{\mathfrak{h}}^\varepsilon(\mathbf{x}) - \mathbf{u}_{\mathfrak{h}}^0(\mathbf{x}) - \frac{1}{-\log\varepsilon}(\mathbf{C}_{\mathfrak{h}}(\mathbf{x}) - \mathbf{U}_{\mathfrak{h}}(\mathbf{x})) \right\|_{\mathbf{H}^1(\Omega_{z,\varepsilon})} \leq \frac{C}{-\log\varepsilon}.$$

As previously mentioned, the two-dimensional problem cannot be approximated by an exterior problem, which in general in this case does not admit a solution which vanishes at infinity. Then the approximation has to be done in a different setting compared to the three-dimensional case, following the same strategy as in [53] (which concerns the Laplace's equation in the plane). This basically consists in building a correction term to the solution given by  $E(\mathbf{x} - \mathbf{z})\mathbf{u}_{\mathfrak{h}}^0$  which has a logarithmic term and then tends to infinity at infinity and is not of finite energy in  $\mathbb{R}^2 \setminus \overline{\omega}$ . Therefore it has to be considered only in  $\Omega$ . To this, we consider the pair  $(\mathbf{U}_{\mathfrak{h}}, \mathbf{P}_{\mathfrak{h}}) \in \mathbf{H}^1(\Omega) \times L_0^2(\Omega)$  solution of Problem (II.1.8) and we combine these solutions with unknown scale parameters  $a(\varepsilon)$  and  $b(\varepsilon)$ . Imposing the desired scales to the error function, we will be able to determine the scale factors  $a(\varepsilon)$  and  $b(\varepsilon)$  which define completely the approximation for  $\mathbf{u}_{\mathfrak{h}}^\varepsilon$ . Here we expose the Dirichlet case, the treatment of Neumann case is analog. In order to simplify the reading, we assume for this part that  $\mathbf{z} = \mathbf{0}$  (the general case is analog) and we use the notation  $\Omega_\varepsilon := \Omega_{0,\varepsilon}$ .

Consider the solution  $(\mathbf{U}_D, \mathbf{P}_D) \in \mathbf{H}^1(\Omega) \times L_0^2(\Omega)$  of Problem (II.1.8) with  $\mathfrak{h} = D$ . The idea is to combine this solution and the function  $\mathbf{C}_D$  to build a proper corrector. To build this, we search coefficients  $a(\varepsilon)$  and  $b(\varepsilon)$  such that the error  $\mathbf{r}_D^\varepsilon$  defined by

$$\mathbf{u}_D^\varepsilon(\mathbf{x}) = \mathbf{u}_D^0(\mathbf{x}) + a(\varepsilon)\mathbf{C}_D(\mathbf{x}) + b(\varepsilon)\mathbf{U}_D(\mathbf{x}) + \mathbf{r}_D^\varepsilon(\mathbf{x})$$

is reduced with respect to  $\mathbf{R}_D^\varepsilon := \mathbf{u}_D^\varepsilon - \mathbf{u}_D^0$ . Notice that the remainder  $\mathbf{r}_D^\varepsilon$  satisfies:

$$\begin{cases} -\nu\Delta\mathbf{r}_D^\varepsilon + \nabla p_{r_D^\varepsilon} = \mathbf{0} & \text{in } \Omega_\varepsilon, \\ \operatorname{div}\mathbf{r}_D^\varepsilon = 0 & \text{in } \Omega_\varepsilon, \\ \mathbf{r}_D^\varepsilon = -(a(\varepsilon) + b(\varepsilon))\mathbf{C}_D(\mathbf{x}) & \text{on } \partial\Omega, \\ \mathbf{r}_D^\varepsilon = -\mathbf{u}_D^0(\mathbf{x}) - a(\varepsilon)\mathbf{C}_D(\mathbf{x}) - b(\varepsilon)\mathbf{U}_D(\mathbf{x}) & \text{on } \partial\omega_\varepsilon, \end{cases}$$

where  $p_{r_D^\varepsilon}$  is defined in analogous way with pressure terms, that is

$$p_{r_D^\varepsilon}(\mathbf{x}) := p_D^\varepsilon(\mathbf{x}) - p_D^0(\mathbf{x}) - a(\varepsilon)\Pi_D(\mathbf{x}) - b(\varepsilon)P_D(\mathbf{x}),$$

with  $\Pi_D(\mathbf{x}) := -4\pi\nu\mathbf{P}(\mathbf{x}) \cdot \mathbf{u}_D^0(\mathbf{0})$ .

For  $\mathbf{x} \in \partial\Omega$ , we have

$$\mathbf{r}_D^\varepsilon(\mathbf{x}) = o(\mathbf{1}) \Leftrightarrow a(\varepsilon) + b(\varepsilon) = o(1).$$

Let us assume for a while that  $\omega$  is a disk. Then, for  $\mathbf{x} \in \partial\omega_\varepsilon$ , there exists  $\mathbf{X} \in \partial B(0,1)$  such that  $\mathbf{x} = \varepsilon\mathbf{X}$  and we have

$$\mathbf{r}_D^\varepsilon(\mathbf{x}) = o(\mathbf{1}) \Leftrightarrow -\mathbf{u}_D^0(\varepsilon\mathbf{X}) - a(\varepsilon)\mathbf{C}_D(\varepsilon\mathbf{X}) - b(\varepsilon)\mathbf{U}_D(\varepsilon\mathbf{X}) = o(\mathbf{1}).$$

We can expand the terms  $\mathbf{U}_D(\varepsilon\mathbf{X})$  and  $\mathbf{u}_D^0(\varepsilon\mathbf{X})$  via Taylor developments:

$$\mathbf{u}_D^0(\varepsilon\mathbf{X}) = \mathbf{u}_D^0(\mathbf{0}) + O(\varepsilon) \quad \text{and} \quad \mathbf{U}_D(\varepsilon\mathbf{X}) = \mathbf{U}_D(\mathbf{0}) + O(\varepsilon),$$

and thus we get (noticing that  $O(\varepsilon)$  is contained in  $o(1)$ ):

$$\mathbf{r}_D^\varepsilon(\mathbf{x}) = o(\mathbf{1}) \Leftrightarrow -\mathbf{u}_D^0(\mathbf{0}) - a(\varepsilon)\mathbf{C}_D(\varepsilon\mathbf{X}) - b(\varepsilon)\mathbf{U}_D(\mathbf{0}) = o(\mathbf{1}).$$

Therefore we have the linear system in unknowns  $(a(\varepsilon), b(\varepsilon))$ :

$$\begin{cases} a(\varepsilon) + b(\varepsilon) = 0, \\ a(\varepsilon) \mathbf{C}_D(\varepsilon \mathbf{X}) + b(\varepsilon) \mathbf{U}_D(\mathbf{0}) = -\mathbf{u}_D^0(\mathbf{0}). \end{cases}$$

We easily get that  $b(\varepsilon) = -a(\varepsilon)$  which implies

$$a(\varepsilon) (\mathbf{C}_D(\varepsilon \mathbf{X}) - \mathbf{U}_D(\mathbf{0})) = -\mathbf{u}_D^0(\mathbf{0}).$$

This vectorial equality implies two possible choices for  $a(\varepsilon)$ : recalling  $\mathbf{C}_D(\varepsilon \mathbf{X}) = -4\pi\nu E(\varepsilon \mathbf{X}) \mathbf{u}_D^0(\mathbf{0})$ , we get (for  $i, j \in \{1, 2\}, i \neq j$ )

$$a(\varepsilon) = \frac{(\mathbf{u}_D^0(\mathbf{0}))_i}{c_1 (\mathbf{u}_D^0(\mathbf{0}))_i - \log \varepsilon \cdot (\mathbf{u}_D^0(\mathbf{0}))_i + c_2 (\mathbf{u}_D^0(\mathbf{0}))_j + (\mathbf{U}_D(\mathbf{0}))_i},$$

where  $c_1$  and  $c_2$  are two positive constants. This leads that  $a(\varepsilon)$  can be expressed as  $a(\varepsilon) = \frac{1}{C - \log \varepsilon}$  for another positive constant denoted by  $C$  in the two possible cases, and then we get the following scale:

$$\frac{1}{-\log \varepsilon} + O\left(\frac{1}{\log^2 \varepsilon}\right) \quad \text{as } \varepsilon \rightarrow 0.$$

It is important to notice, as been pointed in [53, Remark 2.2], that this construction is performed in the case of a disk, where  $\|\mathbf{x}\| = \varepsilon$  for  $\mathbf{x} \in \partial\omega_\varepsilon$ . In the general case,  $\omega$  is not a ball and then  $\log \|\mathbf{x}\| \neq \log \varepsilon$  for all  $\mathbf{x} \in \partial\omega_\varepsilon$  and one has to add correctors as performed by Maz'ya *et al.* in [181, Section 2.4, p. 60–64]. This correction of  $\log \varepsilon$  is of order zero and is then negligible with respect to the logarithmic term. Thus the linear system in  $(a(\varepsilon), b(\varepsilon))$  remains unchanged.

Hence we approximate  $\mathbf{u}_D^\varepsilon$  by

$$\mathbf{u}_D^\varepsilon(\mathbf{x}) = \mathbf{u}_D^0(\mathbf{x}) + \frac{1}{-\log \varepsilon} (\mathbf{C}_D - \mathbf{U}_D) + \mathbf{r}_D^\varepsilon(\mathbf{x}).$$

Analogously we approximate  $\mathbf{u}_N^\varepsilon$  by

$$\mathbf{u}_N^\varepsilon(\mathbf{x}) = \mathbf{u}_N^0(\mathbf{x}) + \frac{1}{-\log \varepsilon} (\mathbf{C}_N - \mathbf{U}_N) + \mathbf{r}_N^\varepsilon(\mathbf{x}).$$

Then several technical lemmas enable to obtain explicit bounds with respect to  $\varepsilon$  of the remainders  $\mathbf{r}_D^\varepsilon$  and  $\mathbf{r}_N^\varepsilon$  and to complete the proof of the previous proposition.

### II.1.3.2 Topological gradient of the Kohn-Vogelius functional

Using the asymptotic expansions of the solutions and explicit bounds with respect to  $\varepsilon$ , we prove the following theorem which gives us the expression of the topological gradient of the Kohn-Vogelius functional  $\mathcal{K}$ .

**Theorem II.1.3.** *For  $\mathbf{z} \in \Omega$ , the functional  $\mathcal{K}$  admits the following topological asymptotic expansion:*

$$\mathcal{K}(\Omega_{\mathbf{z}, \varepsilon}) - \mathcal{K}(\Omega) = \frac{4\pi\nu}{-\log \varepsilon} (|\mathbf{u}_D^0(\mathbf{z})|^2 - |\mathbf{u}_N^0(\mathbf{z})|^2) + o\left(\frac{1}{-\log \varepsilon}\right),$$

where  $\mathbf{u}_D^0 \in \mathbf{H}^1(\Omega)$  and  $\mathbf{u}_N^0 \in \mathbf{H}^1(\Omega)$  solve respectively Problems (II.1.4) and (II.1.5) with  $\omega_\varepsilon = \emptyset$ . Therefore we have

$$\xi(\varepsilon) = \frac{1}{-\log \varepsilon} \quad \text{and} \quad \delta\mathcal{K}(\mathbf{z}) = 4\pi\nu (|\mathbf{u}_D^0(\mathbf{z})|^2 - |\mathbf{u}_N^0(\mathbf{z})|^2)$$

in the general asymptotic expansion (II.1.6).

**Remark II.1.4.** *Notice that, contrary to the three dimensional case [85, Theorem 3.1] the topological gradient does not depend on the geometry of  $\omega$ . The formula applies for all shapes in 2D. This phenomena is closely related to the Stokes paradox as been pointed in [14, 15, 205] and is coherent with the results obtained by several authors in similar problems (see, e.g., [21, 24, 44, 139, 140]).*

### II.1.4 Numerical simulations

Using the topological gradient algorithm, one can detect the number of objects and their qualitative location but we do not have informations about the shapes of the objects. Hence it can provide initial shapes for an optimization method based on the boundary variation method for which we have to know the number of connected objects we want to reconstruct (see, e.g., my previous work [89]). We present here a combination of these two approaches in order to find the number of objects, their locations and their shapes.

We refer to [89] concerning for theoretical results concerning the computation of the shape derivative of the Kohn-Vogelius functional. Particularly it provides the shape gradient of the functional. Then we suggest an algorithm which consists in two steps:

1. the use of a topological algorithm in order to find the number of objects and their rough location (see the “initial shape” in Figure II.1.3);
2. the use of a boundary variation method in order to approximate the shape. Here we follow the same strategy than in [89] using a truncated Fourier parametrization for the obstacles, starting from the previously found initial shapes.

We present in Figure II.1.3 an example of reconstruction with this algorithm.

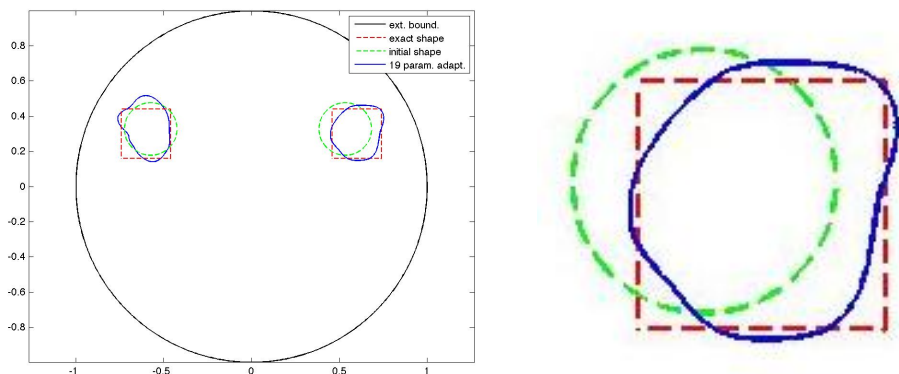


**Figure II.1.3** – Detection of two obstacles with the combined approach (the initial shape is the one obtained after the “topological step”) and zoom on the improvement with the geometrical step

We also underline the fact that, after the topological step, the cost of the functional is here about 1.26 and that, after the geometrical step, we obtain a cost about  $2 \cdot 10^{-2}$  which qualitatively means that we improved the detection. In conclusion this blending method which combines the topological and the geometrical shape methods leads to good results in the identification of obstacle: we detect the number of obstacles, their locations and their shapes at the same time.

## II.2 A Bézier parametrization

This section is devoted to the study of the geometric approximation by parametrization of two-dimensional multiple-component shape using Bézier curves. This work was done in collaboration with Pierre Bonnelie, Loïc Bourdin and Olivier Ruatta (university of Limoges) as part of the PhD thesis of Pierre Bonnelie, and is published in *SMAI Journal of Computational Mathematics* (see [56], 22 pages).

## II.2.1 A way to change the topology of a domain

The previous section presents a blending method, coupling the topological and the geometrical shape optimization approaches in order to numerically solve the inverse obstacle problem. As underlined, the theoretical part, especially concerning the computation of the topological gradient, is technical and may be difficult to prove rigorously, depends on the PDE and on the boundary conditions. The alternative method presented here is based only on mesh variation techniques and on a parametrization by piecewise Bézier curves. The main idea is that this polynomial parametrization can be approximated by its control polygon. Particularly one can easily prevent the potential formation of double points by looking for intersecting control polygons. Once this first step is achieved, one can easily reorganize the control points of the Bézier parametrization in order to modify the topology of the shape, precisely in order to divide one component into two. Hence the *intersecting control polygons detection* and the *flip procedure* enable to dynamically change the topology of the shape in order to find the number of inclusions, and the shape derivatives approach allows to approximate the shape of the inclusions with an explicit representation. This new method seems to be well-suited in order to study the above inverse obstacle problem, especially in the case where the number of inclusions is *a priori* unknown. In order to test these two procedures, we perform numerical simulations on the classical inverse obstacle problem for Laplace’s equation, studied by minimizing a shape least squares functional.

### II.2.1.1 Basics on piecewise Bézier curves

Let us fix our notations and recall some basics about Bézier curves (see, e.g., [129, 200] or [133, from p. 409] for more details). Let  $d \in \mathbb{N}^*$  and a set of  $d + 1$  points  $P_0, \dots, P_d$  of  $\mathbb{R}^2$ . The associated Bézier curve, denoted by  $B([P_0, \dots, P_d])$ , is defined by

$$\forall t \in [0, 1], \quad B([P_0, \dots, P_d], t) := \sum_{j=0}^d P_j b_{j,d}(t),$$

where  $b_{j,d}$  are the classical Bernstein polynomials given by

$$b_{j,d}(t) := \binom{d}{j} t^j (1-t)^{d-j}.$$

The integer  $d$  is the *degree* of the curve and the points  $P_0, \dots, P_d$  are its *control points* (or its *control polygon*). Note that a Bézier curve does not go through its control points in general. However it starts at  $P_0$  and finishes at  $P_d$ . If  $P_0 = P_d$ , the Bézier curve is said to be *closed*. Each point of a Bézier curve is a convex combination of its control points. As a consequence, a Bézier curve lies in the convex hull of its control polygon (see Figure II.2.4).

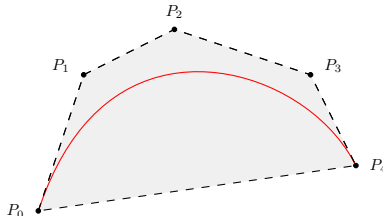


Figure II.2.4 – A non-closed Bézier curve of degree 4 lying in the convex hull of its control polygon.

Using a single closed Bézier curve in order to approximate a two-dimensional shape is not an efficient method for several reasons. Indeed, in order to approximate a shape with a lot of geometric

features, one would need to increase the number of degrees of freedom, i.e. the number of control points. However, as is very well-known, increasing the degree of an approximating polynomial curve leads to a classical oscillation phenomenon and, in the particular case of a Bézier polynomial curve, it leads to numerical instabilities (due to the ill-conditionness of the Bernstein-Vandermonde matrices, see, e.g., [179]). Moreover, since each control point has a global influence on the curve, one could not handle local complexities of a shape with a single Bézier curve. The classical idea is then to divide the curve in several Bézier curves of small degrees. This leads us to recall the following definition of piecewise Bézier curves.

Let  $N \in \mathbb{N}^*$ ,  $d \in \mathbb{N}^*$  and a set of  $N(d + 1)$  control points  $P_{1,0}, \dots, P_{1,d}, \dots, P_{N,d}$  of  $\mathbb{R}^2$  satisfying the *continuity relations*  $P_{i,d} = P_{i+1,0}$  for every  $i = 1, \dots, N - 1$ .<sup>1</sup> The associated piecewise Bézier curve, denoted by  $B([P_{1,0}, \dots, P_{N,d}])$ <sup>2</sup>, is defined by

$$\forall t \in [0, 1], \quad B([P_{1,0}, \dots, P_{N,d}], t) := B([P_{i,0}, \dots, P_{i,d}], Nt - i + 1),$$

$$\text{if } t \in \left[ \frac{i-1}{N}, \frac{i}{N} \right], \text{ } i \text{ ranges from } 1 \text{ to } N.$$

The global curve is then composed of  $N$  Bézier curves called *patches*. Note that a piecewise Bézier curve goes through  $P_{i,0}$  and  $P_{i,d}$  for all  $i = 1, \dots, N$ . If  $P_{1,0} = P_{N,d}$ , the piecewise Bézier curve is said to be *closed*.

**Remark II.2.1.** *In practice we use cubic patches ( $d = 3$ ) because they are sufficient in order to recover many geometrical situations, such as inflexion points (see Figure II.2.5).*

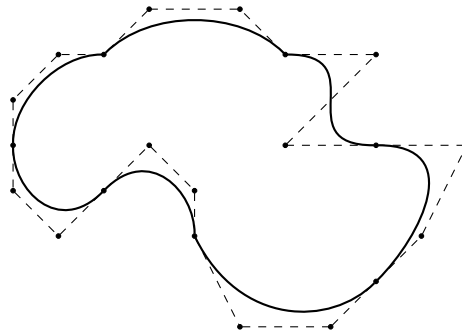


**Figure II.2.5** – A closed piecewise Bézier curve composed of seven cubic patches.

Adapting the proof of the classical Stone-Weierstrass theorem, one can prove the following result (which corresponds to a particular case of the classical Bishop theorem, see [51]). This result fully justifies the use of piecewise Bézier curves in order to approximate two-dimensional bounded shapes.

**Theorem II.2.2.** *Let  $f \in \mathcal{C}([0, 1], \mathbb{R}^2)$ . For all  $\varepsilon > 0$  and all  $d \in \mathbb{N}^*$ , there exist  $N \in \mathbb{N}^*$  and a set of  $N(d + 1)$  control points  $P_{1,0}, \dots, P_{1,d}, \dots, P_{N,d}$ , satisfying the continuity relations, such that  $\|f(t) - B([P_{1,0}, \dots, P_{N,d}], t)\| \leq \varepsilon$  for all  $t \in [0, 1]$ .*

Recall that the use of polar coordinates, where the radius is expanded in a truncated Fourier series, is another common and efficient strategy in order to approximate two-dimensional shapes (see, e.g., [7] in the context of inclusions detection). However it has two main drawbacks. Firstly it allows to represent only star-shaped domains and secondly, due to a classical oscillation phenomenon, it cannot represent rigorously straight lines (see, e.g., [89, Figure 5 p.140] in the context of inclusions

1. The continuity relations guarantee the well-definedness and the continuity of the piecewise Bézier curve.  
 2. One would note here a conflict in notations of a Bézier curve and of a piecewise Bézier curve. In the sequel no confusion is possible since we will only consider piecewise Bézier curves.

detection). The use of piecewise Bézier curves is then an alternative in order to approximate non star-shaped domains and straight lines (see Section II.2.2 for some numerical simulations in the context of inclusions detection). To conclude, let us notice that the *flip procedure*, which is the main feature of this work, is based on the detection of potential collisions between two parts of the boundary of the approximated shape. Thus it is worth specifying that a parametrization based on polar coordinates, where the radius is expanded in a truncated Fourier series, is not suitable to prevent such collisions, in contrary to a piecewise Bézier parametrization.

### II.2.1.2 Intersecting control polygons detection and flip procedure

As mentioned in the introduction of this chapter, the detection of unknown obstacle(s) by starting a classical geometric approximation with a one-component initial shape may lead to the situation depicted in Figure II.2.6, that is, the deformation flow makes the boundary evolve until it surrounds all the components of the target shape. This classical phenomenon tends to create a collision between two parts of the boundary of the approximated shape.

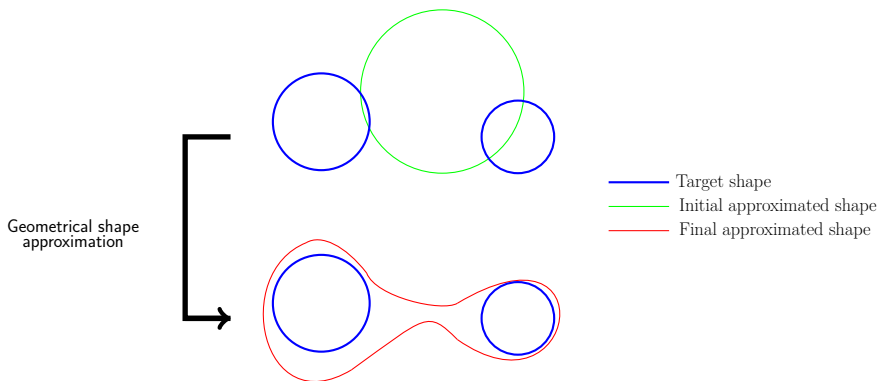


**Figure II.2.6** – A geometric shape approximation of a two-component target shape starting from a one-component initial approximated shape. The final approximated shape surrounds the two components.

Here we propose a simple and new concept (called *flip procedure*) which allows to change the topology of the approximated shape. Precisely, the flip procedure allows to divide a one-component shape into a two-component shape.

Let us consider a general geometric shape approximation algorithm in which the boundary of the approximated shape is parametrized by a piecewise cubic Bézier curve. It starts from a one-component initial shape  $\omega_0$  and produces a sequence of one-component shapes  $(\omega_k)_{k \geq 0}$  by deforming the boundary at each step. The idea consists in two phases (that are summarized in Figure II.2.7):

1. check, at each step of the approximation algorithm, if the current shape  $\omega_k$  is in the situation depicted in Figure II.2.6, that is, if two parts of the boundary are very close to each other. The parametrization by piecewise Bézier curves allows us to prevent such a situation by looking for intersecting control polygons. This procedure is called *intersecting control polygons detection*;
2. if some control polygons intersect each other, we apply the flip procedure in order to obtain a two-component shape by keeping unchanged all other control polygons.

A precise description of this procedure can be found in the corresponding article [56].

## II.2.2 Application to obstacles detection

This section focuses on the problem of reconstructing numerically an obstacle  $\omega^*$  living in a larger bounded domain  $\Omega$  of  $\mathbb{R}^2$  from boundary measurements. Our aim is especially to test the flip procedure

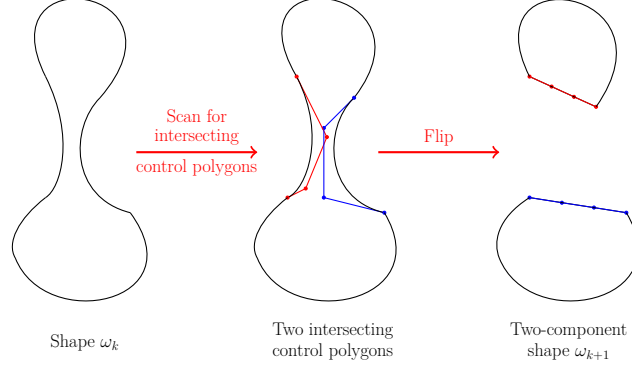


**Figure II.2.7** – Overview of the complete procedure.

introduced before in the case where  $\omega^*$  is a two-component obstacle.

In order to solve numerically the above inverse obstacle problem, we actually consider a shape optimization problem, by minimizing a shape cost functional. We use the classical geometrical shape optimization approach, based on shape derivatives and on a shape gradient descent method. We refer to the classical books of Henrot *et al.* [152] and of Sokolowski *et al.* [210] for more details on the techniques of shape differentiability.

Let  $\Omega$  be a non-empty bounded and connected open set of  $\mathbb{R}^2$  with a  $\mathcal{C}^{1,1}$  boundary and let  $g_D \in \mathbf{H}^{3/2}(\partial\Omega)$  such that  $g_D \neq 0$ . Let  $d_0 > 0$  be fixed (small). In the sequel  $\mathcal{O}$  stands for the set of admissible shapes given by

$$\mathcal{O} := \left\{ \omega \subset\subset \Omega \text{ open set with a } \mathcal{C}^{1,1} \text{ boundary such that } d(\mathbf{x}, \partial\Omega) > d_0, \forall \mathbf{x} \in \omega \right. \\ \left. \text{and such that } \Omega \setminus \overline{\omega} \text{ is connected} \right\}.$$

Finally we also introduce  $\Omega_{d_0}$  an open set with a  $\mathcal{C}^\infty$  boundary such that

$$\{\mathbf{x} \in \Omega; d(\mathbf{x}, \partial\Omega) > d_0/2\} \subset \Omega_{d_0} \subset \{\mathbf{x} \in \Omega; d(\mathbf{x}, \partial\Omega) > d_0/3\}.$$

We focus on the following inverse problem. Assume that an unknown obstacle  $\omega^* \in \mathcal{O}$  is located inside  $\Omega$ . We consider hereafter Laplace's equation in  $\Omega \setminus \overline{\omega^*}$  with homogeneous Dirichlet boundary condition on  $\partial\omega^*$  and non-homogeneous Dirichlet boundary condition on  $\partial\Omega$ . Precisely we denote by  $u_{\text{ex}} \in \mathbf{H}^1(\Omega \setminus \overline{\omega^*})$  the unique solution of the problem

$$\begin{cases} -\Delta u_{\text{ex}} = 0 & \text{in } \Omega \setminus \overline{\omega^*}, \\ u_{\text{ex}} = g_D & \text{on } \partial\Omega, \\ u_{\text{ex}} = 0 & \text{on } \partial\omega^*. \end{cases}$$

Our main purpose is to reconstruct the unknown shape  $\omega^*$ , assuming that a measurement is done on the exterior boundary  $\partial\Omega$ . More precisely let us assume that we know exactly the value of the measure  $g_N := \partial_n u_{\text{ex}} \in \mathbf{H}^{1/2}(\partial\Omega)$  on  $\partial\Omega$ . Thus, for a nontrivial Cauchy pair  $(g_N, g_D) \in \mathbf{H}^{1/2}(\partial\Omega) \times \mathbf{H}^{3/2}(\partial\Omega)$ , we are interested in the following geometric inverse problem:

*Find  $\omega^* \in \mathcal{O}$  and  $u \in \mathbf{H}^1(\Omega \setminus \overline{\omega^*})$  which satisfy the overdetermined problem*

$$\begin{cases} -\Delta u = 0 & \text{in } \Omega \setminus \overline{\omega^*}, \\ u = g & \text{on } \partial\Omega, \\ \partial_n u = g_N & \text{on } \partial\Omega, \\ u = 0 & \text{on } \partial\omega^*. \end{cases} \quad (\text{II.2.1})$$

The existence of a solution is trivial since we assume that the measurement  $g_N$  is exact. From the classical Holmgren's theorem (see, e.g., [158]) one can obtain an identifiability result for this inverse problem which claims that the solution is unique. This fundamental question about uniqueness of a solution to the overdetermined problem (II.2.1) was deeply studied, see for instance [65, Theorem 1.1], [102, Theorem 5.1] or also [112, Proposition 4.4 p. 87]. We recall the identifiability result in our case for the reader's convenience.<sup>3</sup>

**Theorem II.2.3.** *The domain  $\omega^*$  and the function  $u$  that satisfy (II.2.1) are uniquely defined by the Cauchy data  $(g_N, g_D) \neq (0, 0)$ .*

**Remark II.2.4.** *Actually we could assume that the measurement  $g_N$  is done only on a non-empty subset  $\Gamma_{\text{obs}}$  of  $\partial\Omega$ . All the presented result can be adapted to this case (see, e.g., [83]).*

In order to solve the inverse problem (II.2.1) we actually focus on the shape optimization problem

$$\omega^* \in \underset{\omega \in \mathcal{O}}{\operatorname{argmin}} \mathcal{J}(\omega), \quad (\text{II.2.2})$$

where  $\mathcal{J}$  is the nonnegative least squares functional defined by

$$\mathcal{J}(\omega) := \int_{\partial\Omega} |\partial_n u - g_N|^2,$$

where  $u \in H^1(\Omega \setminus \bar{\omega})$  is the unique solution of the problem

$$\begin{cases} -\Delta u = 0 & \text{in } \Omega \setminus \bar{\omega}, \\ u = g_D & \text{on } \partial\Omega, \\ u = 0 & \text{on } \partial\omega. \end{cases}$$

Indeed the identifiability result ensures that  $\mathcal{J}(\omega) = 0$  if and only if  $\omega = \omega^*$ . Finally, in order to solve numerically the shape optimization problem (II.2.2), we easily compute the shape gradient of the cost functional  $\mathcal{J}$  and apply a classical gradient descent method.

We classically obtain the following expression of the shape gradient of the functional  $\mathcal{J}$ .

**Proposition II.2.5.** *The least squares functional  $\mathcal{J}$  is differentiable at  $\omega \in \mathcal{O}$  in the admissible direction  $\mathbf{V} \in \mathcal{U} := \left\{ \mathbf{V} \in \mathbf{W}^{2,\infty}(\mathbb{R}^d); \operatorname{supp}(\mathbf{V}) \subset \bar{\Omega}_{d_0} \text{ and } \|\mathbf{V}\|_{2,\infty} < \min\left(\frac{d_0}{3}, 1\right) \right\}$  with*

$$D\mathcal{J}(\omega) \cdot \mathbf{V} = - \int_{\partial\omega} \partial_n u \partial_n w (\mathbf{V} \cdot \mathbf{n}),$$

where  $w \in H^1(\Omega \setminus \bar{\omega})$  is the unique solution of the adjoint problem given by

$$\begin{cases} -\Delta w = 0 & \text{in } \Omega \setminus \bar{\omega}, \\ w = 2(\partial_n u - g_N) & \text{on } \partial\Omega, \\ w = 0 & \text{on } \partial\omega. \end{cases}$$

From the above explicit formulation of the shape gradient of  $\mathcal{J}$ , we are now in a position to implement some numerical simulations based on a classical gradient descent method and we include the flip procedure introduced previously in order to detect particularly a multiple-component obstacle.

We present here some numerical simulations which underline the efficiency of the proposed method. Particularly we can detect smooth and convex shapes (see Figure II.2.8), non-smooth shape and non-convex shape (see Figure II.2.9) and two-component obstacle starting from a one-component shape (see Figure II.2.10).

To conclude, notice that the flip procedure is a method that enables to divide a one-component shape into a two-component shape. Actually the flip procedure can be easily adapted in order to

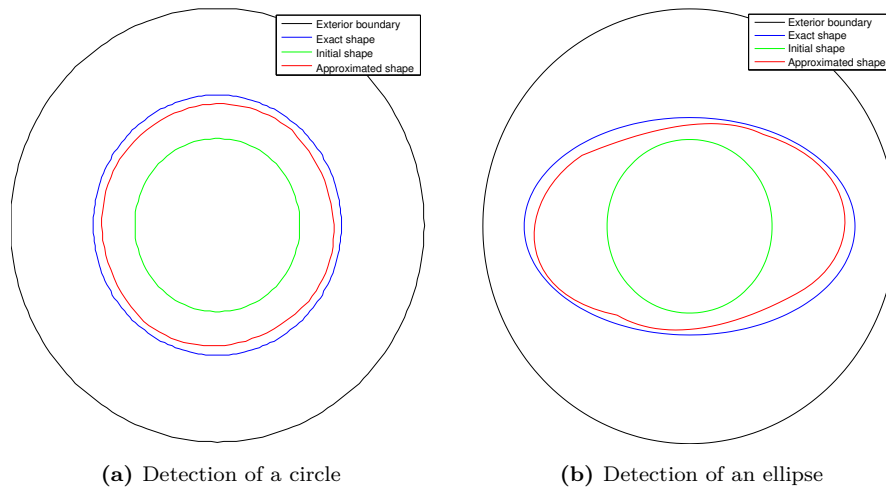


Figure II.2.8 – Detection of convex and smooth obstacles.

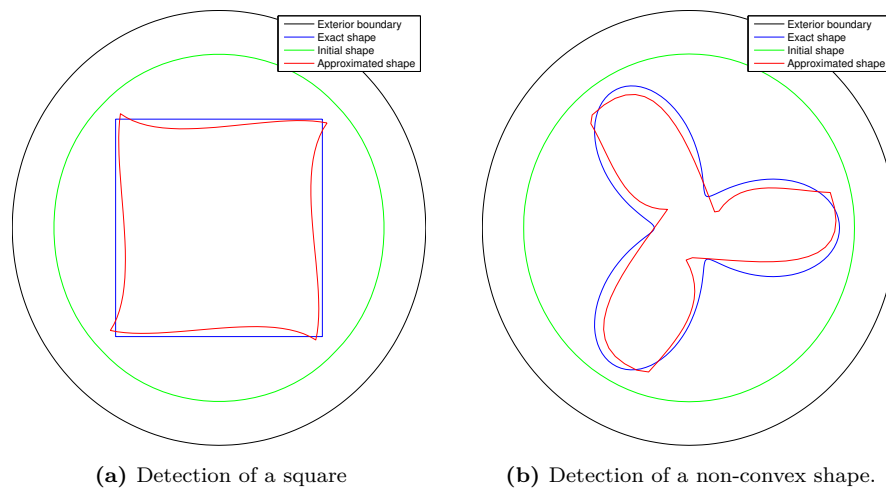


Figure II.2.9 – Detection of a non-smooth obstacle and of a non-convex obstacle.

perform the reverse operation, that is, to merge a two-component shape into a one-component shape (see Figure II.2.11).

## II.3 Perspectives

The two previous methods concern the two dimensional case. Concerning the adaptation of the first one, that is the blending method, in the three-dimensional case, the theoretical part for the computation of the topological gradient already exists and was one of my previous work in [85]. The main difficulty would be to make the numerical simulations, especially for the boundary variation step. The adaptation of the Bézier parametrization method for the three-dimensional case would be

3. Note that Theorem II.2.3 is true even with weaker assumptions, especially on the regularity of the domains, see, e.g., [65, Theorem 1.1].

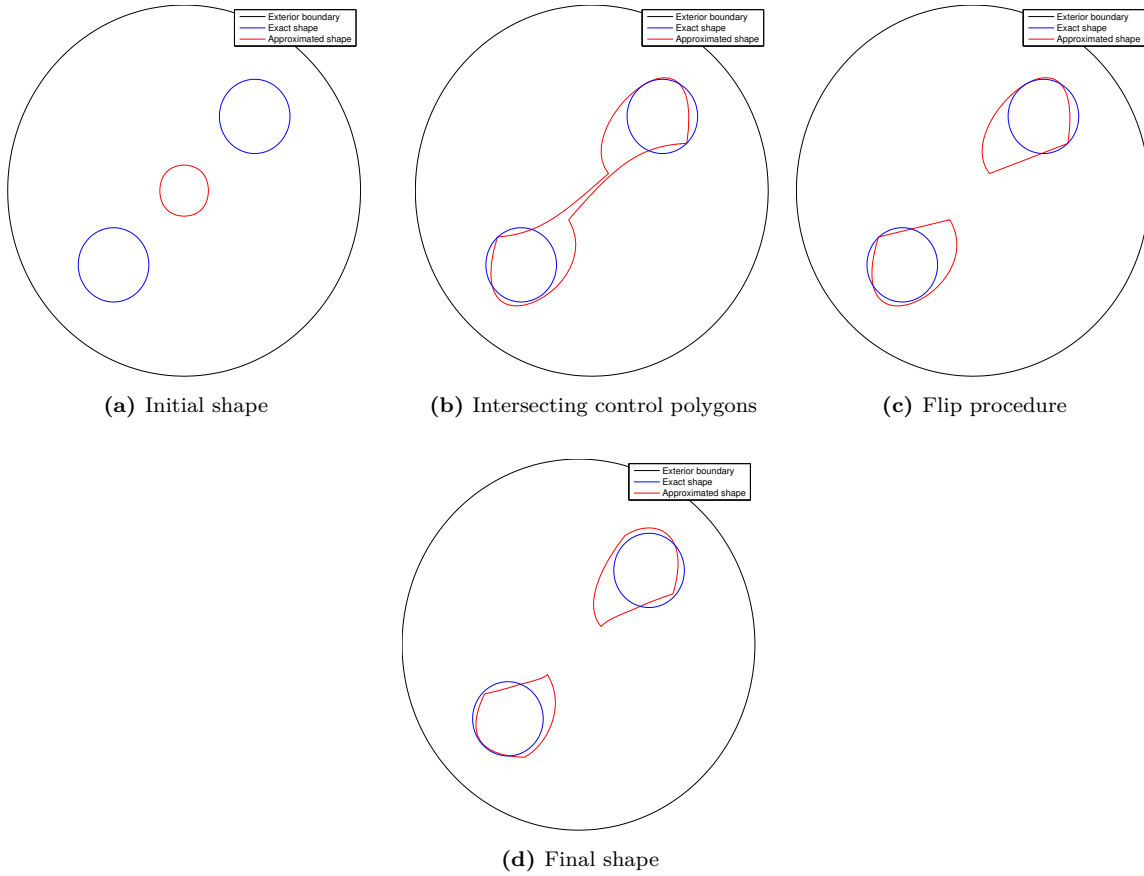
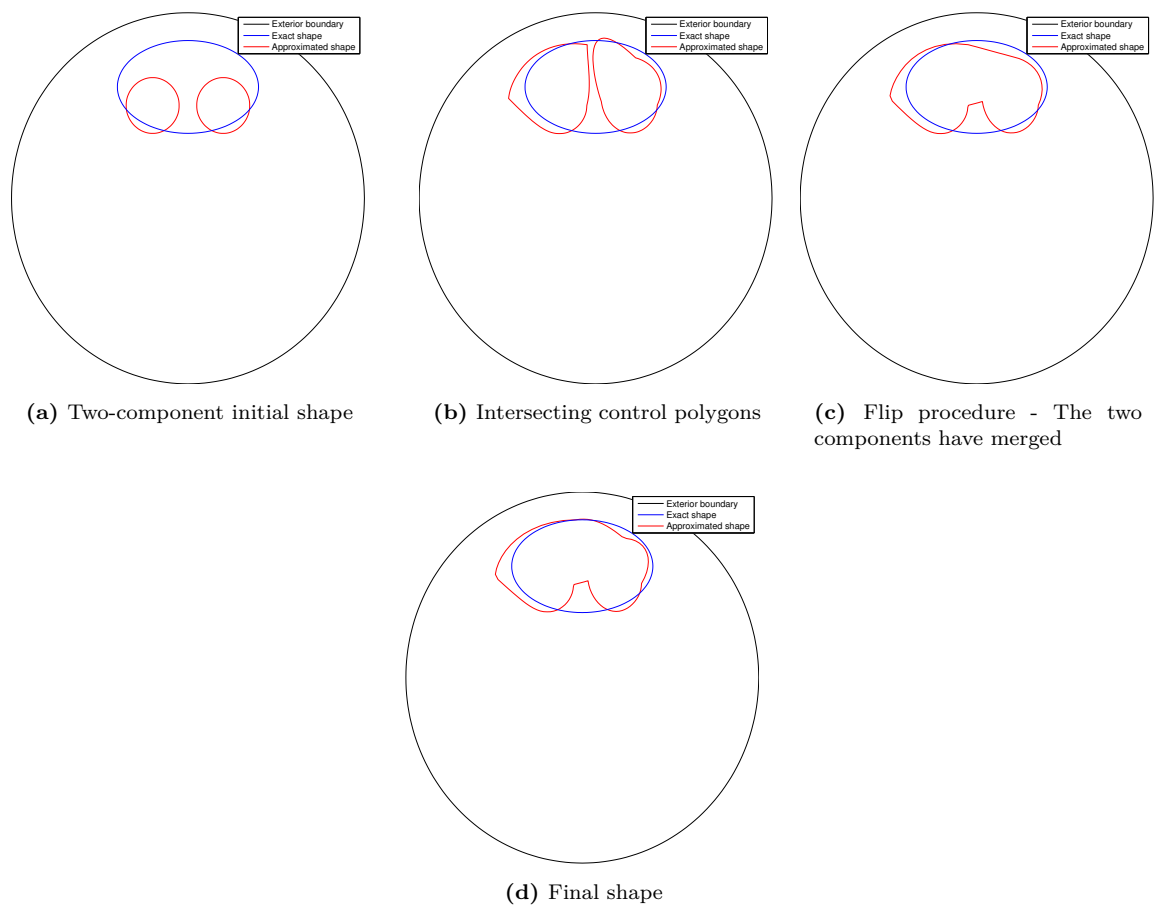


Figure II.2.10 – Detection of two obstacles starting from a one-component shape

interested. We refer for instance to [186] where deformation of piecewise Bézier surfaces is presented with an implementation. However, note that the adaptation of the complete algorithmic setting of the flip procedure to the three-dimensional case would be nontrivial since it would increase the algorithmic and combinatoric complexities.

Let us mention a natural extension of the previous work which concern the case of Navier-Stokes equations, especially to obtain the topological asymptotic expansion of the Kohn-Vogelius functional. Such an adaptation requires to overcome theoretical technical difficulties, due to the nonlinearity. One could use the existing literature on the subject, as for instance [21].

To conclude, as previously mentioned, several methods exist in order to numerically solve the inverse obstacle problem. Additionally to the shape optimization approaches recalled previously, one can also mention the so-called *exterior approach* consisting in the construction of a decreasing sequence of open domains that contain the searched obstacle (see, e.g., the works of Dardé *et al.* [66, 67, 113]). A numerical comparison of these methods, for instance for the Laplacian case, could give information on their respective advantages and drawbacks. This work would be mainly numerical but a rigorous implementation is necessary to obtain objective conclusions. Finally one can notice that the used algorithms in the methods could be obviously improved. Indeed the classical gradient method could be replaced by a Newton kind method. This last point is explored in another work, exposed in the following chapter.



**Figure II.2.11** – Detection of one obstacle starting from a two-component shape



---

---

## Chapter III

---

# The inverse obstacle problem on new models for Laplace's equation

The previous chapter II focuses on the classical inverse obstacle problem and aims at suggesting new methods to numerically solve it. In a perspective of more concrete applications, this chapter explores some more realistic configurations, even if the exposed problems are still academic. Hence two physical constraints are considered. Firstly we consider a partial accessibility of the boundary of the exterior domain, i.e. the domain of measurements: the question is to detect an inclusion from *partial Cauchy data*. Secondly the case of nonclassical boundary conditions imposed on the obstacle is considered: when the obstacle has a thin layer (as, e.g., some corrosion), one can model it using *Generalized Impedance Boundary Conditions* (GIBC). The first section of this chapter summarizes my works concerning the *data completion problem*, that is

- [90] F. Caubet, J. Dardé and M. Godoy. On the data completion problem and the inverse obstacle problem with partial Cauchy data for Laplace's equation. *ESAIM Control Optim. Calc. Var.*, to appear, 2017,
- [87] F. Caubet, M. Dambrine and H. Harbrecht. A new method for the data completion problem and application to obstacle detection. *Submitted*, 2018,

and the second section presents the article on the detection of an obstacle with Wentzell boundary conditions, that is

- [88] F. Caubet, M. Dambrine and D. Kateb. Shape optimization methods for the inverse obstacle problem with generalized impedance boundary conditions. *Inverse Problems*, 29(11):115011, 26, 2013.

Electrical Impedance Tomography (EIT) is used in medical imaging to reconstruct the electric conductivity of a part of a body from measurements of currents and voltages at the surface (see, e.g., [58]). The same technique is also used in geophysical explorations. An important special case consists in reconstructing the shape of an unknown inclusion or void assuming (piecewise) constant conductivities.

In several applications, the aim is then to reconstruct an inclusion (characterized by a Dirichlet condition for instance) from the knowledge of Cauchy data (that is the Dirichlet and the Neumann boundary conditions) on an accessible part of the frontier of the domain of study. Notice that no data at all is provided on a non-empty inaccessible part of the boundary. As already mentioned in this manuscript, it is well-known that this problem admits at most one solution and that the inverse obstacle problem is severely ill-posed: the problem may fail to have a solution and, even when a solution exists, the problem is highly unstable. More precisely, the best one can expect is a logarithmic stability (see, e.g., [10, 118]). Numerous methods have been proposed to solve this problem : sampling methods [188], methods based on conformal mappings [146], on integral equations [166, 196], level-set

method coupled with quasi-reversibility in the exterior approach [65], among others. Among all of them, shape optimization methods (see, e.g., [7, 72, 139]) present interesting features. Especially they are easily adaptable to problems governed by different partial differential equations, such as Stokes system (see, e.g., [21, 84, 89, 140]), and obstacles characterized by different limit conditions, such as Neumann or generalized boundary conditions (see, e.g., [32, 88]). However, since such methods rely on the minimization of a (shape) cost-type functional which in turn needs the resolution of several well-posed direct problems, they need particularly some boundary data on the whole boundary of the domain of study, and therefore cannot be directly used for the partial Cauchy data case. ***Then a data completion step is needed to solve the inverse obstacle problem, which is the topic of the first part of this chapter: Section III.1.1 deals with the case of partial Cauchy data and Section III.1.2 focuses on the use of a Newton approach and of the so-called trial method.***

Another situation can occur in EIT: the inclusion may contain a thin layer, as a membrane or a rough boundary, which can be modeled by some generalized impedance boundary conditions (of order two) on the obstacle, precisely Wentzell boundary conditions for Laplace's equation which deal with the Laplace-Beltrami operator. These boundary conditions appear when one makes an asymptotic analysis of the solution of the problem in the full domain (taking the layer into account) with respect to the thickness of the layer and when one seeks equivalent boundary conditions on the reference domain in order to forget the complex geometry. The construction of generalized impedance boundary conditions is treated for instance by Antoine *et al.* in [26], by Poignard in [187] or by Haddar *et al.* in [144, 145]. This kind of construction is explored more precisely in the next chapter IV. The study of this type of boundary conditions is an emerging research theme and a general analysis of the Wentzell boundary conditions is made by Bonnaillie-Noël *et al.* in [54]. One topic is then to identify the coefficients corresponding to these conditions as treated by Bourgeois *et al.* in [61, 68]. Another is to identify the shape while the coefficients are known. We consider this last problem in the second part of this chapter: ***the aim is to use classical shape optimization methods to solve inverse problems in the case of immersed obstacles modeled by Wentzell boundary conditions (see Section III.2).*** One of the difficulty is the shape sensitivity analysis of such a problem, especially in order to prove the existence and characterize the shape derivatives. Notice that, in the recent work [75], Cakoni *et al.* address the question of recovering simultaneously the unknown boundary and the unknown coefficients by an integral equation approach. We also refer to the recent paper of Bourgeois *et al.* [62] which deals with this topic considering the Helmholtz equation.

### III.1 Taking into account partial Cauchy data: a data completion problem

This section is devoted to the inverse obstacle problem, coupled with the data completion problem. Subsection III.1.1 deals with the inverse obstacle problem in the case of partial Cauchy data and Subsection III.1.2 focuses on the trial method in order to solve the inverse obstacle problem.

Hence, in this section, we deal with the inverse obstacle problem defined as follows. Let  $\Omega$  be a bounded connected Lipschitz open set of  $\mathbb{R}^d$  (with  $d = 2$  or  $d = 3$ ) with a boundary  $\partial\Omega$  divided into two components: the non-empty (relatively) open sets  $\Gamma_{\text{obs}}$  and  $\Gamma_{\text{ina}}$ , such that  $\overline{\Gamma_{\text{obs}}} \cup \overline{\Gamma_{\text{ina}}} = \partial\Omega$ . For some nontrivial data  $(g_N, g_D) \in H^{-1/2}(\Gamma_{\text{obs}}) \times H^{1/2}(\Gamma_{\text{obs}})$ , we consider the following obstacle problem:

$$\begin{aligned}
 & \text{Find } \omega^* \in \mathcal{O} \text{ and } u \in H^1(\Omega \setminus \overline{\omega^*}) \text{ which satisfy the overdetermined problem} \\
 & \left\{ \begin{array}{ll} -\Delta u = 0 & \text{in } \Omega \setminus \overline{\omega^*}, \\ u = g_D & \text{on } \Gamma_{\text{obs}}, \\ \partial_n u = g_N & \text{on } \Gamma_{\text{obs}}, \\ u = 0 & \text{on } \omega^*. \end{array} \right. \tag{III.1.1}
 \end{aligned}$$

### III.1 Taking into account partial Cauchy data: a data completion problem

Here

$$\mathcal{O} := \left\{ \omega \subset\subset \Omega \text{ open set with a } \mathcal{C}^{1,1} \text{ boundary such that } d(\mathbf{x}, \partial\Omega) > d_0, \forall \mathbf{x} \in \omega \right. \\ \left. \text{and such that } \Omega \setminus \bar{\omega} \text{ is connected} \right\}, \quad (\text{III.1.2})$$

with  $d_0 > 0$  a fixed (small) parameter. In other words, the problem is to reconstruct an inclusion  $\omega^*$  characterized by a Dirichlet condition from the knowledge of some data  $(g_N, g_D)$  on the accessible part  $\Gamma_{\text{obs}}$  of the frontier of the domain of study, *no data at all being provided on the inaccessible part of the boundary*  $\Gamma_{\text{ina}}$  (see Figure III.1.1 for an illustration of the notations). This last important point is one the main novelties of this work.

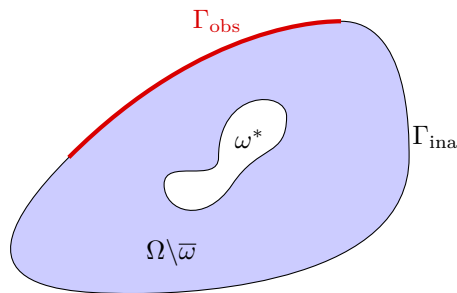


**Figure III.1.1** – A possible configuration for the obstacle problem.

As already mentioned, it is well-known that Problem (III.1.1) admits at most one solution, as claimed by the following identifiability result<sup>1</sup> that we recall in our case for the reader's convenience (see for instance [65, Theorem 1.1], [102, Theorem 5.1] or [112, Proposition 4.4, page 87]).

**Theorem III.1.1.** *The domain  $\omega^*$  and the function  $u$  that satisfy (III.1.1) are uniquely defined by the Cauchy data  $(g_N, g_D) \neq (0, 0)$ .*

It is also well-known that Problem (III.1.1) is severely ill-posed: the problem may fail to have a solution and, even when a solution exists, the problem is highly unstable.

Due to the ill-posedness, regularization techniques are mandatory to solve the problem numerically. Several approaches have been proposed, particularly concerning the data completion problem: among others, we recall the work of Cimetière *et al.* [100] who consider a fixed point scheme for an appropriate operator. In [30, 46, 47], Ben Belgacem *et al.* propose a complete study of the problem based on the Steklov-Poincaré operator and a Lavrentiev regularization. We also mention the works of Bourgeois *et al.* [63, 64] based on the quasi-reversibility method and a generalization to a wider family of systems is presented by Dardé in [114]. Burman in [73] proposes a regularization through discretization: especially he obtains an optimal convergence result of the discretized solution to the exact one. In the particular case of a 2d problem, Leblond *et al.* in [172] use a complex-analytic approach to recover the solution of the Cauchy problem respecting furthermore additional pointwise constraints in the domain. Let us also mention the work of Kozlov *et al.* [165] which presents the classical KMF algorithm used widely for numerical simulations. Several works consider modifications of the KMF algorithm in order to improve the speed of convergence as the work of Abouchabaka *et al.* [1]. The work of Andrieux *et al.* [25] presents another approach considering the minimization of an energy-like functional and presents an algorithm which is equivalent to the KMF algorithm formulation. The work of Aboulaich *et al.* [2] considers a control type method for the numerical resolution of the Cauchy problem for Stokes system and, as an example of regularization techniques employed in this problem, we mention the work of Han *et al.* [147] in which a regularization of an energy functional is considered for an annular domain. In this section, we will use the classical *Tikhonov regularization*.

1. As mentioned previously, Theorem III.1.1 is true even with weaker assumptions, see, e.g., [65, Theorem 1.1].

### III.1.1 Analysis of the data completion problem and numerical reconstruction of an inclusion

The work exposed in this subsection was done in collaboration with Jérémie Dardé (university of Toulouse) and Matías Godoy (university of Chile) as part of the PhD thesis of Matías Godoy, and is published in ESAIM: Control Optimization and Calculus of Variations (see [90], 28 pages).

First notice that, up to my knowledge, among all the methods cited above in order to solve the inverse obstacle problem, only the exterior approach deals with the inverse obstacle problem with partial Cauchy data. However the exterior approach has been specifically developed to deal with obstacles characterized by a Dirichlet-type boundary condition, and its adaptation to a Neumann-type condition is still an open question.

One aim of the method presented here is to overcome this boundary conditions limitation. Indeed the proposed method could be naturally adapted to Neumann boundary conditions for instance and is then an effective alternative method to deal with partial Cauchy data.

Thus we want to use shape optimization methods for the inverse obstacle problem in the case where data are not available on the whole boundary of the domain of study. To do so, our strategy is to solve the inverse obstacle problem and a *data completion problem* in order to reconstruct the obstacle and the missing data at once. We do so through the minimization of a Kohn-Vogelius functional, which will have both the shape  $\omega^*$  and the unknown data as variables. Notice that such type of functional has already been used successfully to solve obstacle problems and data completion problem separately (see, e.g., [7, 25]).

#### III.1.1.1 The data completion problem

Let us assume for a while that the obstacle  $\omega^*$  is known. Then, in order to simplify the notations, let us consider the case  $\omega^* = \emptyset$  but all the presented results can be easily adapted to the case  $\omega^* \neq \emptyset$ . The data completion problem consists in recovering data on the whole boundary, specifically on the inaccessible part  $\Gamma_{\text{ina}}$ , from the overdetermined data  $(g_N, g_D)$  on  $\Gamma_{\text{obs}}$ , that is:

$$\begin{aligned} & \text{Find } u \in H^1(\Omega \setminus \overline{\omega^*}) \text{ such that} \\ & \begin{cases} -\Delta u = 0 & \text{in } \Omega, \\ u = g_D & \text{on } \Gamma_{\text{obs}}, \\ \partial_n u = g_N & \text{on } \Gamma_{\text{obs}}. \end{cases} \end{aligned} \tag{III.1.3}$$

The data completion problem is known to be severely ill-posed, see for instance [45] where the exponential ill-posedness is clearly highlighted. Particularly it has at most one solution but it may have no solution and, when a solution exists, it does not depend continuously on the given data (and therefore the same is true for the missing data); the well-known example of Hadamard [141] is an example of this behavior.

**Definition III.1.2.** A pair  $(g_N, g_D) \in H^{-1/2}(\Gamma_{\text{obs}}) \times H^{1/2}(\Gamma_{\text{obs}})$  will be called **compatible** if there exists (a necessarily unique)  $u \in H^1(\Omega)$  harmonic such that  $u|_{\Gamma_{\text{obs}}} = g_D$  and  $\partial_n u|_{\Gamma_{\text{obs}}} = g_N$ .

If a given pair  $(g_N, g_D)$  is not compatible, we may approximate it by a sequence of compatible data, as the following result asserts (see Fursikov [135, Chapter 3] or Andrieux [25]).

**Lemma III.1.3.** We have the two following density results.

1. For a fixed  $g_D \in H^{1/2}(\Gamma_{\text{obs}})$ , the set of data  $g_N$  for which there exists a function  $u \in H^1(\Omega)$  satisfying the Cauchy problem (III.1.3) is dense in  $H^{-1/2}(\Gamma_{\text{obs}})$ .
2. For a fixed  $g_N \in H^{-1/2}(\Gamma_{\text{obs}})$ , the set of data  $g_D$  for which there exists a function  $u \in H^1(\Omega)$  satisfying the Cauchy problem (III.1.3) is dense in  $H^{1/2}(\Gamma_{\text{obs}})$ .

### III.1 Taking into account partial Cauchy data: a data completion problem

In this work we follow the idea developed in [25, 30, 46, 47]: we study the data completion problem through the minimization of a Kohn-Vogelius type cost functional which admits the solution of Problem (III.1.3) as minimizer, if such a solution exists. In order to deal with the ill-posedness previously mentioned, we consider a Tikhonov regularization of the functional which ensures the existence of a minimizer even for non compatible data thanks to the gained of coerciveness and, in case of compatible data, the convergence towards the exact solution. In case of noisy data, we propose a strategy to choose the regularization parameter in order to preserve convergence to the unpolluted solution.

**The Kohn-Vogelius functional.** We defined the Kohn-Vogelius functional as follows: for all  $(\varphi, \psi) \in H^{-1/2}(\Gamma_{\text{ina}}) \times H^{1/2}(\Gamma_{\text{ina}})$ ,

$$\mathcal{K}(\varphi, \psi) := \frac{1}{2} \int_{\Omega} |\nabla u_{\varphi}^{g_D} - \nabla u_{\psi}^{g_N}|^2, \quad (\text{III.1.4})$$

where  $u_{\varphi}^{g_D}, u_{\psi}^{g_N} \in H^1(\Omega)$  are the respective solutions of

$$\begin{cases} -\Delta u_{\varphi}^{g_D} = 0 & \text{in } \Omega, \\ u_{\varphi}^{g_D} = g_D & \text{on } \Gamma_{\text{obs}}, \\ \partial_n u_{\varphi}^{g_D} = \varphi & \text{on } \Gamma_{\text{ina}}, \end{cases} \quad \text{and} \quad \begin{cases} -\Delta u_{\psi}^{g_N} = 0 & \text{in } \Omega, \\ \partial_n u_{\psi}^{g_N} = g_N & \text{on } \Gamma_{\text{obs}}, \\ u_{\psi}^{g_N} = \psi & \text{on } \Gamma_{\text{ina}}, \end{cases} \quad (\text{III.1.5})$$

where  $(g_N, g_D) \in H^{-1/2}(\Gamma_{\text{obs}}) \times H^{1/2}(\Gamma_{\text{obs}})$  is a given Cauchy pair which may be compatible or not.

We also introduce the solution  $v_{\varphi}, v_{\psi} \in H^1(\Omega)$  of the two following problems (corresponding to the case  $g_D = 0$  and  $g_N = 0$ , i.e.  $v_{\varphi} = u_{\varphi}^0$  and  $v_{\psi} = u_{\psi}^0$ ):

$$\begin{cases} -\Delta v_{\varphi} = 0 & \text{in } \Omega \setminus \bar{\omega}, \\ v_{\varphi} = 0 & \text{on } \Gamma_{\text{obs}}, \\ \partial_n v_{\varphi} = \varphi & \text{on } \Gamma_{\text{ina}}, \end{cases} \quad \text{and} \quad \begin{cases} -\Delta v_{\psi} = 0 & \text{in } \Omega \setminus \bar{\omega}, \\ \partial_n v_{\psi} = 0 & \text{on } \Gamma_{\text{obs}}, \\ v_{\psi} = \psi & \text{on } \Gamma_{\text{ina}}. \end{cases}$$

**Remark III.1.4.** *Note that the two problems appearing in (III.1.5) are well-posed for any given boundary conditions  $(\varphi, \psi) \in H^{-1/2}(\Gamma_{\text{ina}}) \times H^{1/2}(\Gamma_{\text{ina}})$ , without additional compatibility conditions between  $g_D$  and  $\varphi$  for the first problem and between  $g_N$  and  $\psi$  for the second. This is of particular interest for numerical implementations, as the considered setting allows to consider the classical Sobolev spaces and, therefore, the implementations can be done with classical finite element method softwares without any additional adjustments.*

We prove several properties on the Kohn-Vogelius functional. Especially  $\mathcal{K}$  is continuous, convex, positive and its infimum is zero, even for non compatible data. Moreover, if the Cauchy problem (III.1.3) admits a solution  $u_{\text{ex}}$ , we prove that  $u_{\varphi_n}^{g_n^D} \rightharpoonup u_{\text{ex}}$ , weakly in  $H^1(\Omega)$ , for all minimizing sequence  $(\varphi_n^*, \psi_n^*)_n \subset H^{-1/2}(\Gamma_{\text{ina}}) \times H^{1/2}(\Gamma_{\text{ina}})$  of  $\mathcal{K}$ .

**Regularization of the Kohn-Vogelius functional.** As mentioned above, when the data completion problem has no solution, the minimization problem for  $\mathcal{K}$  fails to have one. Additionally, as recalled previously, the data completion problem is ill-posed in the sense that, in case of the existence of solution, there is not a continuous dependence on the given data.

In order to overcome these difficulties, we consider a Tikhonov regularization of the Kohn-Vogelius functional, which, roughly speaking, allows us to get coerciveness and a better behavior with respect to noisy data. There is an extensive literature related to this type of regularization (see, e.g., the book of Engl *et al.* [125] which describes in detail and in full generality the considered regularization).

Then we define the regularized Kohn-Vogelius functional  $\mathcal{K}_{\varepsilon} : H^{-1/2}(\Gamma_{\text{ina}}) \times H^{1/2}(\Gamma_{\text{ina}}) \rightarrow \mathbb{R}$ , for all  $\varepsilon > 0$ , by

$$\mathcal{K}_{\varepsilon}(\varphi, \psi) := \mathcal{K}(\varphi, \psi) + \frac{\varepsilon}{2} \left( \|v_{\varphi}\|_{H^1(\Omega)}^2 + \|v_{\psi}\|_{H^1(\Omega)}^2 \right) = \mathcal{K}(\varphi, \psi) + \frac{\varepsilon}{2} \|(v_{\varphi}, v_{\psi})\|_{(H^1(\Omega))^2}^2,$$

where  $\mathcal{K}$  is the previous Kohn-Vogelius functional given by (III.1.4).  $\mathcal{K}_\varepsilon$  is a regularization of the standard  $\mathcal{K}$  functional, as it always admits a minimizer, regardless of the compatibility of the Cauchy data: for a given  $\varepsilon > 0$ ,  $\mathcal{K}_\varepsilon(\varphi, \psi)$  is continuous, strictly convex and coercive in  $H^{-1/2}(\Gamma_{\text{ina}}) \times H^{1/2}(\Gamma_{\text{ina}})$  and therefore there exists

$$(\varphi_\varepsilon^*, \psi_\varepsilon^*) := \underset{(\varphi, \psi) \in H^{-1/2}(\Gamma_{\text{ina}}) \times H^{1/2}(\Gamma_{\text{ina}})}{\operatorname{argmin}} \mathcal{K}_\varepsilon(\varphi, \psi).$$

Then we prove the following theorem which relates the set of minimizers  $(\varphi_\varepsilon^*, \psi_\varepsilon^*)$  of  $\mathcal{K}_\varepsilon$  with the functional  $\mathcal{K}$  and states a condition to ensure the existence of solution for the Cauchy problem (III.1.3).

**Theorem III.1.5.** *The sequence  $(\varphi_\varepsilon^*, \psi_\varepsilon^*)_\varepsilon$  ( $\varepsilon \rightarrow 0$ ) is a minimizing sequence of  $\mathcal{K}$ . Furthermore, it is a bounded sequence if and only if the Cauchy problem has a (necessarily unique) solution  $u_{\text{ex}}$ . In that case:*

1.  $(\varphi_\varepsilon^*, \psi_\varepsilon^*)$  converges strongly in  $H^{-1/2}(\Gamma_{\text{ina}}) \times H^{1/2}(\Gamma_{\text{ina}})$  when  $\varepsilon \rightarrow 0$  to  $(\varphi^*, \psi^*)$ , a minimizer of  $\mathcal{K}$ ;
2.  $u_{\varphi_\varepsilon^*}^{g_{\text{D}}}$  converges strongly in  $H^1(\Omega)$  when  $\varepsilon \rightarrow 0$  to the solution  $u_{\text{ex}}$  of the Cauchy problem (III.1.3).

Moreover the application  $F(\varepsilon) : (0, +\infty) \rightarrow (u_{\varphi_\varepsilon^*}^{g_{\text{D}}}, u_{\psi_\varepsilon^*}^{g_{\text{N}}}) \in H^1(\Omega) \times H^1(\Omega)$  is continuous for  $\varepsilon > 0$  and, if the data  $(g_{\text{N}}, g_{\text{D}})$  is compatible, it could be continuously extended to 0 with  $F(0) = (u_{\varphi_{\text{ex}}}^{g_{\text{D}}}, u_{\psi_{\text{ex}}}^{g_{\text{N}}})$ .

**The case of noisy data: choosing the parameter of regularization with respect to the noise level.** As one can expect, in real situations, the data  $(g_{\text{N}}, g_{\text{D}})$  cannot be measured with complete precision: noise is intrinsically attached with any measurement method. Hence we consider  $(g_{\text{N}}^\delta, g_{\text{D}}^\delta)$  as a measured data which is assumed to satisfy the following condition

$$\|g_{\text{D}} - g_{\text{D}}^\delta\|_{H^{1/2}(\Gamma_{\text{obs}})} + \|g_{\text{N}} - g_{\text{N}}^\delta\|_{H^{-1/2}(\Gamma_{\text{obs}})} \leq \delta, \quad (\text{III.1.6})$$

where  $\delta > 0$  is the amplitude of noise in the data. Notice that we do not know if the noisy data  $(g_{\text{N}}^\delta, g_{\text{D}}^\delta)$  is compatible or not.

In the following we explore the convergence of minimizers of the regularized Kohn-Vogelius functional  $\mathcal{K}_\varepsilon$  associated to noisy data  $(g_{\text{N}}^\delta, g_{\text{D}}^\delta)$  to the minimum of the Kohn-Vogelius functional without noise, this is, to the solution of the Cauchy problem (III.1.3). For this we consider the following Kohn-Vogelius functional associated to the noisy data  $(g_{\text{N}}^\delta, g_{\text{D}}^\delta)$ :

$$\mathcal{K}^\delta(\varphi, \psi) := \frac{1}{2} \int_{\Omega} |\nabla u_{\varphi}^{g_{\text{D}}^\delta} - \nabla u_{\psi}^{g_{\text{N}}^\delta}|^2.$$

We also consider its regularization (noticing that the regularization term remains unchanged)

$$\mathcal{K}_\varepsilon^\delta(\varphi, \psi) := \mathcal{K}^\delta(\varphi, \psi) + \frac{\varepsilon}{2} \|(v_\varphi, v_\psi)\|_{(H^1(\Omega))^2}^2$$

and the associated minimizers  $(\varphi_{\varepsilon, \delta}^*, \psi_{\varepsilon, \delta}^*)$ . Moreover, if  $(g_{\text{N}}, g_{\text{D}})$  is compatible, we denote

$$(\varphi^*, \psi^*) := \underset{(\varphi, \psi) \in H^{-1/2}(\Gamma_{\text{ina}}) \times H^{1/2}(\Gamma_{\text{ina}})}{\operatorname{argmin}} \mathcal{K}(\varphi, \psi).$$

The key result, in order to obtain the desired convergence from noisy data to the solution of our problem, is the following proposition.

**Proposition III.1.6.** *We have*

$$\|(\varphi_\varepsilon^*, \psi_\varepsilon^*) - (\varphi_{\varepsilon, \delta}^*, \psi_{\varepsilon, \delta}^*)\|_{H^{-1/2}(\Gamma_{\text{ina}}) \times H^{1/2}(\Gamma_{\text{ina}})} \leq C \frac{\delta}{\sqrt{\varepsilon}}.$$

### III.1 Taking into account partial Cauchy data: a data completion problem

---

As a corollary, we deduce in a very general way some conditions on the regularization parameter  $\varepsilon$  in order to have convergence in the noisy case.

**Corollary III.1.7.** *Given a compatible data  $(g_N, g_D)$  associated to the Kohn-Vogelius functional minimizer  $(\varphi^*, \psi^*)$ . Let us consider  $\varepsilon = \varepsilon(\delta)$  such that*

$$\lim_{\delta \rightarrow 0} \varepsilon(\delta) = 0 \quad \text{and} \quad \lim_{\delta \rightarrow 0} \frac{\delta}{\sqrt{\varepsilon}} = 0.$$

Then we have

$$\lim_{\delta \rightarrow 0} \|(\varphi_{\varepsilon, \delta}^*, \psi_{\varepsilon, \delta}^*) - (\varphi^*, \psi^*)\|_{H^{-1/2}(\Gamma_{\text{ina}}) \times H^{1/2}(\Gamma_{\text{ina}})} = 0.$$

The last result gives us a guide on how the regularization parameter  $\varepsilon$  should be chosen in order to have convergence to the real solution (when it exists) in the noisy case. However these conditions are general and do not respond to any precise objective. In the following we explore a criterion for choosing the regularization parameter  $\varepsilon$  based on the definition of a *discrepancy measure*: the so-called *Morozov discrepancy principle* (see [125] for more details in the context of general regularization of inverse problems). We follow the strategy used by Ben Belgacem *et al.* in [47].

**Remark III.1.8.** *Notice that the choice of our parameter will depend on the noise level  $\delta$  and on the noisy data  $(g_N^\delta, g_D^\delta)$ , this is  $\varepsilon = \varepsilon(\delta, (g_N^\delta, g_D^\delta))$ : it is an a posteriori choice parameter rule. One may consider an a priori choice parameter rule which is only based on the noise, that is  $\varepsilon = \varepsilon(\delta)$ . However, in order to obtain optimal order of convergence, one needs some abstract smoothness conditions on the real solution which seems to be unrealistic in our setting (see [125] for more details on those strategies).*

Let us assume that our problem has a solution, i.e. the Kohn-Vogelius functional  $\mathcal{K}$  associated to the compatible data  $(g_N, g_D)$  has a minimizer  $(\varphi^*, \psi^*)$ . Let us define the *discrepancy measure* as the error in the Kohn-Vogelius functional with noisy data when we evaluate it on the solution of our problem, this is:

$$\begin{aligned} \mathcal{K}^\delta(\varphi^*, \psi^*) &= \frac{1}{2} \int_{\Omega} \left| \nabla \left( u_{\varphi^*}^{g_D^\delta} - u_{\psi^*}^{g_N^\delta} \right) \right|^2 \\ &= \mathcal{K}(\varphi^*, \psi^*) + \frac{1}{2} \int_{\Omega} \left| \nabla \left( u_0^{dg_D} - u_0^{dg_N} \right) \right|^2 - \int_{\Omega} \nabla \left( u_{\varphi^*}^{g_D} - u_{\psi^*}^{g_N} \right) \cdot \nabla \left( u_0^{dg_D} - u_0^{dg_N} \right), \end{aligned}$$

where  $(dg_N, dg_D) := (g_N^\delta - g_N, g_D^\delta - g_D)$  and where the second equality is obtained by rewriting  $u_{\varphi^*}^{g_D^\delta} = u_{\varphi^*}^{g_D - g_D + g_D^\delta} = u_0^{dg_D} + u_{\varphi^*}^{g_D}$  and an analogous expression for  $u_{\psi^*}^{g_N^\delta}$ . Now, as  $(\varphi^*, \psi^*)$  is the minimizer of  $\mathcal{K}$ , we have

$$\mathcal{K}(\varphi^*, \psi^*) = 0 \quad \text{and} \quad \int_{\Omega} \nabla \left( u_{\varphi^*}^{g_D} - u_{\psi^*}^{g_N} \right) \cdot \nabla \left( u_0^{dg_D} - u_0^{dg_N} \right) = 0.$$

From the well-posedness of the problems associated to  $u_0^{dg_D}$  and  $u_0^{dg_N}$  and using (III.1.6), we obtain

$$\mathcal{K}^\delta(\varphi^*, \psi^*) = \frac{1}{2} \int_{\Omega} \left| \nabla \left( u_0^{dg_D} - u_0^{dg_N} \right) \right|^2 \leq C \delta^2. \quad (\text{III.1.7})$$

Keeping this in mind, we redefine the noise amount to  $\mathcal{K}^\delta(\varphi^*, \psi^*) = \delta^2$  and we consider the discrepancy principle based on this notion of noise.

One can prove that the application  $\varepsilon \mapsto \mathcal{K}^\delta(\varphi_{\varepsilon, \delta}^*, \psi_{\varepsilon, \delta}^*)$  is strictly increasing and therefore injective. Moreover, if  $\varepsilon \in [0, \infty)$  then  $\mathcal{K}^\delta(\varphi_{\varepsilon, \delta}^*, \psi_{\varepsilon, \delta}^*) \in [0, \mathcal{K}^\delta(0, 0))$ . Let us assume that there exists  $\tau > 1$  such that  $\tau \delta^2 \in [0, \mathcal{K}^\delta(0, 0))$ : indeed we expect that the data we have is not of the same order as the noise,

otherwise  $(\varphi^*, \psi^*) = (0, 0)$  would be an *admissible* approximation of the exact solution. Then the discrepancy principle consists, in our case, in choosing  $\varepsilon$  such that

$$\varepsilon = \sup \{ \varepsilon : \mathcal{K}^\delta(\varphi_{\varepsilon, \delta}^*, \psi_{\varepsilon, \delta}^*) \leq \tau \delta^2 \}. \quad (\text{III.1.8})$$

The idea of choosing the sup is based on the fact that a small regularization parameter involves less stability, so the *natural* strategy is to choose the biggest regularization parameter such that the discrepancy is in the order of the noise. The increasing monotonicity of the application  $\mathcal{K}^\delta$  implies that  $\varepsilon$  is simply the parameter such that

$$\mathcal{K}^\delta(\varphi_{\varepsilon, \delta}^*, \psi_{\varepsilon, \delta}^*) = \tau \delta^2. \quad (\text{III.1.9})$$

**Remark III.1.9.** *It is important to notice that the “redefinition” of the noise estimate does not involve, for real computations, the knowledge of the real solution  $(\varphi^*, \psi^*)$ . Indeed we only use the real solution when we evaluate it into the Kohn-Vogelius functional with noisy data  $(g_N^\delta, g_D^\delta)$  obtaining the estimate (III.1.7). We can observe that this quantity only depends on a constant  $C$  and the error estimate  $\delta$ . Hence, by assuming that  $C \leq 1$  (which is itself a strong assumption, as  $C$  depends on Poincaré inequality constant and trace theorem constant<sup>2</sup>), we can consider  $\mathcal{K}^\delta(\varphi^*, \psi^*) = \delta^2$  as the error measure between the real and measured data which leads to the discrepancy principle formulation given by (III.1.8).*

Finally we prove that this *a posteriori* choice parameter rule satisfies the conditions of Corollary III.1.7.

**Proposition III.1.10.** *The regularization parameter choice given by the Morozov discrepancy principle (III.1.9) satisfies*

$$\lim_{\delta \rightarrow 0} \varepsilon(\delta) = 0 \quad \text{and} \quad \lim_{\delta \rightarrow 0} \frac{\delta}{\sqrt{\varepsilon}} = 0.$$

*This implies particularly that we have the following convergence*

$$\lim_{\delta \rightarrow 0} \|(\varphi_{\varepsilon, \delta}^*, \psi_{\varepsilon, \delta}^*) - (\varphi^*, \psi^*)\|_{H^{-1/2}(\Gamma_{\text{ina}}) \times H^{1/2}(\Gamma_{\text{ina}})} = 0.$$

### III.1.1.2 The inverse obstacle problem with partial Cauchy data

We now come back to our initial inverse problem (III.1.1). As mentioned, these two problems, that is the inverse obstacle problem and the data completion problem, can be studied through the minimization of a cost functional. Thus we focus on the following optimization problem:

$$(\omega^*, \varphi^*, \psi^*) \in \underset{(\omega, \varphi, \psi) \in \mathcal{O} \times H^{-1/2}(\Gamma_{\text{ina}}) \times H^{1/2}(\Gamma_{\text{ina}})}{\operatorname{argmin}} \mathcal{K}(\omega, \varphi, \psi), \quad (\text{III.1.10})$$

where  $\mathcal{K}$  is now the nonnegative Kohn-Vogelius cost functional defined by

$$\mathcal{K}(\omega, \varphi, \psi) := \frac{1}{2} \int_{\Omega \setminus \bar{\omega}} |\nabla u_\varphi^{g_D}(\omega) - \nabla u_\psi^{g_N}(\omega)|^2,$$

where the set of admissible geometries  $\mathcal{O}$  is given by (III.1.2) and where  $u_\varphi^{g_D}(\omega), u_\psi^{g_N}(\omega) \in H^1(\Omega \setminus \bar{\omega})$  are the respective solutions of the following problems

$$\left\{ \begin{array}{ll} -\Delta u_\varphi^{g_D}(\omega) = 0 & \text{in } \Omega \setminus \bar{\omega}, \\ u_\varphi^{g_D}(\omega) = g_D & \text{on } \Gamma_{\text{obs}}, \\ \partial_n u_\varphi^{g_D}(\omega) = \varphi & \text{on } \Gamma_{\text{ina}}, \\ u_\varphi^{g_D}(\omega) = 0 & \text{on } \partial\omega, \end{array} \right. \quad \text{and} \quad \left\{ \begin{array}{ll} -\Delta u_\psi^{g_N}(\omega) = 0 & \text{in } \Omega \setminus \bar{\omega}, \\ \partial_n u_\psi^{g_N}(\omega) = g_N & \text{on } \Gamma_{\text{obs}}, \\ u_\psi^{g_N}(\omega) = \psi & \text{on } \Gamma_{\text{ina}}, \\ u_\psi^{g_N}(\omega) = 0 & \text{on } \partial\omega. \end{array} \right. \quad (\text{III.1.11})$$

---

2. The estimation of the constant  $C$  should be analyzed in detail but is beyond the scope of this work

### III.1 Taking into account partial Cauchy data: a data completion problem

If the inverse problem (III.1.1) has a solution, then the identifiability result III.1.1 ensures that  $\mathcal{K}(\omega, \varphi, \psi) = 0$  if and only if  $(\omega, \varphi, \psi) = (\omega^*, \varphi^*, \psi^*)$  (and in this case  $u_{\varphi^*}^{g_D} = u_{\psi^*}^{g_N} = u_{\text{ex}}$  where  $u_{\text{ex}}$  is the solution of the Cauchy problem in  $\Omega \setminus \bar{\omega}^*$ ).

As previously we introduce the functions  $v_\varphi := u_\varphi^0$  and  $v_\psi := u_\psi^0$  (which also depend on  $\omega$ ) which satisfy respectively

$$\left\{ \begin{array}{ll} -\Delta v_\varphi = 0 & \text{in } \Omega \setminus \bar{\omega}, \\ v_\varphi = 0 & \text{on } \Gamma_{\text{obs}}, \\ \partial_n v_\varphi = \varphi & \text{on } \Gamma_{\text{ina}}, \\ v_\varphi = 0 & \text{on } \partial\omega, \end{array} \right. \quad \text{and} \quad \left\{ \begin{array}{ll} -\Delta v_\psi = 0 & \text{in } \Omega \setminus \bar{\omega}, \\ \partial_n v_\psi = 0 & \text{on } \Gamma_{\text{obs}}, \\ v_\psi = \psi & \text{on } \Gamma_{\text{ina}}, \\ v_\psi = 0 & \text{on } \partial\omega. \end{array} \right. \quad (\text{III.1.12})$$

Hence, using the previous Tikhonov regularization, we consider, instead of (III.1.10), the following optimization problem

$$(\omega^*, \varphi^*, \psi^*) \in \underset{(\omega, \varphi, \psi) \in \mathcal{O} \times H^{-1/2}(\Gamma_{\text{ina}}) \times H^{1/2}(\Gamma_{\text{ina}})}{\text{argmin}} \mathcal{K}_\varepsilon(\omega, \varphi, \psi),$$

where  $\mathcal{K}_\varepsilon$  is the regularized nonnegative Kohn-Vogelius cost functional defined by

$$\mathcal{K}_\varepsilon(\omega, \varphi, \psi) := \mathcal{K}(\omega, \varphi, \psi) + \frac{\varepsilon}{2} \|(v_\varphi, v_\psi)\|_{(H^1(\Omega \setminus \bar{\omega}))^2}^2 = \frac{1}{2} \int_{\Omega \setminus \bar{\omega}} |\nabla u_\varphi^{g_D} - \nabla u_\psi^{g_N}|^2 + \frac{\varepsilon}{2} \|(v_\varphi, v_\psi)\|_{(H^1(\Omega \setminus \bar{\omega}))^2}^2,$$

where  $u_\varphi^{g_D}, u_\psi^{g_N} \in H^1(\Omega \setminus \bar{\omega})$  and  $v_\varphi, v_\psi \in H^1(\Omega \setminus \bar{\omega})$  are the respective solutions of Problems (III.1.11) and (III.1.12).

**Computation of the gradient.** To minimize the functional  $\mathcal{K}_\varepsilon$ , we first compute the gradient in order to consider a descent method to reconstruct numerically the solution. The partial derivatives with respect to  $\varphi$  and  $\psi$  are given by the following proposition.

**Proposition III.1.11.** *For all  $(\varphi, \psi), (\tilde{\varphi}, \tilde{\psi}) \in H^{-1/2}(\Gamma_{\text{ina}}) \times H^{1/2}(\Gamma_{\text{ina}})$ , the partial derivative of the functional  $\mathcal{K}_\varepsilon$  are given by*

$$\frac{\partial \mathcal{K}_\varepsilon}{\partial \varphi}(\varphi, \psi) [\tilde{\varphi}] = \int_{\Gamma_{\text{ina}}} \tilde{\varphi} \cdot (u_\varphi^{g_D} + \varepsilon v_\varphi + w_D - \psi)$$

and

$$\frac{\partial \mathcal{K}_\varepsilon}{\partial \psi}(\varphi, \psi) [\tilde{\psi}] = \langle (\partial_n u_\psi^{g_N} + \varepsilon \partial_n v_\psi + \partial_n w_N - \varphi), \tilde{\psi} \rangle_{-1/2, 1/2, \Gamma_{\text{ina}}},$$

where  $w_N, w_D \in H^1(\Omega)$  are the respective solutions of the following adjoint problems:

$$\left\{ \begin{array}{ll} -\Delta w_N = -\varepsilon v_\psi & \text{in } \Omega, \\ \partial_n w_N = \partial_n u_\varphi^{g_D} - g_N & \text{on } \Gamma_{\text{obs}}, \\ w_N = 0 & \text{on } \Gamma_{\text{ina}}, \end{array} \right. \quad \text{and} \quad \left\{ \begin{array}{ll} -\Delta w_D = \varepsilon v_\varphi & \text{in } \Omega, \\ w_D = u_\psi^{g_N} - g_D & \text{on } \Gamma_{\text{obs}}, \\ \partial_n w_D = 0 & \text{on } \Gamma_{\text{ina}}. \end{array} \right.$$

Particularly the directions  $(\tilde{\varphi}, \tilde{\psi}) \in H^{-1/2}(\Gamma_{\text{ina}}) \times H^{1/2}(\Gamma_{\text{ina}})$  given by

$$\tilde{\varphi} = \psi - u_\varphi^{g_D}|_{\Gamma_{\text{ina}}} - \varepsilon v_\varphi|_{\Gamma_{\text{ina}}} - w_D|_{\Gamma_{\text{ina}}} \quad \text{and} \quad \tilde{\psi} = -v_W|_{\Gamma_{\text{ina}}},$$

with  $W := \varphi - \partial_n u_\psi^{g_N}|_{\Gamma_{\text{ina}}} - \varepsilon \partial_n v_\psi|_{\Gamma_{\text{ina}}} - \partial_n w_N|_{\Gamma_{\text{ina}}} \in H^{-1/2}(\Gamma_{\text{ina}})$ , are descent directions.

**Remark III.1.12.** *The choice of these descent directions can be discussed. The above Proposition III.1.11 gives the natural idea in order to use a gradient method. But a discussion and an improvement of this method will be given below, see the end of Section III.1.2.1.*

Moreover we compute the shape gradient of the functional and obtain the following statement. We recall that  $\Omega_{d_0}$  is an open set with a  $C^\infty$  boundary such that

$$\{\mathbf{x} \in \Omega; d(\mathbf{x}, \partial\Omega) > d_0/2\} \subset \Omega_{d_0} \subset \{\mathbf{x} \in \Omega; d(\mathbf{x}, \partial\Omega) > d_0/3\}.$$

**Proposition III.1.13.** *For  $\mathbf{V} \in \mathcal{U} := \left\{ \mathbf{V} \in \mathbf{W}^{2,\infty}(\mathbb{R}^d); \text{supp}(\mathbf{V}) \subset \overline{\Omega_{d_0}} \text{ and } \|\mathbf{V}\|_{2,\infty} < \min\left(\frac{d_0}{3}, 1\right) \right\}$ , the regularized Kohn-Vogelius cost functional  $\mathcal{K}_\varepsilon$  is differentiable at  $\omega$  in the direction  $\mathbf{V}$  with*

$$\begin{aligned} \text{DK}_\varepsilon(\omega) \cdot \mathbf{V} = & - \int_{\partial\omega} (\partial_n \rho_N^u \cdot \partial_n u_\varphi^{g_D} + \partial_n \rho_N^v \cdot \partial_n v_\varphi)(\mathbf{V} \cdot \mathbf{n}) + \frac{1}{2} \int_{\partial\omega} |\nabla w|^2 (\mathbf{V} \cdot \mathbf{n}) \\ & - \int_{\partial\omega} (\partial_n \rho_D^u \cdot \partial_n u_\psi^{g_N} + \partial_n \rho_D^v \cdot \partial_n v_\psi)(\mathbf{V} \cdot \mathbf{n}) + \frac{\varepsilon}{2} \int_{\partial\omega} (|\nabla v_\varphi|^2 + |\nabla v_\psi|^2 + |v_\varphi|^2 + |v_\psi|^2)(\mathbf{V} \cdot \mathbf{n}), \end{aligned}$$

where  $w := u_\varphi^{g_D} - u_\psi^{g_N}$  and where  $\rho_D^u, \rho_N^u, \rho_D^v, \rho_N^v \in H^1(\Omega \setminus \overline{\omega})$  are the respective solutions of the following adjoint problems

$$\left\{ \begin{array}{ll} -\Delta \rho_N^u = 0 & \text{in } \Omega \setminus \overline{\omega}, \\ \rho_N^u = g_D - u_\psi^{g_N} & \text{on } \Gamma_{\text{obs}}, \\ \partial_n \rho_N^u = 0 & \text{on } \Gamma_{\text{ina}}, \\ \rho_N^u = 0 & \text{on } \partial\omega, \end{array} \right. \quad \left\{ \begin{array}{ll} -\Delta \rho_N^v = -\varepsilon v_\varphi & \text{in } \Omega \setminus \overline{\omega}, \\ \rho_N^v = 0 & \text{on } \Gamma_{\text{obs}}, \\ \partial_n \rho_N^v = 0 & \text{on } \Gamma_{\text{ina}}, \\ \rho_N^v = 0 & \text{on } \partial\omega, \end{array} \right.$$

and

$$\left\{ \begin{array}{ll} -\Delta \rho_D^u = 0 & \text{in } \Omega \setminus \overline{\omega}, \\ \partial_n \rho_D^u = 0 & \text{on } \Gamma_{\text{obs}}, \\ \rho_D^u = \psi - u_\varphi^{g_D} & \text{on } \Gamma_{\text{ina}}, \\ \rho_D^u = 0 & \text{on } \partial\omega, \end{array} \right. \quad \left\{ \begin{array}{ll} -\Delta \rho_D^v = -\varepsilon v_\psi & \text{in } \Omega \setminus \overline{\omega}, \\ \partial_n \rho_D^v = 0 & \text{on } \Gamma_{\text{obs}}, \\ \rho_D^v = \varepsilon \psi & \text{on } \Gamma_{\text{ina}}, \\ \rho_D^v = 0 & \text{on } \partial\omega. \end{array} \right.$$

**Numerical simulations.** As previously mentioned, Theorem 2 in [7] explains the difficulties encountered to solve numerically the reconstruction of  $\omega$ . Indeed the shape gradient has not an uniform sensitivity with respect to the deformation direction. Hence, since the inverse obstacle problem is severely ill-posed, we need some regularization methods to solve it numerically, for instance by adding to the functional a penalization in terms of the perimeter (see [70] or [107]). Here we choose to make a regularization by parametrization using a parametric model of shape variations: following the same strategy as in [7] or in [89], we use a truncated Fourier parametrization for the inclusion.

Then we perform several numerical simulations that we briefly present here (see Figures III.1.2 and III.1.3). The used algorithm is a classical gradient method, updating the boundary condition  $(\varphi, \psi)$  and then the obstacle  $\omega$  at each iteration. Finally we compare numerically the case of partial Cauchy data with the case of complete boundary data in Figure III.1.4.

### III.1.2 Setting of the trial method

The work exposed in this subsection was done in collaboration with Marc Dambrine (university of Pau) and Helmut Harbrecht (university of Basel) and is the topic of the submitted paper [87] (20 pages). We can first notice that, contrary to previously, one can only assume that the admissible shapes  $\omega \in \mathcal{O}$  have Lipschitz boundaries. Moreover we assume now that  $\Gamma_{\text{obs}} = \partial\Omega$ .

The idea is to use the previously mentioned data completion problem in order to use the so-called *trial method* to solve the inverse obstacle problem. We also use the minimization of a regularized Kohn-Vogelius functional in order to approximate the solution of the initial inverse problem (III.1.1).

The first novelty is an improvement of the numerical resolution of the data completion problem using a Newton approach, which is efficient since the functional is quadratic. Then we build an iterative sequence of domains using the combination of a data completion subproblem and the trial method

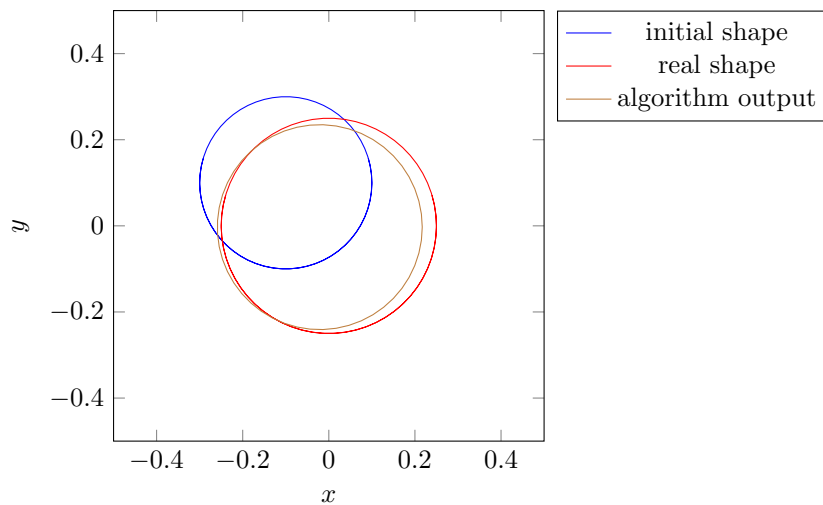


**Figure III.1.2** – Object detection with noise (5%): Real solution, initial guess and obtained obstacle after 10 iterations ( $\varepsilon = 0.01$ ).

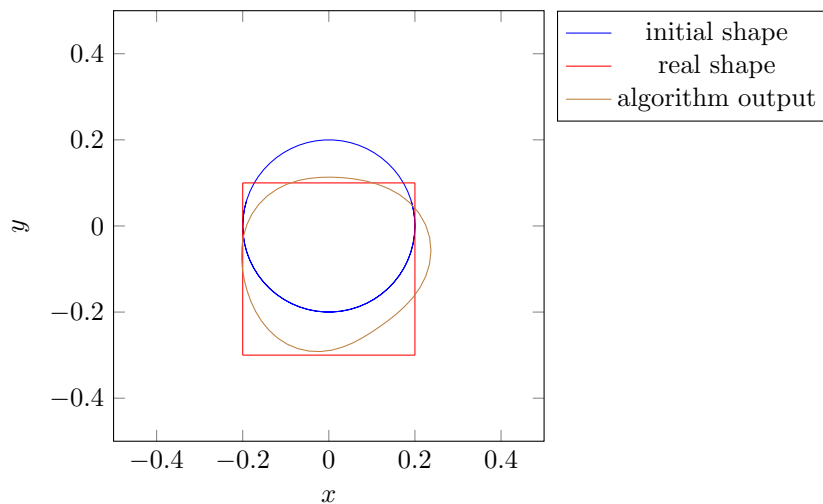


**Figure III.1.3** – Object detection with noise: Real solution, initial guess and obtained obstacle after 55 iterations ( $\varepsilon = 0.001$ ).

which is used to control the evolution of the inclusion boundary. This basically means that, given an inclusion  $\omega$ , we compute an harmonic function  $u \in H^1(\Omega \setminus \bar{\omega})$  which admits the Cauchy data  $(g_N, g_D)$  on the outer boundary  $\partial\Omega$ . With the help of the Cauchy data at the interior boundary  $\partial\omega$ , we aim at updating the interior boundary such that the desired Dirichlet condition  $u = 0$  holds at the new interior boundary.

### III.1.2.1 The data completion problem: a Newton method

Let us consider some nontrivial Cauchy data  $(g_N, g_D) \in H^{-1/2}(\partial\Omega) \times H^{1/2}(\partial\Omega)$  and  $\omega^* \in \mathcal{O}$ . In this context, the data completion problem consists in recovering data on  $\partial\omega^*$ , from the overdetermined

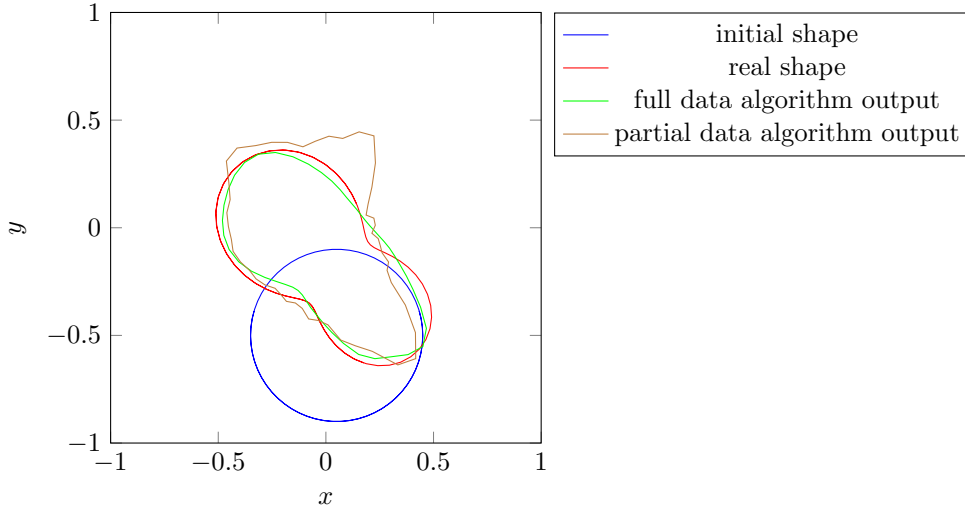


**Figure III.1.4** – Comparison between algorithms in the noisy case (5%) after 200 iterations.

data  $(g_N, g_D)$  on  $\partial\Omega$ , that is:

$$\text{Find } u \in H^1(\Omega \setminus \bar{\omega}^*) \text{ such that} \quad \begin{cases} \Delta u = 0 & \text{in } \Omega \setminus \bar{\omega}^*, \\ u = g_D & \text{on } \partial\Omega, \\ \partial_n u = g_N & \text{on } \partial\Omega. \end{cases} \quad (\text{III.1.13})$$

As previously we solve this problem by minimizing a regularized Kohn-Vogelius functional. Notice that such a functional turns to be quadratic and convex. Surprisingly, to the best of my knowledge, only gradient based numerical schemes have been studied for the resolution of this problem. We describe here the Newton method that is completely suited for quadratic objectives.

In order to deal with the ill-posedness previously mentioned, we consider as before a Tikhonov regularization of the functional which ensures the existence of a minimizer even for non compatible data thanks to the gained of coerciveness and, in case of compatible data, the convergence towards the exact solution (as mentioned in the previous section III.1.1). Then we introduce the two maps  $\mathbf{u}_{DN}$  and  $\mathbf{u}_{ND}$  defined as follows

$$\begin{aligned} \mathbf{u}_{DN} &: H^{1/2}(\partial\Omega) \times H^{-1/2}(\partial\omega) \longrightarrow H^1(\Omega \setminus \bar{\omega}), \\ \mathbf{u}_{ND} &: H^{-1/2}(\partial\Omega) \times H^{1/2}(\partial\omega) \longrightarrow H^1(\Omega \setminus \bar{\omega}), \end{aligned}$$

where  $\mathbf{u}_{DN}(g_D, \varphi) \in H^1(\Omega \setminus \bar{\omega})$  solves the boundary values problem

$$\begin{cases} \Delta u = 0 & \text{in } \Omega \setminus \bar{\omega}, \\ u = g_D & \text{on } \partial\Omega, \\ \partial_n u = \varphi & \text{on } \partial\omega, \end{cases} \quad (\text{III.1.14})$$

and where  $\mathbf{u}_{ND}(g_N, \psi) \in H^1(\Omega \setminus \bar{\omega})$  solves the boundary values problem

$$\begin{cases} \Delta u = 0 & \text{in } \Omega \setminus \bar{\omega}, \\ \partial_n u = g_N & \text{on } \partial\Omega, \\ u = \psi & \text{on } \partial\omega. \end{cases} \quad (\text{III.1.15})$$

Notice that the indices mean the type of boundary condition, where the first one indicates the outer boundary and the second one the inner boundary. Notice also that, using the notations of Section III.1.1, we have  $\mathbf{u}_{DN}(g_D, \varphi) = u_{\varphi}^{g_D}$  and  $\mathbf{u}_{ND}(g_N, \psi) = u_{\psi}^{g_N}$ ; however, here, we reconstruct the

### III.1 Taking into account partial Cauchy data: a data completion problem

---

data on the boundary  $\partial\omega$  which will be an approximation of the unknown inclusion, and not on a fixed part of the exterior boundary. Thus, in order to avoid any confusion between these two parts, we differentiate these notations.

To tackle the inverse problem, we try to solve the problem:

$$\text{Find } (\varphi, \psi) \in \mathbf{H}^{-1/2}(\partial\omega) \times \mathbf{H}^{1/2}(\partial\omega) \text{ such that} \\ \mathbf{u}_{\text{DN}}(g_{\text{D}}, \varphi) = \mathbf{u}_{\text{ND}}(g_{\text{N}}, \psi).$$

Thanks to the linearity of the maps  $\mathbf{u}_{\text{ND}}$  and  $\mathbf{u}_{\text{DN}}$ , this is equivalent to:

$$\text{Find } (\varphi, \psi) \in \mathbf{H}^{-1/2}(\partial\omega) \times \mathbf{H}^{1/2}(\partial\omega) \text{ such that} \\ \mathbf{u}_{\text{DN}}(0, \varphi) - \mathbf{u}_{\text{ND}}(0, \psi) = -(\mathbf{u}_{\text{DN}}(g_{\text{D}}, 0) - \mathbf{u}_{\text{ND}}(g_{\text{N}}, 0)).$$

Notice that this is a standard linear inverse problem associated to the linear operator

$$\mathbf{A} : \mathbf{H}^{-1/2}(\partial\omega) \times \mathbf{H}^{1/2}(\partial\omega) \longrightarrow \mathbf{H}^1(\Omega \setminus \bar{\omega}) \\ (\varphi, \psi) \longmapsto \mathbf{u}_{\text{DN}}(0, \varphi) - \mathbf{u}_{\text{ND}}(0, \psi).$$

Of course, the right hand side  $\mathbf{b} := -(\mathbf{u}_{\text{DN}}(g_{\text{D}}, 0) - \mathbf{u}_{\text{ND}}(g_{\text{N}}, 0))$  may belong or may not belong to the range of  $\mathbf{A}$ , depending on the fact that data are compatible or not.

We try to solve the previous linear equation in a least squares meaning. We thus focus on the following optimization problem

$$(\varphi^*, \psi^*) \in \underset{(\varphi, \psi) \in \mathbf{H}^{-1/2}(\partial\omega) \times \mathbf{H}^{1/2}(\partial\omega)}{\text{argmin}} \mathcal{K}(\varphi, \psi),$$

where  $\mathcal{K} : \mathbf{H}^{-1/2}(\partial\omega) \times \mathbf{H}^{1/2}(\partial\omega) \rightarrow \mathbb{R}$  is the non-negative Kohn-Vogelius cost functional defined by

$$\mathcal{K}(\varphi, \psi) := \frac{1}{2} |\mathbf{A}(\varphi, \psi) - \mathbf{b}|_{\mathbf{H}^1(\Omega \setminus \bar{\omega})}^2.$$

Here again, the functional  $\mathcal{K}$  is convex, positive and its infimum is zero. Notice that the previous criterion also writes

$$\mathcal{K}(\varphi, \psi) = \frac{1}{2} |\mathbf{u}_{\text{DN}}(g_{\text{D}}, \varphi) - \mathbf{u}_{\text{ND}}(g_{\text{N}}, \psi)|_{\mathbf{H}^1(\Omega \setminus \bar{\omega})}^2 = \frac{1}{2} \int_{\Omega \setminus \bar{\omega}} |\nabla \mathbf{u}_{\text{DN}}(g_{\text{D}}, \varphi) - \nabla \mathbf{u}_{\text{ND}}(g_{\text{N}}, \psi)|^2.$$

As previously, the idea is to minimize the functional  $\mathcal{K}$ , noticing that if the inverse problem (III.1.13) has a solution then the minimum of  $\mathcal{K}$  is zero.

The usual theory of linear inverse problems can be applied. That is, we solve the *normal equation*  $\mathbf{A}^* \mathbf{A}(\varphi, \psi) = \mathbf{A}^* \mathbf{b}$  or its *regularized version*  $(\mathbf{A}^* \mathbf{A} + \varepsilon \mathbf{B}^* \mathbf{B})(\varphi, \psi) = \mathbf{A}^* \mathbf{b}$  where  $\mathbf{B}$  is a *regularization operator* and where  $\varepsilon > 0$ . However it involves the adjoint  $\mathbf{A}^*$  of  $\mathbf{A}$  and hence to manipulate the scalar product in the space  $\mathbf{H}^{-1/2}(\partial\omega) \times \mathbf{H}^{1/2}(\partial\omega)$ . The main difficulty of this approach is that the scalar product in the spaces  $\mathbf{H}^{1/2}(\partial\omega)$  and  $\mathbf{H}^{-1/2}(\partial\omega)$  is not so easy to deal with from a practical point of view when we use the optimize then discretize approach. Conversely, if one first discretizes the equations and then computes the discrete adjoint, the usual theory can be applied. In the following we want to remain at the continuous level and reduce the minimization of the Kohn-Vogelius objective to such a linear inverse problem in a simple way thanks to the Newton point of view. Since the objective  $\mathcal{K}$  is quadratic, its hessian is constant and its minimizer can be compute by a single step in a Newton method.

**Remark III.1.14.** *One can note, as in the previous remark III.1.4, that the two problems (III.1.14) and (III.1.15) are well-posed for any given boundary conditions  $(\varphi, \psi) \in \mathbf{H}^{-1/2}(\partial\omega) \times \mathbf{H}^{1/2}(\partial\omega)$ .*

Using the standard Tikhonov regularization, we consider a non-negative real number  $\varepsilon$  and introduce the regularized Kohn-Vogelius cost functional  $\mathcal{K}_\varepsilon : \mathbf{H}^{-1/2}(\partial\omega) \times \mathbf{H}^{1/2}(\partial\omega) \rightarrow \mathbb{R}$  defined by

$$\mathcal{K}_\varepsilon(\varphi, \psi) := \mathcal{K}(\varphi, \psi) + \varepsilon \mathcal{T}(\varphi, \psi),$$

where the regularizing term  $\mathcal{T}(\varphi, \psi)$  is defined by

$$\mathcal{T}(\varphi, \psi) := \frac{1}{2} \left( |\mathbf{u}_{\text{ND}}(0, \psi)|^2 + |\mathbf{u}_{\text{DN}}(0, \varphi)|^2 + \int_{\partial\omega} \psi^2 \right) = \frac{1}{2} \int_{\partial\omega} (\psi + \partial_n \mathbf{u}_{\text{ND}}(0, \psi)) \psi + \mathbf{u}_{\text{DN}}(0, \varphi) \varphi.$$

As in Section III.1.1, this regularization enables to obtain the existence of a minimizer, for all  $\varepsilon > 0$ , even for non compatible data thanks to the gained of coerciveness and, in case of compatible data, the convergence of these minimizers towards the exact solution when  $\varepsilon$  goes to 0.

We have the following expression of the gradient of the objectives with respect to  $(\varphi, \psi)$ .

**Proposition III.1.15.** *The functional  $\mathcal{K}$  is quadratic with gradient*

$$D\mathcal{K}(\varphi, \psi) \cdot [\tilde{\varphi}, \tilde{\psi}] = \int_{\partial\omega} [\partial_n \mathbf{u}_{\text{ND}}(\partial_n \mathbf{u}_{\text{DN}}(g_D, \varphi), \psi) - \varphi] \tilde{\psi} + [\mathbf{u}_{\text{DN}}(\mathbf{u}_{\text{ND}}(g_N, \psi), \varphi) - \psi] \tilde{\varphi},$$

and constant Hessian

$$D^2\mathcal{K}(\varphi, \psi) \cdot \left( [\tilde{\varphi}_1, \tilde{\psi}_1], [\tilde{\varphi}_2, \tilde{\psi}_2] \right) = \langle \mathbf{u}_{\text{DN}}(0, \tilde{\varphi}_1) - \mathbf{u}_{\text{ND}}(0, \tilde{\psi}_1), \mathbf{u}_{\text{DN}}(0, \tilde{\varphi}_2) - \mathbf{u}_{\text{ND}}(0, \tilde{\psi}_2) \rangle.$$

Moreover the derivatives of  $\mathcal{T}$  with respect to  $(\varphi, \psi)$  are

$$D\mathcal{T}(\varphi, \psi) \cdot [\tilde{\varphi}, \tilde{\psi}] = \int_{\partial\omega} \tilde{\psi} (\psi + \partial_n \mathbf{u}_{\text{ND}}(0, \psi)) + \mathbf{u}_{\text{DN}}(0, \varphi) \tilde{\varphi},$$

and

$$D^2\mathcal{T}(\varphi, \psi) \cdot [(\tilde{\varphi}_1, \tilde{\psi}_1), (\tilde{\varphi}_2, \tilde{\psi}_2)] = \int_{\partial\omega} \tilde{\psi}_1 (\tilde{\psi}_2 + \partial_n \mathbf{u}_{\text{ND}}(0, \tilde{\psi}_2)) + \mathbf{u}_{\text{ND}}(0, \tilde{\varphi}_2) \tilde{\varphi}_1.$$

The first natural idea to build a numerical scheme for minimizing the objective is to use a descent method, as what is done previously in Section III.1.1.2. This leads to a sequence  $(\varphi_n, \psi_n)$  by the update rule

$$\begin{pmatrix} \varphi_{n+1} \\ \psi_{n+1} \end{pmatrix} = \begin{pmatrix} \varphi_n \\ \psi_n \end{pmatrix} + s_{n+1} \mathbf{d}_n,$$

where  $s_{n+1}$  is a descent step and where the descent direction  $\mathbf{d}_n$  is naturally chosen as the anti-gradient:

$$\mathbf{d}_n = - \begin{pmatrix} \mathbf{u}_{\text{DN}}(\mathbf{u}_{\text{ND}}(g_N, \varphi_n), \varphi_n) - \psi_n \\ \partial_n \mathbf{u}_{\text{ND}}(\partial_n \mathbf{u}_{\text{DN}}(g_D, \varphi_n), \psi_n) - \varphi_n \end{pmatrix} + \varepsilon \begin{pmatrix} \mathbf{u}_{\text{DN}}(0, \varphi_n) \\ \psi_n + \partial_n \mathbf{u}_{\text{ND}}(0, \psi_n) \end{pmatrix}.$$

However this updates is not in the right spaces: while  $(\varphi_n, \psi_n) \in \mathbf{H}^{-1/2}(\partial\omega) \times \mathbf{H}^{1/2}(\partial\omega)$ , the update  $\mathbf{d}_n$  lies in  $\mathbf{H}^{1/2}(\partial\omega) \times \mathbf{H}^{-1/2}(\partial\omega)$ . In fact,  $\mathbf{d}_n$  is not the gradient that should be computed with respect to the scalar product on  $\mathbf{H}^{-1/2}(\partial\omega) \times \mathbf{H}^{1/2}(\partial\omega)$  and not with respect to  $\mathbf{L}^2(\partial\omega) \times \mathbf{L}^2(\partial\omega)$ . The true gradient is much more complex to compute. Therefore we do not consider the gradient method here and use the Newton method that we describe in our context in the following proposition.

**Proposition III.1.16.** *The Newton update  $(\tilde{\varphi}, \tilde{\psi}) \in \mathbf{H}^{-1/2}(\partial\omega) \times \mathbf{H}^{1/2}(\partial\omega)$  for the regularized Kohn-Vogelius objective  $\mathcal{K}_\varepsilon(\varphi_n, \psi_n)$  is given by the linear system*

$$\begin{cases} \mathbf{u}_{\text{DN}}(\mathbf{u}_{\text{ND}}(0, \tilde{\psi}), \tilde{\varphi}) - \tilde{\psi} + \varepsilon \mathbf{u}_{\text{DN}}(0, \tilde{\varphi}) \\ \quad = \psi_n - \mathbf{u}_{\text{DN}}(\mathbf{u}_{\text{ND}}(g_N, \varphi_n), \varphi_n) - \varepsilon \mathbf{u}_{\text{DN}}(0, \varphi_n), \\ \partial_n \mathbf{u}_{\text{ND}}(\partial_n \mathbf{u}_{\text{DN}}(0, \tilde{\varphi}), \tilde{\psi}) - \tilde{\varphi} + \varepsilon (\tilde{\psi} + \partial_n \mathbf{u}_{\text{ND}}(0, \tilde{\psi})) \\ \quad = \varphi_n - \partial_n \mathbf{u}_{\text{ND}}(\partial_n \mathbf{u}_{\text{DN}}(g_D, \varphi_n), \psi_n) - \varepsilon (\psi_n + \partial_n \mathbf{u}_{\text{ND}}(0, \psi_n)). \end{cases}$$

We underline that the Hessian of the functional  $\mathcal{K}_\varepsilon(\varphi, \psi)$  does not depend on the argument  $(\varphi, \psi)$  and, since the functional is quadratic, the Newton scheme converges in one iteration.

### III.1.2.2 The inverse obstacle problem: the trial method

We now aim at solving numerically the inverse obstacle problem (III.1.1) with the trial method. The general idea is to use the previous data completion step in order to reconstruct  $u|_{\partial\omega}$  and  $\partial_n u|_{\partial\omega}$  on an approximation  $\partial\omega$  of the *real* inclusion and then to use the so-called trial method in order to update the shape of the inclusion.

**Background and motivation.** The trial method is a fixed-point type iterative method, which is well-known from the solution of free boundary problems (see, e.g., [131, 212] and the references therein). In the context of inverse problems, it has been used for instance in [201].

We assume in the following that the domain  $\omega$  is starlike. Hence we represent the inclusion's boundary  $\partial\omega$  by a parametrization  $\gamma : [0, 2\pi] \rightarrow \mathbb{R}^2$  in polar coordinates, that is

$$\partial\omega = \{\gamma(s) = r(s)\mathbf{e}_r(s); s \in [0, 2\pi]\},$$

where  $\mathbf{e}_r(s) = {}^t(\cos(s), \sin(s))$  denotes the unit vector in the radial direction. The radial function  $r(s)$  is supposed to be a positive function in  $\mathcal{C}_{\text{per}}([0, 2\pi])$ , where

$$\mathcal{C}_{\text{per}}([0, 2\pi]) := \{r \in \mathcal{C}([0, 2\pi]); r(0) = r(2\pi)\},$$

such that  $d(\partial\Omega, \partial\omega) > 0$ .

The trial method to solve the conductivity problem (III.1.1) requires an update rule. Suppose that the actual void's boundary is  $\partial\omega_k$ . Then the data completion problem yields a state  $u_k$  which satisfies

$$\begin{cases} \Delta u_k = 0 & \text{in } \Omega \setminus \overline{\omega_k}, \\ u_k = g_D & \text{on } \partial\Omega, \\ \partial_n u_k = g_N & \text{on } \partial\Omega. \end{cases}$$

The new boundary  $\partial\omega_{k+1}$  is now determined by moving the old boundary into the radial direction, which is expressed by the update rule

$$\gamma_{k+1} = \gamma_k + \tilde{r}_k \mathbf{e}_r.$$

The computation of the update function  $\tilde{r}_k$  is the topic of the next paragraph.

**Update rule.** The update function  $\tilde{r}_k \in \mathcal{C}_{\text{per}}([0, 2\pi])$  should be constructed in such a way that the desired homogeneous Dirichlet boundary condition will be (approximately) satisfied at the new boundary  $\partial\omega_{k+1}$ , i.e. we want that the following equality holds:

$$u_k \circ \gamma_{k+1} = 0 \quad \text{on } [0, 2\pi],$$

where  $u_k$  is assumed to be smoothly extended into the exterior of  $\Omega \setminus \overline{\omega_k}$  if required.

The traditional update rule is obtained by linearizing  $u_k \circ (\gamma_k + \tilde{r}_k \mathbf{e}_r)$  with respect to the update function  $\tilde{r}$ . This yields the equation

$$u_k \circ \gamma_{k+1} \approx u_k \circ \gamma_k + \left( \frac{\partial u_k}{\partial \mathbf{e}_r} \circ \gamma_k \right) \tilde{r}_k.$$

We decompose the derivative of  $u_k$  in the direction  $\mathbf{e}_r$  into its normal and tangential components:

$$\frac{\partial u_k}{\partial \mathbf{e}_r} = \frac{\partial u_k}{\partial \mathbf{n}} \langle \mathbf{e}_r, \mathbf{n} \rangle + \frac{\partial u_k}{\partial \boldsymbol{\tau}} \langle \mathbf{e}_r, \boldsymbol{\tau} \rangle \quad \text{on } \partial\omega_k,$$

where  $\boldsymbol{\tau}$  represents the unit tangential vector. Hence, defining  $F(\tilde{r}_k) := u_k \circ \boldsymbol{\gamma}_k + \left( \frac{\partial u_k}{\partial \mathbf{e}_r} \circ \boldsymbol{\gamma}_k \right) \tilde{r}_k$ , we want that  $F(\tilde{r}_k) = 0$  and then we arrive at the update equation

$$F(\tilde{r}_k) = u_k \circ \boldsymbol{\gamma}_k + \left[ \left( \frac{\partial u_k}{\partial \mathbf{n}} \circ \boldsymbol{\gamma}_k \right) \langle \mathbf{e}_r, \mathbf{n} \rangle + \left( \frac{\partial u_k}{\partial \boldsymbol{\tau}} \circ \boldsymbol{\gamma}_k \right) \langle \mathbf{e}_r, \boldsymbol{\tau} \rangle \right] \tilde{r}_k = 0. \quad (\text{III.1.16})$$

**Remark III.1.17.** We mention that the solution of the data completion problem according to Section III.1.2.1 immediately yields the quantities  $u_k|_{\partial\omega_k}$  and  $\partial_{\mathbf{n}}u_k|_{\partial\omega_k}$ . Since  $u_k|_{\partial\omega_k}$  is expressed in terms of trigonometric polynomials, it is also straightforward to compute

$$\left( \frac{\partial u_k}{\partial \boldsymbol{\tau}} \circ \boldsymbol{\gamma}_k \right) (s) = \frac{1}{\|\boldsymbol{\gamma}'_k(s)\|} \frac{\partial u_k}{\partial s}(s).$$

Consequently all terms required in (III.1.16) are available.

**Numerical simulations.** We perform some numerical simulations presented in Figures III.1.5 and III.1.6 which illustrate the efficiency of the proposed method.

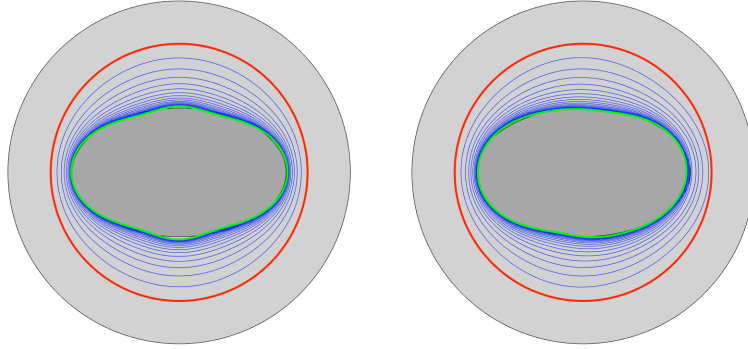


**Figure III.1.5** – Iterates (in blue) and the final reconstructions for the first example (in green) with 1% noise (left-hand side) and with 5% noise (right-hand side).

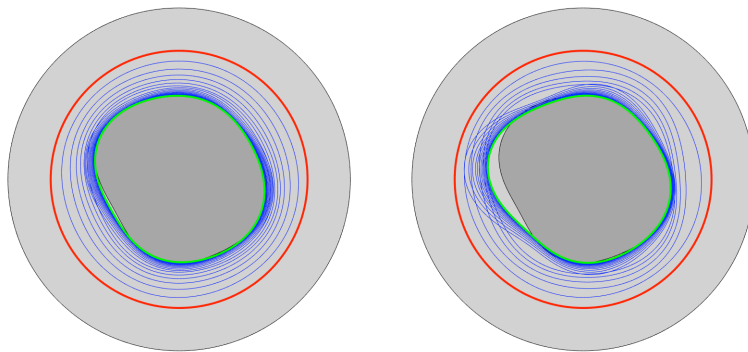


**Figure III.1.6** – Iterates (in blue) and the final reconstructions for the second example (in green) with 1% noise (left-hand side) and with 5% noise (right-hand side).

### III.1.3 Perspectives

The two previous studies concern Laplace's equation. Their adaptations to others PDE, as the (Navier-)Stokes system is natural. Additionally to the numerical difficulties that can appear, the main

novelty could be to adapt to the Stokes system the density lemma on compatible data III.1.3. Indeed this lemma is crucial in order to understand the ill-posedness of the inverse problem and to prove that the infimum of the functional is always zero.

Additionally, another perspective is to take into account uncertainties in the measurements, which is of course more realistic. One could follow the strategy developed recently by Dambrine *et al.* in [108] concerning the inverse obstacle problem for complete Cauchy data. The main assumption is to model the measurements  $g_N$  as a random field. The strategy which consists in minimizing each realization of the functional and in taking the average of the minimizers is obviously too costly numerically. Then Dambrine *et al.* develop in [108] another approach which consists in minimizing an averaged shape functional, that is, for  $0 < \alpha < 1$ ,

$$\mathcal{F}(\omega) = (1 - \alpha)\mathbb{E}(\mathcal{K}(\omega)) + \alpha\mathbb{V}(\mathcal{K}(\omega)),$$

where  $\mathbb{E}$  represents the expectation and  $\mathbb{V}$  the variance. Then, assuming that  $g_N$  has a decomposition with respect to some independent and identically distributed random variables, they show that the expectation and the variance of the random shape functional can be computed from deterministic quantities. Hence the authors compute the shape derivatives and obtain a deterministic shape optimization algorithm in order to solve the inverse obstacle problem for Laplace's equation. We expect to adapt this strategy to the case of partial Cauchy data, studying the data completion problem by the same method. Once again the case of others PDE could be also addressed.

## III.2 With generalized impedance conditions of the Wentzell type

This section focuses on the inverse obstacle problem in the case of corrosion on the obstacle, or if the inclusion has a thin layer. In such a case, one can model the corrosion or the presence of the thin layer by nonclassical boundary conditions on the obstacle called *Generalized Impedance Boundary Conditions* (GIBC). We focus here on the so-called Wentzell boundary conditions given by  $\partial_n u + \alpha u + \beta \Delta_\tau u = 0$ , with  $\alpha > 0$  and  $\beta < 0$ . This work was done in collaboration with Marc Dambrine (university of Pau) and Djalil Kateb (university of Compiègne) and is published in *Inverse Problems* (see [88], 26 pages).

### III.2.1 The inverse obstacle problem with Wentzell boundary conditions

In this section we study the inverse obstacle problem for a corroded obstacle modeled by the Wentzell boundary conditions. In our setting, we assume that the boundary coefficients modeling the corrosion are known and we want to reconstruct the shape of the inclusion from Cauchy data. A study of the problem of corrosion detection, for Robin boundary conditions, is given by Cakoni *et al.* in [74] using a boundary integral equation method, in the spirit of the method proposed by Kress *et al.* in [166]. Especially, in [74], the authors give a non-identifiability result. Even if we do not obtain a general identifiability result (as the one stated for Robin boundary conditions by Bacchelli in [31]), we prove it for annular configurations with the same center using two suitable measurements. Then, following previous works on electric impedance topography (see [7, 8, 126]) or on the same topic in the Stokes and Navier-Stokes cases (see [32, 83, 89]), our strategy is to minimize a least squares functional.

More precisely, let  $\Omega$  be a smooth (at least  $\mathcal{C}^3$ ) bounded open set of  $\mathbb{R}^d$  (with  $d = 2$  or  $d = 3$ ). Let  $d_0 > 0$  be a fixed (small) real number. The set of admissible shapes is now defined by

$$\mathcal{O} := \left\{ \omega \subset\subset \Omega \text{ open set with a } \mathcal{C}^3 \text{ boundary such that } d(\mathbf{x}, \partial\Omega) > d_0, \forall \mathbf{x} \in \omega \right. \\ \left. \text{and such that } \Omega \setminus \bar{\omega} \text{ is connected} \right\}.$$

Let us consider  $\omega^* \in \mathcal{O}$  and  $g_D \in H^{5/2}(\partial\Omega)$  such that  $g_D \neq 0$ , and let  $g_N \in H^{3/2}(\partial\Omega)$  be an admissible boundary measurement, that is  $g_N$  belongs to the range of the Dirichlet-to-Neumann operator defined by  $\Lambda_{\partial\Omega} : g_D \in H^{5/2}(\partial\Omega) \mapsto \partial_n u \in H^{3/2}(\partial\Omega)$ , where  $u$  is solution of Laplace's equation with  $u = g_D$  on  $\partial\Omega$  and  $\partial_n u + \alpha u + \beta \Delta_\tau u = 0$  on  $\partial\omega^*$ . Then we consider the following overdetermined boundary values problem:

$$\begin{cases} -\Delta u = 0 & \text{in } \Omega \setminus \overline{\omega^*}, \\ u = g_D & \text{on } \partial\Omega, \\ \partial_n u + \alpha u + \beta \Delta_\tau u = 0 & \text{on } \partial\omega^*, \\ \partial_n u = g_N & \text{on } \partial\Omega, \end{cases} \quad (\text{III.2.1})$$

where  $\alpha > 0$  and  $\beta < 0$  are fixed real number.

Thus we consider the following geometric inverse problem:

$$\text{Find } \omega^* \in \mathcal{O} \text{ and } u \text{ which satisfy the overdetermined problem (III.2.1).} \quad (\text{III.2.2})$$

To solve this inverse problem, we consider, for  $\omega \in \mathcal{O}$ , the least squares functional

$$\mathcal{J}(\omega) := \frac{1}{2} \int_{\partial\Omega} |\partial_n u(\omega) - g_N|^2,$$

where  $u \in H^1(\Omega \setminus \overline{\omega})$  solves

$$\begin{cases} -\Delta u = 0 & \text{in } \Omega \setminus \overline{\omega}, \\ u = g_D & \text{on } \partial\Omega, \\ \partial_n u + \alpha u + \beta \Delta_\tau u = 0 & \text{on } \partial\omega, \end{cases} \quad (\text{III.2.3})$$

measuring in the misfit to data in the  $L^2$  sense. Notice that one can prove that the boundary value problem (III.2.3) admits a unique solution  $u \in H^3(\Omega \setminus \overline{\omega})$ .

Then, as in Section II.2.2, we try to minimize the least squares criterion  $\mathcal{J}$ :

$$\omega^* \in \underset{\omega \in \mathcal{O}}{\operatorname{argmin}} \mathcal{J}(\omega). \quad (\text{III.2.4})$$

Indeed, as previously, if  $\omega^*$  solves the inverse problem (III.2.2), then  $\mathcal{J}(\omega^*) = 0$  and (III.2.4) holds. Conversely, if  $\omega^*$  solves the optimization problem (III.2.4) with  $\mathcal{J}(\omega^*) = 0$ , then it is a solution of (III.2.2).

**Remark III.2.1.** *Using the local regularity of the solutions in a neighborhood of  $\partial\omega$ , notice that we can only assume that  $\partial\Omega$  is Lipschitz and that  $g_D \in H^{1/2}(\partial\Omega)$  and  $g_N \in H^{-1/2}(\partial\Omega)$  (see for instance [32, 83, 89]). Moreover we could assume that the measurement  $g_N$  is made only on a part  $\Gamma_{\text{obs}} \subset \partial\Omega$  and not on the whole exterior boundary as made for instance in [32, 83].*

Let us recall that  $\Omega_{d_0}$  is an open set with a  $C^\infty$  boundary such that

$$\{\mathbf{x} \in \Omega; d(\mathbf{x}, \partial\Omega) > d_0/2\} \subset \Omega_{d_0} \subset \{\mathbf{x} \in \Omega; d(\mathbf{x}, \partial\Omega) > d_0/3\}$$

and the space of admissible deformations is now defined by

$$\mathcal{U} := \left\{ \mathbf{V} \in \mathbf{W}^{3,\infty}(\mathbb{R}^d); \operatorname{supp}(\mathbf{V}) \subset \overline{\Omega_{d_0}} \text{ and } \|\mathbf{V}\|_{3,\infty} < \min\left(\frac{d_0}{3}, 1\right) \right\}.$$

## III.2.2 The main results and the numerical reconstructions

### III.2.2.1 An identifiability result on rings

The question of the identifiability is the following: *does a measurement (or several measurements) determine uniquely the domain  $\omega^*$ ?* This type of result was proved by Bacchelli in [31] for Robin

### III.2 With generalized impedance conditions of the Wentzell type

boundary conditions. In the case of generalized impedance boundary conditions, one can mention the discussion by Cakoni *et al.* in [75], but, up to my knowledge, this is still an open question.

In order to try to answer to this question concerning the non classical Wentzell boundary conditions, let us focus on particular geometries in the bi-dimensional case. More precisely we consider an annulus with two concentric circles: the inner circle  $\partial\omega = r\mathcal{S}^1$  has a radius  $r$  and we denote by  $R$  the radius of the outer circle  $\partial\Omega = R\mathcal{S}^1$  (where  $\mathcal{S}^1$  denotes the unit sphere). Hence,

$$\Omega \setminus \bar{\omega} := \{ \mathbf{x} \in \mathbb{R}^2, r < \|\mathbf{x}\| < R \}.$$

Then let  $u$  be the solution of the following problem

$$\begin{cases} \Delta u = 0 & \text{in } \Omega \setminus \bar{\omega}, \\ u = g_{\text{D}} & \text{on } \partial\Omega = R\mathcal{S}^1, \\ \partial_{\mathbf{n}} u + \alpha u + \beta \Delta_{\tau} u = 0 & \text{on } \partial\omega = r\mathcal{S}^1. \end{cases} \quad (\text{III.2.5})$$

We deal with the inverse problem of reconstructing the inner circle (i.e. find the radius  $r$ ) from boundary measurements on the outer circle  $\partial\Omega$ . We give a result for identifying uniquely the obstacle from two pairs of Cauchy data  $(g_{\text{D},1}, \partial_{\mathbf{n}} u_1|_{\partial\Omega} = g_{\text{N},1})$  and  $(g_{\text{D},2}, \partial_{\mathbf{n}} u_2|_{\partial\Omega} = g_{\text{N},2})$ , where  $u_1$  and  $u_2$  are the respective solutions of Problem (III.2.5) with the Dirichlet data  $g_{\text{D},1}$  and  $g_{\text{D},2}$ .

Precisely we show the following result: given  $\alpha > 0$  and  $\beta < 0$ , one can determine uniquely  $\partial\omega$  (i.e. the radius  $r$ ) with two pairs of measurements  $(g_{\text{D},1}, g_{\text{N},1})$  and  $(g_{\text{D},2}, g_{\text{N},2})$ , provided  $g_{\text{D},1}$  and  $g_{\text{D},2}$  are suitably chosen (see [88, Theorem 3.1] for a precise statement).

The idea of the proof is the following. We consider two inputs of the form  $g_{\text{D},1} = R^{n_1} \cos(n_1\theta)$  and  $g_{\text{D},2} = R^{n_2} \cos(n_2\theta)$ . We assume that two inner radii  $r$  and  $\tilde{r}$  generate the same Cauchy data for both inputs. We obtain a system of equations in  $t := r/\tilde{r}$  with respect to  $n_1$  and  $n_2$  of the kind

$$h_{n_i}^1(t) = h_{n_i}^2(t), \quad \forall i = 1, 2,$$

where the  $h_{n_i}^j$  are real valued functions of the real variable. We show that for  $n_1$  and  $n_2$  suitably chosen, the unique solution of the previous system is  $t = 1$  meaning  $r = \tilde{r}$ .

#### III.2.2.2 Shape calculus

As before we aim at using shape optimization tools in order to minimize  $\mathcal{J}$ . Then, by the classical method of using a change of variables and the implicit function theorem, we prove the existence of the first and second order shape derivatives. Hence one compute the shape derivatives of the state and of the functional. After lengthly computations, we prove the three following results, where  $\text{H}$  denotes the mean curvature of  $\partial\omega$  and  $b$  is the signed distance to  $\partial\omega$  defined by

$$b(\mathbf{x}) := \begin{cases} -\text{d}(\mathbf{x}, \partial\omega) & \text{if } \mathbf{x} \in \Omega \setminus \bar{\omega}, \\ 0 & \text{if } \mathbf{x} \in \partial\omega, \\ \text{d}(\mathbf{x}, \partial\omega), & \text{if } \mathbf{x} \in \omega. \end{cases}$$

**Proposition III.2.2.** *Let  $\mathbf{V} \in \mathcal{U}$ . The shape derivative  $u'$  of  $u$  which belongs to  $\text{H}^1(\Omega \setminus \bar{\omega})$  is the only solution of the following boundary values problem*

$$\begin{cases} -\Delta u' = 0 & \text{in } \Omega \setminus \bar{\omega}, \\ u' = 0 & \text{on } \partial\Omega, \\ \partial_{\mathbf{n}} u' + \alpha u' + \beta \Delta_{\tau} u' = \xi(u, \mathbf{V} \cdot \mathbf{n}) & \text{on } \partial\omega, \end{cases}$$

with

$$\begin{aligned} \xi(u, \mathbf{V} \cdot \mathbf{n}) := & (\mathbf{V} \cdot \mathbf{n}) (-\alpha \partial_{\mathbf{n}} u - \alpha \text{H} u + \Delta_{\tau} u) + \nabla_{\tau} u \cdot \nabla_{\tau} (\mathbf{V} \cdot \mathbf{n}) \\ & - \beta \Delta_{\tau} ((\mathbf{V} \cdot \mathbf{n}) \partial_{\mathbf{n}} u) - \beta \text{div}_{\tau} ((\mathbf{V} \cdot \mathbf{n}) \text{H} \nabla_{\tau} u - 2(\mathbf{V} \cdot \mathbf{n}) \text{D}^2 b \nabla_{\tau} u). \end{aligned}$$

**Proposition III.2.3.** For  $\mathbf{V}$  in  $\mathcal{U}$ , the least squares functional  $\mathcal{J}$  is differentiable at  $\omega$  in the direction  $\mathbf{V}$  with

$$D\mathcal{J}(\omega) \cdot \mathbf{V} = - \int_{\partial\omega} \left( -\alpha H u w + (-I + \beta(HI - 2D^2b)) (\nabla_\tau u \cdot \nabla_\tau w) + \partial_n u \partial_n w \right) (\mathbf{V} \cdot \mathbf{n}),$$

where  $w \in H^1(\Omega \setminus \bar{\omega})$  is the solution of the following boundary values problem

$$\begin{cases} -\Delta w = 0 & \text{in } \Omega \setminus \bar{\omega}, \\ w = \partial_n u - g_N & \text{on } \partial\Omega, \\ \partial_n w + \alpha w + \beta \Delta_\tau w = 0 & \text{on } \partial\omega. \end{cases}$$

**Proposition III.2.4.** Let  $\omega^* \in \mathcal{O}$  be a solution of the inverse problem (III.2.2). For  $\mathbf{V} \in \mathcal{U}$ , we have

$$D^2\mathcal{J}(\omega^*) \cdot \mathbf{V} \cdot \mathbf{V} = - \int_{\partial\omega^*} \left( -\alpha H u w' + (-I + \beta(HI - 2D^2b)) (\nabla_\tau u \cdot \nabla_\tau w') + \partial_n u \partial_n w' \right) (\mathbf{V} \cdot \mathbf{n}),$$

where  $w' \in H^1(\Omega \setminus \bar{\omega}^*)$  is the solution of the following problem

$$\begin{cases} -\Delta w' = 0 & \text{in } \Omega \setminus \bar{\omega}^*, \\ w' = \partial_n u' & \text{on } \partial\Omega, \\ \partial_n w' + \alpha w' + \beta \Delta_\tau w' = 0 & \text{on } \partial\omega^*. \end{cases}$$

From this expression of the shape hessian, we prove the instability of the inverse problem (III.2.2) using the method already used in [32, 83, 89, 126]. The idea of the proof is to write the shape Hessian as a composition of linear continuous operators whose one is compact. We use a local regularity argument (and a compact imbedding between two Sobolev spaces) in order to prove the compactness of the Riesz operator corresponding to the shape Hessian defined from  $H^{1/2}(\partial\omega^*)$  to  $H^{-1/2}(\partial\omega^*)$  at  $\omega^*$ . Notice that an alternative proof could be to use the potential layers as what is done in [7].

Despite the instability result, we perform numerical simulations (see Figures III.2.7 and III.2.8) using a classical shape variation descent algorithm. Nevertheless the simulations are done without any regularization method in order to solve numerically the optimization problem (III.2.4). Indeed it seems that, in our case, the degeneracy of the functional does not lead to apparition of oscillations in the numerical reconstruction. Surprisingly, this problem seems to be less unstable than the cases of classical boundary conditions, maybe due to the Laplace-Beltrami operator which leads to the presence of the mean curvature in the expression of the gradient of the functional.

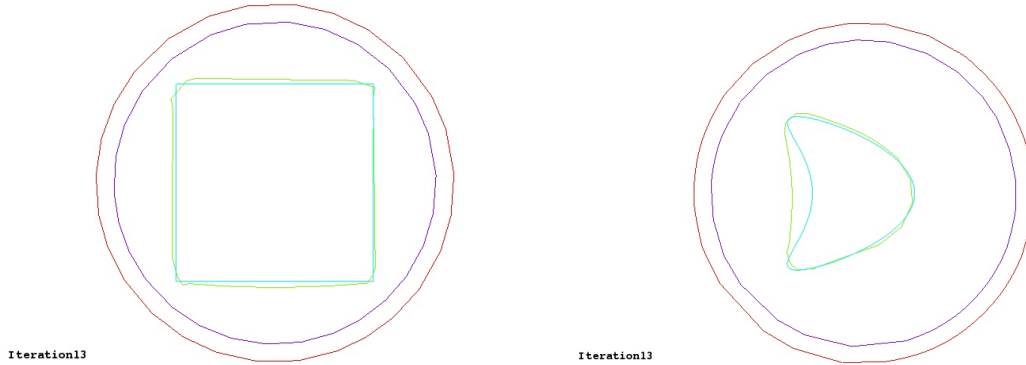


**Figure III.2.7** – Reconstruction of some inclusions (exterior boundary in red, initial shape in purple, exact shape in blue and reconstruction in green)

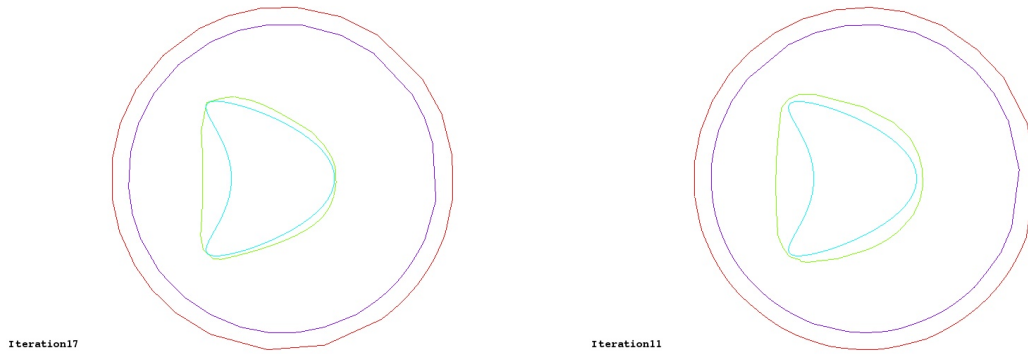


**Figure III.2.8** – Reconstruction with 3% and 10% artificial noise (exterior boundary in red, initial shape in purple, exact shape in blue and reconstruction in green)

### III.2.3 Conclusion

After this work, I pursue my studies on the GIBC, more precisely on the obtention of some GIBC and their shape derivatives in several contexts. This is the topic of the next chapter IV.



---

---

# Chapter IV

---

## Mathematical modeling: taking into account thin layers

The last section of the previous chapter (see Section III.2) focuses on the inverse obstacle problem with Wentzell boundary condition. These nonclassical boundary conditions are usually built using an *asymptotic expansion* of the solution of the considered problem (see, e.g., the PhD thesis of Vial [215]). ***This chapter aims at building boundary conditions modeling a thin layer or a corrosion effect for some problems: Generalized Impedance Boundary Conditions (GIBC) are established in the context of biology in Section IV.1 and in the context of solid mechanics in Section IV.2.*** One of the difficulty is to take into account the characteristics of the layer, as in the first section.

This chapter summarizes the two following articles which concern the construction and the study of GIBC:

- [92] F. Caubet, H. Haddar, J-R. Li and D.V. Nguyen. New transmission condition accounting for diffusion anisotropy in thin layers applied to diffusion MRI. *ESAIM Math. Model. Numer. Anal.*, 51(4):1279–1301, 2017;
- [93] F. Caubet, D. Kateb and F. Le Louër. Shape sensitivity analysis for elastic structures with generalized impedance boundary conditions of the Wentzell type - Application to minimization of the compliance. *Journal of Elasticity*, accepted, 2018.

Diffusion Magnetic Resonance Imaging (dMRI) gives a measure of the average distance traveled by water molecules in a medium and can give useful information on cellular structure and structural change when the medium is biological tissue. A large number of works have appeared in recent years and show that dMRI measurements can be correlated with various physiological or pathological conditions such as cell swelling, demyelinating disorders or the presence of tumors (see, e.g., [157, 161, 170, 177] and references therein). Especially dMRI can be used to detect and quantify abnormalities in the myelin sheath surrounding the axons of neurons (see [29, 52, 130, 132]). The loss of or damage to the myelin sheath can be correlated with many diseases of brain function. A commonly used mathematical model for water proton magnetization in tissue is the *Bloch-Torrey partial differential equation* (see [213]), where intrinsic diffusion tensors are defined in different cellular geometrical compartments. The biological model is usually a three-compartment geometrical model: the three geometrical compartments are 1) the axons, 2) myelin sheath surrounding the axons, 3) the extra-cellular space. This original three-compartment model can then be approximated by a two-compartment geometrical model: the two geometrical compartments are 1) the axons and 2) the extra-cellular space. These two compartments are linked via a *transmission condition*, obtained using an asymptotic expansion of the solution of the Bloch-Torrey equation. One objective of my work is to build such a condition taking into account an *anisotropic diffusion*.

This kind of transmission conditions can appear in several context. Another example concerns the solid mechanics and the mathematical analysis of some elastic structures coated with a thin layer of constant thickness, which can model some corrosion effects for instance (see, e.g., the work of Vogelius *et al.* [217] for the laplacian case). In linear elasticity, it deserves to mention the book of Ciarlet [99], where a local representation of the GIBC is proposed, and others works [57, 128] in the context of thin elastic plates or shells. A very common problem in structural mechanics, even for classical boundary conditions, is then to study the *optimal design of a rigid structure* in order, for instance, to maximize its rigidity. Several works deal with the problem of minimizing the compliance of a structure where standard boundary conditions are imposed on the free boundary. We can here mention the works of Allaire *et al.* [16, 18], Amstutz *et al.* [23], Novotny *et al.* [183] and Dambrine *et al.* [110] (this list of references is far from being exhaustive). Combining these two problems of modeling a thin layer and of optimal design, we address the question of finding the optimal shape of some elastic structures with a corroded part of the boundary.

## IV.1 Generalized Impedance Boundary Conditions for diffusion Magnetic Resonance Imaging (MRI)

This section is devoted to the construction of transmission conditions in the context of diffusion Magnetic Resonance Imaging (dMRI) taking into account an anisotropic diffusion in the membrane of a cell. This work was done in collaboration with Housseem Haddar, Jing-Rebecca Li and Dang Van Nguyen (École Polytechnique) as part of the PhD thesis of Dang Van Nguyen, and is published in *ESAIM: Mathematical Modelling and Numerical Analysis* (see [92], 23 pages).

In order to model the effect of the myelin layer of a cell, a simple and well-known transmission condition can be used when the diffusion inside the layer is assumed to be isotropic. However, since the myelin sheath is composed of layers of lipids or proteins [190] (see Fig. IV.1.1 for an illustration), it is expected that the diffusion tensor in the myelin sheath will have a normal component that is much smaller than the tangential component (see discussion about diffusion inside the myelin sheath in [38, 168, 169]).

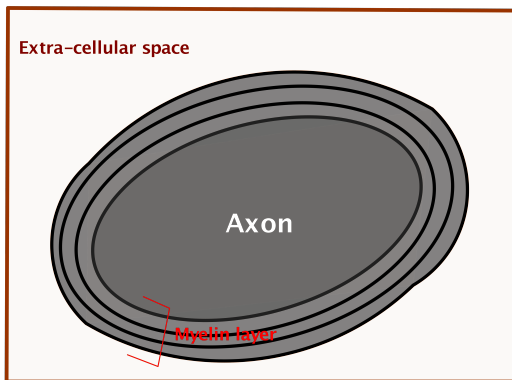


**Figure IV.1.1** – Illustration of the myelin sheath, composed of layers of lipids, surrounding the axon.

Hence, to obtain asymptotic two-compartment models, we rely on a methodology based on classical scaled asymptotic expansions for thin structures (see [98, 115, 187]) and on an appropriate scaling of tangential and normal diffusion inside the myelin layer. This methodology has been extensively used to model thin coatings (see, e.g., [48, 143] and references therein), rough boundaries (see, e.g., [4, 159] and references therein) and imperfectly conducting obstacles (see, e.g., [144, 145] and references therein). We can also mention here the works [123, 185].

To account for low diffusion normal to the layer, we make the following choice for the diffusion inside the layer:

1. for the tangential direction, we use the same scaling as for diffusion in the axons and in the extra-cellular space;
2. for the normal direction, we use a scaling proportional to the layer thickness.

This choice leads to asymptotic transmission conditions. The first order approximation (in the layer thickness) leads to a transmission condition that has the same form as the classical transmission condition associated with isotropic layer diffusion. Anisotropy appears in the second order approximation and gives rise to our new Anisotropic Diffusion Transmission Condition (ADTC). This ADTC couples volumetric diffusion equations with surface diffusion equations. We note that the natural expression of the second order transmission condition does not exhibit uniform time stability with respect to the layer thickness, but this well-known phenomenon for higher order asymptotic models can be corrected by the use of a Padé expansion, as in [98, 142], and our ADTC is corrected in this way. Thus, in its final form, our ADTC has a mass-conservation property, which is important for dMRI modeling.

### IV.1.1 Bloch-Torrey equation to model the diffusion MRI signal

A classic dMRI experiment consists of applying two pulsed gradient magnetic fields with a 180 degree spin reversal between the two pulses in order to encode the displacement of the water molecules between the two pulses (see, e.g., [211]). The complex transverse water proton magnetization  $M$  can be modeled by the following Bloch-Torrey PDE (see, e.g., [213]):

$$\frac{\partial M(\mathbf{x}, t)}{\partial t} + i\mathbf{q} \cdot \mathbf{x} f(t) M(\mathbf{x}, t) - \operatorname{div}(\bar{\boldsymbol{\sigma}}(\mathbf{x}) \nabla M(\mathbf{x}, t)) = 0, \quad (\text{IV.1.1})$$

where  $i := \sqrt{-1}$ ,  $\bar{\boldsymbol{\sigma}}(\mathbf{x})$  is the intrinsic diffusion tensor,  $\mathbf{q}$  contains the amplitude and direction information of the applied diffusion-encoding magnetic field gradient multiplied by the gyro-magnetic ratio of the water proton, and  $f$ , where  $\max_t f(t) = 1$ , is the normalized time profile of the diffusion-encoding magnetic field gradient sequence. The *time profile* of the classic Pulsed Gradient Spin Echo (PGSE) [211] sequence (simplified to include only the parameters relevant to diffusion, i.e., the imaging gradients are ignored) is the following:

$$f(t) := \begin{cases} 1, & 0 < t \leq \delta, \\ -1, & \Delta < t \leq \Delta + \delta, \\ 0, & \text{elsewhere,} \end{cases}$$

where  $0 \leq \delta \leq \Delta$  and where we made  $f(t)$  negative in the second pulse to include the effect of the 180 degree spin reversal between the pulses. The time at which the signal is measured is called the *echo time*  $TE > \delta + \Delta$ .

The *dMRI signal* is the total magnetization:

$$S(\mathbf{q}) := \int M(\mathbf{x}, \delta + \Delta) d\mathbf{x},$$

where  $M$  is the solution of Equation (IV.1.1). The signal is usually plotted against a quantity called the *b-value*, given by

$$b(\mathbf{q}) := \|\mathbf{q}\|^2 \delta^2 \left( \Delta - \frac{\delta}{3} \right),$$

because for a homogeneous domain, where  $\bar{\boldsymbol{\sigma}}(\mathbf{x}) = \bar{\boldsymbol{\sigma}}$  is constant, the signal has the analytical expression

$$S(\mathbf{q}) = \exp\left(-\left(\frac{\mathbf{q}^T \bar{\boldsymbol{\sigma}} \mathbf{q}}{\|\mathbf{q}\|^2}\right) b(\mathbf{q})\right),$$

where the quantity before the *b-value* is the diffusion coefficient in the direction of  $\mathbf{q}$ .

## IV.1.1.1 Geometrical compartments

A standard geometrical model of the brain white matter (for an early example, see [28]) divides the tissue into three compartments:

1.  $\Omega_i^\eta$  is the axons (with associated intrinsic diffusion tensor  $\bar{\sigma}_i$ );
2.  $\Omega_e^\eta$  is the extra-cellular space (with associated intrinsic diffusion tensor  $\bar{\sigma}_e$ );
3.  $\Omega_m^\eta$  is the myelin sheath (with associated intrinsic diffusion tensor  $\bar{\sigma}_m$ ).

We denote by  $\eta$  the thickness of the layer (which is assumed to be constant) and by  $\Gamma$  a fictitious interface inside the myelin layer at equal distance from the two boundaries of the layer. We denote by  $\Omega$  the domain formed by union of  $\Omega_\ell^\eta$ ,  $\ell = e, i, m$ . We also introduce some notations as we consider the geometrical compartments when  $\eta \rightarrow 0$ : we denote the remaining two compartments by  $\Omega_i$  and by  $\Omega_e$  (see Figure IV.1.2). For the ease of notation, we restrict the diffusion tensor,  $\bar{\sigma}(\mathbf{x})$ , for the tissue to be piecewise constant:

$$\bar{\sigma}(\mathbf{x}) := \begin{cases} \bar{\sigma}_i(\mathbf{x}), & \mathbf{x} \in \Omega_i^\eta, \\ \bar{\sigma}_e(\mathbf{x}), & \mathbf{x} \in \Omega_e^\eta, \\ \bar{\sigma}_m(\mathbf{x}), & \mathbf{x} \in \Omega_m^\eta. \end{cases}$$

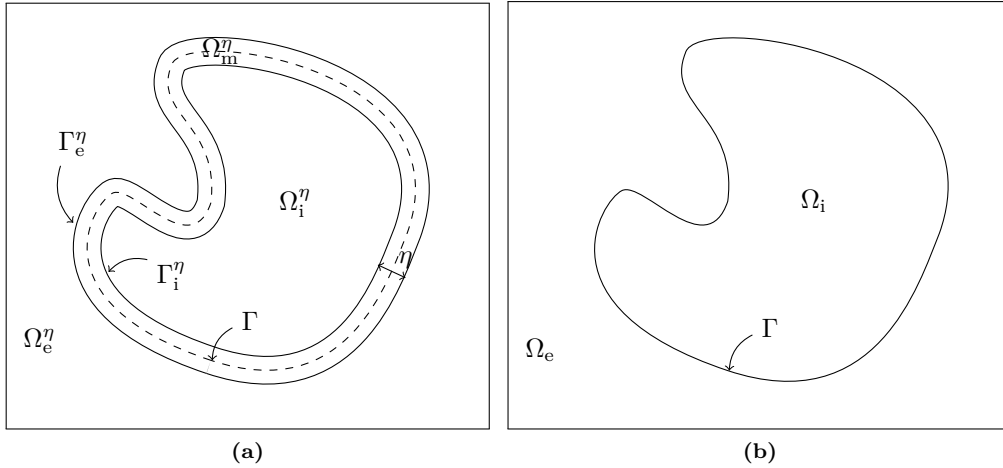


**Figure IV.1.2** – Notations for the three compartment model (left) and the two compartment model (right).

For the three compartment model, the natural continuity conditions (of the magnetization and the flux) on the compartment interfaces result is the following Interface Conditions (IC) on the boundaries  $\Gamma_i^\eta$  and  $\Gamma_e^\eta$  of  $\Omega_i^\eta$  and  $\Omega_e^\eta$ :

$$\text{IC on } \Gamma_e^\eta \text{ and } \Gamma_i^\eta : \begin{cases} [\bar{\sigma} \nabla M \cdot \mathbf{n}] = 0, \\ [M] = 0, \end{cases} \quad (\text{IV.1.2})$$

where  $\mathbf{n}$  is the normal to  $\Gamma_e^\eta$  or  $\Gamma_i^\eta$  and where the symbol  $[\cdot]$  denotes the jump relative to the direction of  $\mathbf{n}$ .

Finally the anisotropy inside the layer is assumed to be such that

$$\bar{\sigma}_m : \begin{cases} \bar{\sigma}_m \mathbf{n} = \sigma_m^n \mathbf{n}, \\ \bar{\sigma}_m \boldsymbol{\tau} = \sigma_m^\tau \boldsymbol{\tau}, \end{cases}$$

where  $\sigma_m^n$  and  $\sigma_m^\tau$  indicate respectively the transverse diffusion coefficient and tangential diffusion coefficient in the layer and  $\boldsymbol{\tau}$  represents the unit tangential vector. The important assumption we make (see (IV.1.6) below) implies that

$$\sigma_m^n \ll \sigma_m^\tau.$$

#### IV.1.1.2 Classical asymptotic model for isotropic diffusion in layer

If the diffusion inside the layer is isotropic, i.e.  $\sigma_m^n = \sigma_m^\tau$ , it is well-known that the following asymptotic transmission condition, which we denote the Isotropic Diffusion Transmission Condition (IDTC), can be imposed on the interface  $\Gamma$  (see, e.g., [101]):

$$\text{IDTC on } \Gamma : \begin{cases} [\boldsymbol{\sigma} \nabla M \cdot \mathbf{n}] = \mathbf{0}, \\ \boldsymbol{\sigma} \nabla M \cdot \mathbf{n} = \kappa_0 [M], \end{cases} \quad (\text{IV.1.3})$$

where  $\kappa_0$  is a given permeability coefficient. We recall that in addition to Equation (IV.1.3), the PDE (IV.1.1) is assumed to hold on  $\Omega_i$  and  $\Omega_e$ . This type of transmission condition corresponds to a first order asymptotic model when the diffusion tensor inside the membrane scales like  $\eta$ . Our aim is to improve this condition by taking into account the  $O(1)$  tangential diffusion.

### IV.1.2 Formal derivation of transmission conditions

The methodology we adopt to derive transmission conditions is similar to the one in [48, 143, 144] and is based on a scaling of the layer with respect to its thickness  $\eta$  and an asymptotic expansion of the fields with respect to  $\eta$ . In this manuscript we restrict ourselves to a formal obtention of these conditions (in the sense that no convergence proof will be established). The latter is technical and is usually valid (for linear problems) as long as the obtained model is proved to be uniformly stable with respect to the thickness. This is why we only discuss this last point hereafter. The convergence proof is given in the appendix of the corresponding article [92]. The following formal technical details in space dimension 2 are inspired by [27] (see also [144] for space dimension 3).

#### IV.1.2.1 Expression of the differential operators in curvilinear coordinates

We assume that  $\Gamma$  is a regular curve (at least  $\mathcal{C}^2$ ) and is the boundary of a simply connected domain  $\Omega_i$  (independent from  $\eta$ ). Notice that we can treat the case of multiply connected domains by treating separately each connected component. Then the boundary  $\Gamma$  can be parametrized in terms of the curvilinear abscissa  $s$  as  $s \mapsto \mathbf{x}_\Gamma(s)$ ,  $s \in [0, L[$ , with  $|\mathrm{d}\mathbf{x}_\Gamma(s)/\mathrm{d}s| = 1$ , where  $L$  is the length of  $\Gamma$ . We assume that this parametrization defines a clockwise orientation. Let  $\mathbf{n}(s)$  be the unitary normal vector at  $\mathbf{x}_\Gamma(s)$  directed to the exterior of  $\Omega_i$  and set  $\boldsymbol{\tau}(s) = \mathrm{d}\mathbf{x}_\Gamma(s)/\mathrm{d}s$  which is a unitary vector tangential to  $\Gamma$  at  $\mathbf{x}_\Gamma(s)$ . The curvature  $c$  can be defined by

$$c(s) := \boldsymbol{\tau}(s) \cdot \mathrm{d}\mathbf{n}(s)/\mathrm{d}s.$$

Then, for  $\eta < \inf_{0 \leq s \leq L} 1/|c(s)|$ ,

$$\forall \mathbf{x} \in \Omega_m^\eta, \exists!(s, r) \in [0, L[\times] - \eta/2, \eta/2[, \mathbf{x} = \mathbf{x}_\Gamma(s) + r \mathbf{n}(s). \quad (\text{IV.1.4})$$

Notice that  $\mathbf{x}_\Gamma$  is the orthogonal projection of  $\mathbf{x}$  on  $\Gamma$ . The couple  $(s, r)$  will be referred to as curvilinear (or parametric) coordinates of  $\mathbf{x} \in \Omega_m^\eta$  (with respect to  $\Gamma$ ). Let  $u$  be a function defined in  $\Omega_m^\eta$  and let  $\tilde{u} : [0, L[\times] - \eta/2, \eta/2[$  be defined by

$$\tilde{u}(s, r) := u(\mathbf{x}),$$

where  $\mathbf{x}$  and  $(s, r)$  satisfy Equation (IV.1.4). Then we have

$$\nabla u(\mathbf{x}) = \frac{1}{1+rc} \partial_s \tilde{u} \boldsymbol{\tau} + \partial_r \tilde{u} \mathbf{n} = \frac{1}{1+rc} \nabla_\tau \tilde{u} + \partial_r \tilde{u} \mathbf{n}$$

and, for a tensor  $\bar{\mathbf{A}}$  such that  $\bar{\mathbf{A}}\boldsymbol{\tau} = A^\tau \boldsymbol{\tau}$  and  $\bar{\mathbf{A}}\mathbf{n} = A^n \mathbf{n}$ , we have

$$\begin{aligned} \operatorname{div}(\bar{\mathbf{A}} \nabla u(\mathbf{x})) &= \frac{1}{1+rc} \partial_s \left( \frac{1}{1+rc} A^\tau \partial_s \tilde{u} \right) + \frac{1}{1+rc} \partial_r \left( (1+rc) A^n \partial_r \tilde{u} \right) \\ &= \frac{1}{1+rc} \operatorname{div}_\tau \left( \frac{1}{1+rc} A^\tau \nabla_\tau \tilde{u} \right) + \frac{1}{1+rc} \partial_r \left( (1+rc) A^n \partial_r \tilde{u} \right). \end{aligned} \quad (\text{IV.1.5})$$

### IV.1.2.2 Scaling and formal asymptotic expansion

In order to take into account the relatively small values of the diffusion tensor along the normal coordinate, we choose the scaling

$$\sigma_m^n = \kappa_0 \eta \quad (\text{IV.1.6})$$

while we assume that  $\bar{\sigma}_e$ ,  $\bar{\sigma}_i$  and  $\sigma_m^\tau$  are independent from  $\eta$ . Physically, the condition (IV.1.6) may be an appropriate choice for dMRI modeling in the case of thin myelin layers and high  $b$ -values (at high  $b$ -values, permeability effects/water exchange become more prominent). We also scale the membrane  $\Omega_m^\eta$  with respect to  $\eta$  and transform this domain into (the  $\eta$  independent domain)  $\Gamma \times ]-1/2, 1/2[$  through the mapping  $\mathbf{x} \mapsto (\mathbf{x}_\Gamma(s), r/\eta)$ . Let us denote by  $M_\ell$  the restriction of  $M$  to the domain  $\Omega_\ell$  for  $\ell = e, i, m$ . We then define  $\widetilde{M}_m$  on  $\Gamma \times ]-1/2, 1/2[ \times [0, \infty)$  as

$$\widetilde{M}_m(\mathbf{x}_\Gamma, R, t) := M_m(\mathbf{x}, t),$$

with  $R := \frac{r}{\eta}$  and  $\mathbf{x}$ ,  $\mathbf{x}_\Gamma$  and  $r$  satisfy (IV.1.4). Since the time plays only the role of a parameter in the process of establishing membrane transmission condition, we omit indicating this variable in the notation. We first observe, using (IV.1.5),

$$\operatorname{div}(\bar{\sigma}_m \nabla M_m) = \frac{1}{1+\eta Rc} \operatorname{div}_\tau \left( \frac{1}{1+\eta Rc} \sigma_m^\tau \nabla_\tau \widetilde{M}_m \right) + \frac{1}{\eta^2} \frac{1}{1+\eta Rc} \partial_R \left( (1+\eta Rc) \eta \kappa_0 \partial_R \widetilde{M}_m \right)$$

and also notice that

$$i\mathbf{q} \cdot \mathbf{x} f(t) M = i(\mathbf{q} \cdot \mathbf{x}_\Gamma + \mathbf{q}^n \eta R) f(t) \widetilde{M}.$$

Assuming that  $\widetilde{M}_m$  has the asymptotic expansion

$$\widetilde{M}_m(\mathbf{x}_\Gamma, R) = \sum_{k=0}^{\infty} \eta^k M_m^k(\mathbf{x}_\Gamma, R),$$

for some functions  $M_m^k$  defined on  $\Gamma \times ]-1/2, 1/2[$ , the Bloch-Torrey equation (multiplied by the factor  $(1+\eta R)^3$ ) implies

$$\begin{aligned} \sum_{k=0}^{\infty} \eta^k \left[ (1+\eta R)^3 \partial_t M_m^k + (1+\eta R)^3 i(\mathbf{q} \cdot \mathbf{x}_\Gamma + \mathbf{q}^n \eta R) f(t) M_m^k - (1+\eta R) \operatorname{div}_\tau (\sigma_m^\tau \nabla_\tau M_m^k) \right. \\ \left. + \eta R \sigma_m^\tau \nabla_\tau M_m^k \nabla_\tau c - \frac{\kappa_0}{\eta} (1+\eta R)^3 \partial_{RR}^2 M_m^k - (1+\eta R)^2 \kappa_0 c \partial_R M_m^k \right] = 0. \end{aligned}$$

Then, by formal identification of powers of  $\eta$ , we obtain particularly for the first two terms

$$\kappa_0 \partial_{RR}^2 M_m^0 = 0, \quad (\text{IV.1.7})$$

$$\kappa_0 \partial_{RR}^2 M_m^1 = \partial_t M_m^0 + i\mathbf{q} \cdot \mathbf{x}_\Gamma f(t) M_m^0 - \operatorname{div}_\tau (\sigma_m^\tau \nabla_\tau M_m^0) - \kappa_0 c \partial_R M_m^0. \quad (\text{IV.1.8})$$

The expression of ADTC will be obtained from explicit expression of the solutions of (IV.1.7) and (IV.1.8) in terms of  $R$  and using the continuity conditions (IV.1.2) that can be written in terms of  $\widetilde{M}_m$  as

$$\begin{aligned} \widetilde{M}_m(\mathbf{x}_\Gamma, -\tfrac{1}{2}) &= M_i(\mathbf{x}_\Gamma - \tfrac{\eta}{2}\mathbf{n}), & \widetilde{M}_m(\mathbf{x}_\Gamma, \tfrac{1}{2}) &= M_e(\mathbf{x}_\Gamma + \tfrac{\eta}{2}\mathbf{n}), \\ \kappa_0 \partial_R \widetilde{M}_m(\mathbf{x}_\Gamma, -\tfrac{1}{2}) &= \bar{\sigma}_i \nabla M_i(\mathbf{x}_\Gamma - \tfrac{\eta}{2}\mathbf{n}) \cdot \mathbf{n}, & \kappa_0 \partial_R \widetilde{M}_m(\mathbf{x}_\Gamma, \tfrac{1}{2}) &= \bar{\sigma}_e \nabla M_e(\mathbf{x}_\Gamma + \tfrac{\eta}{2}\mathbf{n}) \cdot \mathbf{n}. \end{aligned} \quad (\text{IV.1.9})$$

In order to relate these boundary conditions to the asymptotic expansion of  $\widetilde{M}_m$  we postulate that, for  $\ell = i, e$ ,

$$M_\ell = \sum_{k=0}^{\infty} \eta^k M_\ell^k,$$

where the functions  $M_\ell^k$  are defined on  $\Omega_\ell$  and satisfy the Bloch-Torrey equation in  $\Omega_\ell$ . We distinguish two families of ADTC according to the way we choose to match the three asymptotic expansions.

### IV.1.2.3 A first family of ADTC

A first family of ADTC is obtained by imposing the continuity conditions

$$M_m^k(\mathbf{x}_\Gamma, -\tfrac{1}{2}) = M_i^k(\mathbf{x}_\Gamma - \tfrac{\eta}{2}\mathbf{n}), \quad M_m^k(\mathbf{x}_\Gamma, \tfrac{1}{2}) = M_e^k(\mathbf{x}_\Gamma + \tfrac{\eta}{2}\mathbf{n}) \quad (\text{IV.1.10})$$

and

$$\kappa_0 \partial_R M_m^k(\mathbf{x}_\Gamma, -\tfrac{1}{2}) = \bar{\sigma}_i \nabla M_i^k(\mathbf{x}_\Gamma - \tfrac{\eta}{2}\mathbf{n}) \cdot \mathbf{n}, \quad \kappa_0 \partial_R M_m^k(\mathbf{x}_\Gamma, \tfrac{1}{2}) = \bar{\sigma}_e \nabla M_e^k(\mathbf{x}_\Gamma + \tfrac{\eta}{2}\mathbf{n}) \cdot \mathbf{n}, \quad (\text{IV.1.11})$$

for all  $k$ , which is obtained from (IV.1.9) by formal identification of powers of  $\eta$ . We remark that in this way the functions  $M_m^k$  depend also on  $\eta$ . Let us introduce the notations

$$\langle M^k \rangle_\eta(\mathbf{x}_\Gamma) := \frac{M_e^k(\mathbf{x}_\Gamma + \tfrac{\eta}{2}\mathbf{n}) + M_i^k(\mathbf{x}_\Gamma - \tfrac{\eta}{2}\mathbf{n})}{2}, \quad [M^k]_\eta(\mathbf{x}_\Gamma) := M_e^k(\mathbf{x}_\Gamma + \tfrac{\eta}{2}\mathbf{n}) - M_i^k(\mathbf{x}_\Gamma - \tfrac{\eta}{2}\mathbf{n}),$$

and similar definitions for  $\langle \bar{\sigma} \nabla M^k \cdot \mathbf{n} \rangle_\eta$  and  $[\bar{\sigma} \nabla M^k \cdot \mathbf{n}]_\eta$ . We first express  $M_m^k$  (for  $k = 0, 1$ ) in terms of  $\langle M^k \rangle_\eta$  and  $[M^k]_\eta$  by solving with respect to  $R$  Equations (IV.1.7) and (IV.1.8) using the two boundary conditions in (IV.1.10). We then obtain an interface condition by using the two boundary conditions in (IV.1.11). We can already remark that the obtained interface condition will not be a standard interface condition on  $\Gamma$  but will correspond to a condition that couples the boundary values at  $\partial\Omega_e^\eta$  and  $\partial\Omega_i^\eta$ .

**First order term.** From (IV.1.7) and the boundary conditions in (IV.1.10), we readily see that

$$M_m^0 = \langle M^0 \rangle_\eta + R [M^0]_\eta. \quad (\text{IV.1.12})$$

We then immediately get from (IV.1.11)

$$[\bar{\sigma} \nabla M^0 \cdot \mathbf{n}]_\eta = 0 \quad \text{and} \quad \langle \bar{\sigma} \nabla M^0 \cdot \mathbf{n} \rangle_\eta = \kappa_0 [M^0]_\eta. \quad (\text{IV.1.13})$$

**Second order term.** Proceeding as previously, we get from (IV.1.7), (IV.1.10), (IV.1.12) and from (IV.1.11)

$$\begin{aligned} [\bar{\sigma} \nabla M^1 \cdot \mathbf{n}]_\eta &= (\partial_t + i\mathbf{q} \cdot \mathbf{x}_\Gamma f(t)) \langle M^0 \rangle_\eta - \text{div}_\tau \left( \sigma_m^\tau \nabla_\tau \langle M^0 \rangle_\eta \right) - c\kappa_0 [M^0]_\eta, \\ \langle \bar{\sigma} \nabla M^1 \cdot \mathbf{n} \rangle_\eta &= \kappa_0 [M^1]_\eta + \frac{1}{12} (\partial_t + i\mathbf{q} \cdot \mathbf{x}_\Gamma f(t)) [M^0]_\eta - \frac{1}{12} \text{div}_\tau \left( \sigma_m^\tau \nabla_\tau [M^0]_\eta \right). \end{aligned} \quad (\text{IV.1.14})$$

**A first ADTC of order two.** According to the conditions (IV.1.13) and (IV.1.14) and since  $M_\ell = M_\ell^0 + \eta M_\ell^1 + O(\eta^2)$  for  $\ell = e, i$ , we obtain the following interface approximate conditions

$$\begin{aligned} [\bar{\sigma} \nabla M \cdot \mathbf{n}]_\eta &= \eta \left( (\partial_t + i\mathbf{q} \cdot \mathbf{x}_\Gamma f(t)) \langle M \rangle_\eta - \operatorname{div}_\tau \left( \sigma_m^\tau \nabla_\tau \langle M \rangle_\eta \right) - c\kappa_0 [M]_\eta \right) + O(\eta^2), \\ \langle \bar{\sigma} \nabla M \cdot \mathbf{n} \rangle_\eta &= \kappa_0 [M]_\eta + \frac{\eta}{12} \left( (\partial_t + i\mathbf{q} \cdot \mathbf{x}_\Gamma f(t)) [M]_\eta - \operatorname{div}_\tau \left( \sigma_m^\tau \nabla_\tau [M]_\eta \right) \right) + O(\eta^2). \end{aligned} \quad (\text{IV.1.15})$$

A membrane transmission condition of order 2 with respect to  $\eta$  is then obtained from (IV.1.15) by dropping the  $O(\eta^2)$  terms. However it turns out that the obtained expression does not lead to a diffusion problem that respect an energy identity similar to the original problem. This energy identity is important as it is supposed to provide uniform stability with respect to  $\eta$ . This stability is the main ingredient that guarantee the convergence rate at the consistency order (see, e.g., [115, 143, 144] for similar problems).

In order to obtain an expression of ADTC that respects an uniform stability with respect to  $\eta$ , we replace the term  $\eta\kappa_0 [M]_\eta$  by  $\eta \langle \bar{\sigma} \nabla M \cdot \mathbf{n} \rangle_\eta$  in the first equation of (IV.1.15) and add  $\frac{\eta}{4} c [\bar{\sigma} \nabla M \cdot \mathbf{n}]_\eta$  to the left hand side of the second equation (IV.1.15). These substitutions, that have been suggested by the proof of the following energy estimate (IV.1.17), indeed do not change the formal  $O(\eta^2)$  order of the reminders. We therefore propose as second order ADTC the following conditions:

$$\boxed{\begin{cases} [\bar{\sigma} \nabla M \cdot \mathbf{n}]_\eta + \eta c \langle \bar{\sigma} \nabla M \cdot \mathbf{n} \rangle_\eta &= \eta \left( (\partial_t + i\mathbf{q} \cdot \mathbf{x}_\Gamma f(t)) \langle M \rangle_\eta - \operatorname{div}_\tau \left( \sigma_m^\tau \nabla_\tau \langle M \rangle_\eta \right) \right), \\ \langle \bar{\sigma} \nabla M \cdot \mathbf{n} \rangle_\eta + \frac{\eta}{4} c [\bar{\sigma} \nabla M \cdot \mathbf{n}]_\eta &= \kappa_0 [M]_\eta + \frac{\eta}{12} \left( (\partial_t + i\mathbf{q} \cdot \mathbf{x}_\Gamma f(t)) [M]_\eta - \operatorname{div}_\tau \left( \sigma_m^\tau \nabla_\tau [M]_\eta \right) \right). \end{cases}} \quad (\text{IV.1.16})$$

Then we prove the following result, where we use the notation  $\Omega^\eta := \Omega_i^\eta \cup \Omega_e^\eta$ .

**Proposition IV.1.1.** *If  $\bar{\sigma}_e = \sigma_e \mathbf{I}$  and  $\bar{\sigma}_i = \sigma_i \mathbf{I}$ , then the following energy estimate holds:*

$$\begin{aligned} \frac{1}{2} \frac{d}{dt} \int_{\Omega^\eta} |M|^2 + \int_{\Omega^\eta} \sigma |\nabla M|^2 + \kappa_0 \int_\Gamma |[M]_\eta|^2 \\ + \eta \left( \frac{1}{2} \frac{d}{dt} \int_\Gamma |\langle M \rangle_\eta|^2 + \int_\Gamma \sigma_m^\tau |\langle \nabla_\tau M \rangle_\eta|^2 \right) + \frac{\eta}{12} \left( \frac{1}{2} \frac{d}{dt} \int_\Gamma |[M]_\eta|^2 + \int_\Gamma \sigma_m^\tau |\langle \nabla_\tau M \rangle_\eta|^2 \right) = 0. \end{aligned} \quad (\text{IV.1.17})$$

Moreover, if the initial data  $M(\cdot, 0) = M_{\text{init}}$  belongs to  $H^1(\Omega_\ell^\eta)$ , for  $\ell = i, e$ , then the Bloch-Torrey equation (IV.1.1) with the ADTC (IV.1.16) admits a unique solution  $M_\ell \in L^2(0, T; H^1(\Omega_\ell^\eta)) \cap C^0(0, T; L^2(\Omega_\ell^\eta))$  such that  $[M]_\eta$  and  $\langle M \rangle_\eta$  belong to  $L^2(0, T; H^1(\Gamma)) \cap C^0(0, T; L^2(\Gamma))$ .

Finally notice that in dMRI, the measured signal corresponds to  $\int_\Omega M$  and the application of a diffusion-encoding magnetic field gradient ( $\mathbf{q} \neq \mathbf{0}$ ) induces attenuation of this quantity compared to the case  $\mathbf{q} = \mathbf{0}$  (no attenuation). It is therefore important to check that our approximate model does not induce artificial attenuation when  $\mathbf{q} = \mathbf{0}$ . In this case, we check that we have the following mass conservation property, for all  $t > 0$ ,

$$\int_{\Omega_e^\eta \cup \Omega_i^\eta} M(\mathbf{x}, t) + \eta \int_\Gamma \langle M(\mathbf{x}, t) \rangle_\eta = \int_{\Omega_e^\eta \cup \Omega_i^\eta} M(\mathbf{x}, 0) + \eta \int_\Gamma \langle M(\mathbf{x}, 0) \rangle.$$

#### IV.1.2.4 A second family of ADTC

We have to notice that the previous ADTC (IV.1.16) has to be imposed numerically on each interface  $\partial\Omega_m^\eta \cap \partial\Omega_e^\eta$  and  $\partial\Omega_m^\eta \cap \partial\Omega_i^\eta$ . However, in this case, we have to numerically manage a difficulty:

## IV.1 Generalized Impedance Boundary Conditions for dMRI

the vertices on these interfaces would have to be aligned. Given that making powerful finite element mesh generation tools is an active area of research, this is a difficulty that may be resolved by choosing a good mesh generator. For instance the mesh generator ‘‘TetGen’’ [204] allows the specification of element vertices. To overcome this difficulty in another way, we present here some additional computations based on Taylor expansion of  $M_e$  and  $M_i$  in order to obtain new ADTC imposed on the middle  $\Gamma$  of the membrane.

Let us introduce the notations

$$\langle M^k \rangle (\mathbf{x}_\Gamma) := \frac{M_e^k(\mathbf{x}_\Gamma) + M_i^k(\mathbf{x}_\Gamma)}{2} \quad \text{and} \quad [M^k] (\mathbf{x}_\Gamma) := M_e^k(\mathbf{x}_\Gamma) - M_i^k(\mathbf{x}_\Gamma).$$

The second family of ADTC is obtained by using the previous postulate, for  $\ell = i, e$ ,

$$M_\ell = \sum_{k=0}^{\infty} \eta^k M_\ell^k,$$

and by using Taylor expansions of  $M_\ell^k$  for all  $k$ , that is

$$\begin{aligned} M_\ell^k \left( \mathbf{x}_\Gamma + \frac{\eta}{2} \mathbf{n} \right) &= M_\ell^k(\mathbf{x}_\Gamma) + \frac{\eta}{2} \nabla M_\ell^k(\mathbf{x}_\Gamma) \cdot \mathbf{n} + \frac{\eta^2}{4} \nabla^2 M_\ell^k(\mathbf{x}_\Gamma) \cdot \mathbf{n} \cdot \mathbf{n} + O(\eta^3), \\ M_\ell^k \left( \mathbf{x}_\Gamma - \frac{\eta}{2} \mathbf{n} \right) &= M_\ell^k(\mathbf{x}_\Gamma) - \frac{\eta}{2} \nabla M_\ell^k(\mathbf{x}_\Gamma) \cdot \mathbf{n} + \frac{\eta^2}{4} \nabla^2 M_\ell^k(\mathbf{x}_\Gamma) \cdot \mathbf{n} \cdot \mathbf{n} + O(\eta^3). \end{aligned}$$

Proceeding in the same way than for the first family of ADTC, we obtain the following interface approximate conditions

$$\begin{aligned} \langle \bar{\boldsymbol{\sigma}} \nabla M \cdot \mathbf{n} \rangle &= \eta \operatorname{div}_\tau (\langle (\bar{\boldsymbol{\sigma}} - \sigma_m^\tau \mathbf{I}) \nabla_\tau M \rangle) + O(\eta^2), \\ \langle \bar{\boldsymbol{\sigma}} \nabla M \cdot \mathbf{n} \rangle &= \kappa_0 [M] - \frac{\eta}{6} P([M]) + \frac{\eta}{4} \operatorname{div}_\tau ([(\bar{\boldsymbol{\sigma}} - \sigma_m^\tau \mathbf{I}) \nabla_\tau M]) + O(\eta^2), \end{aligned} \tag{IV.1.18}$$

where

$$P([M]) := (\partial_t + i\mathbf{q} \cdot \mathbf{x}_\Gamma f(t)) [M] - \operatorname{div}_\tau (\sigma_m^\tau \nabla_\tau [M]).$$

As previously, the ADTC resulting from (IV.1.18) turns out to be unconditionally unstable. In order to obtain a stable problem, we replace the operator  $\kappa_0 [M] - \frac{\eta}{6} P$  by a Padé approximation up to  $O(\eta^2)$  terms (which is compatible with the ADTC order). More precisely we introduce an auxiliary unknown  $\Psi$  on  $\Gamma$  that satisfies

$$\left( 1 + \frac{\eta}{6\kappa_0} P \right) \Psi = [M],$$

in such a way that

$$\langle \bar{\boldsymbol{\sigma}} \nabla M \cdot \mathbf{n} \rangle = \kappa_0 \Psi + \frac{\eta}{4} \operatorname{div}_\tau ([(\bar{\boldsymbol{\sigma}} - \sigma_m^\tau \mathbf{I}) \nabla_\tau M]) - \frac{1}{2} \frac{\eta^2}{6^2 \kappa_0^2} P(P(\Psi)) + O(\eta^2).$$

By neglecting all  $O(\eta^2)$  terms, we end up with a second order membrane transmission condition on  $\Gamma$  in the following form:

$$\boxed{\begin{cases} \langle \bar{\boldsymbol{\sigma}} \nabla M \cdot \mathbf{n} \rangle &= \eta \operatorname{div}_\tau (\langle (\bar{\boldsymbol{\sigma}} - \sigma_m^\tau \mathbf{I}) \nabla_\tau M \rangle), \\ \langle \bar{\boldsymbol{\sigma}} \nabla M \cdot \mathbf{n} \rangle &= \kappa_0 \Psi + \frac{\eta}{4} \operatorname{div}_\tau ([(\bar{\boldsymbol{\sigma}} - \sigma_m^\tau \mathbf{I}) \nabla_\tau M]), \end{cases}} \tag{IV.1.19}$$

where

$$\boxed{\begin{cases} \left( 1 + \frac{\eta}{6\kappa_0} P \right) \Psi &= [M], \\ \Psi &= 0 \quad \text{at } t = 0. \end{cases}} \tag{IV.1.20}$$

**Remark IV.1.2.** We can note that, in the specific case where  $\bar{\sigma}_e = \bar{\sigma}_i = \sigma_m^\tau \mathbf{I}$ , the second order ADTC has the simple form

$$\begin{cases} [\bar{\sigma} \nabla M \cdot \mathbf{n}] &= \mathbf{0}, \\ \langle \bar{\sigma} \nabla M \cdot \mathbf{n} \rangle &= \kappa_0 \Psi. \end{cases}$$

where  $\Psi$  satisfies (IV.1.20).

As for the first family of ADTC, we prove the following energy estimate, using the following notation:

$$\mathbf{H}(\Omega) := \{ \varphi \in \mathbf{H}^1(\Omega_i \cup \Omega_e); [\varphi] \in \mathbf{H}^1(\Gamma) \text{ and } \langle \varphi \rangle \in \mathbf{H}^1(\Gamma) \}.$$

**Proposition IV.1.3.** If  $\bar{\sigma}_e = \sigma_e \mathbf{I}$  and  $\bar{\sigma}_i = \sigma_i \mathbf{I}$ , then the following energy estimate holds:

$$\begin{aligned} & \frac{1}{2} \frac{d}{dt} \int_{\Omega} |M|^2 + \int_{\Omega} \sigma |\nabla M|^2 + \kappa_0 \int_{\Gamma} |\Psi|^2 + \frac{\eta}{12} \frac{d}{dt} \int_{\Gamma} |\Psi|^2 + \frac{\eta}{6} \int_{\Gamma} \sigma_m^\tau |\nabla_\tau \Psi|^2 \\ & + \eta \int_{\Gamma} \langle \sigma_m^\tau - \sigma \rangle |\langle \nabla_\tau M \rangle|^2 + \frac{\eta}{4} \int_{\Gamma} \langle \sigma_m^\tau - \sigma \rangle |\langle \nabla_\tau M \rangle|^2 - \frac{\eta}{2} \int_{\Gamma} \Re \epsilon ([\sigma] [\nabla_\tau M] \cdot \langle \nabla_\tau \bar{M} \rangle) = 0. \end{aligned} \quad (\text{IV.1.21})$$

Moreover, if the conditions

$$\langle \sigma_m^\tau - \sigma \rangle \geq 0 \quad \text{and} \quad 4 \langle \sigma_m^\tau - \sigma \rangle^2 - [\sigma]^2 \geq 0$$

hold (which guarantee the stability since these conditions lead to the positivity of the terms in the second line of (IV.1.21)) and if the initial data  $M(\cdot, 0) = M_{\text{init}}$  belongs to  $L^2(\Omega)$ , then the Bloch-Torrey equation (IV.1.1) with the ADTC (IV.1.19–IV.1.20) admits a unique solution  $(M, \Psi) \in L^2(0, T; \mathbf{H}(\Omega)) \times L^2(0, T; \mathbf{H}^1(\Gamma))$  such that  $(M, \Psi) \in \mathcal{C}^0(0, T; L^2(\Omega)) \times \mathcal{C}^0(0, T; L^2(\Gamma))$ .

**Remark IV.1.4.** We can notice that the stability is ensured if  $\sigma_e = \sigma_i = \sigma_m^\tau$ . We also notice that in the case  $\sigma_e = \sigma_i = \sigma$  the stability requires  $\sigma_m^\tau \geq \sigma$ , which is compatible with the observations in [115] for the case of the wave equation.

Finally we check again that our approximate model does not induce artificial attenuation in the case  $\mathbf{q} = \mathbf{0}$ . Indeed, if  $\mathbf{q} = \mathbf{0}$ , we prove that

$$\int_{\Omega_e \cup \Omega_i} M(\mathbf{x}, t) = \int_{\Omega_e \cup \Omega_i} M(\mathbf{x}, 0).$$

### IV.1.3 Numerical validation

We numerically solve three models of the dMRI signal in the presence of thin layers:

1. the original three-compartment model where  $\Omega_i^\eta$ ,  $\Omega_m^\eta$ ,  $\Omega_e^\eta$  are linked by the interface conditions on  $\Gamma_i^\eta$  and  $\Gamma_e^\eta$  (see Equation (IV.1.2));
2. the classical asymptotic two-compartment model where  $\Omega_e$  and  $\Omega_i$  are linked by the Isotropic Diffusion Transmission Condition (IDTC, see Equation (IV.1.3));
3. the new asymptotic two-compartment model where  $\Omega_e$  and  $\Omega_i$  are linked by the Anisotropic Diffusion Transmission Condition (ADTC, see Equations (IV.1.19–IV.1.20)).

We compute the dMRI signal associated with each of the three models. We compare the accuracy of the two asymptotic models in approximating the dMRI signal of the original three-compartment model as  $\eta \rightarrow 0$ .

As expected, the signal of the two-compartment model with the ADTC converges quadratically to that of the corresponding three-compartment model whereas the two-compartment model with the IDTC only has first order convergence: see Figure IV.1.3.

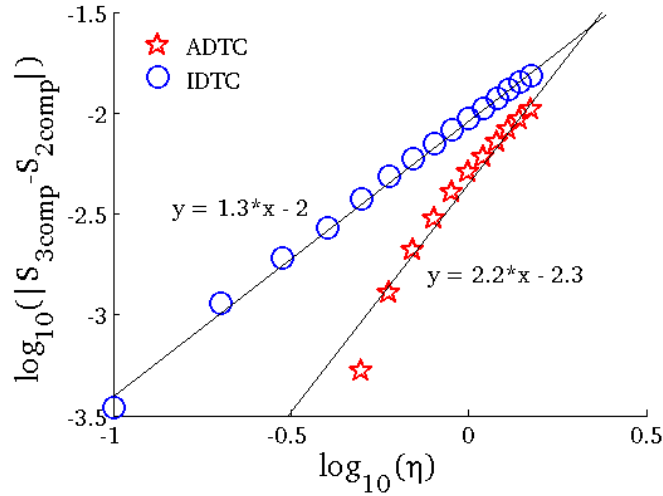


**Figure IV.1.3** – The signal of the new two compartment model with ADTC quadratically converges to that of the corresponding three-compartment model whereas the two compartment model with IDTC only gives the first order convergence.

## IV.2 Generalized Impedance Boundary Conditions (GIBC) and optimal design for linear elasticity

The previous construction of boundary conditions can be applied in several context. The aim of this section is to obtain some Generalized Impedance Boundary Conditions (GIBC) in the context of linear elasticity and general curved interfaces. A condition of the Wentzell type modeling thin layer coatings on some elastic structures is then obtained through an asymptotic analysis of order one of the transmission problem at the thin layer interfaces with respect to the thickness parameter. As mentioned previously, this analysis can model a corrosion effect on the material. A classical question is then to find the optimal shape of a rigid structure in order to maximize its rigidity. To do this we perform a shape sensitivity analysis of the GIBC model and characterize the first shape derivative of this model. A comparison with the asymptotic expansion of the first shape derivative associated to the original thin layer transmission problem shows that we can interchange the asymptotic and shape derivative analysis. Finally we apply these results to the compliance minimization problem: we compute the shape derivative of the compliance in this context and present some numerical simulations.

This work was done in collaboration with Djalil Kateb and Frédérique Le Louër (university of Compiègne), and is the object of a paper accepted for publication in *Journal of Elasticity* (see [93], 37 pages).

### IV.2.1 Setting of the problem

#### IV.2.1.1 Introduction of notations

Let  $\Omega$  be a Lipschitz bounded open set of  $\mathbb{R}^d$  (with  $d = 2$  or  $d = 3$ ). We assume that the solid  $\Omega$  consists of an isotropic material with a linear behavior. The boundary of  $\Omega$  is such that  $\partial\Omega =: \Gamma_D \cup \Gamma_N$  where  $\Gamma_D$  and  $\Gamma_N$  are two non-empty open sets of  $\partial\Omega$  and  $|\Gamma_D| > 0$ . Let  $d_0 > 0$  be a fixed (small) real

number and let us define the following set of admissible shapes:

$$\mathcal{O} := \{ \omega \subset\subset \Omega \text{ open set with a } \mathcal{C}^2 \text{ boundary such that } d(\mathbf{x}, \partial\Omega) > d_0, \forall \mathbf{x} \in \omega \text{ and such that } \Omega \setminus \bar{\omega} \text{ is connected} \}.$$

Let us consider a (non-empty) inclusion  $\omega \in \mathcal{O}$  with boundary  $\partial\omega =: \Gamma$ . Then  $\Omega \setminus \bar{\omega}$  represents a reference configuration of an elastic solid assumed to be built on  $\Gamma_D$ . We denote by  $\mathbf{n}$  the unit normal vector to  $\partial\Omega$  and  $\Gamma$  directed outward to  $\Omega \setminus \bar{\omega}$ . Moreover,  $H$  represents the mean curvature of  $\Gamma$  and  $b$  is the signed distance to  $\Gamma$  defined by

$$b(\mathbf{x}) := \begin{cases} -d(\mathbf{x}, \Gamma) & \text{if } \mathbf{x} \in \Omega \setminus \bar{\omega}, \\ 0 & \text{if } \mathbf{x} \in \Gamma, \\ d(\mathbf{x}, \Gamma), & \text{if } \mathbf{x} \in \omega, \end{cases}$$

so that  $\mathbf{n} = \nabla b|_{\Gamma}$ . Let  $\eta > 0$ . We consider that  $\Gamma$  has an interior thin layer with thickness  $\eta$  bordering  $\omega$  defined by

$$\omega_i^\eta := \{ \mathbf{x} + r\mathbf{n}(\mathbf{x}) \mid \mathbf{x} \in \Gamma \text{ and } 0 < r < \eta \}.$$

We recall that the normal vector  $\mathbf{n}$  is directed inward the inclusion  $\omega$ . We set  $\omega^\eta := \omega \setminus \bar{\omega}_i^\eta$  and we denote its boundary by  $\Gamma^\eta$ . We also denote by  $\mathbf{n}^\eta$  the inward unit normal vector to  $\Gamma^\eta$ , so that  $\mathbf{n}^0 = \mathbf{n}$ . In the sequel we use the lower index e for all quantities related to  $\Omega \setminus \bar{\omega}$  and the lower index i for all quantities related to  $\omega_i^\eta$ . We summarize the notations concerning the domains in Figure IV.2.4 below.

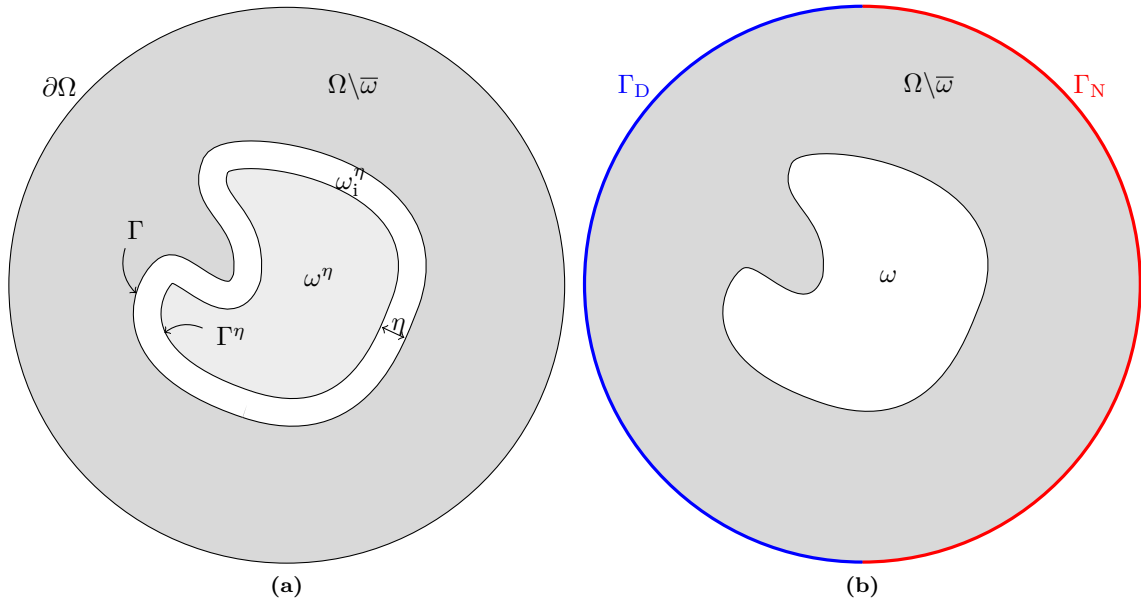


Figure IV.2.4 – Notations for the thin layer model (left) and the obtained GIBC model (right).

We denote by  $A_e$  the *elasticity tensor* defined, for any symmetric matrix  $\xi$ , by

$$A_e \xi := 2\mu_e \xi + \lambda_e \text{Tr}(\xi) \mathbf{I},$$

where  $\mu_e > 0$  and  $\lambda_e > 0$  are two positive constants which represent the *Lamé coefficients* of the material making up the solid and we introduce, for any  $\mathbf{u} \in \mathbf{H}^1(\Omega)$ , the *symmetrized gradient*

$$\mathcal{D}(\mathbf{u}) := \frac{1}{2} (\nabla \mathbf{u} + {}^t \nabla \mathbf{u}).$$

## IV.2 Generalized Impedance Boundary Conditions and optimal design for elasticity

Analogously  $A_i$  represents the elasticity tensor associated to  $\omega_i^\eta$  with Lamé coefficients  $\mu_i > 0$  and  $\lambda_i > 0$ . Moreover the *stress vector* relative to the material properties  $A_i$  on  $\Gamma^\eta$  is defined by

$$\mathbf{T}_i^\eta(\mathbf{u}) := A_i \mathcal{D}(\mathbf{u}) \mathbf{n}^\eta,$$

with the convention  $\mathbf{T}_i^0 = \mathbf{T}_i$  and we define similarly  $\mathbf{T}_e$  the stress vector relative to the material properties  $A_e$  on  $\Gamma$ :

$$\mathbf{T}_e(\mathbf{u}) := A_e \mathcal{D}(\mathbf{u}) \mathbf{n}. \quad (\text{IV.2.1})$$

### IV.2.1.2 Introduction of the transmission problem and the GIBC problem

We introduce the following Sobolev space

$$\mathbf{H}_{\Gamma_D}^1(\Omega \setminus \bar{\omega}) := \{ \mathbf{v} \in \mathbf{H}^1(\Omega \setminus \bar{\omega}) ; \mathbf{v} = \mathbf{0} \text{ on } \Gamma_D \}.$$

Let  $\mathbf{f} \in \mathbf{L}^2(\Omega \setminus \bar{\omega})$  be some exterior forces and a load  $\mathbf{g} \in \mathbf{H}^{-1/2}(\Gamma_N)$ . We are concerned with the following transmission problem

$$\left\{ \begin{array}{lll} -\operatorname{div}(A_e \mathcal{D}(\mathbf{u}_e^\eta)) & = \mathbf{f} & \text{in } \Omega \setminus \bar{\omega}, \\ -\operatorname{div}(A_i \mathcal{D}(\mathbf{u}_i^\eta)) & = \mathbf{0} & \text{in } \omega_i^\eta, \\ \mathbf{u}_e^\eta & = \mathbf{0} & \text{on } \Gamma_D, \\ \mathbf{T}_e(\mathbf{u}_e^\eta) & = \mathbf{g} & \text{on } \Gamma_N, \\ \mathbf{T}_i(\mathbf{u}_i^\eta) & = \mathbf{T}_e(\mathbf{u}_e^\eta) & \text{on } \Gamma, \\ \mathbf{u}_i^\eta & = \mathbf{u}_e^\eta & \text{on } \Gamma, \\ \mathbf{T}_i^\eta(\mathbf{u}_i^\eta) & = \mathbf{0} & \text{on } \Gamma^\eta. \end{array} \right. \quad (\text{IV.2.2})$$

The solution of such a problem exists, is unique and belongs to  $\mathbf{H}_{\Gamma_D}^1(\Omega \setminus \bar{\omega} \cup \omega_i^\eta)$  thanks to the Lax-Milgram theorem and Korn's inequality.

We introduce the following Hilbert space

$$\mathcal{V}(\Gamma) = \{ \boldsymbol{\psi} \in \mathbf{L}^2(\Gamma) ; \mathcal{D}_\Gamma(\boldsymbol{\psi}) \in \mathbf{L}^2(\Gamma) \},$$

endowed with the graph norm  $\| \boldsymbol{\psi} \|_{\mathcal{V}(\Gamma)}^2 := \left( \| \boldsymbol{\psi} \|_{\mathbf{L}^2(\Gamma)}^2 + \| \mathcal{D}_\Gamma(\boldsymbol{\psi}) \|_{\mathbf{L}^2(\Gamma)}^2 \right)^{1/2}$  where

$$\mathcal{D}_\Gamma(\boldsymbol{\psi}) := \frac{1}{2} \Pi_d (\nabla_\tau \boldsymbol{\psi} + {}^t \nabla_\tau \boldsymbol{\psi}) \Pi_d \quad \text{and} \quad \Pi_d := \mathbf{I} - \mathbf{n} \otimes \mathbf{n}.$$

We denote its dual space by  $\mathcal{V}'(\Gamma)$ . Then we set

$$\mathcal{H}(\Omega \setminus \bar{\omega}) := \{ \mathbf{v} \in \mathbf{H}_{\Gamma_D}^1(\Omega \setminus \bar{\omega}) ; \mathbf{v}|_\Gamma \in \mathcal{V}(\Gamma) \}.$$

The space  $\mathcal{H}(\Omega \setminus \bar{\omega})$  endowed with the graph norm  $\| \mathbf{v} \|_{\mathcal{H}(\Omega \setminus \bar{\omega})} := \left( \| \mathbf{v} \|_{\mathbf{H}^1(\Omega \setminus \bar{\omega})}^2 + \| \mathbf{v} \|_{\mathcal{V}(\Gamma)}^2 \right)^{1/2}$  is a Hilbert space. We also introduce, for all  $\boldsymbol{\psi} \in \mathcal{V}(\Gamma)$ , the notation

$$\mathcal{C}^\eta(\boldsymbol{\psi}) := -\eta \operatorname{div}_\tau(\sigma_\Gamma(\boldsymbol{\psi})), \quad (\text{IV.2.3})$$

with

$$\sigma_\Gamma(\boldsymbol{\psi}) := 2\mu_i \mathcal{D}_\Gamma(\boldsymbol{\psi}) + \bar{\lambda}_i (\operatorname{div}_\tau \boldsymbol{\psi}) \Pi_d = \bar{A}_i \mathcal{D}_\Gamma(\boldsymbol{\psi}) \quad \text{and} \quad \bar{A}_i \boldsymbol{\xi} := 2\mu_i \boldsymbol{\xi} + \bar{\lambda}_i \operatorname{Tr}(\boldsymbol{\xi}) \Pi_d,$$

where  $\mu_i$  and  $\bar{\lambda}_i := \frac{2\lambda_i \mu_i}{\lambda_i + 2\mu_i}$  are the modified Lamé constants in the thin layer.

**Remark IV.2.1.** Notice that these modified Lamé coefficients correspond to plane stress situations (see, e.g., [178, Section 8.2, page 514]). Indeed this state of plane stress arises in the thin layer since no buckling or blending occurs (see, e.g., [178, Section 3.5, page 102]).

Using an asymptotic analysis, we prove that the solution of the transmission problem (IV.2.2) can be approximated up to  $O(\eta^2)$  using an asymptotic analysis by the solution  $\mathbf{v}^\eta \in \mathcal{H}(\Omega \setminus \bar{\omega})$  of the following problem with GIBC on  $\Gamma$ :

$$\begin{cases} -\operatorname{div}(A_e \mathcal{D}(\mathbf{v}^\eta)) = \mathbf{f} & \text{in } \Omega \setminus \bar{\omega}, \\ \mathbf{v}^\eta = \mathbf{0} & \text{on } \Gamma_D, \\ \mathbf{T}_e(\mathbf{v}^\eta) = \mathbf{g} & \text{on } \Gamma_N, \\ \mathbf{T}_e(\mathbf{v}^\eta) + \mathbf{C}^\eta(\mathbf{v}^\eta) = \mathbf{0} & \text{on } \Gamma, \end{cases} \quad (\text{IV.2.4})$$

where  $\mathbf{T}_e$  and  $\mathbf{C}^\eta$  are defined respectively in (IV.2.1) and (IV.2.3). We can also prove the well-posedness of this problem applying the classical Lax-Milgram theorem.

**Remark IV.2.2.** (i) *The negative Wentzell-type operator  $\boldsymbol{\psi} \mapsto -\operatorname{div}_\tau(\sigma_\tau(\boldsymbol{\psi}))$  is a positive symmetric operator bounded from  $\mathcal{V}(\Gamma)$  to  $\mathcal{V}'(\Gamma)$ . Indeed we have*

$$\begin{aligned} \langle -\operatorname{div}_\tau(\sigma_\tau(\boldsymbol{\psi})), \boldsymbol{\varphi} \rangle_{\mathcal{V}'(\Gamma), \mathcal{V}(\Gamma)} &= \int_\Gamma \bar{\lambda}_i (\operatorname{div}_\tau \boldsymbol{\psi})(\operatorname{div}_\tau \boldsymbol{\varphi}) + 2\mu_i \int_\Gamma \mathcal{D}_\Gamma(\boldsymbol{\psi}) : \mathcal{D}_\Gamma(\boldsymbol{\varphi}) \\ &= \langle \boldsymbol{\psi}, -\operatorname{div}_\tau(\sigma_\tau(\boldsymbol{\varphi})) \rangle_{\mathcal{V}(\Gamma), \mathcal{V}'(\Gamma)}. \end{aligned}$$

Taking  $\boldsymbol{\psi} = \boldsymbol{\varphi}$ , the resulting quadratic form corresponds to (twice) the strain energy (see, e.g., [178, Equation (8.2.30), page 514]) in plane stress situation.

(ii) *For any  $\boldsymbol{\psi} \in \mathbf{L}^2(\Gamma)$ , let set  $\boldsymbol{\psi}_n := \boldsymbol{\psi} \cdot \mathbf{n}$  and  $\boldsymbol{\psi}_\tau := \boldsymbol{\psi} - \boldsymbol{\psi}_n \mathbf{n}$ . Then we get the following inclusion  $\{\boldsymbol{\psi} \in \mathbf{L}^2(\Gamma); \boldsymbol{\psi}_\tau \in \mathbf{H}^1(\Gamma)\} \subset \mathcal{V}(\Gamma)$  thanks to the equality*

$$\mathcal{D}_\Gamma(\boldsymbol{\psi}) = \mathcal{D}_\Gamma(\boldsymbol{\psi}_\tau) + \boldsymbol{\psi}_n [\mathbf{D}^2 b].$$

Moreover, using the formulas given in [99, page 88], one can check that the operator  $\boldsymbol{\psi} \in \mathcal{V}(\Gamma) \mapsto \mathcal{D}_\Gamma(\boldsymbol{\psi}) \in \mathbf{L}^2(\Gamma)$  corresponds to the operator  $\gamma_{\alpha\beta}$  defined in [99, Theorem 2.7.1]. Using an atlas for the boundary  $\Gamma$ , one can derive an inequality of Korn-type on 2-dimensional compact manifolds without boundary from [99, Theorem 2.7.1] ensuring that there exists a constant  $c_0 > 0$  depending on  $\Gamma$  such that

$$\left( \|\boldsymbol{\psi}_\tau\|_{\mathbf{H}^1(\Gamma)}^2 + \|\boldsymbol{\psi}_n\|_{\mathbf{L}^2(\Gamma)}^2 \right)^{1/2} \leq c_0 \|\boldsymbol{\psi}\|_{\mathcal{V}(\Gamma)}.$$

In other words the two spaces coincide, i.e.

$$\{\boldsymbol{\psi} \in \mathbf{L}^2(\Gamma); \boldsymbol{\psi}_\tau \in \mathbf{H}^1(\Gamma)\} = \mathcal{V}(\Gamma).$$

## IV.2.2 Main results

### IV.2.2.1 Brief description of the asymptotic analysis

This section is devoted to a brief explanation on the derivation of Problem (IV.2.4) and especially to the GIBC

$$\mathbf{T}_e(\mathbf{v}^\eta) + \mathbf{C}^\eta(\mathbf{v}^\eta) = \mathbf{0} \quad \text{on } \Gamma.$$

Let  $N \in \mathbb{N}$ . We want to approximate the solution  $\mathbf{u}_e^\eta \in \mathbf{H}_{\Gamma_D}^1(\Omega \setminus \bar{\omega})$  of the transmission problem (IV.2.2) by the solution  $\mathbf{v}_{[N]}^\eta$  of some boundary value problems of the form

$$\begin{cases} -\operatorname{div}(A_e \mathcal{D}(\mathbf{v}_{[N]}^\eta)) = \mathbf{f} & \text{in } \Omega \setminus \bar{\omega}, \\ \mathbf{v}_{[N]}^\eta = \mathbf{0} & \text{on } \Gamma_D, \\ \mathbf{T}_e(\mathbf{v}_{[N]}^\eta) = \mathbf{g} & \text{on } \Gamma_N, \\ \mathbf{T}_e(\mathbf{v}_{[N]}^\eta) + \mathbf{C}_N^\eta(\mathbf{v}_{[N]}^\eta) = \mathbf{0} & \text{on } \Gamma, \end{cases}$$

## IV.2 Generalized Impedance Boundary Conditions and optimal design for elasticity

where  $\|\mathbf{u}_e^\eta - \mathbf{v}_{[N]}^\eta\|_{\mathbf{H}^1(\Omega \setminus \bar{\omega})} = O(\eta^{N+1})$ . Notice that the linear operator  $\mathbf{C}_N^\eta$  is composed of surface differential operators and depends on the interior Lamé parameters. Also notice that we want here to obtain the expansion for  $N = 1$  in order to obtain a  $O(\eta^2)$  approximation, that is  $\mathbf{v}^\eta = \mathbf{v}_{[1]}^\eta$  and  $\mathbf{C}^\eta = \mathbf{C}_1^\eta$ .

To do so we follow the procedure described, e.g., in [163, 215], in the same spirit as what is done in the previous section in an other context. For any  $\mathbf{x} \in \Gamma$  and  $r \geq 0$ , we set  $\mathbf{u}(\mathbf{x} + r\mathbf{n}(x)) =: \bar{\mathbf{u}}(\mathbf{x}, r)$  and we use the change of variables  $\mathbf{y} = \mathbf{x} + r\mathbf{n}(x) = \mathbf{x} + \eta R\mathbf{n}(x)$  with  $R \in [0, 1]$ . Then we set  $\bar{\mathbf{u}}(\mathbf{x}, r) = \bar{\mathbf{u}}(\mathbf{x}, \eta R) =: \mathbf{U}^\eta(\mathbf{x}, R)$ . Firstly we obtain the following asymptotic expansion when  $\eta \rightarrow 0$ :

$$\operatorname{div}(A_i \mathcal{D}(\mathbf{u}))(\mathbf{x} + \eta R\mathbf{n}(x)) = \frac{1}{\eta^2} \left( \Lambda_0 \partial_R^2 + \eta \Lambda_1 \partial_R + \sum_{n \geq 2} \eta^n \Lambda_n \right) \mathbf{U}^\eta(\mathbf{x}, R),$$

where

$$\begin{aligned} \Lambda_0 &:= (\lambda_i + 2\mu_i) \mathbf{n} \otimes \mathbf{n} + \mu_i (\mathbf{I}_d - \mathbf{n} \otimes \mathbf{n}), \\ \Lambda_1 \mathbf{U}^\eta &:= \mu_i \mathbf{H} \mathbf{U}^\eta + (\lambda_i + \mu_i) (\mathbf{n} \operatorname{div}_\tau \mathbf{U}^\eta + \nabla_\tau (\mathbf{U}^\eta \cdot \mathbf{n})), \\ \Lambda_2 \mathbf{U}^\eta &:= \Lambda_{2,2} \mathbf{U}^\eta + R \Lambda_{2,1} \partial_R \mathbf{U}^\eta, \end{aligned}$$

with

$$\begin{aligned} \Lambda_{2,1} \mathbf{U}^\eta &:= -\mu_i \operatorname{Tr}([\mathbf{D}^2 b]^2) \mathbf{U}^\eta - (\lambda_i + \mu_i) (\mathbf{n} (\operatorname{Tr}([\mathbf{D}^2 b] \nabla_\tau \mathbf{U}^\eta)) + [\mathbf{D}^2 b] \nabla_\tau (\mathbf{U}^\eta \cdot \mathbf{n})), \\ \Lambda_{2,2} \mathbf{U}^\eta &:= (\lambda_i + \mu_i) \nabla_\tau \operatorname{div}_\tau \mathbf{U}^\eta + \mu_i \Delta_\tau \mathbf{U}^\eta - \lambda_i \mathbf{n} (\operatorname{Tr}([\mathbf{D}^2 b] \nabla_\tau \mathbf{U}^\eta)) - \mu_i ([\mathbf{D}^2 b] \nabla_\tau \mathbf{U}^\eta) \mathbf{n}. \end{aligned}$$

Moreover the traction trace operator is defined on  $\Gamma$ , i.e. for  $S = 0$ , by

$$\mathbf{T}_i \mathbf{U}^\eta := \frac{1}{\eta} \Lambda_0 \partial_R \mathbf{U}^\eta + \lambda_i \mathbf{n} \operatorname{div}_\tau \mathbf{U}^\eta + \mu_i [\nabla_\tau \mathbf{U}^\eta] \mathbf{n}$$

and it admits the following expansion on the surface  $\Gamma^\eta$ , i.e. for  $S = 1$ :

$$\mathbf{T}_i^\eta \mathbf{U}^\eta(\cdot, 1) = \frac{1}{\eta} \Lambda_0 \partial_R \mathbf{U}^\eta(\cdot, 1) + \mathbf{B}^0 \mathbf{U}^\eta(\cdot, 1) + \sum_{j \geq 1} \eta^j \mathbf{B}^j \mathbf{U}^\eta(\cdot, 1),$$

with

$$\mathbf{B}^0 \mathbf{U}^\eta := \lambda_i \mathbf{n} \operatorname{div}_\tau \mathbf{U}^\eta + \mu_i [\nabla_\tau \mathbf{U}^\eta] \mathbf{n} \quad \text{and} \quad \mathbf{B}^1 \mathbf{U}^\eta := -\left( \lambda_i \mathbf{n} (\operatorname{Tr}([\mathbf{D}^2 b] \nabla_\tau \mathbf{U}^\eta)) + \mu_i ([\mathbf{D}^2 b] \nabla_\tau \mathbf{U}^\eta) \mathbf{n} \right).$$

Secondly we set  $\mathbf{u}_e^\eta := \sum_{n \geq 0} \eta^n \mathbf{u}_e^n$  in  $\Omega \setminus \bar{\omega}$  and  $\bar{\mathbf{u}}_i^\eta(\mathbf{x}, r) := \mathbf{U}_i^\eta(\mathbf{x}, R) = \sum_{n \geq 0} \eta^n \mathbf{U}_i^n(\mathbf{x}, R)$  in  $\Gamma \times [0, 1]$ .

Hence the transmission problem (IV.2.2) can be rewritten as follows:

$$\left\{ \begin{array}{ll} - \sum_{n \geq 0} \eta^n \operatorname{div}(A_e \mathcal{D}(\mathbf{u}_e^n)) = \mathbf{f} & \text{in } \Omega \setminus \bar{\omega}, \\ \sum_{n \geq 0} \eta^n \partial_R^2 \Lambda_0 \mathbf{U}_i^n = - \sum_{n \geq 1} \eta^n \Lambda_1 \partial_R \mathbf{U}_i^{n-1} - \sum_{n \geq 2} \eta^n \Lambda_2 \mathbf{U}_i^{n-2} - \dots & \text{in } \Gamma \times (0, 1), \\ \sum_{n \geq 0} \eta^n \mathbf{u}_e^n = \mathbf{0} & \text{on } \Gamma_D, \\ \sum_{n \geq 0} \eta^n \mathbf{T}_e(\mathbf{u}_e^n) = \mathbf{g} & \text{on } \Gamma_N, \\ \sum_{n \geq 1} \eta^n \mathbf{T}_e(\mathbf{u}_e^{n-1}) = \sum_{n \geq 0} \eta^n \partial_R \Lambda_0 \mathbf{U}_i^n + \sum_{n \geq 1} \eta^n \mathbf{B}^0 \mathbf{U}_i^{n-1} & \text{on } \Gamma \times \{0\}, \\ \sum_{n \geq 0} \eta^n \Lambda_0 \mathbf{u}_e^n = \sum_{n \geq 0} \eta^n \Lambda_0 \mathbf{U}_i^n & \text{on } \Gamma \times \{0\}, \\ \sum_{n \geq 0} \eta^n \partial_R \Lambda_0 \mathbf{U}_i^n = - \sum_{n \geq 1} \eta^n \mathbf{B}^0 \mathbf{U}_i^{n-1} - \sum_{n \geq 2} \eta^n \mathbf{B}^1 \mathbf{U}_i^{n-2} + \dots & \text{on } \Gamma \times \{1\}. \end{array} \right.$$

Exploring the ranks  $n = 0, 1, 2$ , we obtain the result. One can note that we have  $\mathbf{C}_0^\eta = \mathbf{0}$ .

After these formal computations, we prove (under the additional assumption that  $\mathbf{f} \in \mathbf{H}^{1/2}(\Omega \setminus \bar{\omega})$ ), that the solution  $\mathbf{v}^\eta \in \mathcal{H}(\Omega \setminus \bar{\omega})$  of Problem (IV.2.4) is an approximation up to  $O(\eta^2)$  to the original solution  $\mathbf{u}_e^\eta \in \mathbf{H}_{\Gamma_D}^1(\Omega \setminus \bar{\omega})$  of Problem (IV.2.2). Indeed there exists a constant  $C > 0$ , depending only on the domains  $\Omega$  and  $\omega$ , such that

$$\|\mathbf{v}^\eta - \mathbf{u}_e^\eta\|_{\mathbf{H}^1(\Omega \setminus \bar{\omega})} \leq C \eta^2.$$

#### IV.2.2.2 Shape sensitivity analysis and minimization of the compliance

Another aim of the present work is to make a shape sensitivity analysis of the problem. Hence we prove the existence of shape derivatives with respect to the shape  $\omega$  and characterize the shape derivative of Problem (IV.2.4). To do this, let us recall that  $\Omega_{d_0}$  is an open set with a  $\mathcal{C}^\infty$  boundary such that

$$\{\mathbf{x} \in \Omega; \text{d}(\mathbf{x}, \partial\Omega) > d_0/2\} \subset \Omega_{d_0} \subset \{\mathbf{x} \in \Omega; \text{d}(\mathbf{x}, \partial\Omega) > d_0/3\},$$

and the space of admissible deformations is here given by

$$\mathcal{U} := \left\{ \mathbf{V} \in \mathbf{W}^{3,\infty}(\mathbb{R}^d); \text{supp}(\mathbf{V}) \subset \overline{\Omega_{d_0}} \text{ and } \|\mathbf{V}\|_{3,\infty} < \min\left(\frac{d_0}{3}, 1\right) \right\}.$$

Then we obtain the following second main result.

**Theorem IV.2.3.** *Let  $\mathbf{V} \in \mathcal{U}$ . The shape derivative  $\mathbf{v}^{\eta'}$  of  $\mathbf{v}^\eta$  in the direction  $\mathbf{V}$ , which belongs to  $\mathbf{L}^2(\Omega \setminus \bar{\omega})$ , exists. Moreover, if  $\mathbf{v}^\eta \in \mathbf{H}^2(\Gamma)$ , then  $\mathbf{v}^{\eta'} \in \mathcal{H}(\Omega \setminus \bar{\omega})$  is the only solution of the following boundary value problem*

$$\begin{cases} -\text{div}(A_e \mathcal{D}(\mathbf{v}^{\eta'})) = \mathbf{0} & \text{in } \Omega \setminus \bar{\omega}, \\ \mathbf{v}^{\eta'} = \mathbf{0} & \text{on } \Gamma_D, \\ \mathbf{T}_e(\mathbf{v}^{\eta'}) = \mathbf{0} & \text{on } \Gamma_N, \\ \mathbf{T}_e(\mathbf{v}^{\eta'}) + \mathbf{C}^\eta(\mathbf{v}^{\eta'}) = \xi(\mathbf{v}^\eta, \mathbf{V} \cdot \mathbf{n}) & \text{on } \Gamma, \end{cases}$$

with

$$\begin{aligned} \xi(\mathbf{v}, \mathbf{V} \cdot \mathbf{n}) := & (\mathbf{V} \cdot \mathbf{n}) \mathbf{f} + \text{div}_\tau \left( (\mathbf{V} \cdot \mathbf{n}) \Pi_d (A_e \mathcal{D}(\mathbf{v})) \Pi_d \right) - \eta \text{div}_\tau \left( (\mathbf{V} \cdot \mathbf{n}) ([D^2 b] - \mathbf{H} \Pi_d) \sigma_\Gamma(\mathbf{v}) \right) \\ & - \eta \text{div}_\tau \left( (\mathbf{V} \cdot \mathbf{n}) (\bar{A}_i \Pi_d \left( \frac{1}{2} ([D^2 b] \nabla_\tau \mathbf{v} + {}^t([D^2 b] \nabla_\tau \mathbf{v})) \right) \Pi_d \right) + \eta \text{div}_\tau \left( \sigma_\Gamma((\mathbf{V} \cdot \mathbf{n}) \partial_n \mathbf{v}) \right) \\ & + \eta ([D^2 b] + \mathbf{n} \text{div}_\tau \Pi_d) (\text{div}_\tau((\mathbf{V} \cdot \mathbf{n}) \sigma_\Gamma(\mathbf{v}))) \\ & + \eta \text{div}_\tau \left( \bar{A}_i \left( \frac{1}{2} ([\nabla_\tau \mathbf{v}] \mathbf{n} \otimes \nabla_\tau(\mathbf{V} \cdot \mathbf{n}) + \nabla_\tau(\mathbf{V} \cdot \mathbf{n}) \otimes [\nabla_\tau \mathbf{v}] \mathbf{n}) \right) \right). \end{aligned}$$

We also provide an asymptotic analysis on the shape derivatives for the transmission problem (IV.2.2) and compare it with the shape derivatives of Problem (IV.2.4): we prove (as underlined in [163]) that the asymptotic analysis and the shape derivative calculus can be interchanged.

Finally we give an example of application of this work concerning the minimization of the compliance. We compute the shape derivative of the compliance through the introduction of an adjoint problem and make some numerical simulations in the two-dimensional case in order to illustrate and validate our theoretical results. Thus, defining the compliance of the structure  $\Omega \setminus \bar{\omega}$  as

$$\mathcal{J}^\eta(\Omega \setminus \bar{\omega}) := \int_{\Omega \setminus \bar{\omega}} A_e \mathcal{D}(\mathbf{v}^\eta) : \mathcal{D}(\mathbf{v}^\eta) + \eta \int_\Gamma \bar{A}_i \mathcal{D}_\Gamma(\mathbf{v}^\eta) : \mathcal{D}_\Gamma(\mathbf{v}^\eta), \quad (\text{IV.2.5})$$

where  $\mathbf{v}^\eta \in \mathcal{H}(\Omega \setminus \bar{\omega})$  solves Problem (IV.2.4), we obtain the following expression of the shape gradient of this cost functional.

**Theorem IV.2.4.** *Let  $\mathbf{V} \in \mathcal{U}$ . If  $\mathbf{v}^\eta \in \mathbf{H}^2(\Gamma)$ , then the shape derivative of the cost functional  $\mathcal{J}^\eta$  can be written as*

$$\mathrm{D}\mathcal{J}^\eta(\Omega \setminus \bar{\omega}) \cdot \mathbf{V} = \int_{\Gamma} (\mathbf{V} \cdot \mathbf{n}) \xi^*(\mathbf{v}^\eta, \mathbf{v}^\eta) + \int_{\Gamma} (\mathbf{V} \cdot \mathbf{n}) \mathbf{f} \cdot \mathbf{v}^\eta,$$

where

$$\begin{aligned} \xi^*(\mathbf{v}, \mathbf{w}) := & -(\Pi_d(A_e \mathcal{D}(\mathbf{v})) \Pi_d) : \nabla_\tau \mathbf{w} + \eta \left\{ \left( ([D^2b] - \mathbb{H} \Pi_d) \sigma_\Gamma(\mathbf{v}) \right) : \nabla_\tau \mathbf{w} + ([D^2b] \nabla_\tau \mathbf{v}) : \sigma_\Gamma(\mathbf{w}) \right. \\ & \left. + (\partial_n \mathbf{v}) \operatorname{div}_\tau(\sigma_\Gamma(\mathbf{w})) + \sigma_\Gamma(\mathbf{v}) : (\nabla_\tau([\nabla_\tau \mathbf{w}] \mathbf{n})) + \operatorname{div}_\tau(\sigma_\Gamma(\mathbf{w})[\nabla_\tau \mathbf{v}] \mathbf{n}) \right\} + \mathbf{f} \cdot \mathbf{w}. \end{aligned}$$

**Remark IV.2.5.** *I am confident that the regularity assumption  $\mathbf{v}^\eta \in \mathbf{H}^2(\Gamma)$  made in the two previous theorems is useless since automatically satisfied. Unfortunately, up to my knowledge, the arguments to obtain it are not trivial and this study could be the topic of a future work.*

Notice that we also prove that the considered functional  $\mathcal{J}^\eta$  given by (IV.2.5) is an approximation up to  $O(\eta^2)$  to the original compliance  $\mathcal{J}$  of a structure associated to the original transmission problem (IV.2.2) which is given by

$$\mathcal{J}(\Omega \setminus \bar{\omega}^\eta) := \int_{\Omega \setminus \bar{\omega}^\eta} A_e \mathcal{D}(\mathbf{u}_e^\eta) : \mathcal{D}(\mathbf{u}_e^\eta) + \int_{\omega_1^\eta} A_i \mathcal{D}(\mathbf{u}_i^\eta) : \mathcal{D}(\mathbf{u}_i^\eta).$$

Indeed we have

$$\mathcal{J}(\Omega \setminus \bar{\omega}^\eta) - \mathcal{J}^\eta(\Omega \setminus \bar{\omega}) = O(\eta^2).$$

### IV.2.3 Numerical simulations for a 2D-cantilever

For the numerical simulations presented in this section, we consider the case where we optimize a part of the boundary of the solid which is not necessarily an inclusion. Hence we consider an elastic solid with a reference configuration  $\Omega$ , a bounded open set of  $\mathbb{R}^2$ , built on a part  $\Gamma_D$  of its boundary and subjected to a load  $\mathbf{g}$  on another part  $\Gamma_N$ . We consider here that  $\Gamma := \partial\Omega \setminus (\Gamma_D \cup \Gamma_N)$  is a non-empty set and is the only part of  $\partial\Omega$  which can be optimized (see Figure IV.2.5). We assume that  $\mathbf{f} = \mathbf{0}$ . Then the displacement  $\mathbf{v} \in \mathcal{H}(\Omega)$  of the structure is the solution of

$$\begin{cases} -\operatorname{div}(A_e \mathcal{D}(\mathbf{v})) = \mathbf{0} & \text{in } \Omega, \\ \mathbf{v} = \mathbf{0} & \text{on } \Gamma_D, \\ \mathbf{T}_e \mathbf{v} = \mathbf{g} & \text{on } \Gamma_N, \\ \mathbf{T}_e \mathbf{v} + \mathbf{C}^\eta(\mathbf{v}) = \mathbf{0} & \text{on } \Gamma, \end{cases}$$

where  $\mathbf{T}_e$  and  $\mathbf{C}^\eta$  are defined respectively in (IV.2.1) and (IV.2.3). We want to minimize the compliance adding a penalization on the total mass of the structure. Hence we consider, for  $\ell > 0$ , the functional

$$\mathcal{J}_{\text{pen}}^\eta(\Omega) = \mathcal{J}^\eta(\Omega) + \ell |\Omega| = \int_{\Omega} A_e \mathcal{D}(\mathbf{v}) : \mathcal{D}(\mathbf{v}) + \eta \int_{\Gamma} \bar{A}_i \mathcal{D}_\Gamma(\mathbf{v}) : \mathcal{D}_\Gamma(\mathbf{v}) + \ell |\Omega|.$$

According to Theorem IV.2.4 and taking into account the shape derivative of the volume, the shape derivative of the cost functional  $\mathcal{J}$  can be written in the form

$$\mathrm{D}\mathcal{J}_{\text{pen}}^\eta(\Omega) \cdot \mathbf{V} = \int_{\Gamma} (\mathbf{V} \cdot \mathbf{n}) \left( \xi^*(\mathbf{v}, \mathbf{v}) + \ell \right),$$

where  $\mathbf{V}$  is an admissible deformation and  $\xi^*$  is defined in Proposition IV.2.4.

Using a boundary variation method with a gradient algorithm, we obtain the following result exposed in Figure IV.2.6.

We also make a simulation adding a hole (with the generalized boundary conditions) in the initial shape. We obtain the following result exposed in Figure IV.2.7.

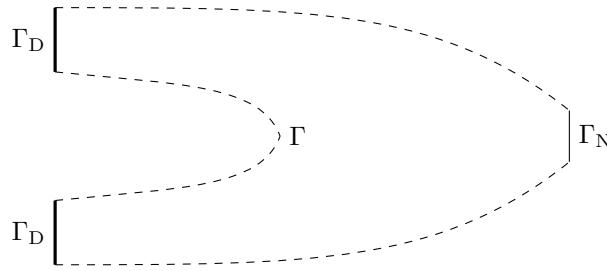


Figure IV.2.5 – A cantilever.

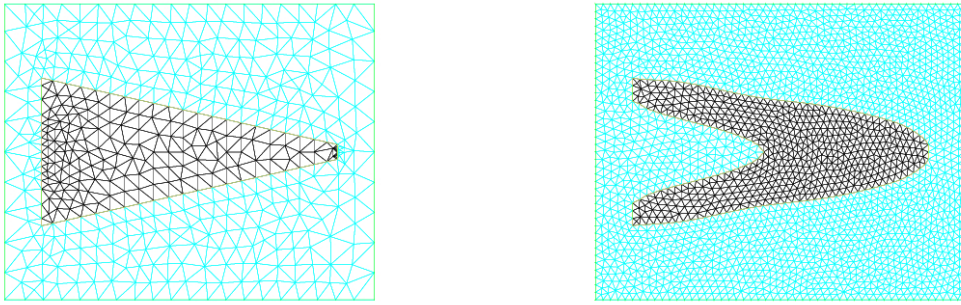
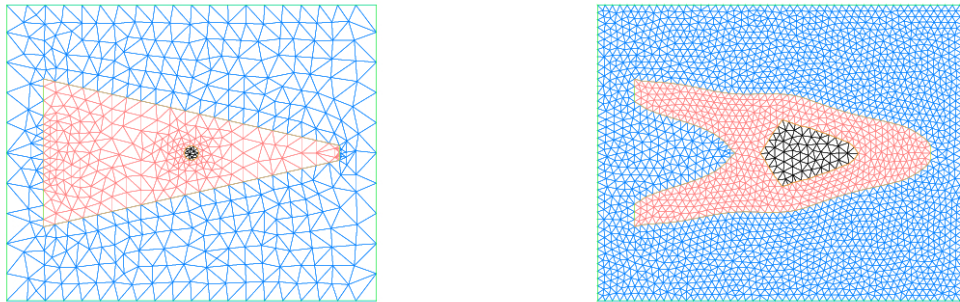


Figure IV.2.6 – Minimization of the compliance for a 2d-cantilever: initial shape (left) and final shape (right).

### IV.3 Perspectives

Concerning the first subject on the Bloch-Torrey equation in the context of dMRI, one perspective could be to adapt the work of Coatléven *et al.* in [101] in order to obtain a macroscopic model for the dMRI taking into account the previously mentioned anisotropic behavior in the myelin layer of a cell. Indeed, assuming that the considered medium in the dMRI is periodic (that is that the disposition of the cells is periodic), the periodic homogenization theory could enable to obtain a macroscopic model from the previously established two compartment model. In [101], the authors obtain the result by expanding the solution of Bloch-Torrey equation using a two-scale asymptotic expansions. Then they explain that one can use it to solve the inverse problem of recovering some macroscopic properties of tissues from dMRI measurements. We expect to adapt this work to our model and compare the obtained results with the ones given in [101].

Concerning the second problem of this chapter, the perspectives could concern mainly the numerical part. Indeed the used optimization algorithm is a very simple one and uses the classical boundary variations method. We can improve this numerical part, using for instance other numerical methods as the so-called level set method which is known to be efficient in this kind of problem (see, e.g., [18]). This could enable to compare these results with the classical problem without GIBC and also to validate numerically the announced order  $O(\eta^2)$  of the GIBC.



**Figure IV.2.7** – Minimization of the compliance for a 2d-cantilever with a hole: initial shape (left) and final shape (right).



---

---

# Chapter V

---

## Sensitivity analysis for contact problems

In the last section of the previous chapter IV, we have considered the linear elasticity equations, arising in solid mechanics. Additionally to the study of a single structure (as, e.g., the optimal design of such a structure), another topic concerns *unilateral constraints and contact problems*. Contact mechanics describes the physical behavior of two solids that touch each other while being subjected to external forces. The bodies may be rigid or flexible; they cannot penetrate each other, but they may deform or slide one against the other, thus causing friction. From the mathematical point of view, this phenomenon translates into a unilateral contact constraint: the non-permeability conditions take the form of inequalities on the contact surface between the bodies and are called *Signorini conditions*; the friction occurring in this region is typically modeled by the so-called *Tresca's or Coulomb's laws* which also appear as a boundary condition with inequalities, but moreover cause nonlinearities in the variational formulation of the problem. This physical model can be mathematically studied from the variational inequality theory and with convex analysis tools (see, e.g., the book [124]).

A project (still in progress) aims at studying the optimal shape of a rigid structure (which minimizes the dissipated energy for instance) in contact situations by taking into account realistic physical constraints, such as the aforementioned mentioned friction phenomena. This question led us to study the sensitivity with respect to a parameter of variational inequalities in which the solution is expressed through the *proximal operator* (some basics are recalled below, in Section V.1). More precisely the proximal operator of the sum of two functions (that is the indicator function of a non-empty closed and convex set of constraints and a convex function) intervenes. Thus ***we wondered if an adapted decomposition of the proximal operator of the sum of two convex functions could be achieved. We obtain such a formula by introducing a new operator and prove a first result of differentiability of the solution with respect to a parameter.*** This is the topic of the following article, written with Samir Adly and Loïc Bourdin (University of Limoges) and accepted in *Journal of Convex Analysis* (20 pages), that I summarized in this chapter:

- [6] S. Adly, L. Bourdin and F. Caubet. On a decomposition formula for the proximal operator of the sum of two convex functions. *Journal of Convex Analysis*, to appear, 2018.

As mentioned, the work presented in this section was initially motivated by the sensitivity analysis, with respect to a nonnegative parameter  $t \geq 0$ , of a parametrized linear variational inequality of second kind in a Hilbert space  $H$ , with a corresponding function  $h \in \Gamma_0(H)$ , where  $\Gamma_0(H)$  is the set of proper, lower semicontinuous and convex functions from  $H$  into  $\mathbb{R} \cup \{+\infty\}$ . More precisely, for all  $t \geq 0$ , we consider the problem of finding  $u(t) \in H$  such that

$$\langle u(t), z - u(t) \rangle + h(z) - h(u(t)) \geq \langle r(t), z - u(t) \rangle, \quad (\text{V.0.1})$$

for all  $z \in H$ , where  $r : \mathbb{R}^+ \rightarrow H$  is assumed to be given and smooth enough. In that framework, the solution  $u(t) \in H$  (which depends on the parameter  $t$ ) can be expressed in terms of the proximal

operator of  $h$  denoted by  $\text{prox}_h$ . Precisely it holds that  $u(t) = \text{prox}_h(r(t))$  for all  $t \geq 0$ . As a consequence, the differentiability of  $u(\cdot)$  at  $t = 0$  is strongly related to the regularity of  $\text{prox}_h$ . If  $h$  is a smooth function, one can easily compute (from the classical inverse mapping theorem for instance) the differential of  $\text{prox}_h$ , and then the sensitivity analysis can be achieved. In that smooth case, note that the variational inequality (V.0.1) can actually be reduced to an equality. On the other hand, if  $h = \iota_K$  is the indicator function of a non-empty closed and convex subset  $K \subset H$ , then  $\text{prox}_h = \text{proj}_K$  is the classical projection operator on  $K$ . In that case, the work of Mignot in [182, Theorem 2.1 p.145] (see also the work of Haraux in [148, Theorem 2 p.620]) provides an asymptotic expansion of  $\text{prox}_h = \text{proj}_K$  and enables to obtain a differentiability result on  $u(\cdot)$  at  $t = 0$ .

Concerning the sensibility analysis of a unilateral contact problem with friction (as the Tresca problem), the considered variational inequality (V.0.1) involves the sum of two functions. Precisely,  $h = f + g$  where  $f = \iota_K$  ( $K$  being a non-empty closed and convex set of constraints), and where  $g \in \Gamma_0(H)$  is a smooth function (derived from the regularization of the friction functional in view of a numerical treatment). Despite the regularity of  $g$ , note that the variational inequality (V.0.1) cannot be reduced to an equality due to the presence of the constraint set  $K$ . In that framework, in order to get an asymptotic expansion of  $\text{prox}_h = \text{prox}_{f+g}$ , a first and natural strategy would be to look for a convenient explicit expression of  $\text{prox}_{f+g}$  in terms of  $\text{prox}_f$  and  $\text{prox}_g$ . Unfortunately, this theoretical question still remains an open challenge in the literature. Let us mention that Yu provides in [218] some necessary and/or sufficient conditions on general functions  $f, g \in \Gamma_0(H)$  under which  $\text{prox}_{f+g} = \text{prox}_f \circ \text{prox}_g$ . Unfortunately, as underlined by the author himself, these conditions are very restrictive and are not satisfied in most of cases (see, e.g., [218, Example 2] for a counterexample). We recall here that a wide literature is already concerned with the sensitivity analysis of parametrized (linear and nonlinear) variational inequalities. We refer for instance to [49, 148, 189, 203] and references therein.

## V.1 Notations and basics of convex analysis

For the reader's convenience, we first recall some basics of convex analysis. We refer to standard books such as [37, 156, 192] and references therein.

Let  $H$  be a real Hilbert space and let  $\langle \cdot, \cdot \rangle$  (respectively  $\| \cdot \|$ ) be the corresponding scalar product (respectively norm). In the sequel we denote by  $I : H \rightarrow H$  the identity operator and by  $L_x : H \rightarrow H$  the affine operator defined by

$$L_x(y) := x - y,$$

for all  $x, y \in H$ .

For a set-valued map  $A : H \rightrightarrows H$ , the *domain* of  $A$  is given by

$$D(A) := \{x \in H \mid A(x) \neq \emptyset\}.$$

We denote by  $A^{-1} : H \rightrightarrows H$  the set-valued map defined by

$$A^{-1}(y) := \{x \in H \mid y \in A(x)\},$$

for all  $y \in H$ . Note that  $y \in A(x)$  if and only if  $x \in A^{-1}(y)$ , for all  $x, y \in H$ . The *range* of  $A$  is given by

$$R(A) := \{y \in H \mid A^{-1}(y) \neq \emptyset\} = D(A^{-1}).$$

We denote by  $\text{Fix}(A)$  the set of all fixed points of  $A$ , that is, the set given by

$$\text{Fix}(A) := \{x \in H \mid x \in A(x)\}.$$

Finally, if  $A(x)$  is a singleton for all  $x \in D(A)$ , we say that  $A$  is *single-valued*.

For all extended-real-valued functions  $g : \mathbb{H} \rightarrow \mathbb{R} \cup \{+\infty\}$ , the *domain* of  $g$  is given by

$$\text{dom}(g) := \{x \in \mathbb{H} \mid g(x) < +\infty\}.$$

We say that  $g$  is *proper* if  $\text{dom}(g) \neq \emptyset$ , and that  $g$  is *lower semicontinuous* if its epigraph is a closed subset of  $\mathbb{H} \times \mathbb{R}$ .

Let  $g : \mathbb{H} \rightarrow \mathbb{R} \cup \{+\infty\}$  be a proper extended-real-valued function. We denote by  $g^* : \mathbb{H} \rightarrow \mathbb{R} \cup \{+\infty\}$  the *conjugate* of  $g$  defined by

$$g^*(y) := \sup_{z \in \mathbb{H}} \{\langle y, z \rangle - g(z)\},$$

for all  $y \in \mathbb{H}$ . Clearly  $g^*$  is lower semicontinuous and convex.

We denote by  $\Gamma_0(\mathbb{H})$  the set of all extended-real-valued functions  $g : \mathbb{H} \rightarrow \mathbb{R} \cup \{+\infty\}$  that are proper, lower semicontinuous and convex. If  $g \in \Gamma_0(\mathbb{H})$ , we recall that  $g^* \in \Gamma_0(\mathbb{H})$  and that the *Fenchel-Moreau equality*  $g^{**} = g$  holds. For all  $g \in \Gamma_0(\mathbb{H})$ , we denote by  $\partial g : \mathbb{H} \rightrightarrows \mathbb{H}$  the *Fenchel-Moreau subdifferential* of  $g$  defined by

$$\partial g(x) := \{y \in \mathbb{H} \mid \langle y, z - x \rangle \leq g(z) - g(x), \forall z \in \mathbb{H}\},$$

for all  $x \in \mathbb{H}$ . It is easy to check that  $\partial g$  is a monotone operator and that, for all  $x \in \mathbb{H}$ ,  $0 \in \partial g(x)$  if and only if  $x \in \text{argmin } g$ . Moreover, for all  $x, y \in \mathbb{H}$ , it holds that  $y \in \partial g(x)$  if and only if  $x \in \partial g^*(y)$ . Recall that, if  $g$  is differentiable on  $\mathbb{H}$ , then  $\partial g(x) = \{\nabla g(x)\}$  for all  $x \in \mathbb{H}$ .

Let  $A : \mathbb{H} \rightarrow \mathbb{H}$  be a single-valued operator defined everywhere on  $\mathbb{H}$ , and let  $g \in \Gamma_0(\mathbb{H})$ . We denote by  $\text{VI}(A, g)$  the variational inequality which consists of finding  $y \in \mathbb{H}$  such that

$$-A(y) \in \partial g(y), \tag{V.1.1}$$

or equivalently,

$$\langle A(y), z - y \rangle + g(z) - g(y) \geq 0,$$

for all  $z \in \mathbb{H}$ . Then we denote by  $\text{Sol}_{\text{VI}}(A, g)$  the set of solutions of  $\text{VI}(A, g)$ . Recall that if  $A$  is Lipschitz and strongly monotone, then  $\text{VI}(A, g)$  admits a unique solution, i.e.  $\text{Sol}_{\text{VI}}(A, g)$  is a singleton.

Let  $g \in \Gamma_0(\mathbb{H})$ . The classical *proximal operator* of  $g$  is defined by

$$\text{prox}_g := (\text{I} + \partial g)^{-1}.$$

Recall that  $\text{prox}_g$  is a single-valued operator defined everywhere on  $\mathbb{H}$ . Moreover it can be characterized as follows:

$$\text{prox}_g(x) = \text{argmin} \left( g + \frac{1}{2} \|\cdot - x\|^2 \right) = \text{Sol}_{\text{VI}}(-L_x, g),$$

for all  $x \in \mathbb{H}$ . It is also well-known that

$$\text{Fix}(\text{prox}_g) = \text{argmin } g.$$

The classical *Moreau's envelope*  $M_g : \mathbb{H} \rightarrow \mathbb{R}$  of  $g$  is defined by

$$M_g(x) := \min \left( g + \frac{1}{2} \|\cdot - x\|^2 \right),$$

for all  $x \in \mathbb{H}$ . Recall that  $M_g$  is convex and differentiable on  $\mathbb{H}$  with  $\nabla M_g = \text{prox}_{g^*}$ .

Finally it is well-known that if  $g = \iota_K$  is the *indicator function* of a non-empty closed and convex subset  $K$  of  $\mathbb{H}$ , that is,  $\iota_K(x) = 0$  if  $x \in K$  and  $\iota_K(x) = +\infty$  if not, then  $\text{prox}_g = \text{proj}_K$ , where  $\text{proj}_K$  denotes the classical projection operator on  $K$ .

## V.2 The $f$ -proximal operator

### V.2.1 Introduction of the $f$ -proximal operator and main result

Let us consider general functions  $f, g \in \Gamma_0(\mathbb{H})$ . In order to avoid trivialities, we assume in the whole chapter that  $\text{dom}(f) \cap \text{dom}(g) \neq \emptyset$  when dealing with the sum  $f + g$ .

We first introduce a new operator  $\text{prox}_g^f : \mathbb{H} \rightrightarrows \mathbb{H}$  called  *$f$ -proximal operator of  $g$* .

**Definition V.2.1.** *Let us consider  $f, g \in \Gamma_0(\mathbb{H})$ . The  $f$ -proximal operator of  $g$  is the set-valued map  $\text{prox}_g^f : \mathbb{H} \rightrightarrows \mathbb{H}$  defined by*

$$\text{prox}_g^f := (\text{I} + \partial g \circ \text{prox}_f)^{-1}. \quad (\text{V.2.1})$$

This new operator can be seen as a generalization of  $\text{prox}_g$  in the sense that, if  $f$  is constant for instance, then  $\text{prox}_g^f = \text{prox}_g$ . More general sufficient (and necessary) conditions under which  $\text{prox}_g^f = \text{prox}_g$  are provided in the following proposition. We will base our discussion on the following conditions:

$$\partial(f + g) = \partial f + \partial g, \quad (\text{C}_1)$$

$$\forall x \in \mathbb{H}, \quad \partial g(x) \subset \partial g(\text{prox}_f(x)), \quad (\text{C}_2)$$

and

$$\forall x \in \mathbb{H}, \quad \partial g(\text{prox}_f(x)) \subset \partial g(x). \quad (\text{C}_3)$$

Note that Condition (C<sub>2</sub>) has been introduced by Yu in [218] as a sufficient condition under which  $\text{prox}_{f+g} = \text{prox}_f \circ \text{prox}_g$ .

**Proposition V.2.2.** *Let  $f, g \in \Gamma_0(\mathbb{H})$  with  $\text{dom}(f) \cap \text{dom}(g) \neq \emptyset$ .*

(i) *If Condition (C<sub>2</sub>) is satisfied, then  $\text{prox}_g^f(x) \in \text{prox}_g^f(x)$  for all  $x \in \mathbb{H}$ .*

(ii) *If Conditions (C<sub>1</sub>) and (C<sub>3</sub>) are satisfied, then  $\text{prox}_g^f(x) = \text{prox}_g(x)$  for all  $x \in \mathbb{H}$ .*

*In both cases, Condition (C<sub>1</sub>) is satisfied and the equality  $\text{prox}_{f+g} = \text{prox}_f \circ \text{prox}_g$  holds true.*

Note that  $\text{prox}_g^f$  is a set-valued operator *a priori*. Indeed we illustrate this by the following example.

**Example V.2.3.** *Let us assume that  $\mathbb{H} = \mathbb{R}$ . We consider  $f = \iota_{\{0\}}$  and  $g(x) = |x|$  for all  $x \in \mathbb{R}$ . In that case we obtain that  $\partial g \circ \text{prox}_f(x) = [-1, 1]$  for all  $x \in \mathbb{R}$ . As a consequence  $\text{prox}_g^f(x) = [x-1, x+1]$  for all  $x \in \mathbb{R}$ . See Figure V.2.1 for graphical representations of  $\text{prox}_g$  and  $\text{prox}_g^f$  in that case.*

Example V.2.3 provides a simple illustration where  $\text{prox}_g^f$  is not single-valued. Especially it follows that  $\text{prox}_g^f$  cannot be written as a proximal operator  $\text{prox}_\varphi$  for some  $\varphi \in \Gamma_0(\mathbb{H})$ . We provide some sufficient conditions under which  $\text{prox}_g^f$  is single-valued in the following proposition.

**Proposition V.2.4.** *Let  $f, g \in \Gamma_0(\mathbb{H})$  with  $\text{dom}(f) \cap \text{dom}(g) \neq \emptyset$  and such that  $\partial(f + g) = \partial f + \partial g$ . If either  $\partial f$  or  $\partial g$  is single-valued, then  $\text{prox}_g^f$  is single-valued.*

Moreover notice that Example V.2.3 provides a simple situation where  $\partial g \circ \text{prox}_f$  is not a monotone operator. As a consequence, it may be possible that  $\text{D}(\text{prox}_g^f) \subsetneq \mathbb{H}$ . However we prove the following characterization.

**Proposition V.2.5.** *Let  $f, g \in \Gamma_0(\mathbb{H})$  such that  $\text{dom}(f) \cap \text{dom}(g) \neq \emptyset$ . It holds that  $\text{D}(\text{prox}_g^f) = \mathbb{H}$  if and only if the additivity condition (C<sub>1</sub>) is satisfied.*

Finally, if the additivity condition (C<sub>1</sub>) is satisfied, the following main result presents an original decomposition formula of  $\text{prox}_{f+g}$ .

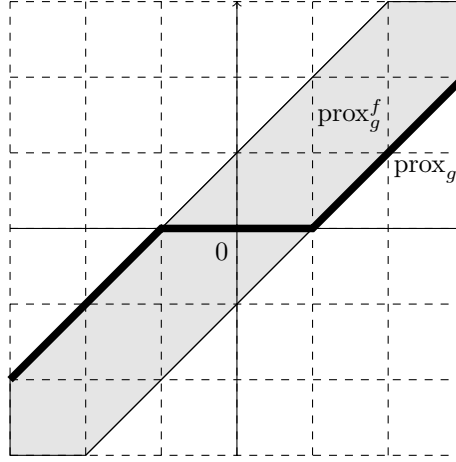


**Figure V.2.1** – Example V.2.3, graph of  $\text{prox}_g$  in bold line, and graph of  $\text{prox}_g^f$  in gray.

**Theorem V.2.6.** *Let  $f, g \in \Gamma_0(\mathbb{H})$  such that  $\text{dom}(f) \cap \text{dom}(g) \neq \emptyset$ . If  $\partial(f + g) = \partial f + \partial g$ , then the decomposition formula*

$$\text{prox}_{f+g} = \text{prox}_f \circ \text{prox}_g^f \quad (\text{V.2.2})$$

*holds true. In other words, for every  $x \in \mathbb{H}$ , we have  $\text{prox}_{f+g}(x) = \text{prox}_f(z)$  for all  $z \in \text{prox}_g^f(x)$ .*

**Remark V.2.7.** *Let  $f, g \in \Gamma_0(\mathbb{H})$  with  $\text{dom}(f) \cap \text{dom}(g) \neq \emptyset$  and such that  $\partial(f + g) = \partial f + \partial g$  and let  $x \in \mathbb{H}$ . Theorem V.2.6 states that, even if  $\text{prox}_g^f(x)$  is not a singleton, all elements of  $\text{prox}_g^f(x)$  have the same value through the proximal operator  $\text{prox}_f$ , and this value is equal to  $\text{prox}_{f+g}(x)$ .*

**Remark V.2.8.** *Let us consider  $f, g \in \Gamma_0(\mathbb{H})$  such that  $\text{dom}(f) \cap \text{dom}(g) \neq \emptyset$ . Note that the additivity condition  $\partial(f + g) = \partial f + \partial g$  is not only sufficient, but also necessary for the validity of the equality  $\text{prox}_{f+g} = \text{prox}_f \circ \text{prox}_g^f$ . Indeed, from Proposition V.2.5, if  $\partial f + \partial g \subsetneq \partial(f + g)$ , then there exists  $x \in \mathbb{H}$  such that  $\text{prox}_g^f(x) = \emptyset$  and thus  $\text{prox}_{f+g}(x) \neq \text{prox}_f \circ \text{prox}_g^f(x)$ .*

**Remark V.2.9.** *Let  $f, g \in \Gamma_0(\mathbb{H})$  with  $\text{dom}(f) \cap \text{dom}(g) \neq \emptyset$  and such that  $\partial(f + g) = \partial f + \partial g$ . From Theorem V.2.6, we deduce that  $\text{R}(\text{prox}_{f+g}) \subset \text{R}(\text{prox}_f) \cap \text{R}(\text{prox}_g)$ . If the additivity condition  $\partial(f + g) = \partial f + \partial g$  is not satisfied, this remark does not hold true anymore.*

Let us now give a simple illustration of the previous Theorem V.2.6.

**Example V.2.10.** *Following the idea of Yu in [218, Example 2], let us consider  $\mathbb{H} = \mathbb{R}$  and let  $f(x) = \frac{1}{2}x^2$  for all  $x \in \mathbb{R}$ . Since  $\text{prox}_{\gamma f} = \frac{1}{1+\gamma}\text{I}$  for all  $\gamma \geq 0$  and  $\text{prox}_f^f = \frac{2}{3}\text{I}$ , we retrieve that*

$$\frac{1}{3}\text{I} = \text{prox}_{2f} = \text{prox}_{f+f} = \text{prox}_f \circ \text{prox}_f^f = \frac{1}{3}\text{I} \neq \frac{1}{4}\text{I} = \text{prox}_f \circ \text{prox}_f.$$

It is well-known in the literature that obtaining a theoretical formula for  $\text{prox}_{f+g}$  is not an easy task in general, even if  $\text{prox}_f$  and  $\text{prox}_g$  are known. In our article [6], we give a more precise description of the difficulty to obtain an easy computable formula of  $\text{prox}_{f+g}$  by proving that there is no closed formula, independent of  $f$  and  $g$ , allowing to write  $\text{prox}_{f+g}$  as a linear combination of compositions of linear combinations of  $\text{I}$ ,  $\text{prox}_f$ ,  $\text{prox}_g$ ,  $\text{prox}_f^{-1}$  and  $\text{prox}_g^{-1}$ . In the decomposition formula (V.2.2), it should be noted that the difficulty of computing  $\text{prox}_{f+g}$  is only transferred to the computation of  $\text{prox}_g^f$  which is not an easier task. Note that other rewritings, which are not suitable for an easy computation of  $\text{prox}_{f+g}$  neither, can be considered such as

$$\text{prox}_{f+g} = (\text{prox}_f^{-1} + \text{prox}_g^{-1} - \text{I})^{-1} = (\text{prox}_{2f}^{-1} + \text{prox}_{2g}^{-1})^{-1} \circ 2\text{I},$$

the second equality being provided in [37, Corollary 25.35 p.458]. However our decomposition formula (V.2.2) is of theoretical interest in order to prove in a concise and elegant way almost all other new statements of this chapter, and also to recover in a simple way some well-known results making it central in our work. We provide an illustration of this feature in the next section about the classical Douglas-Rachford algorithm. Moreover, as explained above, we also prove the usefulness of the decomposition formula (V.2.2) in the context of sensitivity analysis of the variational inequality (V.0.1).

## V.2.2 Relationship with the classical Douglas-Rachford operator

Recall that the proximal operator  $\text{prox}_{f+g}$  is strongly related to the minimization problem

$$\operatorname{argmin} f + g,$$

since the set of solutions is exactly the set of fixed points of  $\text{prox}_{f+g}$  denoted by  $\text{Fix}(\text{prox}_{f+g})$ . In the sequel, we assume that the above minimization problem admits at least one solution. The classical *Douglas-Rachford operator*  $\mathcal{DR}_{f,g} : \mathbb{H} \rightarrow \mathbb{H}$  associated to  $f$  and  $g$ , introduced in [122], is usually defined by

$$\mathcal{DR}_{f,g}(y) := y - \text{prox}_f(y) + \text{prox}_g(2\text{prox}_f(y) - y),$$

for all  $y \in \mathbb{H}$ . We refer for instance to [37, Section 28.3 p.517] where details can be found on this classical operator. This operator provides an algorithm  $x_{n+1} = \mathcal{DR}_{f,g}(x_n)$  that is weakly convergent to some  $x^* \in \mathbb{H}$  satisfying

$$\text{prox}_f(x^*) \in \operatorname{argmin} f + g.$$

Even if the *Douglas-Rachford algorithm* is not a *proximal point algorithm* in general, in the sense that  $\mathcal{DR}_{f,g}$  is not equal to  $\text{prox}_\varphi$  for some  $\varphi \in \Gamma_0(\mathbb{H})$  in general, it is a very powerful tool since it allows to solve the above minimization problem, requiring only the knowledge of  $\text{prox}_f$  and  $\text{prox}_g$  (see, e.g., [37, Section 28.3 p.517] for more details).

We underline here the relations between the  $f$ -proximal operator  $\text{prox}_g^f$  and the Douglas-Rachford operator  $\mathcal{DR}_{f,g}$ . For this purpose, we introduce an extension  $\overline{\mathcal{DR}}_{f,g} : \mathbb{H} \times \mathbb{H} \rightarrow \mathbb{H}$  of the classical Douglas-Rachford operator defined by

$$\overline{\mathcal{DR}}_{f,g}(x, y) := y - \text{prox}_f(y) + \text{prox}_g(x + \text{prox}_f(y) - y),$$

for all  $x, y \in \mathbb{H}$ .

Note that  $\mathcal{DR}_{f,g}(y) = \overline{\mathcal{DR}}_{f,g}(\text{prox}_f(y), y)$  for all  $y \in \mathbb{H}$ , and that the definition of  $\overline{\mathcal{DR}}_{f,g}$  only depends on the knowledge of  $\text{prox}_f$  and  $\text{prox}_g$ .

Then we prove that

$$\text{prox}_g^f(x) = \text{Fix}(\overline{\mathcal{DR}}_{f,g}(x, \cdot)),$$

for all  $x \in \mathbb{H}$ . More precisely we have the following proposition.

**Proposition V.2.11.** *Let  $f, g \in \Gamma_0(\mathbb{H})$ . It holds that*

$$\text{prox}_g^f(x) = \text{Sol}_{\text{VI}}(\text{prox}_f, g^* \circ L_x) = \operatorname{argmin} (M_{f^*} + g^* \circ L_x) = \text{Fix}(\overline{\mathcal{DR}}_{f,g}(x, \cdot)),$$

for all  $x \in \mathbb{H}$ , where  $\text{Sol}_{\text{VI}}$  denotes the set of solutions of  $\text{VI}(A, g)$  given by (V.1.1) with  $A = \text{prox}_f$  and  $g = g^* \circ L_x$ .

Let us now show that the above statements, especially the decomposition formula (V.2.2), allow to recover in a concise way the well-known inclusion

$$\text{prox}_f(\text{Fix}(\mathcal{DR}_{f,g})) \subset \operatorname{argmin} f + g = \text{Fix}(\text{prox}_{f+g}). \quad (\text{V.2.3})$$

Indeed, if  $x^* \in \text{Fix}(\mathcal{DR}_{f,g})$ , then  $x^* \in \text{Fix}(\overline{\mathcal{DR}}_{f,g}(\text{prox}_f(x^*), \cdot)) = \text{prox}_g^f(\text{prox}_f(x^*))$ . From the decomposition formula (V.2.2), we conclude that

$$\text{prox}_f(x^*) = \text{prox}_f \circ \text{prox}_g^f(\text{prox}_f(x^*)) = \text{prox}_{f+g}(\text{prox}_f(x^*)).$$

This proof of only few lines is an illustration of the theoretical interest of the decomposition formula (V.2.2). Note that the above inclusion (V.2.3) is, as well-known, an equality.

Finally the  $f$ -proximal operator  $\text{prox}_g^f$  is also of interest from a numerical point of view. Indeed we have the following convergence result for the fixed-point algorithm  $y_{k+1} = \overline{\mathcal{DR}}_{f,g}(x, y_k)$ .

**Theorem V.2.12.** *Let  $f, g \in \Gamma_0(\mathbb{H})$  and let  $x \in \text{D}(\text{prox}_g^f)$  be fixed. Then Algorithm  $(\mathcal{A}_1)$  given by*

$$\begin{cases} y_0 \in \mathbb{H}, \\ y_{k+1} = \overline{\mathcal{DR}}_{f,g}(x, y_k), \end{cases} \quad (\mathcal{A}_1)$$

*weakly converges to an element  $y^* \in \text{prox}_g^f(x)$ . Moreover, if the conditions  $\text{dom}(f) \cap \text{dom}(g) \neq \emptyset$  and  $\partial(f+g) = \partial f + \partial g$  are satisfied, it holds that  $\text{prox}_f(y^*) = \text{prox}_{f+g}(x)$ .*

We conclude that Algorithm  $(\mathcal{A}_1)$  allows to compute numerically  $\text{prox}_{f+g}(x)$  with the only knowledge of  $\text{prox}_f$  and  $\text{prox}_g$ . It turns out that Algorithm  $(\mathcal{A}_1)$  was already considered, up to some translations, and implemented in previous works (see, e.g., the so-called *dual forward-backward splitting* in [103, Algorithm 3.5]), showing that the  $f$ -proximal operator  $\text{prox}_g^f$  is already present (in a hidden form) and useful for numerical purposes in the existing literature. However, to the best of my knowledge, it has never been explicitly expressed in a closed formula such as (V.2.1) and neither been deeply studied from a theoretical point of view. This contribution aims at filling this gap in the literature.

**Remark V.2.13.** *Let  $f, g \in \Gamma_0(\mathbb{H})$  and let  $x \in \text{D}(\text{prox}_g^f)$ . Algorithm  $(\mathcal{A}_1)$  consists in a fixed-point algorithm from the characterization given in Proposition V.2.11 by*

$$\text{prox}_g^f(x) = \text{Fix}(\overline{\mathcal{DR}}_{f,g}(x, \cdot)).$$

*Actually, one can see that Algorithm  $(\mathcal{A}_1)$  also coincides with the well-known Forward-Backward algorithm (see [104, Section 10.3 p.191] for details) from the characterization given in Proposition V.2.11 by*

$$\text{prox}_g^f(x) = \text{argmin}(\text{M}_{f^*} + g^* \circ L_x).$$

*Indeed we recall that  $\text{M}_{f^*}$  is differentiable with  $\nabla \text{M}_{f^*} = \text{prox}_f$ .*

## V.3 Conclusion

### V.3.1 Application to sensitivity analysis

Let us come back to our initial motivation, namely the sensitivity analysis, with respect to a nonnegative parameter  $t \geq 0$ , of some parametrized linear variational inequalities of second kind in a real Hilbert space  $\mathbb{H}$ . More precisely, for all  $t \geq 0$ , we consider the variational inequality which consists of finding  $u(t) \in \text{K}$  such that

$$\langle u(t), z - u(t) \rangle + g(z) - g(u(t)) \geq \langle r(t), z - u(t) \rangle,$$

for all  $z \in \text{K}$ , where  $\text{K} \subset \mathbb{H}$  is a non-empty closed and convex set of constraints, and where  $g \in \Gamma_0(\mathbb{H})$  and  $r : \mathbb{R}^+ \rightarrow \mathbb{H}$  are assumed to be given and smooth enough. The above problem admits a unique solution given by

$$u(t) = \text{prox}_{f+g}(r(t)),$$

where  $f = \iota_K$  is the indicator function of  $K$ .

Our aim is to provide from Theorem V.2.6 a simple and compact formula for the derivative  $u'(0)$ . Following the idea of Mignot in [182] (see also [148, Theorem 2 p.620]), we first introduce the following sets

$$\begin{aligned} O_v &:= \{w \in H \mid \exists \lambda > 0, \text{proj}_K(v) + \lambda w \in K\} \cap [v - \text{proj}_K(v)]^\perp, \\ C_v &:= \text{cl}\left(\{w \in H \mid \exists \lambda > 0, \text{proj}_K(v) + \lambda w \in K\}\right) \cap [v - \text{proj}_K(v)]^\perp, \end{aligned}$$

for all  $v \in H$ , where  $\perp$  denotes the classical orthogonal of a set. Then we prove the following result.

**Proposition V.3.1.** *Let  $v(t) := r(t) - \nabla g(u(t))$  for all  $t \in \mathbb{R}$ . If the following conditions are satisfied:*

- (i)  $r$  is differentiable at  $t = 0$ ;
- (ii)  $g$  is twice differentiable on  $H$ ;
- (iii)  $O_{v(0)}$  is dense in  $C_{v(0)}$ ;
- (iv)  $u$  is differentiable at  $t = 0$ ;

then the derivative  $u'(0)$  is given by

$$u'(0) = \text{prox}_{\varphi_f + \psi_g}(r'(0)),$$

where  $\varphi_f := \iota_{C_{v(0)}}$  and  $\psi_g(x) := \frac{1}{2} \langle D^2 g(u(0))(x), x \rangle$  for all  $x \in H$ .

**Remark V.3.2.** *Proposition V.3.1 provides an expression of  $u'(0)$  in terms of the proximal operator of a sum of two proper, lower semicontinuous and convex functions. Hence it could be numerically computed from Algorithm  $(\mathcal{A}_1)$ , requiring the knowledge of  $\text{proj}_{C_{v(0)}}$  and  $\text{prox}_{\psi_g}$ .*

The relaxations in special frameworks of the assumptions of Proposition V.3.1 should be the subject of future works. Particularly it would be relevant to provide sufficient conditions ensuring that  $u$  is differentiable at  $t = 0$ . A promising idea in this sense is to invoke the concepts of *twice epi-differentiability* and *proto-differentiability* introduced by Rockafellar in [193, 194].

### V.3.2 Perspectives

As mentioned in the introduction of this chapter, our original aim is to contribute to the shape optimization theory under unilateral constraints. To do this, we could begin by considering one of the most standard model in contact mechanics which is the so-called *Tresca friction problem* given by the following PDE system:

$$\begin{cases} -\Delta u + u = f, & \text{in } \Omega, \\ |\partial_n u| \leq g, \partial_n u = -g \frac{u}{|u|} \text{ if } u \neq 0, & \text{on } \partial\Omega, \end{cases}$$

where  $f, g : \mathbb{R}^d \rightarrow \mathbb{R}$  are given functions, corresponding respectively to external forces and nonnegative friction threshold. This model is a simplified, scalar counterpart of the more realistic setting of contact mechanics in elasticity. The above classical problem involves non-smooth boundary conditions; in terms of variational framework, these translate into the variational inequality:

$$\int_{\Omega} \nabla u \cdot \nabla(\varphi - u) + \int_{\Omega} u(\varphi - u) + \int_{\partial\Omega} g|\varphi| - \int_{\partial\Omega} g|u| \geq \int_{\Omega} f(\varphi - u), \quad (\text{V.3.1})$$

for all  $\varphi : \Omega \rightarrow \mathbb{R}$ . Using classical results of convex analysis, this variational inequality turns out to have a unique solution denoted by  $u_{\Omega}$ .

The shape sensitivity analysis of solutions to (both linear and nonlinear) variational equalities has been extensively studied by several authors (see, e.g., the book [152]). However the literature about

the shape sensitivity analysis of solutions to variational inequalities still matures and is promising [50, 121, 134], with various remaining theoretical challenges. Most investigations on this topic are based on regularization techniques: the non-smoothness  $|\varphi|$  in (V.3.1) is approximated by a smooth, penalized counterpart. At the opposite, we expect to develop a new approach based on technical tools of non-smooth analysis in order to derive the existence and an explicit formulation of the shape derivative of  $u_\Omega$  with respect to small perturbations of the domain  $\Omega$ . A first step towards fulfilling this objective is to express  $u_\Omega$  as  $u_\Omega = \text{prox}_j(v_\Omega)$ , where  $v_\Omega$  is the unique solution to the variational equality

$$\int_{\Omega} \nabla v \cdot \nabla \varphi + \int_{\Omega} v \varphi = \int_{\Omega} f \varphi,$$

for all test functions  $\varphi : \Omega \rightarrow \mathbb{R}$ , where  $j$  is the non-smooth functional defined by

$$j(\varphi) := \int_{\partial\Omega} g|\varphi|.$$

Since the shape differentiability of  $v_\Omega$  is well-known in the literature, we deduce that the existence of the shape derivative of  $u_\Omega$  is strongly related to the regularity of the proximity operator  $\text{prox}_j$ . Then we could use the notion of twice epi-differentiability and proto-differentiability (see [193, 194]): these notions from non-smooth analysis allow to derive asymptotic developments of proximity operators. However note that the classical techniques of shape sensitivity analysis would involve a parametrized perturbation  $j_t$  of the functional  $j$ . Nevertheless we do believe that this difficulty can be overcome by using the recent work of Adly *et al.* in [5] where the notions introduced by Rockafellar have been extended in order to handle parametrized functionals  $j_t$ .

Then the expression of the shape derivative of  $u_\Omega$  resulting from the above approach will make it possible to compute explicitly the shape gradient of cost functionals of the domain in view of the numerical resolution of some shape optimization problems involving contact friction.



---

---

# Chapter VI

---

## Optimal location of resources in population dynamics

This last chapter is a little bit independent of others but we give a brief presentation of this work due to its application and its perspectives. This chapter summarizes the following article in collaboration with Thibaut Dehevels (École Normale Supérieure de Rennes) and Yannick Privat (University of Strasbourg), published in *SIAM Journal of Applied Mathematics* (28 pages):

- [91] F. Caubet, T. Dehevels and Y. Privat. Optimal location of resources for biased movement of species: the 1D case. *SIAM J. Appl. Math.*, 77(6):1876–1903, 2017.

*The aim of this work is to investigate an optimal design problem motivated by some issues arising in population dynamics. In a nutshell, we aim at determining the optimal shape of a region occupied by resources for maximizing the survival ability of a species in a given box and we consider the general case of Robin boundary conditions on its boundary.* Mathematically, this issue can be modeled with the help of an extremal indefinite weight linear eigenvalue problem. The optimal spatial arrangement is obtained by minimizing the positive principal eigenvalue with respect to the weight, under a  $L^1$  constraint standing for limitation of the total amount of resources. The specificity of such a problem lays upon the presence of nonlinear functions of the weight both in the numerator and denominator of the Rayleigh quotient. By using suitable rearrangement procedures, an adapted change of variable, as well as necessary optimality conditions, we completely solve this optimization problem in the unidimensional case by showing first that every minimizer is unimodal and *bang-bang*. This leads to investigate a finite dimensional optimization problem. This allows to show especially that every minimizer is (up to additive constants) the characteristic function of three possible domains: an interval that sticks on the boundary of the box, an interval that is symmetrically located at the middle of the box, or, for a precise value of the Robin coefficient, all intervals of a given fixed length

This work can be seen as an extension of the previous works of Laurain *et al.* [155, 167] adding an advection term in the considered equation. Notice that, additionally to the advection term, the general Robin boundary conditions also lead to mathematical difficulties in the resolution of the problem.

### VI.1 The biological model and the state of the art

#### VI.1.1 The biological model

In this chapter we consider a reaction-diffusion model for population dynamics. We assume that the environment is spatially heterogeneous and present both favorable and unfavorable regions. More

specifically we assume that the intrinsic growth rate of the population is spatially dependent. Such models have been introduced in the pioneering work of Skellam [208], see also [76, 77] and references therein. We also assume that the population tends to move toward the favorable regions of the habitat, that is, we add to the model an advection term (or drift) along the gradient of the habitat quality. This model has been introduced by Belgacem and Cosner in [39].

Precisely we assume that the flux of the population density  $u(\mathbf{x}, t)$  is of the form  $-\nabla u + \alpha u \nabla m$ , where  $m$  represents the growth rate of the population, and will be assumed to be bounded and to change sign. From a biological point of view, the function  $m$  can be seen as a measure of the access to resources at a location  $\mathbf{x}$  of the habitat. The nonnegative constant  $\alpha$  measures the rate at which the population moves up the gradient of the growth rate  $m$ . With a slight abuse of language, we will also say that  $m(\mathbf{x})$  stands for the local rate of resources or simply the resources at location  $\mathbf{x}$ .

This leads to the following diffusive-logistic equation

$$\begin{cases} \partial_t u = \operatorname{div}(\nabla u - \alpha u \nabla m) + \lambda u(m - u) & \text{in } \Omega \times (0, \infty), \\ e^{\alpha m}(\partial_n u - \alpha u \partial_n m) + \beta u = 0 & \text{on } \partial\Omega \times (0, \infty), \end{cases} \quad (\text{VI.1.1})$$

where  $\Omega$  is a bounded region of  $\mathbb{R}^d$  (with  $d = 1, 2, 3$ ) which represents the habitat,  $\beta \geq 0$ , and  $\lambda$  is a positive constant. The case  $\beta = 0$  in (VI.1.1) corresponds to the no-flux boundary condition: the boundary acts as a barrier for the population. The Dirichlet case, where the boundary condition on  $\partial\Omega$  is replaced by  $u = 0$ , corresponds to the case when the boundary is lethal to the population, and can be seen as the limit case when  $\beta \rightarrow \infty$ . The choice  $0 < \beta < \infty$  corresponds to the case where a part of the population dies when reaching the boundary, while a part of the population turns back.

Plugging the change of function  $v = e^{-\alpha m} u$  into Problem (VI.1.1) yields to

$$\begin{cases} \partial_t v = \Delta v + \alpha \nabla v \cdot \nabla m + \lambda v(m - e^{\alpha m} v) & \text{in } \Omega \times (0, \infty), \\ e^{\alpha m} \partial_n v + \beta v = 0 & \text{on } \partial\Omega \times (0, \infty). \end{cases} \quad (\text{VI.1.2})$$

The relation  $v = e^{-\alpha m} u$  ensures that the behavior of models (VI.1.1) and (VI.1.2) in terms of growth, extinction or equilibrium is the same. Therefore we only deal with Problem (VI.1.2) in the following.

It would be natural *a priori* to consider weights  $m$  belonging to  $L^\infty(\Omega)$  without assuming additional regularity assumption. Nevertheless, for technical reasons that will be made clear in the following, we will temporarily assume that  $m \in C^2(\overline{\Omega})$ . Moreover we also make the following additional assumptions on the weight  $m$ , motivated by biological reasons. Given  $m_0 \in (0, 1)$  and  $\kappa > 0$ , we consider that

- the total resources in the heterogeneous environment are limited:

$$\int_{\Omega} m \leq -m_0 |\Omega|, \quad (\text{VI.1.3})$$

- $m$  is a bounded measurable function which changes sign in  $\Omega$ , i.e.

$$|\{\mathbf{x} \in \Omega, m(\mathbf{x}) > 0\}| > 0, \quad (\text{VI.1.4})$$

and using an easy renormalization argument leads to assume that

$$-1 \leq m \leq \kappa \quad \text{a.e. in } \Omega. \quad (\text{VI.1.5})$$

Observe that the combination of (VI.1.3) and (VI.1.4) guarantees that the weight  $m$  changes sign in  $\Omega$ .

In the following we introduce and investigate an optimization problem in which roughly speaking, we look at configurations of resources maximizing the survival ability of the population. The main unknown is the weight  $m$  and for this reason, it is convenient to introduce the set of admissible weights:

$$\mathcal{M}_{m_0, \kappa} := \{m \in L^\infty(\Omega), m \text{ satisfies assumptions (VI.1.3), (VI.1.4) and (VI.1.5)}\}. \quad (\text{VI.1.6})$$

### VI.1.2 A principal eigenvalue problem with indefinite weight

It is well known that the behavior of Problem (VI.1.2) can be predicted from the study of the following eigenvalue problem with indefinite weight (see [39, 76, 153])

$$\begin{cases} -\Delta\varphi - \alpha\nabla m \cdot \nabla\varphi = \Lambda m\varphi & \text{in } \Omega, \\ e^{\alpha m}\partial_n\varphi + \beta\varphi = 0 & \text{on } \partial\Omega, \end{cases} \quad (\text{VI.1.7})$$

which also rewrites

$$\begin{cases} -\operatorname{div}(e^{\alpha m}\nabla\varphi) = \Lambda m e^{\alpha m}\varphi & \text{in } \Omega, \\ e^{\alpha m}\partial_n\varphi + \beta\varphi = 0 & \text{on } \partial\Omega. \end{cases} \quad (\text{VI.1.8})$$

Recall that an eigenvalue  $\Lambda$  of Problem (VI.1.8) is said to be a principal eigenvalue if  $\Lambda$  has a positive eigenfunction. Using the same arguments as in [9, 154], the following proposition can be proved.

**Proposition VI.1.1.** *1. In the case of Dirichlet boundary condition, there exists a unique positive principal eigenvalue denoted  $\lambda_1^\infty(m)$ , which is characterized by*

$$\lambda_1^\infty(m) = \inf_{\varphi \in \mathcal{S}_0} \frac{\int_{\Omega} e^{\alpha m} |\nabla\varphi|^2}{\int_{\Omega} m e^{\alpha m} \varphi^2},$$

where  $\mathcal{S}_0 = \{\varphi \in H_0^1(\Omega), \int_{\Omega} m e^{\alpha m} \varphi^2 > 0\}$ .

*2. In the case of Robin boundary condition with  $\beta > 0$ , the situation is similar to the Dirichlet case, and  $\lambda_1^\beta(m)$  is characterized by*

$$\lambda_1^\beta(m) = \inf_{\varphi \in \mathcal{S}} \frac{\int_{\Omega} e^{\alpha m} |\nabla\varphi|^2 + \beta \int_{\partial\Omega} \varphi^2}{\int_{\Omega} m e^{\alpha m} \varphi^2}, \quad (\text{VI.1.9})$$

where  $\mathcal{S} = \{\varphi \in H^1(\Omega), \int_{\Omega} m e^{\alpha m} \varphi^2 > 0\}$ .

*3. In the case of Neumann boundary condition ( $\beta = 0$ ),*

- *if  $\int_{\Omega} m e^{\alpha m} < 0$ , then the situation is similar as the Robin case, and  $\lambda_1^\beta(m) > 0$  is given by (VI.1.9) with  $\beta = 0$ ,*
- *if  $\int_{\Omega} m e^{\alpha m} \geq 0$ , then  $\lambda_1^\beta(m) = 0$  is the only non-negative principal eigenvalue.*

**Remark VI.1.2.** *According to the existing literature (see e.g. [39]), the existence of  $\lambda_1^\beta(m)$  defined as the principal eigenvalue of Problem (VI.1.8) for  $C^2$  weights follows from the Krein Rutman theory. Nevertheless one can extend the definition of  $\lambda_1^\beta(m)$  to a larger class of weights by using Rayleigh quotients, as done in Proposition VI.1.1.*

Following [154, Theorem 28.1] (applied in the special case where the operator coefficients are periodic with an arbitrary period), one has the following time asymptotic behavior characterization of the solution of the logistic equation (VI.1.2):

- *if  $\lambda > \lambda_1^\beta(m)$ , then (VI.1.2) has a unique positive equilibrium, which is globally attracting among non-zero non-negative solutions;*
- *if  $\lambda_1^\beta(m) > 0$  and  $0 < \lambda < \lambda_1^\beta(m)$ , then all non-negative solutions of (VI.1.2) converge to zero as  $t \rightarrow \infty$ .*

From a biological point of view, the above characterization yields a criterion for extinction or persistence of the species.

A consequence is that the smaller  $\lambda_1^\beta(m)$  is, the more likely the population will survive. This biological consideration led Cantrell *et al.* to raise the question of finding  $m$  such that  $\lambda_1^\beta(m)$  is minimized, see [76, 77]. This problem writes

$$\inf_{m \in \mathcal{M}_{m_0, \kappa}} \lambda_1^\beta(m), \quad (\text{VI.1.10})$$

or respectively

$$\inf_{m \in \mathcal{M}_{m_0, \kappa}} \lambda_1^\infty(m).$$

in the case of Dirichlet conditions.

Biologically this corresponds to finding the optimal arrangement of favorable and unfavorable regions in the habitat so the population can survive.

**Remark VI.1.3.** *It is notable that, in the Neumann case ( $\beta = 0$ ), if we replace Assumption (VI.1.3) with  $\int_\Omega m \geq 0$  in the definition of  $\mathcal{M}_{m_0, \kappa}$ , then  $\lambda_1^0(m) = 0$  for every  $m \in \mathcal{M}_{m_0, \kappa}$ . Biologically this means that any choice of distribution of the resources will ensure the survival of the population.*

### VI.1.3 State of the art

**Analysis of the biological model (with an advection term).** Problem (VI.1.2) was introduced in [39], and studied particularly in [39, 106], where the question of the effect of adding the drift term is raised. The authors investigate if increasing  $\alpha$ , starting from  $\alpha = 0$ , has a beneficial or harmful impact on the population, in the sense that it decreases or increases the principal eigenvalue of Problem (VI.1.8).

It turns out that the answer depends critically on the condition imposed on the boundary of the habitat. Under Dirichlet boundary conditions, adding the advection term can be either favorable or detrimental to the population, see [39]. This can be explained by the fact that if the favorable regions in the habitat are located near the hostile boundary, this could result in harming the population. In contrast, under no-flux boundary conditions, it is proved in [39] that a sufficiently fast movement up the gradient of the resources is always beneficial. Also, according to [106], if we start with no drift ( $\alpha = 0$ ), adding the advection term is always beneficial if the habitat is convex. The authors however provide examples of non-convex habitats such that introducing advection up the gradient of  $m$  is harmful to the population.

**Optimal design issues.** The study of extremal eigenvalue problems with indefinite weights like Problem (VI.1.10), with slight variations on the parameter choices (typically  $\alpha = 0$  or  $\alpha > 0$ ) and with different boundary conditions (in general Dirichlet, Neumann or Robin ones) is a long-standing question in calculus of variations. In the survey [151, Chapter 9], results of existence and qualitative properties of optimizers when dealing with non-negative weights are gathered.

In the survey article [175], the biological motivations for investigating extremal problems for principal eigenvalue with sign-changing weights are recalled, as well as the first existence and analysis properties of such problems, mainly in the 1D case.

A wide literature has been devoted to Problem (VI.1.7) (or close variants) without the drift term, i.e. with  $\alpha = 0$ . Monotonicity properties of eigenvalues and *bang-bang* properties of minimizers<sup>1</sup> were established in [9], [176] and [160] for Neumann boundary conditions ( $\beta = 0$ ) in the 1D case. In [195], the same kind of results were obtained for periodic boundary conditions. We also mention [116], for an extension of these results to principal eigenvalues associated to the one dimensional  $p$ -Laplacian operator.

In this work, we investigate a similar optimal design problem for a more general model in which a drift term with Robin boundary conditions is considered. In the simpler case where no advection term was included in the population dynamics equation, a fine study of the optimal design problem [155, 167] allowed to emphasize existence properties of *bang-bang* minimizers, as well as several geometrical properties they satisfy. Concerning now the drift case model with Dirichlet or Neumann boundary conditions, the existence of principal eigenvalues and the characterization of survival ability of the

---

1. It means that the  $L^\infty$  constraints on the unknown  $m$  are saturated a.e. in  $\Omega$ , in other words that every optimizer  $m^*$  satisfies  $m^*(x) \in \{-1, \kappa\}$  a.e. in  $\Omega$ .

population in terms of such eigenvalues has been performed in [39, 106]. However and up to my knowledge, nothing was known about the related optimal design problem (VI.1.10) or any variant.

## VI.2 Modeling of the optimal design problem and main results

### VI.2.1 Modeling

From now on, we focus on the 1D case  $d = 1$ . Hence, for sake of simplicity, we consider that

$$\Omega := (0, 1).$$

If  $\omega$  is a subset of  $(0, 1)$ , we denote by  $\chi_\omega$  the *characteristic function* of  $\omega$ , that is  $\chi_\omega(x) = 1$  if  $x \in \omega$  and  $\chi_\omega(x) = 0$  if not.

As mentioned previously (see Section VI.1.1), we aim at finding the optimal  $m$  (whenever it exists) which minimizes the positive principal eigenvalue  $\lambda_1^\beta(m)$  of Problem (VI.1.8). For technical reasons, most of the results concerning the qualitative analysis of System (VI.1.2) (especially the persistence/survival ability of the population as  $t \rightarrow +\infty$ , the characterization of the principal eigenvalue  $\lambda_1^\beta(m)$ , and so on) are established by considering smooth weights, say  $\mathcal{C}^2$ . The following theorem emphasizes the link between the problem of minimizing  $\lambda_1^\beta(m)$  over the class  $\mathcal{M}_{m_0, \kappa} \cap \mathcal{C}^2(\overline{\Omega})$  and a relaxed one, where one aims at minimizing  $\lambda_1^\beta$  over the larger class  $\mathcal{M}_{m_0, \kappa}$ .

**Theorem VI.2.1.** *When  $\alpha$  is sufficiently small, the infimum  $\inf \left\{ \lambda_1^\beta(m), m \in \mathcal{M}_{m_0, \kappa} \cap \mathcal{C}^2(\overline{\Omega}) \right\}$  is not attained for any  $m \in \mathcal{M}_{m_0, \kappa} \cap \mathcal{C}^2(\overline{\Omega})$ . Moreover, one has*

$$\inf_{m \in \mathcal{M}_{m_0, \kappa} \cap \mathcal{C}^2(\overline{\Omega})} \lambda_1^\beta(m) = \min_{m \in \mathcal{M}_{m_0, \kappa}} \lambda_1^\beta(m),$$

and every minimizer  $m^*$  of  $\lambda_1^\beta$  over  $\mathcal{M}_{m_0, \kappa}$  is a bang-bang function, i.e. can be represented as  $m^* = \kappa \chi_E - \chi_{\Omega \setminus E}$ , where  $E \subset \Omega$  is a measurable set.

As a consequence, we consider the following optimal design problem. Fix  $\beta \in [0, \infty]$ . We consider the extremal eigenvalue problem

$$\lambda_*^\beta = \inf \left\{ \lambda_1^\beta(m), m \in \mathcal{M}_{m_0, \kappa} \right\}, \quad (\text{VI.2.1})$$

where  $\mathcal{M}_{m_0, \kappa}$  is defined by (VI.1.6) and where  $\lambda_1^\beta(m)$  is the positive principal eigenvalue of

$$\begin{cases} -(e^{\alpha m} \varphi')' = \lambda m e^{\alpha m} \varphi & \text{in } (0, 1), \\ e^{\alpha m(0)} \varphi'(0) = \beta \varphi(0), \quad e^{\alpha m(1)} \varphi'(1) = -\beta \varphi(1). \end{cases} \quad (\text{VI.2.2})$$

Problem (VI.2.2) above is understood in a weak sense, that is, in the sense of the variational formulation:

$$\begin{aligned} & \text{Find } \varphi \in \mathbf{H}^1(0, 1) \text{ such that for all } \psi \in \mathbf{H}^1(0, 1), \\ & \int_0^1 e^{\alpha m} \varphi' \psi' + \beta(\varphi(0)\psi(0) + \varphi(1)\psi(1)) = \lambda_1^\beta(m) \int_0^1 m e^{\alpha m} \varphi \psi. \end{aligned}$$

## VI.2.2 Solving of the optimal design problem

Let us first provide a brief summary of the main results of this work which concern the resolution of the optimal design problem (VI.2.1).

In a nutshell, we prove that under an additional smallness assumption on the non-negative parameter  $\alpha$ , the problem of minimizing  $\lambda_1^\beta(\cdot)$  over  $\mathcal{M}_{m_0, \kappa}$  has a solution writing

$$m^* = \kappa \chi_{E^*} - \chi_{\Omega \setminus E^*}, \quad (\text{VI.2.3})$$

where  $E^*$  is (up to a zero Lebesgue measure set) an interval. Moreover one has the following alternative: except for one critical value of the parameter  $\beta$  denoted  $\beta_{\alpha, \delta}$ , either  $E^*$  is stuck to the boundary, or  $E^*$  is centered at the middle point of  $\Omega$ . More precisely there exists  $\delta \in (0, 1)$  such that:

- for Neumann boundary conditions, one has  $E^* = (0, \delta)$  or  $E^* = (1 - \delta, 1)$ ;
- for Dirichlet boundary conditions, one has  $E^* = ((1 - \delta)/2, (1 + \delta)/2)$ ;
- for Robin boundary conditions, there exists a threshold  $\beta_{\alpha, \delta} > 0$  such that, if  $\beta < \beta_{\alpha, \delta}$  then the situation is similar to the Neumann case, whereas if  $\beta > \beta_{\alpha, \delta}$  the situation is similar to the Dirichlet case.

Figure VI.2.1 illustrates different profiles of minimizers. The limit case  $\beta = \beta_{\alpha, \delta}$  is a bit more intricate. For a more precise statement of these results, we refer to Theorems VI.2.5, VI.2.6 and VI.2.8 below.

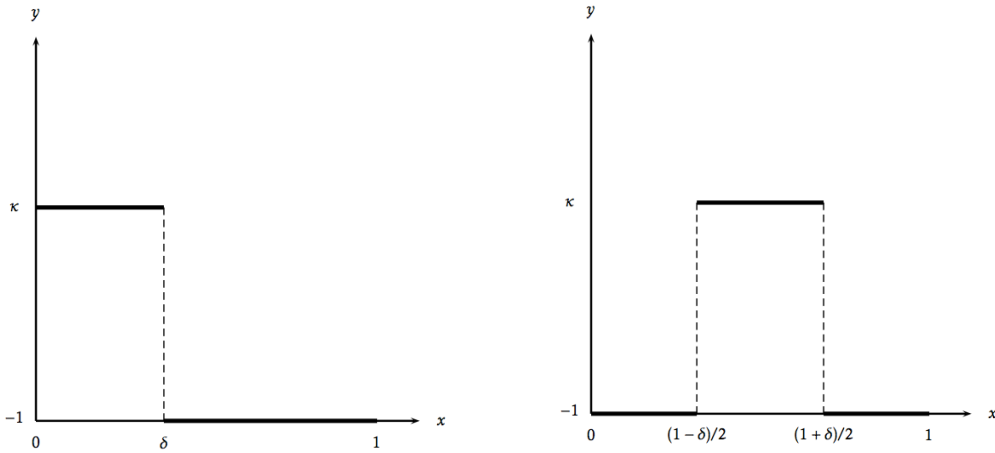


**Figure VI.2.1** – Graph of a minimizer for small  $\beta$  (left) and graph of the unique minimizer for large  $\beta$  (right).

We will say that a solution  $m_*^\beta$  (whenever it exists) of Problem (VI.2.1) is of *Dirichlet type* if  $m_*^\beta = (\kappa + 1)\chi_{((1-\delta)/2, (1+\delta)/2)} - 1$  for some parameter  $\delta > 0$ . We first investigate the Neumann and Robin cases. The Dirichlet case is a byproduct of our results on the Robin problem.

**Neumann boundary conditions.** In the limit case where Neumann boundary conditions are imposed (i.e.  $\beta = 0$ ), we have the following characterization of persistence, resulting from the Neumann case in Proposition VI.1.1 (see [106]).

**Proposition VI.2.2.** *Let  $m \in \mathcal{M}_{m_0, \kappa}$ . There exists a unique  $\alpha^*(m) > 0$  such that*

- if  $\alpha < \alpha^*(m)$ , then  $\int_0^1 m e^{\alpha m} < 0$  and  $\lambda_1^0(m) > 0$ ,
- if  $\alpha \geq \alpha^*(m)$ , then  $\int_0^1 m e^{\alpha m} \geq 0$  and  $\lambda_1^0(m) = 0$ .

## VI.2 Modeling of the optimal design problem and main results

As a consequence, in order to analyze the optimal design problem (VI.2.1) which minimizes the positive principal eigenvalue  $\lambda_1^\beta(m)$ , it is relevant to consider (at least for the Neumann boundary conditions)  $\alpha$  uniformly small with respect to  $m$ . This is the purpose of the following theorem.

**Theorem VI.2.3** (Neumann case). *The infimum*

$$\bar{\alpha} = \inf_{m \in \mathcal{M}_{m_0, \kappa}} \alpha^*(m)$$

is attained at every function  $m_* \in \mathcal{M}_{m_0, \kappa}$  having the bang-bang property and such that  $\int_\Omega m_* = -m_0$ . In other words, the infimum is attained at every  $m_* \in \mathcal{M}_{m_0, \kappa}$  which can be represented as  $m_* = \kappa \chi_E - \chi_{\Omega \setminus E}$ , where  $E$  is a measurable subset of  $\Omega$  of measure  $(1 - m_0)/(\kappa + 1)$ . Moreover, one computes  $\bar{\alpha} = \frac{1}{1+\kappa} \ln \left( \frac{\kappa + m_0}{\kappa(1 - m_0)} \right) > 0$ .

**Remark VI.2.4.** A consequence of the combination of Theorem VI.2.3 and Proposition VI.1.1 is that  $\int_\Omega m e^{\alpha m} < 0$  for every  $m \in \mathcal{M}_{m_0, \kappa}$  whenever  $\alpha < \bar{\alpha}$ .

**Theorem VI.2.5** (Neumann case). *Let  $\beta = 0$  and  $\alpha \in [0, \bar{\alpha}]$ . The optimal design problem (VI.2.1) has a solution.*

If one assumes moreover that  $\alpha \in [0, \min\{1/2, \bar{\alpha}\}]$ , then the inequality constraint (VI.1.3) is active, and the only solutions of Problem (VI.2.1) are  $m = (\kappa + 1)\chi_{(0, \delta^*)} - 1$  and  $m = (\kappa + 1)\chi_{(1 - \delta^*, 1)} - 1$ , where  $\delta^* := \frac{1 - m_0}{1 + \kappa}$ .

**Robin boundary conditions.** The next result is devoted to the investigation of the Robin boundary conditions case, for an intermediate value of  $\beta$  in  $(0, +\infty)$ . For that purpose, let us introduce the positive real number  $\beta_{\alpha, \delta}$  such that

$$\beta_{\alpha, \delta} := \begin{cases} \frac{e^{-\alpha}}{\sqrt{\kappa\delta}} \arctan \left( \frac{2\sqrt{\kappa}e^{\alpha(\kappa+1)}}{\kappa e^{2\alpha(\kappa+1)} - 1} \right) & \text{if } \kappa e^{2\alpha(\kappa+1)} > 1, \\ \frac{\pi e^{-\alpha}}{2\sqrt{\kappa\delta}} & \text{if } \kappa e^{2\alpha(\kappa+1)} = 1, \\ \frac{e^{-\alpha}}{\sqrt{\kappa\delta}} \arctan \left( \frac{2\sqrt{\kappa}e^{\alpha(\kappa+1)}}{\kappa e^{2\alpha(\kappa+1)} - 1} \right) + \frac{\pi e^{-\alpha}}{\sqrt{\kappa\delta}} & \text{if } \kappa e^{2\alpha(\kappa+1)} < 1. \end{cases}$$

We also introduce

$$\delta^* := \frac{1 - m_0}{1 + \kappa} \quad \text{and} \quad \xi^* := \frac{\kappa + m_0}{2(1 + \kappa)},$$

and we denote by  $\beta_\alpha^*$  the real number  $\beta_{\alpha, \delta^*}$ .

Note that the particular choice  $|\{m = \kappa\}| = \delta^*$  corresponds to choosing  $\int_0^1 m = -m_0$  if  $m$  is bang-bang. It is also notable that if  $E^* = (\xi^*, \xi^* + \delta^*)$  in (VI.2.3), then  $\{m = \kappa\}$  is a centered subinterval of  $(0, 1)$ .

**Theorem VI.2.6** (Robin case). *Let  $\beta \geq 0$  and  $\alpha \in [0, \bar{\alpha}]$ . The optimal design problem (VI.2.1) has a solution  $m_*^\beta$ .*

Defining  $\delta := \frac{1 - \tilde{m}_0}{1 + \kappa}$ , where  $\tilde{m}_0 = -\int_0^1 m_*^\beta$  and assuming moreover that  $\alpha \in [0, \min\{1/2, \bar{\alpha}\}]$ , one has the following.

- If  $\beta < \beta_{\alpha, \delta}$ , then  $\int_0^1 m_*^\beta = -m_0$  and the solutions of Problem (VI.2.1) coincide with the solutions of Problem (VI.2.1) in the Neumann case.
- If  $\beta > \beta_{\alpha, \delta}$ , then the solutions of Problem (VI.2.1) are of Dirichlet type. Moreover, if we further assume that

$$\alpha < \frac{\sinh^2(\beta_{1/2}^* \xi^*)}{1 + 2 \sinh^2(\beta_{1/2}^* \xi^*)}, \quad (\text{VI.2.4})$$

- then  $\int_0^1 m_*^\beta = -m_0$  and the solutions of Problem (VI.2.1) coincide with the solutions of Problem (VI.2.1) in the Dirichlet case.
- If  $\beta = \beta_{\alpha,\delta}$ , then  $\int_0^1 m_*^\beta = -m_0$  and every function  $m = (\kappa + 1)\chi_{(\xi,\xi+\delta^*)} - 1$  where  $\xi \in [0, 1 - \delta^*]$  solves Problem (VI.2.1).

This result is illustrated on Figure VI.2.1. It can be seen as a generalization of [167, Theorem 1], where the case  $\alpha = 0$  is investigated.

Let us comment on these results. It is notable that standard symmetrization argument cannot be directly applied. Indeed this is due to the presence of the term  $e^{\alpha m}$  at the same time in the numerator and the denominator of the Rayleigh quotient defining  $\lambda_1^\beta(m)$ . The proofs rest upon the use of a change of variable to show some monotonicity properties of the minimizers, combined with an appropriate rearrangement procedure as well as a refined study of the necessary first and second order optimality conditions to show the *bang-bang* property of the minimizers.

Let us now comment on the activeness of the inequality constraint (VI.1.3). In the case  $\alpha = 0$ , one can prove that a comparison principle holds (see [176], Lemma 2.3). A direct consequence is that the constraint (VI.1.3) is always active. In our case however, it can be established that the comparison principle fails to hold, and the activeness of the constraint has to be studied *a posteriori*.

**Remark VI.2.7.** We can prove that, if assumption (VI.2.4) fails to hold, then there exist sets of parameters such that  $\int_0^1 m_*^\beta < m_0$ .

**Dirichlet boundary conditions.** Finally, as a byproduct of Theorem VI.2.6, we have the following result in the case of Dirichlet boundary conditions.

**Theorem VI.2.8** (Dirichlet case). *Let  $\beta = +\infty$  and  $\alpha \geq 0$ . The optimal design problem (VI.2.1) has a solution. If one assumes moreover that  $\alpha \in [0, 1/2)$ , then any solution of Problem (VI.2.1) writes  $m = (\kappa + 1)\chi_{((1-\delta)/2, (1+\delta)/2)} - 1$  for some  $\delta \in (0, 1)$ .*

**Remark VI.2.9.** Note that under the assumptions of Theorem VI.2.6, with the additional assumption (VI.2.4), Theorem VI.2.6 rewrites:

- if  $\beta < \beta_\alpha^*$ , then the only solutions of Problem (VI.2.1) are the Neumann solutions;
- if  $\beta > \beta_\alpha^*$ , then the only solution of Problem (VI.2.1) is the Dirichlet solution;
- if  $\beta = \beta_\alpha^*$ , then every function  $m = (\kappa + 1)\chi_{(\xi,\xi+\delta^*)} - 1$  where  $\xi \in [0, 1 - \delta^*]$  solves Problem (VI.2.1).

The proofs of Theorems VI.2.5, VI.2.6 and VI.2.8 are split into four steps that can be summed up as follows: (i) proof that one can restrict the search of minimizers to unimodal weights, (ii) proof of existence, (iii) proof of the *bang-bang* character of minimizers. The consequence of these three steps is that there exists a minimizer of the form  $m^* = \kappa\chi_E - \chi_{\Omega \setminus E}$ , where  $E$  is an interval. The fourth step hence writes: (iv) optimal location of  $E$  whenever  $E$  is an interval of fixed length.

### VI.2.3 Qualitative properties and comments on the results

It is interesting to notice that, after some computations, we prove that the optimal eigenvalue  $\lambda_*^\beta$  is the first positive solution of an algebraic equation, the so-called *transcendental equation*. More precisely,

- in the case  $\beta < \beta_{\alpha,\delta}$ , the optimal eigenvalue  $\lambda_*^\beta$  is the first positive root of the equation (of unknown  $\lambda$ )

$$\tan(\sqrt{\lambda\kappa\delta}) = \sqrt{\kappa}e^{\alpha(\kappa+1)} \frac{(\lambda + \beta^2 e^{2\alpha}) \tanh(\sqrt{\lambda}(1-\delta)) + 2\beta e^\alpha \sqrt{\lambda}}{\beta e^\alpha \sqrt{\lambda} (\kappa e^{2\alpha(\kappa+1)} - 1) \tanh(\sqrt{\lambda}(1-\delta)) + e^{2\alpha} (\lambda \kappa e^{2\alpha\kappa} - \beta^2)},$$

- in the case  $\beta > \beta_{\alpha, \delta}$ , the optimal eigenvalue  $\lambda_*^\beta$  is the first positive root of the equation (of unknown  $\lambda$ )

$$\tan(\sqrt{\lambda\kappa}\delta) = \sqrt{\kappa}e^{\alpha(\kappa+1)} \frac{(\lambda + \beta^2 e^{2\alpha}) \sinh(\sqrt{\lambda}(1-\delta)) + 2\beta\sqrt{\lambda}e^\alpha \cosh(\sqrt{\lambda}(1-\delta))}{\mathcal{A}_\alpha(\beta, \lambda)},$$

where

$$\begin{aligned} \mathcal{A}_\alpha(\beta, \lambda) := & \frac{1}{2}(\kappa e^{2\alpha(1+\kappa)} - 1)(\beta^2 e^{2\alpha} + \lambda) \cosh(\sqrt{\lambda}(1-\delta)) \\ & + \beta e^\alpha \sqrt{\lambda}(\kappa e^{2\alpha(\kappa+1)} - 1) \sinh(\sqrt{\lambda}(1-\delta)) + \frac{1}{2}(1 + \kappa e^{2\alpha(1+\kappa)})(\lambda - \beta^2 e^{2\alpha}). \end{aligned}$$

These formulae provide an efficient way to compute the numbers  $\lambda_*^\beta$  since it comes to the resolution of a one-dimensional algebraic equation.

On Figure VI.2.2, we used this technique to draw the graph of  $\beta \mapsto \lambda_*^\beta$  for a given choice of the parameters  $\alpha$ ,  $\kappa$  and  $m_0$ . It is notable that one can recover from this figure, the values  $\lambda_*^0$  (optimal value of  $\lambda_1$  in the Neumann case) as the ordinate of the most left hand point of the curve and  $\lambda_*^\infty$  (optimal value of  $\lambda_1$  in the Dirichlet case) as the ordinate of all points of the horizontal asymptotic axis of the curve. Finally the concavity of the function  $\beta \mapsto \lambda_*^\beta$  can be observed on Figure VI.2.2. This can be seen as a consequence of the fact that  $\lambda_*^\beta$  writes as the infimum of linear functions of the real variable  $\beta$ .

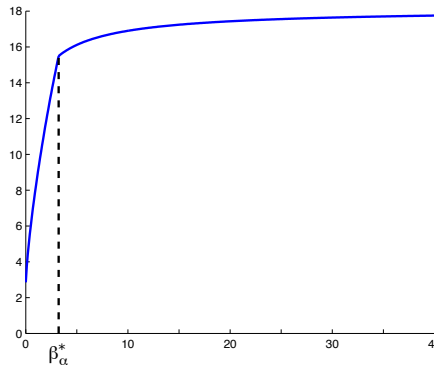


**Figure VI.2.2** – Graph of  $\beta \mapsto \lambda_*^\beta$  for  $\alpha = 0.2$ ,  $\kappa = 1$  and  $m_0 = 0.4$ . In that case,  $\beta_\alpha^* \simeq 3.2232$ .

## VI.3 Perspectives

The same issues as those investigated in this work remain relevant in the multi-dimensional case, from the biological as well as the mathematical point of view. Indeed the same considerations as in Section VI.1.1 lead to investigate the problem

$$\inf_{m \in \mathcal{M}_{m_0, \kappa}} \lambda_1^\beta(m) \quad \text{with} \quad \lambda_1^\beta(m) = \inf_{\varphi \in \mathcal{S}} \frac{\int_{\Omega} e^{\alpha m} |\nabla \varphi|^2 + \beta \int_{\partial \Omega} \varphi^2}{\int_{\Omega} m e^{\alpha m} \varphi^2}.$$

Such a problem needs a very careful analysis. It is likely that such analysis will strongly differ from the one led in this article. Indeed we claim that except maybe for some particular sets  $\Omega$  enjoying symmetry properties, we cannot use directly the same kind of rearrangement/symmetrization techniques.

Furthermore the change of variable introduced in the proofs of the main theorem (especially in order to prove that every minimizer is unimodal), that is

$$y = \int_0^x e^{-\alpha m(s)} ds, \quad x \in [0, 1],$$

is proper to the study of Sturm-Liouville equations. We used it to characterize persistence properties of the diffusive logistic equation with an advection term and to exploit the first and second order optimality conditions of the optimal design problem above, but such a rewriting has *a priori* no equivalent in higher dimensions.

The following issues could be investigated:

- (*biological model*) existence, simplicity of a principal eigenvalue for weights  $m$  in the class  $\mathcal{M}_{m_0, \kappa}$ , without additional regularity assumption;
- (*biological model*) time asymptotic behavior of the solution of the logistic diffusive equation with an advection term, and characterization of the alternatives in terms of the principal eigenvalue;
- (*optimal design problem*) existence and *bang-bang* properties of minimizers;
- (*optimal design problem*) development of a numerical approach to compute the minimizers.

It is notable that, in the case where  $\alpha = 0$ , several theoretical and numerical results gathered in [162] suggest that properties of optimal shapes, whenever they exist, strongly depend on the value of  $m_0$ .

Another interesting issue (relevant as well in the one and multi-D models) concerns the sharpness of the smallness assumptions on  $\alpha$  made in Theorems VI.2.5, VI.2.6 and VI.2.8. From these results, one is driven to wonder whether this assumption can be relaxed or even removed.

---

## Références bibliographiques

- [1] J. Abouchabaka and C. Tajani. An alternating KMF algorithm to solve the Cauchy problem for Laplace's equation. *International Journal of Computer Applications*, 38(8), 2012.
- [2] R. Aboulaich, A. B. Abda, and M. Kallel. A control type method for solving the Cauchy–Stokes problem. *Applied Mathematical Modelling*, 37(6):4295–4304, 2013.
- [3] E. Acerbi, N. Fusco, and M. Morini. Minimality via second variation for a nonlocal isoperimetric problem. *Comm. Math. Phys.*, 322(2):515–557, 2013.
- [4] Y. Achdou, O. Pironneau, and F. Valentin. Effective boundary conditions for laminar flows over periodic rough boundaries. *J. Comput. Phys.*, 147(1):187–218, 1998.
- [5] S. Adly and L. Bourdin. Sensitivity analysis of variational inequalities via twice epi-differentiability and proto-differentiability of the proximity operator. *SIAM J. Optim.*, 2018.
- [6] S. Adly, L. Bourdin, and F. Caubet. On a decomposition formula for the proximal operator of the sum of two convex functions. *Journal of Convex Analysis*, 2018.
- [7] L. Afraites, M. Dambrine, K. Eppler, and D. Kateb. Detecting perfectly insulated obstacles by shape optimization techniques of order two. *Discrete Contin. Dyn. Syst. Ser. B*, 8(2):389–416 (electronic), 2007.
- [8] L. Afraites, M. Dambrine, and D. Kateb. On second order shape optimization methods for electrical impedance tomography. *SIAM J. Control Optim.*, 47(3):1556–1590, 2008.
- [9] G. A. Afrouzi and K. J. Brown. On principal eigenvalues for boundary value problems with indefinite weight and Robin boundary conditions. *Proc. Amer. Math. Soc.*, 127(1):125–130, 1999.
- [10] G. Alessandrini, E. Beretta, E. Rosset, and S. Vessella. Optimal stability for inverse elliptic boundary value problems with unknown boundaries. *Annali della Scuola Normale Superiore di Pisa - Classe di Scienze*, 29(4):755–806, 2000.
- [11] G. Alessandrini, L. Del Piero, and L. Rondi. Stable determination of corrosion by a single electrostatic boundary measurement. *Inverse Problems*, 19(4):973–984, 2003.
- [12] G. Alessandrini, L. Rondi, E. Rosset, and S. Vessella. The stability for the Cauchy problem for elliptic equations. *Inverse Problems*, 25(12):123004, 47, 2009.

## Références bibliographiques

---

- [13] G. Alessandrini and E. Sincich. Detecting nonlinear corrosion by electrostatic measurements. *Appl. Anal.*, 85(1-3):107–128, 2006.
- [14] G. Allaire. Continuity of the darcy’s law in the low-volume fraction limit. *Annali della Scuola Normale Superiore di Pisa-Classe di Scienze*, 18(4):475–499, 1991.
- [15] G. Allaire. Homogenization of the navier-stokes equations in open sets perforated with tiny holes i. abstract framework, a volume distribution of holes. *Archive for Rational Mechanics and Analysis*, 113(3):209–259, 1991.
- [16] G. Allaire and C. Dapogny. A deterministic approximation method in shape optimization under random uncertainties. *SMAI-Journal of computational mathematics*, 1:83–143, 2015.
- [17] G. Allaire, F. de Gournay, F. Jouve, and A.-M. Toader. Structural optimization using topological and shape sensitivity via a level set method. *Control Cybernet.*, 34(1):59–80, 2005.
- [18] G. Allaire, F. Jouve, and A.-M. Toader. Structural optimization using sensitivity analysis and a level-set method. *J. Comput. Phys.*, 194(1):363–393, 2004.
- [19] C. Alvarez, C. Conca, L. Friz, O. Kaviani, and J. H. Ortega. Identification of immersed obstacles via boundary measurements. *Inverse Problems*, 21(5):1531–1552, 2005.
- [20] H. Ammari and H. Kang. *Reconstruction of small inhomogeneities from boundary measurements*, volume 1846 of *Lecture Notes in Mathematics*. Springer-Verlag, Berlin, 2004.
- [21] S. Amstutz. The topological asymptotic for the Navier-Stokes equations. *ESAIM Control Optim. Calc. Var.*, 11(3):401–425 (electronic), 2005.
- [22] S. Amstutz. Topological sensitivity analysis for some nonlinear pde systems. *Journal de mathématiques pures et appliquées*, 85(4):540–557, 2006.
- [23] S. Amstutz and M. Ciligot-Travain. A notion of compliance robustness in topology optimization. *ESAIM Control Optim. Calc. Var.*, 22(1):64–87, 2016.
- [24] S. Amstutz, M. Masmoudi, and B. Samet. The topological asymptotic for the Helmholtz equation. *SIAM J. Control Optim.*, 42(5):1523–1544 (electronic), 2003.
- [25] S. Andrieux, T. Baranger, and A. Ben Abda. Solving Cauchy problems by minimizing an energy-like functional. *Inverse problems*, 22(1):115, 2006.
- [26] X. Antoine and H. Barucq. Approximation by generalized impedance boundary conditions of a transmission problem in acoustic scattering. *M2AN Math. Model. Numer. Anal.*, 39(5):1041–1059, 2005.
- [27] B. Aslanyürek, H. Haddar, and H. Şahintürk. Generalized impedance boundary conditions for thin dielectric coatings with variable thickness. *Wave Motion*, 48(7):681–700, 2011.
- [28] Y. Assaf, R. Z. Freidlin, G. K. Rohde, and P. J. Basser. New modeling and experimental framework to characterize hindered and restricted water diffusion in brain white matter. *Magnetic Resonance in Medicine*, 52(5):965–978, 2004.
- [29] W. Y. Aung, S. Mar, and T. L. Benzinger. Diffusion tensor MRI as a biomarker in axonal and myelin damage. *Imaging in Medicine*, 5(5):427–440, 2013.
- [30] M. Azaïez, F. Ben Belgacem, and H. El Fekih. On Cauchy’s problem: II. Completion, regularization and approximation. *Inverse problems*, 22(4):1307, 2006.
- [31] V. Bacchelli. Uniqueness for the determination of unknown boundary and impedance with the homogeneous Robin condition. *Inverse Problems*, 25(1):015004, 4, 2009.

- [32] M. Badra, F. Caubet, and M. Dambrine. Detecting an obstacle immersed in a fluid by shape optimization methods. *Math. Models Methods Appl. Sci.*, 21(10):2069–2101, 2011.
- [33] M. Badra, F. Caubet, and J. Dardé. Stability estimates for Navier-Stokes equations and application to inverse problems. *Discrete Contin. Dyn. Syst. Ser. B*, 21(8):2379–2407, 2016.
- [34] L. Baffico, C. Grandmont, and B. Maury. Multiscale modeling of the respiratory tract. *Math. Models Methods Appl. Sci.*, 20(1):59–93, 2010.
- [35] A. Ballerini. Stable determination of an immersed body in a stationary Stokes fluid. *Inverse Problems*, 26(12):125015, 25, 2010.
- [36] A. Ballerini. Stable determination of a body immersed in a fluid: the nonlinear stationary case. *Appl. Anal.*, 92(3):460–481, 2013.
- [37] H. H. Bauschke and P. L. Combettes. *Convex analysis and monotone operator theory in Hilbert spaces*. CMS Books in Mathematics/Ouvrages de Mathématiques de la SMC. Springer, New York, 2017 (2nd edition).
- [38] C. Beaulieu. The basis of anisotropic water diffusion in the nervous system – a technical review. *NMR in Biomedicine*, 15(7-8):435–455, 2002.
- [39] F. Belgacem and C. Cosner. The effects of dispersal along environmental gradients on the dynamics of populations in heterogeneous environments. *Canad. Appl. Math. Quart.*, 3(4):379–397, 1995.
- [40] M. Bellassoued, J. Cheng, and M. Choulli. Stability estimate for an inverse boundary coefficient problem in thermal imaging. *J. Math. Anal. Appl.*, 343(1):328–336, 2008.
- [41] J. A. Bello, E. Fernández-Cara, J. Lemoine, and J. Simon. The differentiability of the drag with respect to the variations of a Lipschitz domain in a Navier-Stokes flow. *SIAM J. Control Optim.*, 35(2):626–640, 1997.
- [42] J. A. Bello, E. Fernández Cara, and J. Simon. Optimal shape design for Navier-Stokes flow. In *System modelling and optimization (Zurich, 1991)*, volume 180 of *Lecture Notes in Control and Inform. Sci.*, pages 481–489. Springer, Berlin, 1992.
- [43] J. A. Bello, E. Fernández Cara, and J. Simon. The variation of the drag with respect to the domain in Navier-Stokes flow. In *Optimization, optimal control and partial differential equations (Iasi, 1992)*, volume 107 of *Internat. Ser. Numer. Math.*, pages 287–296. Birkhäuser, Basel, 1992.
- [44] A. Ben Abda, M. Hassine, M. Jaoua, and M. Masmoudi. Topological sensitivity analysis for the location of small cavities in Stokes flow. *SIAM J. Control Optim.*, 48(5):2871–2900, 2009/10.
- [45] F. Ben Belgacem. Why is the Cauchy problem severely ill-posed? *Inverse Problems*, 23(2):823, 2007.
- [46] F. Ben Belgacem and H. El Fekih. On Cauchy’s problem: I. A variational Steklov–Poincaré theory. *Inverse Problems*, 21(6):1915, 2005.
- [47] F. Ben Belgacem, H. El Fekih, and F. Jelassi. The Lavrentiev regularization of the data completion problem. *Inverse Problems*, 24(4):045009, 2008.
- [48] A. Bendali and K. Lemrabet. The effect of a thin coating on the scattering of a time-harmonic wave for the Helmholtz equation. *SIAM J. Appl. Math.*, 56(6):1664–1693, 1996.
- [49] A. Bensoussan and J.-L. Lions. Inéquations quasi-variationnelles dépendant d’un paramètre. *Ann. Scuola Norm. Sup. Pisa Cl. Sci. (4)*, 4(2):231–255, 1977.

## Références bibliographiques

---

- [50] P. Beremlijski, J. Haslinger, M. Kočvara, R. Kučera, and J. V. Outrata. Shape optimization in three-dimensional contact problems with Coulomb friction. *SIAM J. Optim.*, 20(1):416–444, 2009.
- [51] E. Bishop. A generalization of the Stone-Weierstrass theorem. *Pacific J. Math.*, 11(3):777–783, 1961.
- [52] I. E. Biton, I. D. Duncan, and Y. Cohen. High b-value q-space diffusion MRI in myelin-deficient rat spinal cords. *Magn Reson Imaging*, 24(2):161–166, 2006.
- [53] V. Bonnaillie-Noël and M. Dambrine. Interactions between moderately close circular inclusions: the Dirichlet-Laplace equation in the plane. *Asymptot. Anal.*, 84(3-4):197–227, 2013.
- [54] V. Bonnaillie-Noël, M. Dambrine, F. Hérau, and G. Vial. On generalized Ventcel’s type boundary conditions for Laplace operator in a bounded domain. *SIAM J. Math. Anal.*, 42(2):931–945, 2010.
- [55] V. Bonnaillie-Noël, M. Dambrine, S. Tordeux, and G. Vial. Interactions between moderately close inclusions for the Laplace equation. *Math. Models Methods Appl. Sci.*, 19(10):1853–1882, 2009.
- [56] P. Bonnelie, L. Bourdin, F. Caubet, and O. Ruatta. Flip procedure in geometric approximation of multiple-component shapes—application to multiple-inclusion detection. *SMAI J. Comput. Math.*, 2:255–276, 2016.
- [57] M. Bonnet, A. Burel, M. Duruffé, and P. Joly. Effective transmission conditions for thin-layer transmission problems in elastodynamics. The case of a planar layer model. *ESAIM: Mathematical Modelling and Numerical Analysis*, 50:43–75, 2016.
- [58] A. Borsic, W. Lionheart, and N. Polydorides. Electrical impedance tomography: Methods, history and applications. *IOP Series in Medical Physics and Biomedical Engineering*, pages 3–64, 2005.
- [59] M. Boulakia, A.-C. Egloffé, and C. Grandmont. Stability estimates for a Robin coefficient in the two-dimensional Stokes system. *Math. Control Relat. Fields*, 3(1):21–49, 2013.
- [60] M. Boulakia, A.-C. Egloffé, and C. Grandmont. Stability estimates for the unique continuation property of the Stokes system and for an inverse boundary coefficient problem. *Inverse Problems*, 29(11):115001, 21, 2013.
- [61] L. Bourgeois, N. Chaulet, and H. Haddar. Stable reconstruction of generalized impedance boundary conditions. *Inverse Problems*, 27(9):095002, 26, 2011.
- [62] L. Bourgeois, N. Chaulet, and H. Haddar. On simultaneous identification of the shape and generalized impedance boundary condition in obstacle scattering. *SIAM J. Sci. Comput.*, 34(3):A1824–A1848, 2012.
- [63] L. Bourgeois and J. Dardé. A duality-based method of quasi-reversibility to solve the Cauchy problem in the presence of noisy data. *Inverse Problems*, 26(9):095016, 2010.
- [64] L. Bourgeois and J. Dardé. About stability and regularization of ill-posed elliptic Cauchy problems: the case of Lipschitz domains. *Applicable Analysis*, 89(11):1745–1768, 2010.
- [65] L. Bourgeois and J. Dardé. A quasi-reversibility approach to solve the inverse obstacle problem. *Inverse Probl. Imaging*, 4(3):351–377, 2010.
- [66] L. Bourgeois and J. Dardé. The “exterior approach” to solve the inverse obstacle problem for the Stokes system. *Inverse Probl. Imaging*, 8(1):23–51, 2014.

- 
- [67] L. Bourgeois and J. Dardé. The “exterior approach” applied to the inverse obstacle problem for the heat equation. *SIAM J. Numer. Anal.*, 55(4):1820–1842, 2017.
- [68] L. Bourgeois and H. Haddar. Identification of generalized impedance boundary conditions in inverse scattering problems. *Inverse Probl. Imaging*, 4(1):19–38, 2010.
- [69] F. Boyer and P. Fabrie. *Éléments d’analyse pour l’étude de quelques modèles d’écoulements de fluides visqueux incompressibles*, volume 52 of *Mathématiques & Applications (Berlin) [Mathematics & Applications]*. Springer-Verlag, Berlin, 2006.
- [70] D. Bucur and G. Buttazzo. *Variational methods in shape optimization problems*. Progress in Nonlinear Differential Equations and their Applications, 65. Birkhäuser Boston Inc., Boston, MA, 2005.
- [71] M. Burger, B. Hackl, and W. Ring. Incorporating topological derivatives into level set methods. *J. Comput. Phys.*, 194(1):344–362, 2004.
- [72] M. Burger and S. J. Osher. A survey on level set methods for inverse problems and optimal design. *European J. Appl. Math.*, 16(2):263–301, 2005.
- [73] E. Burman. A stabilized nonconforming finite element method for the elliptic Cauchy problem. *Math. Comp.*, 86(303):75–96, 2017.
- [74] F. Cakoni and R. Kress. Integral equations for inverse problems in corrosion detection from partial Cauchy data. *Inverse Probl. Imaging*, 1(2):229–245, 2007.
- [75] F. Cakoni and R. Kress. Integral equations methods for the inverse obstacle problems with generalized impedance boundary condition. *Inverse Problems*, 29:015005, 2012.
- [76] R. Cantrell and C. Cosner. Diffusive logistic equations with indefinite weights: population models in disrupted environments. II. *SIAM J. Math. Anal.*, 22(4):1043–1064, 1991.
- [77] R. S. Cantrell and C. Cosner. The effects of spatial heterogeneity in population dynamics. *J. Math. Biol.*, 29(4):315–338, 1991.
- [78] A. Carpio and M.-L. Rapún. Solving inhomogeneous inverse problems by topological derivative methods. *Inverse Problems*, 24(4):045014, 32, 2008.
- [79] A. Carpio and M.-L. Rapún. Hybrid topological derivative and gradient-based methods for electrical impedance tomography. *Inverse Problems*, 28(9):095010, 22, 2012.
- [80] A. Carpio and M.-L. Rapún. Parameter identification in photothermal imaging. *J. Math. Imaging Vision*, 49(2):273–288, 2014.
- [81] F. Caubet. Detecting an obstacle immersed in a fluid: the Stokes case. In *Eleventh International Conference Zaragoza-Pau on Applied Mathematics and Statistics*, volume 37 of *Monogr. Mat. García Galdeano*, pages 91–101. Prensas Univ. Zaragoza, Zaragoza, 2012.
- [82] F. Caubet. *Détection d’un objet immergé dans un fluide*. PhD thesis, Thèse de doctorat dirigée par Marc Dambrine, Mathématiques appliquées Pau, 2012.
- [83] F. Caubet. Instability of an Inverse Problem for the Stationary Navier–Stokes Equations. *SIAM J. Control Optim.*, 51(4):2949–2975, 2013.
- [84] F. Caubet, C. Conca, and M. Godoy. On the detection of several obstacles in 2D Stokes flow: topological sensitivity and combination with shape derivatives. *Inverse Probl. Imaging*, 10(2):327–367, 2016.

## Références bibliographiques

---

- [85] F. Caubet and M. Dambrine. Localization of small obstacles in Stokes flow. *Inverse Problems*, 28(10):105007, 31, 2012.
- [86] F. Caubet and M. Dambrine. Stability of critical shapes for the drag minimization problem in Stokes flow. *J. Math. Pures Appl. (9)*, 100(3):327–346, 2013.
- [87] F. Caubet, M. Dambrine, and H. Harbrecht. A new method for the data completion problem and application to obstacle detection. *Submitted*, 2018.
- [88] F. Caubet, M. Dambrine, and D. Kateb. Shape optimization methods for the inverse obstacle problem with generalized impedance boundary conditions. *Inverse Problems*, 29(11):115011, 26, 2013.
- [89] F. Caubet, M. Dambrine, D. Kateb, and C. Z. Timimoun. A Kohn-Vogelius formulation to detect an obstacle immersed in a fluid. *Inverse Probl. Imaging*, 7(1):123–157, 2013.
- [90] F. Caubet, J. Dardé, and M. Godoy. On the data completion problem and the inverse obstacle problem with partial Cauchy data for Laplace’s equation. *ESAIM Control Optim. Calc. Var.*, to appear, 2017.
- [91] F. Caubet, T. Deheuvels, and Y. Privat. Optimal location of resources for biased movement of species: the 1D case. *SIAM J. Appl. Math.*, 77(6):1876–1903, 2017.
- [92] F. Caubet, H. Haddar, J.-R. Li, and D. V. Nguyen. New transmission condition accounting for diffusion anisotropy in thin layers applied to diffusion MRI. *ESAIM Math. Model. Numer. Anal.*, 51(4):1279–1301, 2017.
- [93] F. Caubet, D. Kateb, and F. Le Louër. Shape sensitivity analysis for elastic structures with generalized impedance boundary conditions of the wentzell type - application to minimization of the compliance. *Journal of Elasticity*, to appear, 2018.
- [94] S. Chaabane, I. Fellah, M. Jaoua, and J. Leblond. Logarithmic stability estimates for a Robin coefficient in two-dimensional Laplace inverse problems. *Inverse Problems*, 20(1):47–59, 2004.
- [95] S. Chaabane and M. Jaoua. Identification of Robin coefficients by the means of boundary measurements. *Inverse Problems*, 15(6):1425–1438, 1999.
- [96] J. Cheng, M. Choulli, and J. Lin. Stable determination of a boundary coefficient in an elliptic equation. *Math. Models Methods Appl. Sci.*, 18(1):107–123, 2008.
- [97] A. N. Christiansen, M. Nobel-Jørgensen, N. Aage, O. Sigmund, and J. A. Bærentzen. Topology optimization using an explicit interface representation. *Structural and Multidisciplinary Optimization*, 49(3):387–399, 2014.
- [98] S. Chun, H. Haddar, and J. S. Hesthaven. High-order accurate thin layer approximations for time-domain electromagnetics, Part II: transmission layers. *J. Comput. Appl. Math.*, 234(8):2587–2608, 2010.
- [99] P. G. Ciarlet. *Mathematical elasticity. Vol. III*, volume 29 of *Studies in Mathematics and its Applications*. North-Holland Publishing Co., Amsterdam, 2000. Theory of shells.
- [100] A. Cimetiere, F. Delvare, M. Jaoua, and F. Pons. Solution of the Cauchy problem using iterated Tikhonov regularization. *Inverse Problems*, 17(3):553, 2001.
- [101] J. Coatléven, H. Haddar, and J.-R. Li. A macroscopic model including membrane exchange for diffusion MRI. *SIAM J. Appl. Math.*, 74(2):516–546, 2014.

- [102] D. Colton and R. Kress. *Inverse acoustic and electromagnetic scattering theory*, volume 93 of *Applied Mathematical Sciences*. Springer-Verlag, Berlin, second edition, 1998.
- [103] P. L. Combettes, D. Dũng, and B. C. Vũ. Dualization of signal recovery problems. *Set-Valued Var. Anal.*, 18(3-4):373–404, 2010.
- [104] P. L. Combettes and J.-C. Pesquet. Proximal splitting methods in signal processing. In *Fixed-point algorithms for inverse problems in science and engineering*, volume 49 of *Springer Optim. Appl.*, pages 185–212. Springer, New York, 2011.
- [105] C. Conca, M. Malik, and A. Munnier. Detection of a moving rigid solid in a perfect fluid. *Inverse Problems*, 26(9):095010, 18, 2010.
- [106] C. Cosner and Y. Lou. Does movement toward better environments always benefit a population? *J. Math. Anal. Appl.*, 277(2):489–503, 2003.
- [107] M. Dambrine. On variations of the shape Hessian and sufficient conditions for the stability of critical shapes. *RACSAM Rev. R. Acad. Cienc. Exactas Fís. Nat. Ser. A Mat.*, 96(1):95–121, 2002.
- [108] M. Dambrine, H. Harbrecht, and B. Puig. Incorporating knowledge on the measurement noise in electrical impedance tomography. *ESAIM Control Optim. Calc. Var.*, 2018.
- [109] M. Dambrine and J. Lamboley. Stability in shape optimization with second variation. *soumis*, 2017.
- [110] M. Dambrine and A. Laurain. A first order approach for worst-case shape optimization of the compliance for a mixture in the low contrast regime. *Struct. Multidiscip. Optim.*, 54(2):215–231, 2016.
- [111] M. Dambrine and M. Pierre. About stability of equilibrium shapes. *M2AN Math. Model. Numer. Anal.*, 34(4):811–834, 2000.
- [112] J. Dardé. *Quasi-reversibility and level set methods applied to elliptic inverse problems*. Theses, Université Paris-Diderot - Paris VII, Dec. 2010.
- [113] J. Dardé. The ‘exterior approach’: a new framework to solve inverse obstacle problems. *Inverse Problems*, 28(1):015008, 22, 2012.
- [114] J. Dardé. Iterated quasi-reversibility method applied to elliptic and parabolic data completion problems. *Inverse Probl. Imaging*, 10(2):379–407, 2016.
- [115] B. Delourme, H. Haddar, and P. Joly. Approximate models for wave propagation across thin periodic interfaces. *J. Math. Pures Appl. (9)*, 98(1):28–71, 2012.
- [116] A. Derlet, J.-P. Gossez, and P. Takáč. Minimization of eigenvalues for a quasilinear elliptic Neumann problem with indefinite weight. *J. Math. Anal. Appl.*, 371(1):69–79, 2010.
- [117] J. Descloux. On the two dimensional magnetic shaping problem without surface tension. *Report, Analysis and numerical analysis*, (07.90), 1990. Ecole polytechnique fédérale de Lausanne.
- [118] M. Di Cristo and L. Rondi. Examples of exponential instability for inverse inclusion and scattering problems. *Inverse Problems*, 19(3):685–701, 2003.
- [119] O. Dorn and D. Lesselier. Level set methods for inverse scattering. *Inverse Problems*, 22(4):R67–R131, 2006.
- [120] O. Dorn and D. Lesselier. Level set methods for inverse scattering—some recent developments. *Inverse Problems*, 25(12):125001, 11, 2009.

## Références bibliographiques

---

- [121] Z. Dostál, D. Horák, J. Szweda, and V. Vondrák. Scalabilities of FETI for variational inequalities and contact shape optimization. In *Domain decomposition methods in science and engineering (Lyon, 2000)*, Theory Eng. Appl. Comput. Methods, pages 361–369. Internat. Center Numer. Methods Eng. (CIMNE), Barcelona, 2002.
- [122] J. Douglas and H. H. Rachford. On the numerical solution of heat conduction problems in two and three space variables. *Trans. Amer. Math. Soc.*, 82:421–439, 1956.
- [123] M. Duruflé, V. Péron, and C. Poinard. Thin layer models for electromagnetism. *Commun. Comput. Phys.*, 16(1):213–238, 2014.
- [124] G. Duvaut and J.-L. Lions. *Inequalities in mechanics and physics*. Springer-Verlag, Berlin-New York, 1976. Translated from the French by C. W. John, Grundlehren der Mathematischen Wissenschaften, 219.
- [125] H. W. Engl, M. Hanke, and A. Neubauer. *Regularization of inverse problems*, volume 375. Springer Science & Business Media, 1996.
- [126] K. Eppler and H. Harbrecht. A regularized Newton method in electrical impedance tomography using shape Hessian information. *Control Cybernet.*, 34(1):203–225, 2005.
- [127] C. Fabre and G. Lebeau. Prolongement unique des solutions de l’équation de Stokes. *Comm. Partial Differential Equations*, 21(3-4):573–596, 1996.
- [128] E. Faou. Elasticity on a thin shell: formal series solution. *Asymptot. Anal.*, 31(3-4):317–361, 2002.
- [129] G. Farin. *Curves and Surfaces for CAGD: A Practical Guide*. Morgan Kaufmann Publishers Inc., San Francisco, CA, USA, 5th edition, 2002.
- [130] J. Farrell. Q-space diffusion imaging of axon and myelin damage in the human and rat spinal cord. *Johns Hopkins University*, 2009.
- [131] M. Flucher and M. Rumpf. Bernoulli’s free-boundary problem, qualitative theory and numerical approximation. *J. Reine Angew. Math.*, 486:165–204, 1997.
- [132] R. Fox, T. Cronin, J. Lin, X. Wang, K. Sakaie, D. Ontaneda, S. Mahmoud, M. Lowe, and M. Phillips. Measuring myelin repair and axonal loss with diffusion tensor imaging. *American Journal of Neuroradiology*, 32(1):85–91, 2011.
- [133] P. Frey and P. George. *Mesh Generation: Application to Finite Elements, Second Edition*. Wiley-ISTE, 2008.
- [134] P. Fulmański, A. Laurain, J.-F. Scheid, and J. Sokołowski. A level set method in shape and topology optimization for variational inequalities. *Int. J. Appl. Math. Comput. Sci.*, 17(3):413–430, 2007.
- [135] A. V. Fursikov. *Optimal control of distributed systems. Theory and applications*. American Mathematical Soc., 1999.
- [136] A. V. Fursikov and O. Y. Imanuvilov. *Controllability of evolution equations*, volume 34 of *Lecture Notes Series*. Seoul National University Research Institute of Mathematics Global Analysis Research Center, Seoul, 1996.
- [137] N. Fusco and M. Morini. Equilibrium configurations of epitaxially strained elastic films: second order minimality conditions and qualitative properties of solutions. *Arch. Ration. Mech. Anal.*, 203(1):247–327, 2012.

- [138] G. P. Galdi. *An introduction to the mathematical theory of the Navier-Stokes equations.*, volume 38 of *Springer Tracts in Natural Philosophy*. Springer-Verlag, New York, 1994. Linearized steady problems.
- [139] P. Guillaume and K. Sid Idris. The topological asymptotic expansion for the Dirichlet problem. *SIAM J. Control Optim.*, 41(4):1042–1072 (electronic), 2002.
- [140] P. Guillaume and K. Sid Idris. Topological sensitivity and shape optimization for the Stokes equations. *SIAM J. Control Optim.*, 43(1):1–31 (electronic), 2004.
- [141] J. Hadamard. *Le probleme de Cauchy et les équations aux dérivées partielles linéaires hyperboliques*, volume 220. Paris, 1932.
- [142] H. Haddar and P. Joly. Effective boundary conditions for thin ferromagnetic coatings. Asymptotic analysis of the 1D model. *Asymptot. Anal.*, 27(2):127–160, 2001.
- [143] H. Haddar and P. Joly. Stability of thin layer approximation of electromagnetic waves scattering by linear and nonlinear coatings. *J. Comput. Appl. Math.*, 143(2):201–236, 2002.
- [144] H. Haddar, P. Joly, and H.-M. Nguyen. Generalized impedance boundary conditions for scattering by strongly absorbing obstacles: the scalar case. *Math. Models Methods Appl. Sci.*, 15(8):1273–1300, 2005.
- [145] H. Haddar, P. Joly, and H.-M. Nguyen. Generalized impedance boundary conditions for scattering problems from strongly absorbing obstacles: the case of Maxwell’s equations. *Math. Models Methods Appl. Sci.*, 18(10):1787–1827, 2008.
- [146] H. Haddar and R. Kress. Conformal mappings and inverse boundary value problems. *Inverse Problems*, 21(3):935–953, 2005.
- [147] H. Han, L. Ling, and T. Takeuchi. An energy regularization for Cauchy problems of Laplace equation in annulus domain. *Communications in Computational Physics*, 9(4):878, 2011.
- [148] A. Haraux. How to differentiate the projection on a convex set in Hilbert space. Some applications to variational inequalities. *J. Math. Soc. Japan*, 29(4):615–631, 1977.
- [149] M. Hassine. Shape optimization for the Stokes equations using topological sensitivity analysis. *ARIMA*, 5:216–229, 2006.
- [150] L. He, C.-Y. Kao, and S. Osher. Incorporating topological derivatives into shape derivatives based level set methods. *J. Comput. Phys.*, 225(1):891–909, 2007.
- [151] A. Henrot. *Extremum problems for eigenvalues of elliptic operators*. Frontiers in Mathematics. Birkhäuser Verlag, Basel, 2006.
- [152] A. Henrot and M. Pierre. *Variation et optimisation de formes*, volume 48 of *Mathématiques & Applications (Berlin) [Mathematics & Applications]*. Springer, Berlin, 2005. Une analyse géométrique. [A geometric analysis].
- [153] P. Hess. *Periodic-parabolic boundary value problems and positivity*, volume 247 of *Pitman Research Notes in Mathematics Series*. Longman Scientific & Technical, Harlow; copublished in the United States with John Wiley & Sons, Inc., New York, 1991.
- [154] P. Hess and T. Kato. On some linear and nonlinear eigenvalue problems with an indefinite weight function. *Comm. Partial Differential Equations*, 5(10):999–1030, 1980.
- [155] M. Hintermüller, C.-Y. Kao, and A. Laurain. Principal eigenvalue minimization for an elliptic problem with indefinite weight and Robin boundary conditions. *Appl. Math. Optim.*, 65(1):111–146, 2012.

## Références bibliographiques

---

- [156] J.-B. Hiriart-Urruty and C. Lemaréchal. *Fundamentals of convex analysis*. Grundlehren Text Editions. Springer-Verlag, Berlin, 2001.
- [157] M. A. Horsfield and D. K. Jones. Applications of diffusion-weighted and diffusion tensor MRI to white matter diseases, a review. *NMR Biomed.*, 15(7-8):570–577, 2002.
- [158] V. Isakov. *Inverse problems for partial differential equations*, volume 127. Springer Science & Business Media, 2006.
- [159] W. Jäger and A. Mikelić. On the roughness-induced effective boundary conditions for an incompressible viscous flow. *J. Differential Equations*, 170(1):96–122, 2001.
- [160] K. Jha and G. Porru. Minimization of the principal eigenvalue under Neumann boundary conditions. *Numer. Funct. Anal. Optim.*, 32(11):1146–1165, 2011.
- [161] D. Jones. Diffusion MRI: theory, methods, and applications. *Oxford University Press, USA*, 2010.
- [162] C.-Y. Kao, Y. Lou, and E. Yanagida. Principal eigenvalue for an elliptic problem with indefinite weight on cylindrical domains. *Math. Biosci. Eng.*, 5(2):315–335, 2008.
- [163] D. Kateb and F. Le Louër. Generalized impedance boundary conditions and shape derivatives for 3D Helmholtz problems. *Math. Models Methods Appl. Sci.*, 26(10):1995–2033, 2016.
- [164] M. V. Klibanov. Carleman estimates for the regularization of ill-posed Cauchy problems. *Appl. Numer. Math.*, 94:46–74, 2015.
- [165] V. A. Kozlov, V. G. Maz'ya, and A. Fomin. An iterative method for solving the Cauchy problem for elliptic equations. *Zhurnal Vychislitel'noi Matematiki i Matematicheskoi Fiziki*, 31(1):64–74, 1991.
- [166] R. Kress and W. Rundell. Nonlinear integral equations and the iterative solution for an inverse boundary value problem. *Inverse Problems*, 21(4):1207–1223, 2005.
- [167] J. Lamboley, A. Laurain, G. Nadin, and Y. Privat. Properties of optimizers of the principal eigenvalue with indefinite weight and Robin conditions. *Calc. Var. Partial Differential Equations*, 55(6):55:144, 2016.
- [168] L. J. Lanyon. *Neuroimaging - Methods*. Chapter: Diffusion tensor imaging: structural connectivity insights, limitations and future directions. InTech, 2012.
- [169] D. Le Bihan. The 'wet mind': water and functional neuroimaging. *Physics in medicine and biology*, 52(7), 2007.
- [170] D. Le Bihan and H. Johansen-Berg. Diffusion MRI at 25: Exploring brain tissue structure and function. *NeuroImage*, 61(2):324–341, 2012.
- [171] J. Le Rousseau and G. Lebeau. On Carleman estimates for elliptic and parabolic operators. Applications to unique continuation and control of parabolic equations. *ESAIM Control Optim. Calc. Var.*, 18(3):712–747, 2012.
- [172] J. Leblond and D. Ponomarev. Recovery of harmonic functions from partial boundary data respecting internal pointwise values. *J. Inverse Ill-Posed Probl.*, 25(2):157–174, 2017.
- [173] C.-L. Lin, G. Uhlmann, and J.-N. Wang. Optimal three-ball inequalities and quantitative uniqueness for the Stokes system. *Discrete Contin. Dyn. Syst.*, 28(3):1273–1290, 2010.
- [174] A. Litman, D. Lesselier, and F. Santosa. Reconstruction of a two-dimensional binary obstacle by controlled evolution of a level-set. *Inverse Problems*, 14(3):685–706, 1998.

- [175] Y. Lou. Some challenging mathematical problems in evolution of dispersal and population dynamics. In *Tutorials in mathematical biosciences. IV*, volume 1922 of *Lecture Notes in Math.*, pages 171–205. Springer, Berlin, 2008.
- [176] Y. Lou and E. Yanagida. Minimization of the principal eigenvalue for an elliptic boundary value problem with indefinite weight, and applications to population dynamics. *Japan J. Indust. Appl. Math.*, 23(3):275–292, 2006.
- [177] S. E. Maier, Y. Sun, and R. V. Mulkern. Diffusion imaging of brain tumors. *NMR Biomed.*, 23(7):849–864, 2010.
- [178] L. E. Malvern. *Introduction to the mechanics of a continuous medium*. Prentice Hall, 1969.
- [179] A. Marco, , and J.-J. Martinez. A fast and accurate algorithm for solving bernstein-vandermonde linear systems. *Linear Algebra and its Applications*, 422(2):616 – 628, 2007.
- [180] V. Maz'ya and A. Movchan. Asymptotic treatment of perforated domains without homogenization. *Math. Nachr.*, 283(1):104–125, 2010.
- [181] V. Maz'ya, S. Nazarov, and B. Plamenevskij. *Asymptotic theory of elliptic boundary value problems in singularly perturbed domains. Vol. I*, volume 111 of *Operator Theory: Advances and Applications*. Birkhäuser Verlag, Basel, 2000. Translated from the German by Georg Heinig and Christian Posthoff.
- [182] F. Mignot. Contrôle dans les inéquations variationelles elliptiques. *J. Functional Analysis*, 22(2):130–185, 1976.
- [183] A. A. Novotny, R. A. Feijóo, E. Taroco, and C. Padra. Topological sensitivity analysis for three-dimensional linear elasticity problem. *Comput. Methods Appl. Mech. Engrg.*, 196(41-44):4354–4364, 2007.
- [184] O. Pantz and K. Trabelsi. Simultaneous shape, topology, and homogenized properties optimization. *Struct. Multidiscip. Optim.*, 34(4):361–365, 2007.
- [185] R. Perrussel and C. Poignard. Asymptotic expansion of steady-state potential in a high contrast medium with a thin resistive layer. *Appl. Math. Comput.*, 221:48–65, 2013.
- [186] T. D. M. Phan. *3D Free Form Method and Applications to Robotics*. PhD thesis, Université de Limoges, 2014.
- [187] C. Poignard. Generalized impedance boundary condition at high frequency for a domain with thin layer: the circular case. *Appl. Anal.*, 86(12):1549–1568, 2007.
- [188] R. Potthast. A survey on sampling and probe methods for inverse problems. *Inverse Problems*, 22(2):R1–R47, 2006.
- [189] Y. Qiu and T. L. Magnanti. Sensitivity analysis for variational inequalities. *Math. Oper. Res.*, 17(1):61–76, 1992.
- [190] R. Quarles, W. Macklin, and P. Morell. *Basic neurochemistry: molecular, cellular and medical aspects*. Chapter: Myelin formation, structure and biochemistry. Elsevier Science, 2006.
- [191] A. Quarteroni and A. Veneziani. Analysis of a geometrical multiscale model based on the coupling of ODEs and PDEs for blood flow simulations. *Multiscale Model. Simul.*, 1(2):173–195 (electronic), 2003.
- [192] R. T. Rockafellar. *Convex analysis*. Princeton Mathematical Series, No. 28. Princeton University Press, Princeton, N.J., 1970.

## Références bibliographiques

---

- [193] R. T. Rockafellar. Maximal monotone relations and the second derivatives of nonsmooth functions. *Ann. Inst. H. Poincaré Anal. Non Linéaire*, 2(3):167–184, 1985.
- [194] R. T. Rockafellar. Proto-differentiability of set-valued mappings and its applications in optimization. *Ann. Inst. H. Poincaré Anal. Non Linéaire*, 6:449–482, 1989. *Analyse non linéaire* (Perpignan, 1987).
- [195] L. Roques and F. Hamel. Mathematical analysis of the optimal habitat configurations for species persistence. *Math. Biosci.*, 210(1):34–59, 2007.
- [196] W. Rundell. Recovering an obstacle using integral equations. *Inverse Probl. Imaging*, 3(2):319–332, 2009.
- [197] F. Santosa. A level-set approach for inverse problems involving obstacles. *ESAIM, Control Optim. Calc. Var.*, 1:17–33, 1996.
- [198] M. Schäfer, S. Turek, and R. Rannacher. Evaluation of a CFD benchmark for laminar flows. *Proceedings ENUMATH 1997*, (Heidelberg, Germany, 28 September–3 October 1997. World Scientific: Singapore):549–563, 1998.
- [199] A. Schumacher. Topologieoptimisierung von Bauteilstrukturen unter Verwendung von Lopchpositionierungskriterien. *Thesis*, 1995. Universität-Gesamthochschule-Siegen.
- [200] T. W. Sederberg. Computer aided geometric design, October 2014.
- [201] P. Serranho. *A hybrid method for inverse obstacle scattering problems*. PhD thesis, Georg-August-Universität Gottingen, 2007.
- [202] J. Sethian. *Level set methods and fast marching methods. Evolving interfaces in computational geometry, fluid mechanics, computer vision, and materials science*. Cambridge: Cambridge University Press, 1999.
- [203] A. Shapiro. Sensitivity analysis of parameterized variational inequalities. *Math. Oper. Res.*, 30(1):109–126, 2005.
- [204] H. Si. Tetgen, a delaunay-based quality tetrahedral mesh generator. *ACM Trans. Math. Software*, 41(12), 2015.
- [205] K. Sid Idris. *Sensibilité topologique en optimisation de forme*. PhD thesis, Thèse de doctorat dirigée par Philippe Guillaume, Mathématiques appliquées Toulouse, INSA, 2001.
- [206] J. Simon. Domain variation for drag in Stokes flow. In *Control theory of distributed parameter systems and applications (Shanghai, 1990)*, volume 159 of *Lecture Notes in Control and Inform. Sci.*, pages 28–42. Springer, Berlin, 1991.
- [207] E. Sincich. Lipschitz stability for the inverse Robin problem. *Inverse Problems*, 23(3):1311–1326, 2007.
- [208] J. G. Skellam. Random dispersal in theoretical populations. *Biometrika*, 38:196–218, 1951.
- [209] J. Sokołowski and A. Żochowski. On the topological derivative in shape optimization. *SIAM J. Control Optim.*, 37(4):1251–1272 (electronic), 1999.
- [210] J. Sokołowski and J.-P. Zolésio. *Introduction to shape optimization*, volume 16 of *Springer Series in Computational Mathematics*. Springer-Verlag, Berlin, 1992. Shape sensitivity analysis.
- [211] E. O. Stejskal and J. E. Tanner. Spin diffusion measurements: Spin echoes in the presence of a time-dependent field gradient. *The Journal of Chemical Physics*, 42(1):288–292, 1965.

- [212] T. Tiihonen and J. Järvinen. On fixed point (trial) methods for free boundary problems. In *Free boundary problems in continuum mechanics (Novosibirsk, 1991)*, volume 106 of *Internat. Ser. Numer. Math.*, pages 339–350. Birkhäuser, Basel, 1992.
- [213] H. Torrey. Bloch equations with diffusion terms. *Physical Review Online Archive (Prola)*, 104(3):563–565, 1956.
- [214] M. Tucsnak and G. Weiss. *Observation and control for operator semigroups*. Birkhäuser Advanced Texts: Basler Lehrbücher. [Birkhäuser Advanced Texts: Basel Textbooks]. Birkhäuser Verlag, Basel, 2009.
- [215] G. Vial. *Analyse multi-échelle et conditions aux limites approchées pour un problème avec couche mince dans un domaine à coin*. PhD thesis, Thèse de doctorat dirigée par Gabriel Caloz, Mathématiques, Rennes 1, 2003.
- [216] I. E. Vignon-Clementel, C. A. Figueroa, K. E. Jansen, and C. A. Taylor. Outflow boundary conditions for three-dimensional finite element modeling of blood flow and pressure in arteries. *Comput. Methods Appl. Mech. Engrg.*, 195(29-32):3776–3796, 2006.
- [217] M. Vogelius and J.-M. Xu. A nonlinear elliptic boundary value problem related to corrosion modeling. *Quart. Appl. Math.*, 56(3):479–505, 1998.
- [218] Y.-L. Yu. On decomposing the proximal map. *Advances in Neural Information Processing Systems*, 26:91–99, 2013.





## Résumé

Ce manuscrit contient une partie de mes activités de recherche depuis mon arrivée à l'Institut de Mathématiques de Toulouse de l'Université Toulouse III - Paul Sabatier, en 2013.

Il traite de deux domaines mathématiques principaux : l'**optimisation de forme** et les **problèmes inverses**. Il présente un résumé des mes contributions sur ces thématiques sur quelques **équations aux dérivées partielles** et souligne les champs d'applications possibles de ces résultats.

Ce travail a été motivé par les questions principales suivantes :

- comment **justifier théoriquement l'efficacité d'une méthode numérique** ou le besoin de régularisation pour résoudre un problème ?
- comment **résoudre numériquement le problème inverse d'obstacles** en fonction du contexte physique ?
- comment **modéliser mathématiquement un problème d'optimisation de forme** dans différents champs d'applications ?

**Mots clés** : optimisation de forme, problèmes inverses, équations aux dérivées partielles, problème de minimisation de la traînée, problème inverse d'obstacle, problème de Cauchy, problème de complétion de données, conditions de Wentzell, développement asymptotique, analyse convexe, opérateur proximal

## Abstract

This manuscript contains some of my research activities since my arrival at the Institut de Mathématiques de Toulouse at the University Toulouse III - Paul Sabatier, in 2013.

It deals with two main mathematical areas: **shape optimization** and **inverse problems**. It presents a summary of my contributions about these themes on some **partial differential equations** and underlines the fields of possible applications of the results.

This work was motivated by the following main questions:

- how to **justify theoretically the efficiency of a numerical method** or the need of regularization to solve a problem?
- how to **solve numerically the inverse obstacle problem** according to the physical context?
- how to **model mathematically a shape optimization problem** in several fields of applications?

**Keywords** : shape optimization, inverse problems, partial differential equations, drag minimization problem, inverse obstacle problem, Cauchy problem, data completion problem, Wentzell boundary conditions, asymptotic expansion, convex analysis, proximal operator